

Comprehensive Nanorobotic Cure for Male Erectile Dysfunction

[Robert A. Freitas Jr.](#)

Senior Research Fellow

[Institute for Molecular Manufacturing](#)

Abstract. This paper presents the first detailed technical analysis of the application of atomically precise nanorobots to the treatment of erectile dysfunction (ED) in human males. A summary of the normal physiological processes by which male erections occur, and fail, and are currently treated in conventional clinical medicine, is followed by descriptions of how medical nanorobotics can provide (1) actual permanent cures for the underlying medical conditions that cause ED, (2) symptomatic relief from ED without correcting the underlying organic pathologies, and (3) nanorobotic penile prostheses that can reliably substitute for erectile functionality without directly curing or treating the biological pathologies of ED, but with greatly improved sexual performance characteristics.

© 2024 Robert A. Freitas Jr. All Rights Reserved.

Cite as: Robert A. Freitas Jr., “Comprehensive Nanorobotic Cure for Male Erectile Dysfunction” IMM Report No. 55, 15 Nov 2024; <http://www.imm.org/Reports/rep055.pdf>.

Table of Contents

1. Introduction.....	4
2. The Normal Process of Erection.....	7
2.1 Sexual Arousal.....	7
2.2 Neural Initiation.....	9
2.3 Vascular Response	10
2.4 Blood Flow Increase.....	13
2.5 Pressure and Expansion	14
2.6 Maintenance of Erection and Detumescence.....	15
3. How Erectile Dysfunction Occurs	17
3.1 Impaired Blood Flow	17
3.2 Neurological Disorders	18
3.3 Hormonal Imbalances.....	20
3.4 Enzymatic Abnormalities	21
3.5 Pelvic Muscle Weakness	21
3.6 Psychological Disorders.....	22
3.7 Co-Morbidities	22
3.8 Lifestyle Choices.....	23
4. Conventional Treatments for Erectile Dysfunction.....	26
4.1 PDE5 Inhibitors	26
4.2 Intracavernosal Injections of Vasoactive Agents	27
4.3 Testosterone Replacement Therapy	28
4.4 Penile Vibratory Stimulation (PVS).....	28
4.5 Low-Intensity Extracorporeal Shock Wave Therapy.....	29
4.6 Penile Implants.....	31
4.7 Vascular Surgery.....	33
4.8 Vacuum Erection Devices.....	35
4.9 Possible Future Conventional Treatments.....	37
4.9.1 Melanocortin Receptor Agonists	39
4.9.2 Botulinum Neurotoxin A	41
4.9.3 Stem Cell Therapy	41
4.9.4 Gene Therapy.....	44
4.9.5 Penile Transplants.....	46
4.10 Lifestyle Changes	50
5. Nanorobotic Treatments for Erectile Dysfunction	51
5.1 Examples of Medical Nanorobots.....	52
5.1.1 Respirocyte-Class Nanorobots.....	56

5.1.2 Microbivore-Class Nanorobots.....	60
5.1.3 Chromalloyte-Class Nanorobots	63
5.2 Nanorobotic Curative Treatments for ED.....	67
5.2.1 Nanorobotic Cure for ED-Related Impaired Blood Flow.....	68
5.2.1.1 Arterial Obstruction	68
5.2.1.2 Venous Leakage.....	77
5.2.2 Nanorobotic Cure for ED-Related Neurological Disorders.....	79
5.2.3 Nanorobotic Cure for Other ED-Related Pathologies	81
5.2.4 Nanocatheter-Based Interventions.....	84
5.2.4.1 Nanocatheter Pain Avoidance.....	90
5.2.4.2 Plaque Debridement.....	92
5.2.4.3 Whole Cell Transport and Emplacement	95
5.2.4.4 Cytosolic Intervention in Individual Cells.....	98
5.2.4.5 Tissue and Nerve Repair	99
5.3 Nanorobotic Symptomatic Treatments for ED	100
5.3.1 Erection via Vasodilator or Inflatable Nanorobots (Lifters).....	101
5.3.1.1 Bloodstream Diffusion of Nitric Oxide	102
5.3.1.2 Endothelial Cell Injection of Nitric Oxide	107
5.3.1.3 Mechanical Sinusoid Inflation	108
5.3.1.4 Venous Occlusion.....	110
5.3.1.5 Nanorobot Infusion.....	112
5.3.1.6 Nanorobot Extraction	118
5.3.1.7 Nanorobot Control	123
5.3.2 Nanorobotic Stimulation of Sexual Arousal in Men (Lustbots)	126
5.3.2.1 Physiological Requirements	126
5.3.2.2 Technical Details.....	128
5.3.2.3 Nanorobot Control	137
5.3.2.4 Female Arousal.....	139
5.3.3 Male Orgasms on Demand (Ecstasytes).....	145
5.3.3.1 Penile Orgasm Management	145
5.3.3.2 Virtual Orgasms.....	152
5.3.3.3 Continuous Orgasms	155
5.4 Nanorobotic Prostheses for ED.....	159
5.4.1 Maypole Implant.....	159
5.4.2 Nanorobotic Condom (Nanoglove)	161
5.4.3 Lifter Mesh Implant.....	164
5.4.4 Utility Penis	165
5.5 Why Physical Sex?	169
6. Conclusions.....	171

1. Introduction

Penile erection is considered to be the main component of the male sexual response. The ability of men to create and maintain an erection is important for several reasons that span both physical and psychological domains, and has been enshrined in culture and architecture at least since the ancient days of Pompeii (image, right).¹ Physically, it is a key function in the process of human bonding and sexual reproduction, allowing for the possibility of conceiving children. Psychologically, erectile function is closely tied to self-esteem and emotional well-being (and makes life fun).² Difficulties in achieving or maintaining an erection can lead to feelings of inadequacy, anxiety, and depression. Moreover, since sexual health is an integral part of overall health, erectile dysfunction can also be an indicator of underlying health issues such as cardiovascular disease or diabetes. The ability to maintain erectile function is often seen as a marker of general health and vitality.



Erectile dysfunction (ED),³ also known as impotence, is characterized by the persistent inability to achieve or maintain an erection sufficient for satisfactory sexual performance. ED mainly affects men above the age of 40. Clinically, its worldwide prevalence in men under 40 is 1%-10%, increasing to 2%-15% in men aged 40-49 years, 20%-40% in men 60-69 years of age, finally rising to 50%-75 % in men in their 70s and 80s.⁴ It has been estimated that the prevalence of ED worldwide will be over 300 million cases by the year 2025.⁵

ED is a multifactorial condition that can be influenced by psychological, neurological, hormonal, arterial, and penile anatomical components. Risk factors for ED include cardiovascular disease, diabetes mellitus, obesity, and certain lifestyle choices such as smoking and excessive alcohol consumption. Neurogenic causes are linked to disorders that affect the central or peripheral nervous system such as multiple sclerosis and spinal cord injuries. Psychological contributors to ED may include anxiety, depression, and stress.

¹ https://en.wikipedia.org/wiki/Erotic_art_in_Pompeii_and_Herculaneum.

² Love B. Encyclopedia of Unusual Sex Practices, Barricade Books, 1992; <https://www.amazon.com/Encyclopedia-Unusual-Practices-Brenda-Love/dp/1569800111/>.

³ https://en.wikipedia.org/wiki/Erectile_dysfunction.

⁴ Lewis RW, Fugl-Meyer KS, Corona G, Hayes RD, Laumann EO, Moreira ED Jr, Rellini AH, Segraves T. Definitions/epidemiology/risk factors for sexual dysfunction. J Sex Med. 2010 Apr;7(4 Pt 2):1598-607; <https://www.arca.fiocruz.br/bitstream/handle/icict/9060/Lewis%20RW%20Definitions....pdf>.

⁵ Maiorino MI, Bellastella G, Esposito K. Lifestyle modifications and erectile dysfunction: what can be expected? Asian J Androl. 2015 Jan-Feb;17(1):5-10; <https://www.ncbi.nlm.nih.gov/pmc/articles/PMC4291878/pdf>.

This paper outlines future nanorobotic complete cures and effective symptomatic treatments for erectile dysfunction in a coming era when atomically precise molecular manufacturing using nanofactories⁶ will be widespread, and medical nanorobots⁷ (Section 5.1) can be fabricated and deployed in standard clinical practice. After more than four decades of detailed exploratory engineering and related technical studies,⁸ it appears that atomically precise manufacturing of both microscale and macroscale products using nanofactories is a realistic prospect that lies “a few decades from now”,⁹ given the recent accelerating pace of developments.¹⁰

Herein we describe the normal physiological process by which male erections occur (Section 2), how this normal process can fail, leading to erectile dysfunction (Section 3), the conventional treatments for ED in clinical medicine today (Section 4), and future nanorobotic complete cures,

⁶ Drexler KE. Nanosystems: Molecular Machinery, Manufacturing, and Computation, John Wiley & Sons, New York, 1992, Section 14.4, “An exemplar manufacturing system architecture”, pp. 421-427; <https://www.amazon.com/dp/0471575186/>. Freitas RA Jr., Merkle RC. Kinematic Self-Replicating Machines, Landes Bioscience, Georgetown, TX, 2004; Section 5.9.4, “Performance of Convergent Assembly Nanofactory Systems”; <http://www.MolecularAssembler.com/KSRM/5.9.4.htm>. See also: <http://www.molecularassembler.com/Nanofactory/>.

⁷ Freitas RA Jr. Nanomedicine, Volume I: Basic Capabilities, Landes Bioscience, Georgetown, TX, 1999; <http://www.nanomedicine.com/NMI.htm>. Freitas RA Jr. Nanomedicine, Volume IIA: Biocompatibility, Landes Bioscience, Georgetown, TX, 2003; <http://www.nanomedicine.com/NMIIA.htm>. Freitas RA Jr. Chapter 23. Comprehensive Nanorobotic Control of Human Morbidity and Aging. In: Fahy GM, West MD, Coles LS, Harris SB, eds, The Future of Aging: Pathways to Human Life Extension, Springer, New York, 2010; <http://www.nanomedicine.com/Papers/Aging.pdf>. Freitas RA Jr. Cryostasis Revival: The Recovery of Cryonics Patients through Nanomedicine. Alcor Life Extension Foundation, Scottsdale AZ, 2022; Section 1.2, “Medical Nanorobotics”; <https://www.alcor.org/cryostasis-revival/>. See also: <http://www.nanomedicine.com/#NanorobotAnalyses>.

⁸ Drexler KE. Molecular engineering: An approach to the development of general capabilities for molecular manipulation. Proc Natl Acad Sci U S A. 1981 Sep;78(9):5275-8; <https://www.pnas.org/doi/pdf/10.1073/pnas.78.9.5275>. Drexler KE. Nanosystems: Molecular Machinery, Manufacturing, and Computation, John Wiley & Sons, New York, 1992; http://e-drexler.com/d/09/00/Drexler_MIT_dissertation.pdf. Freitas RA Jr. Nanomedicine, Volume I: Basic Capabilities. Landes Bioscience, Georgetown, TX, 1999; <http://www.nanomedicine.com/NMI.htm>. Freitas RA Jr., Merkle RC. Kinematic Self-Replicating Machines. Landes Bioscience, Georgetown, TX, 2004; <http://www.MolecularAssembler.com/KSRM.htm>. Freitas RA Jr., Merkle RC. A minimal toolset for positional diamond mechanosynthesis. J Comput Theor Nanosci. 2008;5:760-861; <http://www.molecularassembler.com/Papers/MinToolset.pdf>. Freitas RA Jr. Cryostasis Revival: The Recovery of Cryonics Patients through Nanomedicine. Alcor Life Extension Foundation, Scottsdale AZ, 2022; <https://www.alcor.org/cryostasis-revival/>. See also <http://www.molecularassembler.com/Nanofactory/> and https://en.wikipedia.org/wiki/Molecular_assembler#Nanofactories.

⁹ Dr. Marie OMahony. The Age of Atomically Precise Manufacturing: Talking Nanotechnology with David Forrest. Intl Fiber J, 30 May 2024; <https://www.fiberjournal.com/the-age-of-atomically-precise-manufacturing/>.

¹⁰ Kurzweil R. The Singularity is Nearer: When We Merge with AI. Viking Press, 2024; <https://www.amazon.com/Singularity-Nearer-Ray-Kurzweil/dp/0399562761>.

relevant symptomatic treatments, and prosthetic aids for erectile dysfunction ([Section 5](#)), followed by our conclusions ([Section 6](#)).

2. The Normal Process of Erection

The transition of the male human penis from the flaccid state to the erect state is a complex multi-step physiological process involving vascular, neural, and hormonal components, primarily mediated by the relaxation of smooth muscle in the corpora cavernosa¹¹ and subsequent arterial dilation. The process normally proceeds from sexual arousal ([Section 2.1](#)) to neural initiation ([Section 2.2](#)), followed by vascular response ([Section 2.3](#)), increase in blood flow ([Section 2.4](#)), then pressure and expansion ([Section 2.5](#)), after which the erection must be maintained, later followed by detumescence ([Section 2.6](#)).

This entire process is coordinated with input from the central nervous system and is influenced by hormonal, cardiovascular, and psychological factors that can affect both the initiation and maintenance of an erection.

2.1 Sexual Arousal

The process of erection begins with sexual arousal.¹² Arousal can be induced by sensory perceptions, which might include tactile, visual, olfactory, auditory, or imaginative stimuli. Erotic stimuli which can result in sexual arousal can include conversation, reading, films or images, or a smell or setting, any of which can generate erotic thoughts and memories in a person.

These sensory inputs are processed by the respective sensory areas of the brain. The limbic system,¹³ which includes structures such as the amygdala¹⁴ and hippocampus,¹⁵ plays a critical role in emotional processing of sensory inputs. Seeing or thinking about a sexual partner can trigger emotional responses. The prefrontal cortex¹⁶ is involved in higher cognitive functions and helps to assess the context and appropriateness of the stimuli, contributing to sexual desire. Increased libido¹⁷ can lead to enhanced cognitive focus on sexual thoughts and fantasies, anticipation of sex, and more pronounced responsiveness to potential sexual opportunities. This cognitive aspect is directly tied to the brain's processing of erotic stimuli and can influence overall attention towards sexual activity.

Once the brain processes the stimuli as sexually arousing, it activates specific neural pathways. Sexual arousal involves both the sympathetic¹⁸ and parasympathetic¹⁹ branches of the autonomic

¹¹ The corpora cavernosa are a pair of sponge-like regions of erectile tissue that contain most of the blood in the penis during an erection; https://en.wikipedia.org/wiki/Corpus_cavernosum_penis.

¹² https://en.wikipedia.org/wiki/Sexual_arousal.

¹³ https://en.wikipedia.org/wiki/Limbic_system.

¹⁴ <https://en.wikipedia.org/wiki/Amygdala>.

¹⁵ <https://en.wikipedia.org/wiki/Hippocampus>.

¹⁶ https://en.wikipedia.org/wiki/Prefrontal_cortex.

¹⁷ <https://en.wikipedia.org/wiki/Libido>.

¹⁸ https://en.wikipedia.org/wiki/Sympathetic_nervous_system.

¹⁹ https://en.wikipedia.org/wiki/Parasympathetic_nervous_system.

nervous system.²⁰ While the parasympathetic nervous system is primarily responsible for promoting blood flow to the genital area (facilitating an erection), the sympathetic system can modulate the physical expressions of arousal and prepare the body for orgasm. The autonomic nervous system adjusts heart rate, blood pressure, and respiratory rate, preparing the body for sexual activity, often manifesting as increased heart rate, flushed skin and pupil dilation. The hypothalamus,²¹ crucial for regulating hormonal and autonomic responses, becomes activated. The hypothalamus communicates with the pituitary gland and other parts of the nervous system to initiate physiological responses, including the release of neurotransmitters such as dopamine²² (which enhances sexual pleasure and desire) and serotonin²³ (modulating mood and arousal levels). Sexual desire often coincides with improved mood states, heightened energy, and a general sense of well-being, influenced by the above neurotransmitters. Thyroid hormones²⁴ also influence mood, energy levels, and overall metabolic rate, all of which can indirectly affect erectile function. These biochemicals affect both the brain and the peripheral nervous system.²⁵

The hypothalamus also triggers the release of hormones from the testes, enhancing libido and sexual function. Testosterone²⁶ is the primary male sex hormone and plays a pivotal role in modulating libido and sexual desire, which are crucial for initiating the neural processes that lead to an erection. Testosterone acts on the brain, influencing the limbic system which is involved in emotion and mood regulation. Higher levels of testosterone are generally associated with increased sexual desire. (Testosterone also affects the structural integrity of penile tissue and the function of nitric oxide synthase, the enzyme responsible for producing nitric oxide in the penis.) Gonadotropins²⁷ (luteinizing hormone or LH, and follicle-stimulating hormone, or FSH) are involved in the regulation of testosterone production by the testes. LH stimulates the Leydig cells in the testes to produce testosterone, which is necessary for normal erectile function. Oxytocin,²⁸ aka. the “love hormone,” is apparently released only after orgasm in males, hence appears unrelated to initial male sexual arousal.

²⁰ The autonomic nervous system is a division of the nervous system that operates internal organs, smooth muscle and glands, and regulates unconscious activities and bodily functions such as heart rate, digestion, respiratory rate, and sexual arousal; https://en.wikipedia.org/wiki/Autonomic_nervous_system.

²¹ <https://en.wikipedia.org/wiki/Hypothalamus>.

²² <https://en.wikipedia.org/wiki/Dopamine#Pleasure>.

²³ https://en.wikipedia.org/wiki/Serotonin#Biological_role.

²⁴ https://en.wikipedia.org/wiki/Thyroid_hormones.

²⁵ The peripheral nervous system consists of nerves and ganglia outside the brain and spinal cord that serves to connect the central nervous system (i.e., brain and spine) to the limbs and organs; https://en.wikipedia.org/wiki/Peripheral_nervous_system.

²⁶ <https://en.wikipedia.org/wiki/Testosterone>.

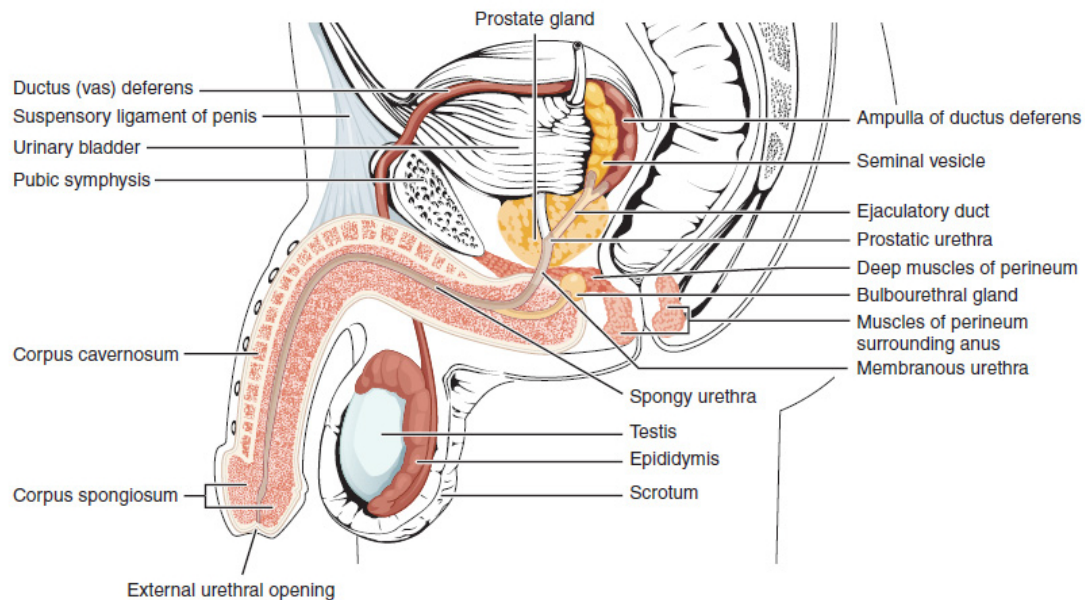
²⁷ <https://en.wikipedia.org/wiki/Gonadotropin>.

²⁸ <https://en.wikipedia.org/wiki/Oxytocin>.

2.2 Neural Initiation

Sexual arousal triggers the release of neurotransmitters from nerve endings in the human penis.²⁹ The primary neurotransmitter involved is **nitric oxide (NO)**,³⁰ which plays a crucial role in the relaxation of the smooth muscle cells within the corpora cavernosa (the bulk of the penis) during an erection. Several other neurotransmitters play important ancillary roles alongside nitric oxide, often with overlapping and regulatory roles that help initiate and maintain an erection, including acetylcholine (ACh),³¹ vasoactive intestinal peptide (VIP),³² and dopamine.³³

The nerve endings responsible for the release of neurotransmitters during sexual arousal are predominantly located in the corpus cavernosum and the corpus spongiosum, two key structures within the penis (image, below).³⁴



²⁹ https://en.wikipedia.org/wiki/Human_penis.

³⁰ https://en.wikipedia.org/wiki/Biological_functions_of_nitric_oxide#Vasodilation_and_smooth_muscles.

³¹ Released from parasympathetic nerve endings, acetylcholine also contributes to the relaxation of penile smooth muscle. It can act on endothelial cells to promote the production of NO and on smooth muscle cells directly through muscarinic receptors;
https://en.wikipedia.org/wiki/Acetylcholine#Direct_vascular_effects.

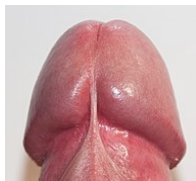
³² Vasoactive intestinal peptide (https://en.wikipedia.org/wiki/Vasoactive_intestinal_peptide) is a neuropeptide that is co-released with acetylcholine from parasympathetic nerves. VIP has a potent vasodilatory effect on the penile arteries and facilitates increased blood flow into the corpora cavernosa.

³³ Released from nerves within the penis, dopamine can enhance the erection process by its action on specific dopamine receptors, which promotes smooth muscle relaxation and vasodilation.

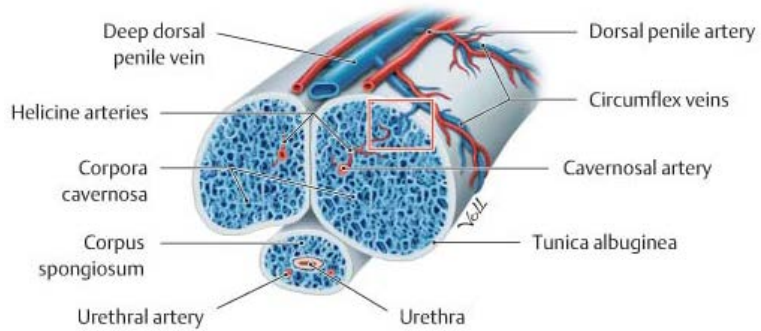
³⁴ https://en.wikipedia.org/wiki/Human_penis#/media/File:Penis_lateral_cross_section.jpg.

The **corpus cavernosum**³⁵ is a pair of cylindrical, sponge-like regions that runs along the length of the penis near the top (image, right).³⁶ They house a large proportion of the autonomic nerves that initiate erections by releasing neurotransmitters like nitric oxide (NO) and acetylcholine, triggering the relaxation of

smooth muscle and increased blood flow necessary for an erection. The **corpus spongiosum**³⁷ is a single, spongy body that runs along the underside of the penis near the bottom, encompassing the urethra. It contains nerves that are important for the modulation of the erection and also



ensures that the urethra is kept open during an erection for the passage of semen and urine. Nerve endings in the **glans penis** (image, left)³⁸ are primarily sensory nerves involved in sexual pleasure and arousal feedback, but they also contribute to the overall erectile response by communicating sensory information to the central nervous system, which then modulates the autonomic output to the penis. The dorsal nerve of the penis,³⁹ a branch of the pudendal nerve, runs along the dorsal (top) side of the organ and is primarily responsible for sensory innervation but also carries some autonomic fibers that contribute to the erectile process.



The autonomic nerves in these regions are crucial for the vascular changes that lead to an erection. They are intricately linked with both sensory and motor functions, creating a feedback loop between arousal and physical erectile response. These nerves facilitate the release of neurotransmitters directly into the tissues of the corpus cavernosum and corpus spongiosum, initiating the biochemical processes that result in an erection.

2.3 Vascular Response

The smooth muscle cells in the penis are normally contracted, restricting the flow of blood into the organ to just a trickle. The release of neurotransmitters into the corpus cavernosum and the corpus spongiosum ([Section 2.2](#)) in response to sexual arousal ([Section 2.1](#)) provokes an immediate vascular response.

The neuronal enzyme nitric oxide synthase (nNOS)⁴⁰ in the nerve endings of the penis is initially activated, producing NO that is released immediately, diffuses, and acts directly on the smooth muscle cells within the corpora cavernosa. The diffused NO activates guanylate cyclase,⁴¹ an

³⁵ https://en.wikipedia.org/wiki/Corpus_cavernosum_penis.

³⁶ <https://radiologykey.com/diseases-of-the-penis-with-functional-evaluation/>.

³⁷ [https://en.wikipedia.org/wiki/Corpus_spongiosum_\(penis\)](https://en.wikipedia.org/wiki/Corpus_spongiosum_(penis)).

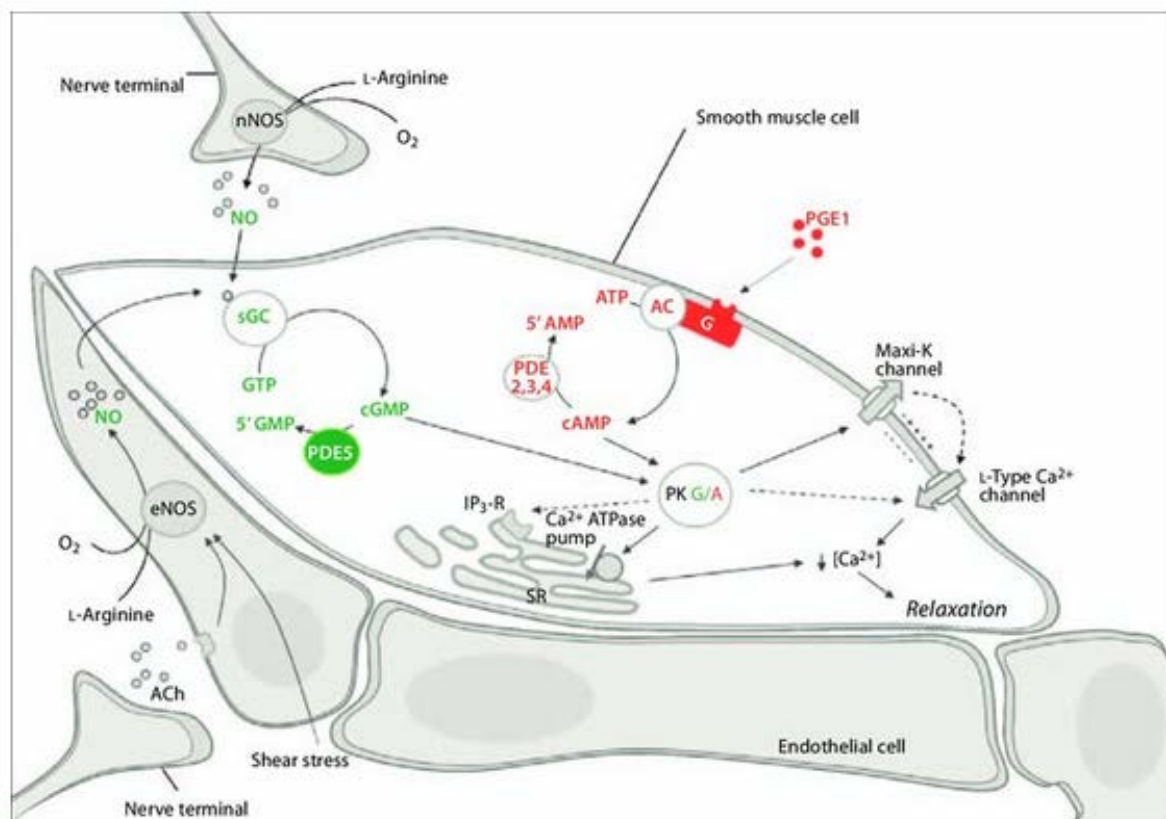
³⁸ https://en.wikipedia.org/wiki/Glans_penis.

³⁹ https://en.wikipedia.org/wiki/Dorsal_nerve_of_the_penis.

⁴⁰ https://en.wikipedia.org/wiki/Nitric_oxide_synthase#nNOS.

⁴¹ https://en.wikipedia.org/wiki/Guanylate_cyclase.

enzyme that produces cyclic guanosine monophosphate (cGMP)⁴² in the smooth muscle cells. This secondary messenger causes the smooth muscle cells to relax,⁴³ allowing for the initial dilation of penile arteries and an increase in blood flow into the corpora cavernosa of the penis. The enhanced blood flow and shear stress on the vessel walls resulting from initial vasodilation⁴⁴ also stimulates the endothelial cells lining the blood vessels of the penis to produce more NO via the endothelial nitric oxide synthase (eNOS) enzyme.⁴⁵ Once released, this additional NO diffuses into the smooth muscle cells in the walls of the blood vessels and the corpora cavernosa, further contributing to the relaxation of vascular smooth muscle cells, amplifying and sustaining the vasodilation initiated by neuronal NO (image, below).⁴⁶



⁴² https://en.wikipedia.org/wiki/Cyclic_guanosine_monophosphate.

⁴³ cGMP induces relaxation of smooth muscle cells by reducing intracellular calcium levels and modifying the phosphorylation state of key proteins involved in muscle contraction.

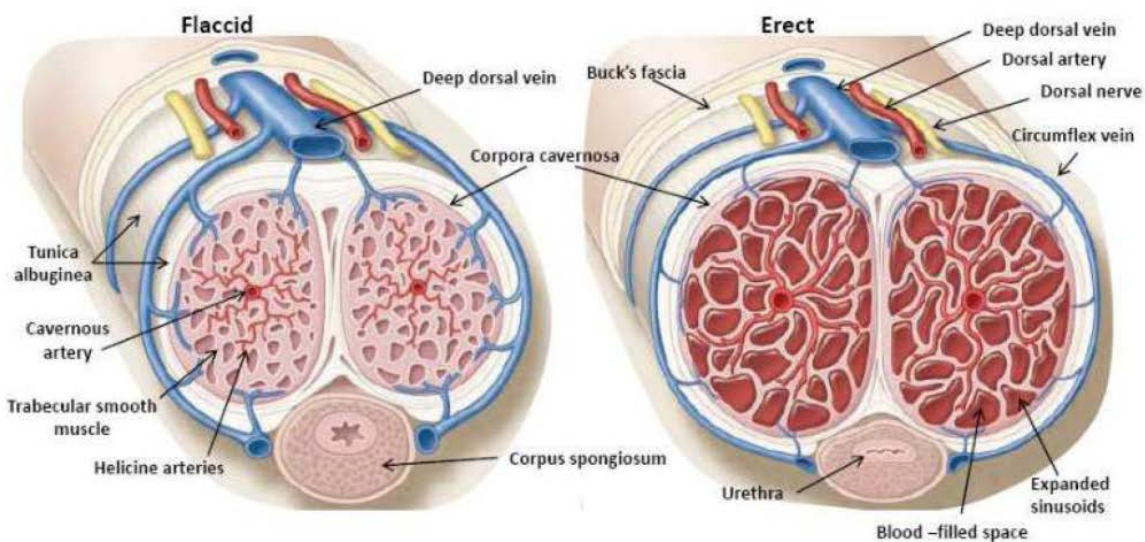
⁴⁴ https://en.wikipedia.org/wiki/Vasodilation#Smooth_muscle_physiology.

⁴⁵ https://en.wikipedia.org/wiki/Endothelial_NOS.

⁴⁶ Albersen M, Orabi H, Lue TF. Evaluation and treatment of erectile dysfunction in the aging male: a mini-review. Gerontology. 2012;58(1):3-14; <https://karger.com/Article/PDF/329598>.

The increase in blood flow itself can enhance endothelial NO production, creating a positive feedback loop that maintains vasodilation as long as sexual arousal continues. This ensures that the erection is not only initiated but also maintained until sexual activity concludes or arousal decreases. NO also directly inhibits platelet aggregation within the penile vasculature⁴⁷ – the NO diffuses into platelets and directly activates a signaling pathway that inhibits an internal calcium release needed for platelet activation and aggregation – helping to maintain a smooth and unrestricted blood flow during erection with no serious risk of blood clotting or coagulation.

The smooth muscle cells in the corpus cavernosum are an integral component of the penile architecture and play a crucial role in the erectile process. The smooth muscle cells are primarily located in the walls of the sinusoids within the corpora cavernosa. These cells are embedded within a framework of fibrous connective tissue and elastin, forming the trabeculae that separate individual sinusoidal spaces. During an erection, the relaxation of these smooth muscle cells, mediated by nitric oxide and other vasodilators, allows the sinusoids to fill with blood, expanding the corpora cavernosa and compressing the vessels carrying the venous outflow (images, below).⁴⁸



The helicine arteries, which are responsible for delivering blood directly into the sinusoids, are also surrounded by smooth muscle cells. These smooth muscle cells help regulate the flow of blood into the sinusoids by contracting or relaxing, which controls the diameter and thus the blood flow rate through these arteries. During sexual arousal, the relaxation of the smooth muscle cells in the helicine arteries facilitates increased blood flow into the sinusoids, essential for achieving an erection.

⁴⁷ Moncada S. Nitric oxide: discovery and impact on clinical medicine. *J R Soc Med.* 1999 Apr;92(4):164-9; <https://www.ncbi.nlm.nih.gov/pmc/articles/PMC1297136/pdf>.

⁴⁸ Nunes KP, Webb RC. Mechanisms in Erectile Function and Dysfunction: An Overview. In: Kenia Nunes, ed. *Erectile Dysfunction – Disease-Associated Mechanisms and Novel Insights into Therapy*. InTech, Feb 2012; https://openresearchlibrary.org/ext/api/media/68138c9b-5617-4453-989f-98924609d424/assets/external_content.pdf.

Endothelial cells form the inner lining (luminal wall) of all blood vessels, including the helicine arteries and the sinusoids. In the helicine arteries, endothelial cells are crucial for producing nitric oxide in response to shear stress and other stimuli, which then acts on the smooth muscle cells to induce relaxation. Within the sinusoids, endothelial cells contribute to the regulation of blood flow and the permeability of the sinusoidal walls, affecting the filling and emptying of these spaces.

2.4 Blood Flow Increase

As the penile smooth muscles relax, the arteries and arterioles dilate, leading to an increased flow of blood into the spongy erectile tissues of the penis. This blood flow is primarily into the corpora cavernosa, the two cylindrical structures that run the length of the penis. In the flaccid state, the steady-state blood flow to the penis is relatively low, about 2-5 cm³/min, sufficient to provide oxygen and nutrients to the penile tissues. During the erection process lasting perhaps ~20-200 sec for stress-free healthy young males, blood flow increases dramatically to as much as 50-120 cm³/min,⁴⁹ due to the relaxation of the smooth muscles in the corpora cavernosa and the dilation of the penile arteries. These rates are highly dependent on individual factors such as age, overall cardiovascular health, and the extent of sexual arousal.

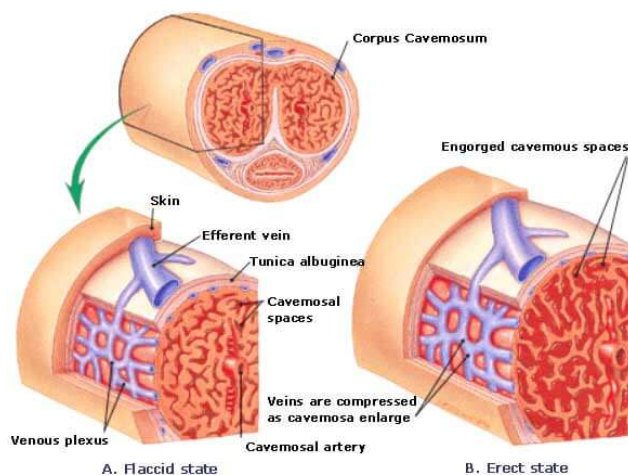
The corpus spongiosum that surrounds the urethra and runs along the underside of the penis also fills with blood during an erection, though its vascular capacity and the amount of blood it receives are less than that of the corpora cavernosa. The corpus spongiosum ensures that the urethra remains open during an erection, allowing for the passage of semen during ejaculation. The glans penis (the tip of the penis, an expanded part of the corpus spongiosum) also receives increased blood flow, contributing to the sensitivity of the glans and enhancing sexual pleasure. The corpus spongiosum and the glans probably account for 20-30% of the penile volume during an erection, compared to 70-80% for the corpora cavernosa.

The dorsal (topmost) arteries of the penis supply the skin and other tissues of the penis with blood. These arteries and the corresponding veins experience increased blood flow during an erection, contributing to the overall engorgement and rigidity of the penis.

⁴⁹ e.g., Engel G, Burnham SJ, Carter MF. Penile blood pressure in the evaluation of erectile impotence. *Fertil Steril*. 1978 Dec;30(6):687-90; <https://www.sciencedirect.com/science/article/pii/S0015028216436976/pdf>. Simonsen U, García-Sacristán A, Prieto D. Penile arteries and erection. *J Vasc Res*. 2002 Jul-Aug;39(4):283-303 ; <https://pubmed.ncbi.nlm.nih.gov/12187119/>. Ma M, Yu B, Qin F, Yuan J. Current approaches to the diagnosis of vascular erectile dysfunction. *Transl Androl Urol*. 2020 Apr;9(2):709-721; <https://www.ncbi.nlm.nih.gov/pmc/articles/PMC7215019/pdf>.

2.5 Pressure and Expansion

The blood outflow from the flaccid penis is relatively unimpeded. The veins are in an uncompressed state, allowing for the free return of blood to the systemic circulation, with the rate of blood outflow essentially matching the inflow rate to maintain tissue oxygenation and nutrient supply without engorgement. During an erection, the corpora cavernosa expand due to the increased arterial inflow (images, right).⁵⁰ The surrounding tunica albuginea⁵¹ compresses the subtunical venules against the firm fibrous tissue of the tunica albuginea (a fibrous sheath



surrounding the corpora cavernosa), significantly reducing the venous outflow and trapping the blood within the corpora cavernosa. This venous compression reduces blood outflow and maintains the erection. The venous outflow rate decreases significantly, although not completely to zero, as some blood flow is necessary to maintain tissue viability and prevent ischemia. The rate of outflow can decrease by as much as 70-90% compared to the inflow rate, depending on the degree of venous compression and the efficiency of the veno-occlusive mechanism.

The blood pressure within the corpora cavernosa varies significantly between the flaccid and erect states of the penis. In the flaccid state, when there is no sexual arousal and blood flow is minimal at around 2-5 cm³/min, the blood pressure in the corpora cavernosa is roughly equivalent to systemic venous pressure, typically in the range of 10-20 mmHg which is just enough to maintain sufficient blood flow to supply oxygen and nutrients to the penile tissue. When sexual arousal occurs and the corpora cavernosa fill with blood due to venous compression, the intracavernosal pressure (ICP) rises sharply. An ICP of 90 mmHg is the starting point for erection of the penile shaft,⁵² but the pressure in the corpora cavernosa typically rises to ~100 mmHg and ~35 mmHg in the corpus spongiosum, sometimes matching or even exceeding normal systolic systemic blood pressure ($p_{\text{erect}} \sim 120$ mmHg) during the peak of sexual arousal and rigidity.⁵³

⁵⁰ <https://diabetesindia.com/diabetes-causes-preventions/medical-cme/erectile-dysfunction-doctor/penile-erection-doctor.html>.

⁵¹ The tunica albuginea is the fibrous envelope that extends the length of the corpus cavernosum and the corpus spongiosum in the penis; [https://en.wikipedia.org/wiki/Tunica_albuginea_\(penis\)](https://en.wikipedia.org/wiki/Tunica_albuginea_(penis)).

⁵² Hsu GL, Hung YP, Tsai MH, Chang HC, Liu SP, Molodysky E, Hsu MC. The venous drainage of the corpora cavernosa in the human penis. Arab J Urol. 2013 Dec;11(4):384-91; <https://www.ncbi.nlm.nih.gov/pmc/articles/pmid/26558109/>.

⁵³ Pamchatsharam PK, Durland J, Zito PM. Physiology, Erection. StatPearls [Internet], 2023 May 1; <https://www.ncbi.nlm.nih.gov/books/NBK513278/>.

Penile volume before and after erection varies widely among individuals, but average values have been compiled.⁵⁴ An average flaccid penis that is $L_{\text{flaccid}} \sim 9.2$ cm in length and $D_{\text{flaccid}} \sim 3$ cm in diameter would have an ideal cylindrical volume of $V_{\text{flaccid}} = (\pi/4) D_{\text{flaccid}}^2 L_{\text{flaccid}} \sim 64 \text{ cm}^3$, whereas an erect penis that is $L_{\text{erect}} \sim 13.1$ cm in length and $D_{\text{erect}} \sim 3.7$ cm in diameter would have an ideal cylindrical volume of $V_{\text{erect}} = (\pi/4) D_{\text{erect}}^2 L_{\text{erect}} \sim 141 \text{ cm}^3$. The average erection angle of men aged 21-67 years is about 60° as measured downward from a vertical position pressed against the abdomen (table, right).⁵⁵ For the curious, the record length of the world's longest (functional) erect penis is 34 cm,⁵⁶ but its sexual employment would risk causing pain during male/female intercourse because the average length of the stretched (sexually aroused) vagina is only $\sim 13 \pm 3$ cm.⁵⁷

Occurrence of erection angles

Angle ($^\circ$) from vertically upwards	Percent of males
0–30	4.9
30–60	29.6
60–85	30.9
85–95	9.9
95–120	19.8
120–180	4.9

2.6 Maintenance of Erection and Detumescence

To prolong the erection, continued sexual stimulation and ongoing neural signaling are necessary to sustain NO release and maintain high cGMP levels in smooth muscle cells, keeping them relaxed.⁵⁸ Phosphodiesterase type 5 (PDE5),⁵⁹ an enzyme present in those cells, gradually degrades cGMP, reducing the concentration of this second messenger molecule⁶⁰ and leading to detumescence (i.e., return to the flaccid state) within minutes after ejaculation or when sexual arousal diminishes.

Detumescence is initiated by the cessation of neural inputs that promote erection. During sexual arousal, parasympathetic⁶¹ nervous activity induces the release of nitric oxide, which relaxes the smooth muscle in the arterial walls, leading to increased blood flow into the penile tissues. Detumescence begins when sympathetic⁶² nervous activity predominates, causing a reduction in arterial blood flow to the penis and an increase in venous outflow. The primary vascular change in detumescence is the contraction of penile smooth muscle cells. This contraction reduces the diameter of the arterioles and the cavernosal spaces within the penis, decreasing the inflow of

⁵⁴ Veale D, Miles S, Bramley S, Muir G, Hodsoll J. Am I normal? A systematic review and construction of nomograms for flaccid and erect penis length and circumference in up to 15,521 men. BJU Int. 2015 Jun;115(6):978-86; <https://pubmed.ncbi.nlm.nih.gov/25487360/>. See also: https://en.wikipedia.org/wiki/Human_penis_size.

⁵⁵ Sparling J. Penile erections: shape, angle, and length. J Sex Marital Ther. 1997 Fall;23(3):195-207; <https://pubmed.ncbi.nlm.nih.gov/9292834/>.

⁵⁶ https://en.wikipedia.org/wiki/Jonah_Falcon.

⁵⁷ https://en.wikipedia.org/wiki/Penile-vaginal_intercourse#Injury_risks.

⁵⁸ https://en.wikipedia.org/wiki/Smooth_muscle#Relaxation.

⁵⁹ https://en.wikipedia.org/wiki/CGMP-specific_phosphodiesterase_type_5.

⁶⁰ https://en.wikipedia.org/wiki/Second_messenger_system.

⁶¹ “feed and breed response”; https://en.wikipedia.org/wiki/Parasympathetic_nervous_system.

⁶² “fight or flight response”; https://en.wikipedia.org/wiki/Sympathetic_nervous_system.

blood while increasing the venous outflow. The sinusoids of the corpora cavernosa, which had been engorged with blood to maintain erection, empty as the blood drains away.

Following ejaculation, a refractory period⁶³ ensues during which further erection is inhibited in most, but not all,⁶⁴ men. During this time, the penis returns to its flaccid state and physiological systems stabilize to pre-arousal conditions. The refractory period varies among individuals and increases with age, ranging from ~15 minutes for 18-year-old males to ~20 hours for males in their 70s, with ~30 minutes average for all men.⁶⁵

Failure to detumesce after sex is called priapism.⁶⁶ In this condition, the penis remains erect for hours after all sexual activity or arousal has ended. Most cases involve painful ischemic (low-flow) priapism, in which most of the penis remains hard because blood does not adequately drain from the tissues. Treatment usually involves administering a nerve block to the penis followed by aspiration of blood from the corpora cavernosa.⁶⁷ Priapism is considered a medical emergency because of the increased risk of permanent scarring of the penis after four hours and the near-certainty of scarring after 48 hours.

⁶³ Seizert CA. The neurobiology of the male sexual refractory period. *Neurosci Biobehav Rev.* 2018 Sep;92:350-377; <https://pubmed.ncbi.nlm.nih.gov/29940235/>.

⁶⁴ Whipple B, Myers BR, Komisaruk BR. Male multiple ejaculatory orgasms: a case study. *J Sex Educ and Therapy* 1998; 23(2):157-162; <https://www.tandfonline.com/doi/abs/10.1080/01614576.1998.11074222>.
Haake P, Exton MS, Haverkamp J, Krämer M, Leygraf N, Hartmann U, Schedlowski M, Krueger TH. Absence of orgasm-induced prolactin secretion in a healthy multi-orgasmic male subject. *Int J Impot Res.* 2002 Apr;14(2):133-5; <https://pubmed.ncbi.nlm.nih.gov/11979330/>.

⁶⁵ [https://en.wikipedia.org/wiki/Refractory_period_\(sex\)](https://en.wikipedia.org/wiki/Refractory_period_(sex)).

⁶⁶ <https://en.wikipedia.org/wiki/Priapism>.

⁶⁷ Podolej GS, Babcock C. Emergency Department Management Of Priapism. *Emerg Med Pract.* 2017 Jan;19(1):1-16; <https://pubmed.ncbi.nlm.nih.gov/28027457/>.

3. How Erectile Dysfunction Occurs

Disruptions in the erectile function pathway, causing erectile dysfunction, can occur due to vascular impairments ([Section 3.1](#)), neurological disorders ([Section 3.2](#)), hormonal imbalances ([Section 3.3](#)), enzymatic abnormalities ([Section 3.4](#)), pelvic muscle weakness ([Section 3.5](#)), psychological disorders ([Section 3.6](#)), various co-morbidities each affecting the process differently ([Section 3.7](#)), and lifestyle choices ([Section 3.8](#)).

3.1 Impaired Blood Flow

Adequate blood flow through the cavernosal arteries is crucial for achieving and maintaining an erection. Conditions that lead to vascular insufficiency or damage, such as atherosclerosis,⁶⁸ hypertension,⁶⁹ and smoking, can reduce arterial blood flow to the penis. Indeed, atherosclerotic disease is estimated to account for 40% of ED in men over 50 years,⁷⁰ and ED is often viewed as a harbinger of future cardiovascular disease events.⁷¹ The reduced blood flow can prevent the sufficient filling of the corpora cavernosa that is essential for an erection. Endothelial dysfunction,⁷² often caused by diabetes and hypertension, compromises the ability of blood vessels to properly dilate, further inhibiting blood flow.

⁶⁸ Kloner RA, Speakman M. Erectile dysfunction and atherosclerosis. *Curr Atheroscler Rep.* 2002 Sep;4(5):397-401; <https://pubmed.ncbi.nlm.nih.gov/12162940/>. Sangiorgi G, Cereda A, Benedetto D, Bonanni M, Chiricolo G, Cota L, Martuscelli E, Greco F. Anatomy, Pathophysiology, Molecular Mechanisms, and Clinical Management of Erectile Dysfunction in Patients Affected by Coronary Artery Disease: A Review. *Biomedicines.* 2021 Apr 16;9(4):432; <https://www.ncbi.nlm.nih.gov/pmc/articles/PMC8074129/pdf>.

⁶⁹ Koroglu G, Kaya-Sezginer E, Yilmaz-Oral D, Gur S. Management of Erectile Dysfunction: An Under-Recognition of Hypertension. *Curr Pharm Des.* 2018;24(30):3506-3519; <https://pubmed.ncbi.nlm.nih.gov/30152279/>. de Oliveira AA, Nunes KP. Hypertension and Erectile Dysfunction: Breaking Down the Challenges. *Am J Hypertens.* 2021 Mar 11;34(2):134-142; <https://pubmed.ncbi.nlm.nih.gov/32866225/>.

⁷⁰ Wyllie MG. The underlying pathophysiology and causes of erectile dysfunction. *Clin Cornerstone.* 2005;7(1):19-27; <https://pubmed.ncbi.nlm.nih.gov/16156420/>.

⁷¹ Montorsi F, Briganti A, Salonia A, Rigatti P, Margonato A, Macchi A, Galli S, Ravagnani PM, Montorsi P. Erectile dysfunction prevalence, time of onset and association with risk factors in 300 consecutive patients with acute chest pain and angiographically documented coronary artery disease. *Eur Urol.* 2003 Sep;44(3):360-4; discussion 364-5; <https://pubmed.ncbi.nlm.nih.gov/12932937/>. Corona G, Rastrelli G, Isidori AM, Pivonello R, Bettocchi C, Reisman Y, Sforza A, Maggi M. Erectile dysfunction and cardiovascular risk: a review of current findings. *Expert Rev Cardiovasc Ther.* 2020 Mar;18(3):155-164; https://edisciplinas.usp.br/pluginfile.php/5317149/mod_resource/content/1/14.1..pdf.

⁷² De Leonardis F, Colalillo G, Finazzi Agrò E, Miano R, Fuschi A, Asimakopoulos AD. Endothelial Dysfunction, Erectile Deficit and Cardiovascular Disease: An Overview of the Pathogenetic Links. *Biomedicines.* 2022 Aug 1;10(8):1848; <https://www.ncbi.nlm.nih.gov/pmc/articles/PMC9405076/pdf>.

Additionally, venous leakage,⁷³ also known as venogenic erectile dysfunction, penile venous insufficiency, or veno-occlusive dysfunction, refers to a condition where the veins of the penis are unable to properly restrict the outflow of blood during an erection in order to trap blood within the penile corpora cavernosa.⁷⁴ Possible causes include:

Structural Abnormalities: The connective tissue of the tunica albuginea⁷⁵ might be defective or damaged, which can prevent it from adequately compressing the venous plexuses, most importantly the deep dorsal vein of the penis, a pair of cavernosal veins, and two pairs of para-arterial veins between the Buck's fascia⁷⁶ and the tunica albuginea. This scenario can arise from congenital defects, Peyronie's disease⁷⁷ (which causes fibrous scar tissue), or trauma to the penis.

Failure of Smooth Muscle to Relax: If the smooth muscle within the corpora cavernosa fails to relax fully, the pressure needed to compress the subtunical venular plexuses adequately might not be achieved. This issue can be exacerbated by underlying conditions such as diabetes or high cholesterol, which can cause endothelial dysfunction and impaired nitric oxide signaling.

Venous Structural Defects: Anomalies in the venous anatomy itself, such as the presence of excessive or aberrant venous channels that should not be there, can also prevent proper venous occlusion. Surgical intervention might involve ligation or embolization of the leaking veins.

3.2 Neurological Disorders

Normal erectile function relies on an intact neural pathway from the brain and spinal cord to the penile tissues. Neurological disorders such as Parkinson's disease,⁷⁸ multiple sclerosis,⁷⁹

⁷³ https://en.wikipedia.org/wiki/Venous_leak.

⁷⁴ Kaba R, Pearce I. Venous leak and erectile dysfunction – an important differential. J Clin Urology 2020; 13(1):33-39; <https://journals.sagepub.com/doi/full/10.1177/2051415819847318>.

⁷⁵ The tunica albuginea is the fibrous envelope that extends the length of the corpus cavernosum and the corpus spongiosum in the penis; [https://en.wikipedia.org/wiki/Tunica_albuginea_\(penis\)](https://en.wikipedia.org/wiki/Tunica_albuginea_(penis)).

⁷⁶ https://en.wikipedia.org/wiki/Buck%27s_fascia.

⁷⁷ https://en.wikipedia.org/wiki/Peyronie%27s_disease.

⁷⁸ Bronner G, Vodušek DB. Management of sexual dysfunction in Parkinson's disease. Ther Adv Neurol Disord. 2011 Nov;4(6):375-83; <https://www.ncbi.nlm.nih.gov/pmc/articles/PMC3229252/pdf>. Shalash A, Hamid E, Elrassas H, Abushouk AI, Salem HH. Sexual dysfunction in male patients with Parkinson's disease: related factors and impact on quality of life. Neurol Sci. 2020 Aug;41(8):2201-2206; <https://pubmed.ncbi.nlm.nih.gov/32172403/>. Vafaeimastanabad M, Salemi MH, Jodki T, Sabri V, Talab EK, Babaei FN, Manesh SE, Emami D. Sexual dysfunction among patients with Parkinson's disease: A systematic review and meta-analysis. J Clin Neurosci. 2023 Nov;117:1-10; <https://pubmed.ncbi.nlm.nih.gov/37717275/>.

stroke,⁸⁰ and spinal cord injuries⁸¹ can interrupt this pathway. Damage or degeneration of nerves can impair the transmission of signals necessary to initiate the release of nitric oxide, thus preventing the relaxation of smooth muscle in the corpora cavernosa. Erectile impairment following radical prostate cancer surgery is thought to be due to the damage to the cavernous nerves, aka. neuropraxia.⁸² The incidence of iatrogenic impotence from various procedures has been reported as 43% to 100% following radical prostatectomy, 29% after perineal prostatectomy for benign disease, 15% to 100% after abdominal perineal resection, and 2% to 49% after external sphincterotomy at the 3- and 9-o'clock positions.⁸³ Additionally, peripheral neuropathy⁸⁴ and neuropathies secondary to diabetes mellitus⁸⁵ often damage the peripheral nerves involved in

⁷⁹ Kirkeby HJ, Poulsen EU, Petersen T, Dørup J. Erectile dysfunction in multiple sclerosis. *Neurology*. 1988 Sep;38(9):1366-71 ; <https://pubmed.ncbi.nlm.nih.gov/3412584/>. Betts CD, Jones SJ, Fowler CG, Fowler CJ. Erectile dysfunction in multiple sclerosis. Associated neurological and neurophysiological deficits, and treatment of the condition. *Brain*. 1994 Dec;117 (Pt 6):1303-10 ; <https://citeseerx.ist.psu.edu/document?repid=rep1&type=pdf&doi=a3a48e4f3be95375abdc48047eccfb364e4cd3>. Landtblom AM. Treatment of erectile dysfunction in multiple sclerosis. *Expert Rev Neurother*. 2006 Jun;6(6):931-5 ; <https://pubmed.ncbi.nlm.nih.gov/16784415/>. Shaygannejad V, Mirmosayyeb O, Vaheb S, Nehzat N, Ghajarzadeh M. The prevalence of sexual dysfunction and erectile dysfunction in men with multiple sclerosis: A systematic review and meta-analysis. *Neurologia (Engl Ed)*. 2022 Aug 10:S2173-5808(22)00088-8; <https://pubmed.ncbi.nlm.nih.gov/35963537/>.

⁸⁰ Zhao S, Wu W, Wu P, Ding C, Xiao B, Xu Z, Hu Y, Shen M, Feng L. Significant Increase of Erectile Dysfunction in Men With Post-stroke: A Comprehensive Review. *Front Neurol*. 2021 Jul 28;12:671738; <https://www.ncbi.nlm.nih.gov/pmc/articles/PMC8355431/pdf>. Calabrò RS. Post-stroke Sexual Dysfunction in Men: Epidemiology, Diagnostic Work-up, and Treatment. *Innov Clin Neurosci*. 2022 Jul-Sep;19(7-9):12-16; https://www.ncbi.nlm.nih.gov/pmc/articles/PMC9507142/pdf/icns_19_7-9_12.pdf.

⁸¹ Barbonetti A, DAndrea S, Castellini C, Totaro M, Muselli M, Cavallo F, Felzani G, Necozone S, Francavilla S. Erectile Dysfunction Is the Main Correlate of Depression in Men with Chronic Spinal Cord Injury. *J Clin Med*. 2021 May 13;10(10):2090; <https://www.ncbi.nlm.nih.gov/pmc/articles/PMC8152485/pdf>. Di Bello F, *et al.* Male Sexual Dysfunction and Infertility in Spinal Cord Injury Patients: State-of-the-Art and Future Perspectives. *J Pers Med*. 2022 May 26;12(6):873; <https://www.ncbi.nlm.nih.gov/pmc/articles/PMC9225464/pdf>.

⁸² Burnett AL. Rationale for cavernous nerve restorative therapy to preserve erectile function after radical prostatectomy. *Urology*. 2003 Mar;61(3):491-7; <https://pubmed.ncbi.nlm.nih.gov/12639630/>.

⁸³ Dean RC, Lue TF. Physiology of penile erection and pathophysiology of erectile dysfunction. *Urol Clin North Am*. 2005 Nov;32(4):379-95; <https://www.ncbi.nlm.nih.gov/pmc/articles/PMC1351051/pdf>.

⁸⁴ Hicks CW, Wang D, Windham BG, Selvin E. Association of Peripheral Neuropathy with Erectile Dysfunction in US Men. *Am J Med*. 2021 Feb;134(2):282-284; <https://www.ncbi.nlm.nih.gov/pmc/articles/PMC7870518/pdf>.

⁸⁵ Agochukwu-Mmonu N, Pop-Busui R, Wessells H, Sarma AV. Autonomic neuropathy and urologic complications in diabetes. *Auton Neurosci*. 2020 Dec;229:102736; <https://www.ncbi.nlm.nih.gov/pmc/articles/PMC10248950/pdf>.

erection, resulting in decreased penile sensation and impaired neural input necessary for arousal. It has been estimated that 10-19% of ED is of neurogenic origin.⁸⁶

3.3 Hormonal Imbalances

Hormones play a significant role in regulating sexual function, with testosterone⁸⁷ being particularly critical for libido and erectile function. Testosterone is primarily produced in the Leydig cells of the testes, with smaller amounts produced in the adrenal glands located above the kidneys. Low levels of testosterone, a condition known as hypogonadism,⁸⁸ can diminish libido and reduce erectile function via diminished NO production and endothelial dysfunction (impairing the blood vessels ability to dilate). Low levels can lead to depression,⁸⁹ anxiety, insomnia, mood disturbances, and decreased cognitive function, which in turn can negatively affect sexual performance. Chronic low testosterone can also lead to structural changes in the penile tissues, including the loss of penile muscle mass and increased fibrosis.⁹⁰ The decrease in testosterone can be due to testicular failure, hypothalamic-pituitary axis disorders, or age-related decline.

Hormonal imbalances involving the thyroid and adrenal glands can also influence erectile function. For example, hyperthyroidism or hypothyroidism can alter metabolic and cardiovascular functions, impacting the mechanisms responsible for erection.⁹¹

⁸⁶ Abicht J. Testing the autonomic system. In: Jonas U, Thoh W, Steif C, eds. *Erectile Dysfunction*. SpringerVerlag, Berlin, 1991, pp. 187-194; <https://www.amazon.com/Erectile-Dysfunction-U-Jonas/dp/0387527486>. Aboseif S, Shinohara K, Borirakchanyavat S, Deirmenjian J, Carroll PR. The effect of cryosurgical ablation of the prostate on erectile function. *Br J Urol*. 1997 Dec;80(6):918-22; <https://pubmed.ncbi.nlm.nih.gov/9439410/>.

⁸⁷ <https://en.wikipedia.org/wiki/Testosterone>.

⁸⁸ <https://en.wikipedia.org/wiki/Hypogonadism>.

⁸⁹ Indirli R, Lanzi V, Arosio M, Mantovani G, Ferrante E. The association of hypogonadism with depression and its treatments. *Front Endocrinol (Lausanne)*. 2023 Aug 10;14:1198437; <https://www.ncbi.nlm.nih.gov/pmc/articles/PMC10449581/pdf>.

⁹⁰ Iacono F, Prezioso D, Ruffo A, Illiano E, Romis L, Di Lauro G, Romeo G, Amato B. Testosterone deficiency causes penile fibrosis and organic erectile dysfunction in aging men. Evaluating association among Age, TDS and ED. *BMC Surg*. 2012;12 Suppl 1(Suppl 1):S24; <https://www.ncbi.nlm.nih.gov/pmc/articles/PMC3499353/pdf>.

⁹¹ Bates JN, Kohn TP, Pastuszak AW. Effect of Thyroid Hormone Derangements on Sexual Function in Men and Women. *Sex Med Rev*. 2020 Apr;8(2):217-230; <https://www.ncbi.nlm.nih.gov/pmc/articles/PMC6525090/pdf>.

3.4 Enzymatic Abnormalities

The presence of phosphodiesterase type 5 (PDE5) in the penis degrades cGMP (the second messenger that activates and maintains vasodilation),⁹² thus regulating the duration and magnitude of the erectile response. If PDE5 is overactive, it can break down cGMP at a faster rate than cGMP is produced. This rapid degradation of cGMP can lead to insufficient relaxation of the smooth muscle, thereby preventing adequate penile engorgement which leads to erectile dysfunction. Conditions such as diabetes mellitus⁹³ and hypertension⁹⁴ have been associated with increased expression or activity of PDE5.

3.5 Pelvic Muscle Weakness

The pelvic floor muscles play a important role in sexual function, including the maintenance and strength of an erection. In particular, the two **bulbocavernosus muscles**⁹⁵ (one on either side of the midline) assist in the compression of the penile veins, which helps to maintain the erection by limiting the outflow of blood from the penis. A weaker muscle may be less effective at this task, potentially reducing the rigidity and duration of erections. This muscle is also involved in the ejaculation process by contracting to expel semen. The **ischiocavernosus muscles**⁹⁶ also assist in the rigidity of the penis during an erection by compressing the base of the penile corpora cavernosa, thereby restricting venous outflow and maintaining the tumescence of the penis, working in tandem with the bulbocavernosus muscles to maintain erection and the force of ejaculation, functions that would be degraded if the muscles were weak.

Other pelvic floor muscles contribute to erectile function and can impact the symptoms of erectile dysfunction (ED) if they are weakened, including the **pubococcygeus muscles**,⁹⁷ the **transverse perineal muscles**,⁹⁸ and the **external anal sphincter**.⁹⁹ Weakness in these pelvic floor muscles can lead to suboptimal control over the penile venous outflow, potentially resulting in difficulties

⁹² https://en.wikipedia.org/wiki/Cyclic_guanosine_monophosphate.

⁹³ Wang L, Chopp M, Szalad A, Liu Z, Bolz M, Alvarez FM, Lu M, Zhang L, Cui Y, Zhang RL, Zhang ZG. Phosphodiesterase-5 is a therapeutic target for peripheral neuropathy in diabetic mice. *Neuroscience*. 2011 Oct 13;193:399-410; <https://www.ncbi.nlm.nih.gov/pmc/articles/PMC3391742/pdf>.

⁹⁴ Black SM, Sanchez LS, Mata-Greenwood E, Bekker JM, Steinhorn RH, Fineman JR. sGC and PDE5 are elevated in lambs with increased pulmonary blood flow and pulmonary hypertension. *Am J Physiol Lung Cell Mol Physiol*. 2001 Nov;281(5):L1051-7; <https://journals.physiology.org/doi/epdf/10.1152/ajplung.2001.281.5.L1051>. Murray F, MacLean MR, Pyne NJ. Increased expression of the cGMP-inhibited cAMP-specific (PDE3) and cGMP binding cGMP-specific (PDE5) phosphodiesterases in models of pulmonary hypertension. *Br J Pharmacol*. 2002 Dec;137(8):1187-94; <https://www.ncbi.nlm.nih.gov/pmc/articles/PMC1573609/pdf>.

⁹⁵ https://en.wikipedia.org/wiki/Bulbospongiosus_muscle.

⁹⁶ https://en.wikipedia.org/wiki/Ischiocavernosus_muscle.

⁹⁷ https://en.wikipedia.org/wiki/Levator_anii#Pubococcygeus_muscle.

⁹⁸ https://en.wikipedia.org/wiki/Transverse_perineal_muscles.

⁹⁹ https://en.wikipedia.org/wiki/External_anal_sphincter.

maintaining an erection. Pelvic floor dysfunction can also lead to issues with the neurological feedback and vascular responses necessary for initiating and maintaining erections.

3.6 Psychological Disorders

Erectile dysfunction can be significantly influenced by psychological factors which are often interwoven with the physiological aspects of sexual function.¹⁰⁰ Psychological causes of ED generally involve conditions that affect mental health and emotional well-being, leading to difficulties with sexual arousal and performance. Common psychological contributors include anxiety, particularly performance anxiety where the fear of sexual failure leads to a self-fulfilling prophecy of dysfunction. Depression is another major factor, dampening sexual desire and interfering with neurochemical messages between the brain and the penis that are essential for erection. Stress, whether related to work, relationships, or other personal issues, can distract an individual and impede the focus necessary for initiating sexual responses. Psychological trauma and negative sexual experiences can lead to sexual aversions or psychological blocks that manifest as erectile problems.

3.7 Co-Morbidities

Erectile dysfunction is associated with a long list of co-morbid conditions that can affect or exacerbate the underlying mechanisms of ED, including:

(1) Cardiovascular Disease. ED and cardiovascular disease share common risk factors such as atherosclerosis, hypertension, hyperlipidemia, and smoking. The same endothelial dysfunction and reduced blood flow that contribute to heart disease can also impede the blood flow necessary for an erection, and ED can be an early marker of vascular disease.

(2) Diabetes Mellitus. High blood sugar levels associated with diabetes cause damage to small blood vessels and nerves throughout the body, including those in the penis, leading to impaired blood flow and nerve function crucial for achieving an erection.

(3) Obesity. Obesity contributes to ED through several mechanisms, including endothelial dysfunction, low-grade inflammation, and hormonal changes such as reduced testosterone levels which can impact libido and erectile function. Obesity is also a risk factor for diabetes and cardiovascular disease, further increasing the risk of ED.

(4) Neurological Disorders. Conditions such as Parkinson's disease, multiple sclerosis, and spinal cord injuries can impair the nerve signals necessary for initiating an erection, and

¹⁰⁰ Swindle RW, Cameron AE, Lockhart DC, Rosen RC. The psychological and interpersonal relationship scales: assessing psychological and relationship outcomes associated with erectile dysfunction and its treatment. Arch Sex Behav. 2004 Feb;33(1):19-30; <https://pubmed.ncbi.nlm.nih.gov/14739687/>. Rastrelli G, Maggi M. Erectile dysfunction in fit and healthy young men: psychological or pathological? Transl Androl Urol. 2017 Feb;6(1):79-90; <https://www.ncbi.nlm.nih.gov/pmc/articles/PMC5313296/pdf>.

peripheral nerve damage, as seen in diabetic neuropathy, can significantly impact erectile function.

(5) Enlarged Prostate. An enlarged prostate (aka. benign prostatic hyperplasia, or BPH) can influence the progression of ED due to several interconnected mechanisms:

(A) Shared Risk Factors: Both BPH and ED share common risk factors including age, diabetes, hypertension, and cardiovascular diseases – systemic conditions that can contribute to both prostate enlargement and the deterioration of erectile function.

(B) Urinary Symptoms and Lifestyle Impact: BPH often leads to lower urinary tract symptoms (LUTS), such as frequent urination, nocturia (nighttime urination), urinary urgency, and incomplete bladder emptying, which can significantly affect quality of life and sleep patterns, which in turn can reduce sexual desire and lead to ED. Chronic sleep deprivation and the stress of dealing with persistent urinary symptoms can also exacerbate psychological components of sexual dysfunction.

(C) Vascular and Neurological Factors: The mechanisms underlying BPH may also affect the vascular and neurological systems that are crucial for achieving and maintaining an erection. For instance, chronic inflammation, a factor in BPH, can also cause endothelial dysfunction in penile vessels, impacting erectile function. The prostate surrounds the urethra and is located near nerves and blood vessels that control erectile function, so enlargement of the prostate may exert pressure on these structures, potentially impairing their function.

(D) Medication Side Effects: Treatments for BPH, particularly certain medications such as alpha-blockers and 5-alpha-reductase inhibitors, can have side effects that include ED or other sexual dysfunction. For example, alpha-blockers can cause ejaculatory dysfunction and sometimes hypotension, which might indirectly affect sexual performance; 5-alpha-reductase inhibitors can decrease libido, ejaculate volume, and potentially cause ED directly by altering hormonal levels.

(6) Chronic Kidney Disease. Reduced kidney function is linked to changes in hormone levels, blood flow, and nerve function. Patients with kidney disease often experience various degrees of sexual dysfunction, including ED.

(7) Chronic Liver Disease. Liver cirrhosis and other liver diseases can lead to hormonal imbalances and changes in blood flow, both of which can contribute to ED.

(8) Sleep Disorders. Conditions like obstructive sleep apnea are associated with a higher prevalence of ED. Sleep apnea leads to poor oxygenation during sleep, which can cause physiological stresses on the body, including reduced testosterone levels and endothelial dysfunction.

3.8 Lifestyle Choices

Poor lifestyle choices can impact vascular, neurological, and hormonal systems essential for erectile function. The most important lifestyle contributors to erectile dysfunction may be

smoking.¹⁰¹ Tobacco use contributes to the development of atherosclerosis,¹⁰² a condition that narrows and hardens the arteries which may reduce blood flow to the penis. The toxic chemicals in cigarette smoke also damage the lining of blood vessels, impairing endothelial function which is crucial for the nitric oxide mediated dilation of blood vessels necessary for an erection.¹⁰³

The use of drugs such as amphetamines¹⁰⁴ and opiates¹⁰⁵ may have a detrimental effect on erectile function.¹⁰⁶ These substances can alter the central nervous systems response to sexual stimuli and impair the hormonal balance necessary for sexual function. The lifestyle associated with drug abuse, including psychological stress and poor general health, can further exacerbate erectile problems. The consumption of alcohol depresses the nervous system (impairing nerve sensitivity) and impairs cardiovascular function,¹⁰⁷ reducing the ability to increase blood flow that is needed to achieve and maintain an erection – although light to moderate alcohol consumption¹⁰⁸ may actually be beneficial for erectile function.¹⁰⁹

¹⁰¹ Verze P, Margreiter M, Esposito K, Montorsi P, Mulhall J. The Link Between Cigarette Smoking and Erectile Dysfunction: A Systematic Review. *Eur Urol Focus*. 2015 Aug;1(1):39-46; <https://pubmed.ncbi.nlm.nih.gov/28723353/>.

¹⁰² Ishida M, Sakai C, Kobayashi Y, Ishida T. Cigarette Smoking and Atherosclerotic Cardiovascular Disease. *J Atheroscler Thromb*. 2024 Mar 1;31(3):189-200; <https://www.ncbi.nlm.nih.gov/pmc/articles/PMC10918046/pdf>.

¹⁰³ Kovac JR, Labbate C, Ramasamy R, Tang D, Lipshultz LI. Effects of cigarette smoking on erectile dysfunction. *Andrologia*. 2015 Dec;47(10):1087-92; <https://www.ncbi.nlm.nih.gov/pmc/articles/PMC4485976/pdf>. Allen MS, Tostes RC. Cigarette smoking and erectile dysfunction: an updated review with a focus on pathophysiology, e-cigarettes, and smoking cessation. *Sexual Med Reviews* 2023 Jan; 11(1):61-73; <https://academic.oup.com/smr/article/11/1/61/6985842>.

¹⁰⁴ Chou NH, Huang YJ, Jiann BP. The Impact of Illicit Use of Amphetamine on Male Sexual Functions. *J Sex Med*. 2015 Aug;12(8):1694-702; <https://pubmed.ncbi.nlm.nih.gov/26147855/>.

¹⁰⁵ Zhao S, Deng T, Luo L, Wang J, Li E, Liu L, Li F, Luo J, Zhao Z. Association Between Opioid Use and Risk of Erectile Dysfunction: A Systematic Review and Meta-Analysis. *J Sex Med*. 2017 Oct;14(10):1209-1219; <https://pubmed.ncbi.nlm.nih.gov/28923307/>. Salata B, Kluczna A, Dzierżanowski T. Opioid-Induced Sexual Dysfunction in Cancer Patients. *Cancers (Basel)*. 2022 Aug 22;14(16):4046; <https://www.ncbi.nlm.nih.gov/pmc/articles/PMC9406921/pdf>.

¹⁰⁶ Sivaratnam L, Selimin DS, Abd Ghani SR, Nawi HM, Nawi AM. Behavior-Related Erectile Dysfunction: A Systematic Review and Meta-Analysis. *J Sex Med* 2021 Jan; 18(1):121-143; <https://academic.oup.com/jsm/article-abstract/18/1/121/6956083>.

¹⁰⁷ <https://www.healthline.com/health/alcohol-and-erectile-dysfunction>.

¹⁰⁸ Typically defined as consuming up to 14 standard drinks per week or no more than 4 drinks on any day for men.

¹⁰⁹ Li S, Song JM, Zhang K, Zhang CL. A Meta-Analysis of Erectile Dysfunction and Alcohol Consumption. *Urol Int*. 2021;105(11-12):969-985; <https://karger.com/uin/article/105/11-12/969/829299/>.

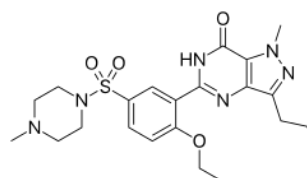
A diet high in processed and saturated fat and low in fruits and vegetables can contribute to high cholesterol levels, high blood pressure, and diabetes, all of which can impair blood flow to the penis. Physical inactivity also reduces cardiovascular health, makes weight management more difficult, and lowers overall energy levels, potentially further impeding sexual performance.

4. Conventional Treatments for Erectile Dysfunction

Conventional treatment strategies for the management of erectile dysfunction are primarily pharmacological and mechanical. They offer, at best, modest and temporary restoration of sexual function in some patients, though often accompanied by physical discomfort or undesirable side effects. Psychosexual counseling is often advocated to address psychological contributors in ED cases, while encouraging lifestyle changes such as weight management, cessation of smoking, and regular exercise¹¹⁰ that might improve overall cardiovascular health and ED outcomes.

4.1 PDE5 Inhibitors

Currently the frontline and perhaps the most effective treatments for the symptoms of ED are the oral pharmaceutical agents known as phosphodiesterase type 5 (PDE5) inhibitors,¹¹¹ including Viagra (sildenafil; image, right),¹¹² Cialis (tadalafil),¹¹³ Levitra (vardenafil),¹¹⁴ and Stendra (avanafil),¹¹⁵ all of which are available in pill form.¹¹⁶ These medications work by blocking the action of PDE5,¹¹⁷ thus increasing cGMP¹¹⁸ levels in the penis, thereby prolonging smooth muscle relaxation and improving blood flow to facilitate an erection. They offer symptomatic relief by enhancing erectile response to sexual stimulation through increased nitric oxide-mediated vasodilation¹¹⁹ in penile tissues (Section 2.3). These drugs do not directly initiate an erection. Rather, they interfere with the normal counter-erectile process in which PDE5 breaks down cGMP already present in the penis (because of nitric oxide that is also already present in the penis), precipitating flaccidity. These drugs have a very narrow window of operability. If any other aspect of the pro-erectile process is malfunctioning (e.g., if no nitric oxide or cGMP is being generated or delivered), these drugs will not reverse impotence. ED patients must have an intact molecular and nervous system pathway, as well as a degree of sexual stimulation, for the drugs to work. Furthermore, these medications can decline in effectiveness over many years of use and eventually stop producing erections altogether, due to the natural progression of underlying health issues such as diabetes, cardiovascular disease, or hypertension, which may eventually worsen the vascular or nerve functions necessary for an erection.



¹¹⁰ https://en.wikipedia.org/wiki/Kegel_exercise#Men.

¹¹¹ https://en.wikipedia.org/wiki/PDE5_inhibitor.

¹¹² <https://en.wikipedia.org/wiki/Sildenafil>.

¹¹³ <https://en.wikipedia.org/wiki/Tadalafil>.

¹¹⁴ <https://en.wikipedia.org/wiki/Vardenafil>.

¹¹⁵ <https://en.wikipedia.org/wiki/Avanafil>.

¹¹⁶ These drugs are generally safe and effective for most men suffering from ED but they can have unwanted side effects and interactions, particularly with certain cardiac medications.

¹¹⁷ https://en.wikipedia.org/wiki/CGMP-specific_phosphodiesterase_type_5.

¹¹⁸ https://en.wikipedia.org/wiki/Cyclic_guanosine_monophosphate.

¹¹⁹ https://en.wikipedia.org/wiki/Biological_functions_of_nitric_oxide#Vasodilation_and_smooth_muscles.

4.2 Intracavernosal Injections of Vasoactive Agents

Injections of vasoactive agents directly into the corpora cavernosa¹²⁰ via a hypodermic needle (ouch!)¹²¹ applied to the side of the penis is an uncomfortable alternative treatment for the symptoms of ED for patients who are unresponsive to the oral PDE5 inhibitors described in [Section 4.1](#). The three most common agents – alprostadil (prostaglandin E1)¹²² and papaverine (an opium alkaloid),¹²³ which facilitate cavernous smooth muscle relaxation, and phentolamine,¹²⁴ an alpha-adrenergic blocker that inhibits cavernous smooth muscle contraction – are vasodilators that open blood vessels and relax smooth muscle cells. Alprostadil is available alone as an injectable, but the three are often combined by a compounding pharmacy in a more effective “Trimix” formulation¹²⁵ with fewer side effects. Alternative mixes called “Bimix” (papaverine and phentolamine) or “Quadmix” (prostaglandin, papaverine, phentolamine, and atropine or forskolin) are sometimes used. When injected, these vasodilators produce tumescence within ~15 minutes, but sometimes with such common side effects as priapism, bruising, Peyronie’s disease, and pain. All will produce an erection even in the absence of sexual arousal or nitric oxide production in the penis.

As with PDE5 inhibitors, and for similar reasons, these injections can decline in effectiveness over many years of use. Repeated use of intracavernosal injections sometimes leads to fibrosis (scarring) of the penile tissue, affecting the erectile tissues ability to expand and contract, potentially further decreasing the effectiveness of the injections over time.

Alprostadil and papaverine are also available as a less-effective urethral suppository,¹²⁶ with a small pellet inserted through the tip of the penis into the urethra at least ten minutes before the erection is needed.¹²⁷ The most common side effect and cause of suppository discontinuation is penile or urethral pain.¹²⁸

¹²⁰ https://en.wikipedia.org/wiki/Intracavernous_injection.

¹²¹ Nelson CJ, Hsiao W, Balk E, Narus J, Tal R, Bennett NE, Mulhall JP. Injection anxiety and pain in men using intracavernosal injection therapy after radical pelvic surgery. *J Sex Med*. 2013 Oct;10(10):2559-65; <https://pubmed.ncbi.nlm.nih.gov/23898886/>.

¹²² https://en.wikipedia.org/wiki/Prostaglandin_E1.

¹²³ <https://en.wikipedia.org/wiki/Papaverine>.

¹²⁴ <https://en.wikipedia.org/wiki/Phentolamine>.

¹²⁵ Typically 20 µg alprostadil, 30 mg of papaverine, and 2 mg of phentolamine; https://en.wikipedia.org/wiki/Prostaglandin_E1#Sexual_dysfunction.

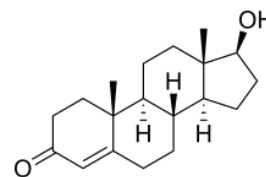
¹²⁶ <https://www.cancer.gov/publications/dictionaries/cancer-terms/def/medicated-urethral-system-for-erection>.

¹²⁷ https://en.wikipedia.org/wiki/Prostaglandin_E1#Sexual_dysfunction.

¹²⁸ Guay AT, Perez JB, Velásquez E, Newton RA, Jacobson JP. Clinical experience with intraurethral alprostadil (MUSE) in the treatment of men with erectile dysfunction. A retrospective study. Medicated urethral system for erection. *Eur Urol*. 2000 Dec;38(6):671-6; <https://pubmed.ncbi.nlm.nih.gov/11111182/>. Costa P, Potempa AJ. Intraurethral alprostadil for erectile dysfunction: a review of the literature. *Drugs*. 2012 Dec 3;72(17):2243-54; <https://pubmed.ncbi.nlm.nih.gov/23170913/>.

4.3 Testosterone Replacement Therapy

Testosterone (image, right)¹²⁹ plays a crucial role in regulating libido or sexual desire. Abnormally low levels of this hormone can result in decreased interest in sexual activity, making it more challenging to achieve and maintain an erection. The hormone influences mood, energy levels, and the overall sense of well-being, with low levels sometimes leading to depression, anxiety, and a reduced sense of vitality. Reduced testosterone levels can lead to reduced nitric oxide availability, directly impairing erectile function, and can also lead to physical changes that may indirectly affect erectile function such as increased body fat, reduced muscle mass, and changes in cholesterol metabolism which can influence cardiovascular health and blood flow. Low serum testosterone due to hypogonadism¹³⁰ is often treated with supplemental hormone available in oral, dermal gel, and many other forms,¹³¹ and in some cases may be treated with selective estrogen receptor modulators (SERMs) such as clomiphene, enclomiphene, and tamoxifen.¹³²



Testosterone supplementation carries numerous long-term risks which may include: (1) increased risk of cardiovascular events such as heart attacks and strokes; (2) higher levels of red blood cells (polycythemia) which can increase blood viscosity and the likelihood of thrombosis (blood clots); (3) growth of the prostate gland leading to benign prostatic hyperplasia (BPH) while exacerbating symptoms like urinary retention and difficulty urinating, and even growth of prostate cancer; (4) liver toxicity ranging from mild elevations in liver enzymes to more serious conditions like liver damage; (5) suppression of the body's natural hormone production, leading in the long-term to a reduction in sperm production and testicular shrinkage, potentially causing infertility; (6) acceleration of male pattern baldness in genetically predisposed men; and (7) mood swings, irritability, aggression, and gynecomastia (enlargement of breast tissue) in some individuals.

4.4 Penile Vibratory Stimulation (PVS)

PVS was first used to induce penile erection and ejaculation in men without spinal cord injury in 1965,¹³³ and the FDA approved the use of PVS for erectile dysfunction in 2011. Viberec (image, right) is an FDA



¹²⁹ <https://en.wikipedia.org/wiki/Testosterone>.

¹³⁰ <https://en.wikipedia.org/wiki/Hypogonadism#Men>.

¹³¹ https://en.wikipedia.org/wiki/Androgen_replacement_therapy#Males.

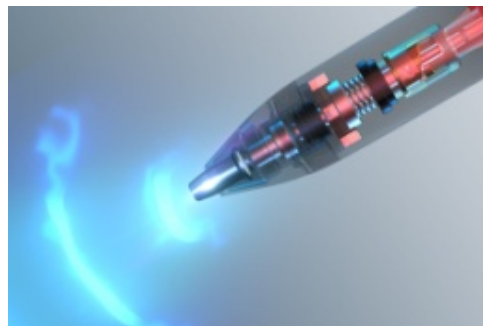
¹³² Khodamoradi K, Khosravizadeh Z, Parmar M, Kuchakulla M, Ramasamy R, Arora H. Exogenous testosterone replacement therapy versus raising endogenous testosterone levels: current and future prospects. *F S Rev.* 2021 Jan;2(1):32-42; <https://pmc.ncbi.nlm.nih.gov/articles/PMC7894643/>.

¹³³ Sobrero AJ, Stearns HE, Blair JH. Technic for the induction of ejaculation in humans. *Fertil Steril.* 1965 Nov-Dec;16(6):765-7; <https://www.sciencedirect.com/science/article/pii/S0015028216357673/pdf?md5=2769b1069d8f7305796822d1c66a46a9&pid=1-s2.0-S0015028216357673-main.pdf>.

approved class II medical device developed by Reflexonic (Chambersburg, PA) to provoke penile erection in men with ED by providing vibratory stimulation to branches of the pudendal nerve along the penile shaft.¹³⁴ The most effective vibratory amplitude and frequency appears to be 2.5 mm and 100 Hz.¹³⁵ Vibrating cock rings¹³⁶ are sometimes effective as well.

4.5 Low-Intensity Extracorporeal Shock Wave Therapy

Low-intensity extracorporeal shockwave therapy (Li-ESWT),¹³⁷ also known as focused shockwave therapy,¹³⁸ is a treatment that involves passing short, high-frequency, powerful acoustic pulses through the skin and into the penis. These mechanically-generated waves (conceptual image, at right) break down any plaques within the blood vessels and encourage the formation of new vessels (revascularization via angiogenesis) by creating microtraumas that stimulate repair and tissue regeneration.



Focused shockwave therapy appears to work best for males with vasculogenic ED, which is a blood vessel disorder that affects blood flow to tissue in the penis. The treatment is mostly painless with few known side effects, but requires running the tip of a handheld device (e.g., image, left)¹³⁹ up and down the shaft of the flaccid penis for ~15 minutes per treatment, typically requiring 2-3 treatments per week for one or more months to show results.¹⁴⁰ Exposure to shockwave therapy can lead to a significant improvement of the IIEF (International Index of Erectile Function),¹⁴¹ but as with other ED treatments it can decline in effectiveness over time as vascular and neural health continue to deteriorate with age.

¹³⁴ Segal RL, Tajkarimi K, Burnett AL. Viberect penile vibratory stimulation system: evaluation of its erectogenic efficacy. *Can J Urol*. 2013 Aug;20(4):6844-7; <https://scholar.archive.org/work/gejr2axj2rgo7bdifxssip3fxi/access/wayback/http://www.viberect.com.tr/download/evaluation%20of%20its%20erectogenic%20efficacy.pdf>.

¹³⁵ Sønksen J, Biering-Sørensen F, Kristensen JK. Ejaculation induced by penile vibratory stimulation in men with spinal cord injuries. The importance of the vibratory amplitude. *Paraplegia*. 1994 Oct;32(10):651-60; <https://www.nature.com/articles/sc1994105.pdf>.

¹³⁶ https://en.wikipedia.org/wiki/Cock_ring#Variations.

¹³⁷ https://en.wikipedia.org/wiki/Extracorporeal_shockwave_therapy.

¹³⁸ https://en.wikipedia.org/wiki/Erectile_dysfunction#Focused_shockwave_therapy.

¹³⁹ <https://www.getmyphoenix.com/phoenix/>.

¹⁴⁰ Hayon S, Panken EJ, Bennett NE. Variations in Low Intensity Shockwave Treatment Protocols for Erectile Dysfunction: A Review of the Literature and Guide to Offering Treatment. *World J Men's Health*. 2024 Apr;42(2):283-289; <https://www.ncbi.nlm.nih.gov/pmc/articles/PMC10949028/pdf>.

Patients who received shockwave therapy¹⁴² were more likely to experience improvements in their ED symptoms compared to those who didn't receive any treatment,¹⁴³ and people with mild to moderate ED tend to respond best to shockwave therapy treatment,¹⁴⁴ but clinical trials are continuing. As of mid-2024, ESWT was not yet formally FDA-approved for treating ED.¹⁴⁵

Unlike the continuous waveforms in typical ultrasound imaging, low-intensity pulsed ultrasound (LIPUS) therapy delivers pulses of ultrasound waves at lower intensities ($<3 \text{ W/cm}^2$) to penile

¹⁴¹ <https://reference.medscape.com/calculator/377/international-index-of-erectile-function-ief-5>.

¹⁴² Radial Shockwave Therapy (RSWT) and Low-Intensity Extracorporeal Shock Wave Therapy (Li-ESWT) are two different modalities used in shockwave therapy, each having distinct mechanisms and applications. RSWT produces shockwaves that spread out radially from the point of application. These shockwaves are generally lower in energy compared to those used in focused shockwave therapies. RSWT is often used for treating superficial musculoskeletal issues, such as plantar fasciitis or tennis elbow. The energy is dispersed over a wider area and is less targeted, which can make it less effective for deeper tissues, so RSWT is typically not used for erectile dysfunction. Li-ESWT, on the other hand, involves the use of lower-energy shockwaves that are more focused compared to RSWT. This technology is particularly noted for its ability to promote healing and regeneration at a cellular level. Li-ESWT has been extensively studied and used for conditions like chronic tendon issues, cardiac conditions, and erectile dysfunction (ED). The focused nature of these waves allows for deeper penetration and targeted treatment of specific areas.

¹⁴³ Angulo JC, Arance I, de Las Heras MM, Meilán E, Esquinas C, Andrés EM. Efficacy of low-intensity shock wave therapy for erectile dysfunction: A systematic review and meta-analysis. *Actas Urol Esp*. 2017 Oct;41(8):479-490; <https://pubmed.ncbi.nlm.nih.gov/27521134/>. Sokolakis I, Hatzichristodoulou G. Clinical studies on low intensity extracorporeal shockwave therapy for erectile dysfunction: a systematic review and meta-analysis of randomised controlled trials. *Int J Impot Res*. 2019 May;31(3):177-194; <https://www.psjedclinics.co.uk/pdf/sokolakis.pdf>. Drury R, Natale C, Hellstrom WJG. Reviewing the evidence for shockwave- and cell-based regenerative therapies in the treatment of erectile dysfunction. *Ther Adv Urol*. 2021 Mar 15;13:17562872211002059; <https://www.ncbi.nlm.nih.gov/pmc/articles/PMC7968013/pdf>. Vena W, Vaccalluzzo L, LA Vignera S, Morengi E, D'Agostino C, Perri A, Giammusso B, Lania AG, Aversa A, Pizzocaro A. Low-intensity shockwave treatment (LISWT) improves penile rigidity in eugonadal subjects with erectile dysfunction: a pilot study. *Minerva Endocrinol (Torino)*. 2023 Mar;48(1):4-11; <https://pubmed.ncbi.nlm.nih.gov/34931511/>. Medrano-Sánchez EM, Peña-Cantonero B, Candón-Ballester P, Blanco-Díaz M, Díaz-Mohedo E. Effectiveness of Low-Intensity Extracorporeal Shock Wave Therapy in Erectile Dysfunction: An Analysis of Sexual Function and Penile Hardness at Erection: An Umbrella Review. *J Pers Med*. 2024 Feb 4;14(2):177; <https://www.ncbi.nlm.nih.gov/pmc/articles/PMC10890328/pdf>.

¹⁴⁴ Yao H, Wang X, Liu H, Sun F, Tang G, Bao X, Wu J, Zhou Z, Ma J. Systematic Review and Meta-Analysis of 16 Randomized Controlled Trials of Clinical Outcomes of Low-Intensity Extracorporeal Shock Wave Therapy in Treating Erectile Dysfunction. *Am J Men's Health*. 2022 Mar-Apr;16(2):15579883221087532.; <https://www.ncbi.nlm.nih.gov/pmc/articles/PMC8949743/pdf>. Kaynak Y, Gruenwald I. Long-term effects of combination treatment comprising low-intensity extracorporeal shockwave therapy and tadalafil for patients with erectile dysfunction: a retrospective study. *Int J Impot Res*. 2023 Aug 29; <https://pubmed.ncbi.nlm.nih.gov/37644168/>.

¹⁴⁵ <https://www.goodrx.com/conditions/erectile-dysfunction/shockwave-therapy-for-erectile-dysfunction>.

tissues in order to stimulate cellular processes like protein synthesis, cell proliferation, and angiogenesis, and to promote tissue healing.¹⁴⁶ The mechanism is more about promoting cellular activity and less about inducing microtrauma as in the case of Li-ESWT. In a randomized clinical trial conducted in mild to moderate ED patients,¹⁴⁷ LIPUS therapy improved erectile function with no treatment-related adverse events reported. LIPUS is traditionally used for bone healing and tissue repair, but investigation of its therapeutic effects on human erectile dysfunction remains limited and more research is needed.

4.6 Penile Implants

Penile implants,¹⁴⁸ also known as penile prostheses, are devices surgically implanted within the penis to allow men with erectile dysfunction to achieve an erection. These devices are typically considered when other treatments for ED have failed, are unsuitable, or are contraindicated. Penile implants allow for spontaneous sexual activity, requiring no preparation time beyond manipulating the device, and don't generally affect the sensation in the penis or the ability to achieve orgasm. The procedure to emplace a penile implant does require surgery,¹⁴⁹ involving risks such as infection or implant problems, and recovery time can vary during which period sexual activity must be avoided.

There are two main types of penile implants that can achieve erections suitable for sexual intercourse: **inflatable** and **malleable** (or semi-rigid).

Inflatable implants are the most common type of penile implant and most closely mimic the natural erection process while remaining visibly unobtrusive.¹⁵⁰ The system consists of a pair of sterile-saline fluid-filled cylinders implanted into the cavernous body of the penis, a pump placed in the scrotum, and a fluid reservoir placed in the abdomen. To achieve an erection, the man squeezes the pump in the scrotum, which transfers 10-15 cm³ of fluid from the reservoir into each

¹⁴⁶ Cui W, Li H, Guan R, Li M, Yang B, Xu Z, Lin M, Tian L, Zhang X, Li B, Liu W, Dong Z, Wang Z, Zheng T, Zhang W, Lin G, Guo Y, Xin Z. Efficacy and safety of novel low-intensity pulsed ultrasound (LIPUS) in treating mild to moderate erectile dysfunction: a multicenter, randomized, double-blind, sham-controlled clinical study. *Transl Androl Urol*. 2019 Aug;8(4):307-319; <https://www.ncbi.nlm.nih.gov/pmc/articles/PMC6732092/pdf>.

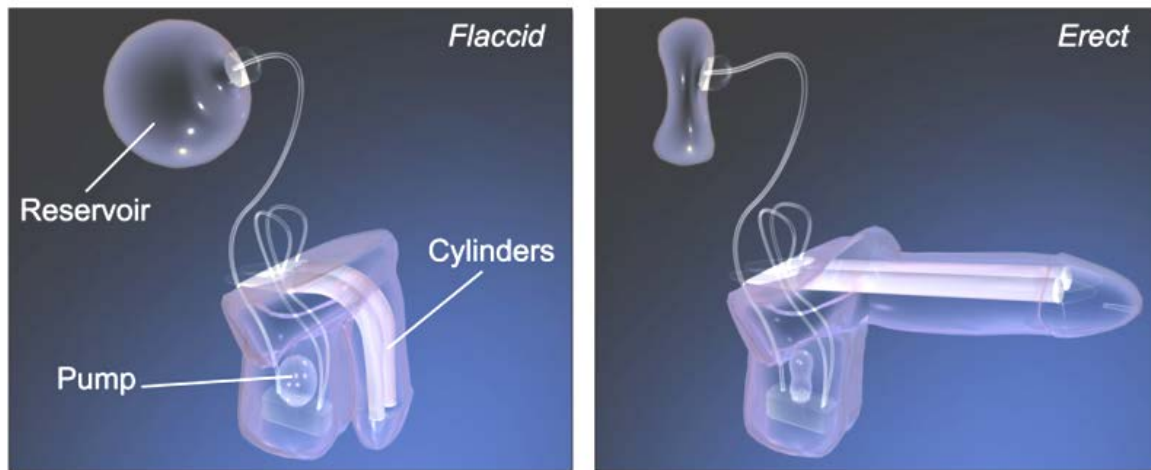
¹⁴⁷ Chen H, Li Z, Li X, Yang Y, Dai Y, Xie Z, Xiao J, Liu X, Yang L, Shi C, Zhi E, Tian R, Li P, Chen H, Zhao F, Hu J, Yao C, Lin G, Lue TF, Xia S. The Efficacy and Safety of Thrice vs Twice per Week Low-Intensity Pulsed Ultrasound Therapy for Erectile Dysfunction: A Randomized Clinical Trial. *J Sex Med*. 2022 Oct;19(10):1536-1545; <https://pubmed.ncbi.nlm.nih.gov/35999130/>.

¹⁴⁸ https://en.wikipedia.org/wiki/Penile_implant.

¹⁴⁹ Readers who have no fear of queasiness can view the entire fully-illustrated installation surgery, with color photographs, at https://cdn.prod.website-files.com/62a6f71fe682453a7fe6cb66/6314c1b61f547d780bb65f70_ZSI%20475%20Procedure%20Flyer%20EN%20V6.pdf.

¹⁵⁰ e.g., “Your ZSI implant cannot be detected by airport scanners”; <https://en.zsimplants.ch/products/zsi-475/about>.

of the cylinders in the penis, causing them to inflate and the penis to become erect. For example, the Model ZSI 475 manufactured by Zephyr Surgical Implants¹⁵¹ in Switzerland creates an erection “that resists a pressure over 500 gm [4.9 N], which is the minimum pressure to penetrate a vagina.”¹⁵² Various models of this device feature “extremely stable pressure up to >3 bar” and are available “for corpora cavernosa from 12 cm to 24 cm [4.7-9.4 inches] and more with extenders” (images, below).¹⁵³ After sexual activity, a release valve on the pump can be activated, allowing the fluid to flow back into the reservoir, deflating the penis and returning it to a natural flaccid state.



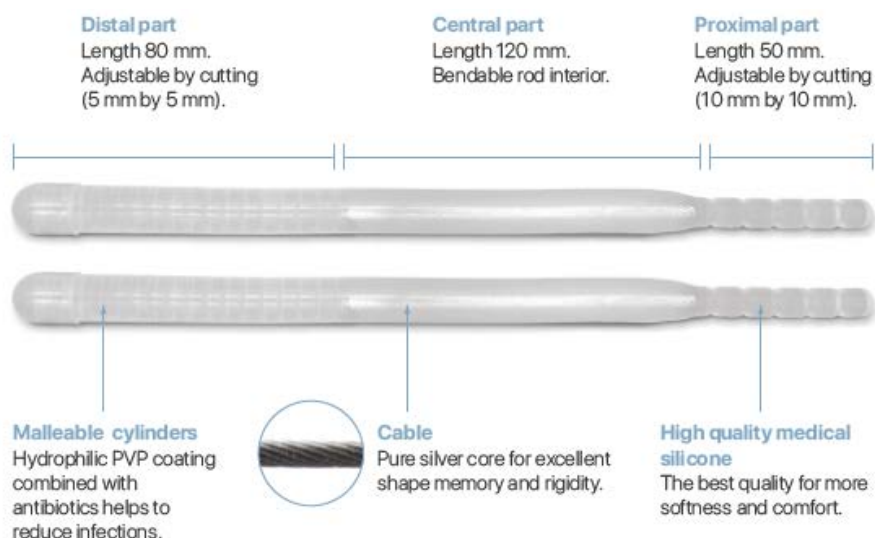
Malleable (semi-rigid) implants are simpler and easier to use than inflatable types but offer less natural-looking erections. Malleable implants consist of bendable rods that are surgically inserted into the erection chambers of the penis. The penis can be positioned upward for sex or bent away from the body for concealment under clothing when not in use. The rods have a certain firmness which allows them to keep the penis stiff enough for sexual intercourse. A diagram of the Model ZSI 100 from by Zephyr Surgical Implants¹⁵⁴ is illustrated below. The distal and central part measure ~20 cm in length and ~1.25 cm in width, giving a solid volume of ~25 cm³.

¹⁵¹ <https://en.zsimplants.ch/products/zsi-475/about>.

¹⁵² The normal resting (and maximum) vaginal closing force has been measured as 3.6 N (7.5 N) while supine and 6.9 N (10.1 N) while standing. Morgan DM, Kaur G, Hsu Y, Fenner DE, Guire K, Miller J, Ashton-Miller JA, Delancey JO. Does vaginal closure force differ in the supine and standing positions? Am J Obstet Gynecol. 2005 May;192(5):1722-8; <https://pubmed.ncbi.nlm.nih.gov/15902185/>.

¹⁵³ https://en.wikipedia.org/wiki/Penile_implant#/media/File:Penile_Implant.png.

¹⁵⁴ <https://en.zsimplants.ch/products/zsi-100/documents/surgeons>.



The 5- and 10-year overall survival of modern penile prosthetics is estimated to be 90.4% and 86.6%, respectively,¹⁵⁵ with patient satisfaction ranging from 90% to 100%,¹⁵⁶ but has a high cost, high invasiveness, and myriad potential complications including infection, distal cylinder erosion (cavernous tissue is irreversibly damaged by the implantation procedure), auto-inflation, pump migration, and reservoir displacement.¹⁵⁷ The volume of penile implant surgeries has dropped significantly¹⁵⁸ since the advent of PDE5 inhibitor pharmaceuticals ([Section 4.1](#)).

4.7 Vascular Surgery

Besides penile implants, other surgical interventions for erectile dysfunction are relatively limited and are typically reserved for special cases. These surgical options are still considered

¹⁵⁵ Dick B, Tsambarlis P, Reddy A, Hellstrom WJ. An update on: long-term outcomes of penile prostheses for the treatment of erectile dysfunction. *Expert Rev Med Devices*. 2019 Apr;16(4):281-286; <https://pubmed.ncbi.nlm.nih.gov/30898042/>.

¹⁵⁶ Bernal RM, Henry GD. Contemporary patient satisfaction rates for three-piece inflatable penile prostheses. *Adv Urol*. 2012;2012:707321; <https://www.ncbi.nlm.nih.gov/pmc/articles/PMC3412090/pdf>. Levine LA, Becher EF, Bella AJ, Brant WO, Kohler TS, Martinez-Salamanca JI, Trost L, Morey AF. Penile Prosthesis Surgery: Current Recommendations From the International Consultation on Sexual Medicine. *J Sex Med*. 2016 Apr;13(4):489-518; <http://drmartinezsalamanca.com/wp-content/uploads/2016/08/Pub.Intl.2016-2.pdf>.

¹⁵⁷ Hellstrom WJ, Montague DK, Moncada I, Carson C, Minhas S, Faria G, Krishnamurti S. Implants, mechanical devices, and vascular surgery for erectile dysfunction. *J Sex Med*. 2010 Jan;7(1 Pt 2):501-23; <https://pubmed.ncbi.nlm.nih.gov/20092450/>.

¹⁵⁸ Kohn TP, Rajanahally S, Hellstrom WJG, Hsieh TC, Raheem OA. Global Trends in Prevalence, Treatments, and Costs of Penile Prosthesis for Erectile Dysfunction in Men. *Eur Urol Focus*. 2022 May;8(3):803-813; <https://pubmed.ncbi.nlm.nih.gov/34034995/>.

experimental due to the need of elevated vascular microsurgery expertise and the lack of standardization in patient selection, hemodynamic evaluation, and surgical technique, and limited long-term outcome data using validated instruments.¹⁵⁹ Vascular surgeries are generally less common due to the higher effectiveness and lower risk profiles of pharmacological treatments and devices like penile implants as compared to surgeries.¹⁶⁰ Types of surgeries may include:

Arteriogenic Vascular Surgery: This is generally considered in younger men who have experienced significant pelvic trauma leading to arteriogenic ED (i.e., insufficiency of blood supply). Vascular surgery aims to repair or bypass blocked arteries that impede blood flow to the penis. Success rates of 57% have been reported using vascular stents,¹⁶¹ but application is quite selective, given the mixed outcomes and the availability of less invasive treatments.

Venous Ligation Surgery: This procedure involves tying off leaky veins that prevent the retention of blood within the penile tissue despite adequate arterial inflow – that is, vein ligation to interrupt at least one of the branches of penile and pelvic veins¹⁶² – which is necessary for maintaining an erection. The long-term success of venous surgeries is only ~25%,¹⁶³ so they are seldom performed due to the effectiveness of other non-surgical therapies.

Venous Embolization Surgery: This procedure involves inserting a blocking bolus of cyanoacrylic glue into leaky veins, with greater reported success for patients with venogenic erectile dysfunction.¹⁶⁴

¹⁵⁹ Munarriz R, Uberoi J, Fantini G, Martinez D, Lee C. Microvascular arterial bypass surgery: long-term outcomes using validated instruments. *J Urol.* 2009 Aug;182(2):643-8; <https://pubmed.ncbi.nlm.nih.gov/19539333/>.

¹⁶⁰ Hsieh CH, Hsu GL, Chang SJ, Yang SS, Liu SP, Hsieh JT. Surgical niche for the treatment of erectile dysfunction. *Int J Urol.* 2020 Feb;27(2):117-133; <https://pubmed.ncbi.nlm.nih.gov/31812157/>.

¹⁶¹ Schönhofen J, Räber L, Knöchel J, Keo HH, Regli C, Kostal F, Schumacher MC, Sammarchi L, Bechir M, Diehm N. Endovascular Therapy for Arteriogenic Erectile Dysfunction With a Novel Sirolimus-Eluting Stent. *J Sex Med.* 2021 Feb;18(2):315-326; <https://pubmed.ncbi.nlm.nih.gov/33454205/>.

¹⁶² Afsar H, Metin A, Sozduyar N, Salih M, Gulsoy U. Erectile dysfunction due to venous incompetence treated by dorsal vein ligation. *Int Urol Nephrol.* 1992;24(1):65-8; <https://pubmed.ncbi.nlm.nih.gov/1624245/>. Hassan AA, Hassouna MM, Elhilali MM. Long-term results of penile venous ligation for corporeal venous occlusive dysfunction. *Can J Surg.* 1995 Dec;38(6):537-41; <https://pubmed.ncbi.nlm.nih.gov/7497370/>. Rahman NU, Dean RC, Carrion R, Bochinski D, Lue TF. Crural ligation for primary erectile dysfunction: a case series. *J Urol.* 2005 Jun;173(6):2064-6; <https://pubmed.ncbi.nlm.nih.gov/15879835/>.

¹⁶³ Lewis RW. Venous surgery for impotence. *Urol Clin North Am.* 1988 Feb;15(1):115-21; <http://ndl.ethernet.edu.et/bitstream/123456789/23503/1/Wayne%20L.G.%20Hellstrom.pdf#page=536>. Katzenwadel A, Popken G, Wetterauer U. Penile venous surgery for cavernosal venous leakage: long-term results and retrospective studies. *Urol Int.* 1993;50(2):71-6; <https://pubmed.ncbi.nlm.nih.gov/8460451/>.

¹⁶⁴ Diehm N, Pelz S, Kalka C, Keo HH, Mohan V, Schumacher MC, Do DD, Hoppe H. Venous Leak Embolization in Patients with Venogenic Erectile Dysfunction via Deep Dorsal Penile Vein Access: Safety and Early Efficacy. *Cardiovasc Intervent Radiol.* 2023 May;46(5):610-616; <https://www.ncbi.nlm.nih.gov/pmc/articles/PMC10156837/pdf>.

Cavernous Nerve Grafting: Procedures aimed at reconstructing damaged nerves at the pelvic and cavernous level are based on cavernous nerve graft reconstruction, a challenging procedure requiring microsurgical expertise, in which sural nerve grafts and/or neuroorrhaphy are used to reinstate lesioned nerve function at the cavernous level after pelvic trauma and after radical prostatectomy.¹⁶⁵

Electrode Array Implantation: In one study involving 24 patients enrolled for radical prostatectomy,¹⁶⁶ a 2D flexible electrode array was implanted such that at least one electrode optimally contacted the cavernous nerve. Electrical stimulation was found to induce penile erection as assessed by visual change of penile tumescence in 75% of patients under intraoperative conditions.

4.8 Vacuum Erection Devices

Vacuum erection devices, also known as vacuum constriction devices or “penis pumps”, are a non-invasive treatment option for erectile dysfunction.¹⁶⁷ They work by creating a vacuum around the penis which mechanically induces blood to flow into the penile tissue, aiding the development of an erection in 30-60 sec,¹⁶⁸ often in concert with cock rings¹⁶⁹ to restrict outflow of venous blood after the erection has been established.

¹⁶⁵ Hanson GR, Borden LS Jr, Backous DD, Bayles SW, Corman JM. Erectile function following unilateral cavernosal nerve replacement. *Can J Urol*. 2008 Apr;15(2):3990-3; <https://pubmed.ncbi.nlm.nih.gov/18405447/>. Jacobs MA, Avellino AM, Shurtleff D, Lendvay TS. Reinnervating the penis in spina bifida patients in the United States: ilioinguinal-to-dorsal-penile neuroorrhaphy in two cases. *J Sex Med*. 2013 Oct;10(10):2593-7; <https://thetomaxprocedure.com/wp-content/uploads/2018/09/TOMAX-Seattle-.pdf>. Souza Trindade J.C., Viterbo F., Petean Trindade A., Fávare W.J., Trindade-Filho J.C.S. Long-term follow-up of treatment of erectile dysfunction after radical prostatectomy using nerve grafts and end-to-side somatic-autonomic neuroorrhaphy: A new technique. *BJU Int*. 2017;119:948-954; <https://assets.auanet.org/SITES/AUANet/PDFs/AUA2018-Posters-MP84-01.pdf>.

¹⁶⁶ Skoufias S, Sturny M, Fraga-Silva R, Papaioannou TG, Stergiopoulos N, Adamakis I, Constantinides CA. Novel Concept Enabling an Old Idea: A Flexible Electrode Array to Treat Neurogenic Erectile Dysfunction. *J Sex Med*. 2018 Nov;15(11):1558-1569; <https://pubmed.ncbi.nlm.nih.gov/30415811/>.

¹⁶⁷ Yuan J, Hoang AN, Romero CA, Lin H, Dai Y, Wang R. Vacuum therapy in erectile dysfunction--science and clinical evidence. *Int J Impot Res*. 2010 Jul-Aug;22(4):211-9; <https://quintet.no/wp-content/uploads/2020/11/Vacuum-ED-oversiktsartikkel-10.2019.pdf>. Lin H, Wang R. The science of vacuum erectile device in penile rehabilitation after radical prostatectomy. *Transl Androl Urol*. 2013 Mar;2(1):61-6; <https://www.ncbi.nlm.nih.gov/pmc/articles/PMC4708600/pdf>.

¹⁶⁸ Diederichs W, Kaula NF, Lue TF, Tanagho EA. The effect of subatmospheric pressure on the simian penis. *J Urol*. 1989 Oct;142(4):1087-9; <https://pubmed.ncbi.nlm.nih.gov/2795736/>.

¹⁶⁹ https://en.wikipedia.org/wiki/Cock_ring.

Typically, the device (image, right)¹⁷⁰ includes a plastic tube that is placed over the penis, with the base of the tube padded to create a tight seal against the body.

Once the penis is inside the tube, the air is pumped out of the tube using a hand-powered or battery-powered pump. The removal of air creates a vacuum that lowers the pressure inside the tube,



causing blood to flow into the penis and helping it to become engorged. After an adequate erection is achieved, a constriction ring or band is slipped from the base of the tube to the base of the penis before the tube is removed. This ring helps to maintain the erection by preventing blood from flowing back out of the penis. The ring should not be left in place for more than 30 minutes to prevent ischemic damage and associated complications.¹⁷¹ To remove the ring and end the erection, the user stretches or adjusts the ring to allow blood to flow out of the penis.

Using vacuum erection devices is generally safe. However, some men may not like the quality of the erection which can feel different from a natural erection due to the constriction ring. Patients may feel discomfort or pain if the vacuum is too intense or if the constriction ring is too tight, impeding proper blood flow. The vacuum action can cause tiny blood vessels on the surface of the skin to burst, resulting in small red spots (petechiae) or bruising (hematoma).¹⁷² The constriction ring can also cause numbness or a cold sensation in the penis if it restricts blood flow too much or is left on for too long. If the device is not used correctly, skin at the base of the penis or pubic hair can get pulled into the device, causing discomfort or pinching. The constriction ring can sometimes inhibit ejaculation, which some users may find uncomfortable or unsatisfactory. Leaving the constriction ring on for longer than recommended can cause serious damage to penile tissue due to prolonged lack of oxygenated blood, resulting in permanent damage to erectile function. Discontinuation rates are up to 30% due to bruising, pivoting at the base of penis, decreased orgasm, and problems related to constriction band including pain, and temporary change to penile sensation.¹⁷³ Usage has declined in recent decades due to the greater ease and effectiveness of PDE5 inhibitor treatments ([Section 4.1](#)).

¹⁷⁰ https://en.wikipedia.org/wiki/Penis_enlargement#/media/File:Water-based_Penis_Enlargement_Pump.jpg.

¹⁷¹ Broderick GA, McGahan JP, Stone AR, White RD. The hemodynamics of vacuum constriction erections: assessment by color Doppler ultrasound. J Urol. 1992 Jan;147(1):57-61; <https://www.sciencedirect.com/science/article/pii/S002253471737132X/pdf>.

¹⁷² Ganem JP, Lucey DT, Janosko EO, Carson CC. Unusual complications of the vacuum erection device. Urology. 1998 Apr;51(4):627-31; <https://pubmed.ncbi.nlm.nih.gov/9586618/>.

¹⁷³ Levine LA, Dimitriou RJ. Vacuum constriction and external erection devices in erectile dysfunction. Urol Clin North Am. 2001 May;28(2):335-41, ix-x; <https://pubmed.ncbi.nlm.nih.gov/11402585/>.

4.9 Possible Future Conventional Treatments

Various possible future treatments for erectile dysfunction involving novel molecular pathways have been conceived or are under development, such as melanocortin receptor agonists (Section 4.9.1) and botulinum neurotoxin A (Section 4.9.2) among the pharmacological approaches. Numerous other potential drug molecules have been or are being investigated,¹⁷⁴ including apomorphine,¹⁷⁵ arginase inhibitors,¹⁷⁶ dopamine agonists,¹⁷⁷ hexarelin analogues,¹⁷⁸ maxi-K channel activators,¹⁷⁹ nitric oxide-independent guanylate cyclase activators,¹⁸⁰ oxytocin,¹⁸¹

¹⁷⁴ Argiolas A, Argiolas FM, Argiolas G, Melis MR. Erectile Dysfunction: Treatments, Advances and New Therapeutic Strategies. *Brain Sci.* 2023 May 15;13(5):802; <https://www.ncbi.nlm.nih.gov/pmc/articles/PMC10216368/pdf>.

¹⁷⁵ Lal S, Laryea E, Thavundayil JX, Nair NP, Negrete J, Ackman D, Blundell P, Gardiner RJ. Apomorphine-induced penile tumescence in impotent patients--preliminary findings. *Prog Neuropsychopharmacol Biol Psychiatry.* 1987;11(2-3):235-42; <https://pubmed.ncbi.nlm.nih.gov/3628831/>. Gontero P, D'Antonio R, Pretti G, Fontana F, Panella M, Kocjancic E, Allochis G, Frea B. Clinical efficacy of Apomorphine SL in erectile dysfunction of diabetic men. *Int J Impot Res.* 2005 Jan-Feb;17(1):80-5; <https://pubmed.ncbi.nlm.nih.gov/15510184/>.

¹⁷⁶ Abdelkawy KS, Lack K, Elbarbry F. Pharmacokinetics and Pharmacodynamics of Promising Arginase Inhibitors. *Eur J Drug Metab Pharmacokinet.* 2017 Jun;42(3):355-370; <https://pubmed.ncbi.nlm.nih.gov/27734327/>.

¹⁷⁷ Giuliano F, Allard J. Dopamine and male sexual function. *Eur Urol.* 2001 Dec;40(6):601-8; https://www.angelfire.com/d20/medicina_ucsm/revistas/revisao/003.pdf. Simonsen U, Comerma-Steffensen S, Andersson KE. Modulation of Dopaminergic Pathways to Treat Erectile Dysfunction. *Basic Clin Pharmacol Toxicol.* 2016 Oct;119 Suppl 3:63-74; <https://onlinelibrary.wiley.com/doi/epdf/10.1111/bcpt.12653>.

¹⁷⁸ Melis MR, Succu S, Spano MS, Locatelli V, Torsello A, Muller EE, Deghenghi R, Argiolas A. EP 60761 and EP 50885, two hexarelin analogues, induce penile erection in rats. *Eur J Pharmacol.* 2000 Sep 15;404(1-2):137-43; <https://pubmed.ncbi.nlm.nih.gov/10980272/>. Argiolas A, Melis MR, Deghenghi R. Hexarelin analogues as inducers of penile erection. *Drugs of the Future* 2002; 27(8):0771; <https://access.portico.org/stable?au=pjbf78xdddg>.

¹⁷⁹ Király I, Pataricza J, Bajory Z, Simonsen U, Varro A, Papp JG, Pajor L, Kun A. Involvement of large-conductance Ca(2+) -activated K(+) channels in both nitric oxide and endothelium-derived hyperpolarization-type relaxation in human penile small arteries. *Basic Clin Pharmacol Toxicol.* 2013 Jul;113(1):19-24; <https://onlinelibrary.wiley.com/doi/pdf/10.1111/bcpt.12059>. Bentzen BH, Olesen SP, Rønn LC, Grønnet M. BK channel activators and their therapeutic perspectives. *Front Physiol.* 2014 Oct 9;5:389; <https://www.ncbi.nlm.nih.gov/pmc/articles/PMC4191079/pdf>.

¹⁸⁰ Mónica FZ, Antunes E. Stimulators and activators of soluble guanylate cyclase for urogenital disorders. *Nat Rev Urol.* 2018 Jan;15(1):42-54; <https://pubmed.ncbi.nlm.nih.gov/29133940/>. Chrysant SG. A novel approach for the treatment of hypertension with the soluble guanylate cyclase stimulating drug. *Expert Opin Drug Saf.* 2021 Jun;20(6):635-640; <https://pubmed.ncbi.nlm.nih.gov/33734912/>.

¹⁸¹ Melis MR, Argiolas A. Oxytocin, Erectile Function and Sexual Behavior: Last Discoveries and Possible Advances. *Int J Mol Sci.* 2021 Sep 26;22(19):10376; <https://www.ncbi.nlm.nih.gov/pmc/articles/PMC8509000/pdf>.

RhoA/Rho kinase inhibitors,¹⁸² topical glyceryl trinitrate,¹⁸³ trazodone,¹⁸⁴ and yohimbine,¹⁸⁵ each with its own set of clinical complications.

The pharmacological therapies described above are mostly aimed at providing symptomatic relief to erectile dysfunction, thus providing a temporary resolution of the problem rather than a cure aimed at permanently resolving the cause of the dysfunction.¹⁸⁶ Attempts at genuine cures for ED using the techniques of biotechnology include stem cell therapies (Section 4.9.3) and gene therapies (Section 4.9.4). Finally, penile transplantation (Section 4.9.5) may be the most extreme of the conventional curative approaches.

¹⁸² Sopko NA, Hannan JL, Bivalacqua TJ. Understanding and targeting the Rho kinase pathway in erectile dysfunction. *Nat Rev Urol*. 2014 Nov;11(11):622-8; <https://www.ncbi.nlm.nih.gov/pmc/articles/PMC4696116/pdf>. Zewdie KA, Ayza MA, Tesfaye BA, Wondafrash DZ, Berhe DF. A Systematic Review on Rho-Kinase as a Potential Therapeutic Target for the Treatment of Erectile Dysfunction. *Res Rep Urol*. 2020 Jul 17;12:261-272; <https://www.ncbi.nlm.nih.gov/pmc/articles/PMC7373493/pdf>.

¹⁸³ Ralph DJ, Eardley I, Taubel J, Terrill P, Holland T. Efficacy and Safety of MED2005, a Topical Glyceryl Trinitrate Formulation, in the Treatment of Erectile Dysfunction: A Randomized Crossover Study. *J Sex Med*. 2018 Feb;15(2):167-175; <https://www.sciencedirect.com/science/article/pii/S1743609517318520>. Davis A, Reisman Y. Development of a novel topical formulation of glyceryl trinitrate for the treatment of erectile dysfunction. *Int J Impot Res*. 2020 Nov;32(6):569-577; <https://pubmed.ncbi.nlm.nih.gov/32001815/>.

¹⁸⁴ Fink HA, MacDonald R, Rutks IR, Wilt TJ. Trazodone for erectile dysfunction: a systematic review and meta-analysis. *BJU Int*. 2003 Sep;92(4):441-6; <https://pubmed.ncbi.nlm.nih.gov/12930437/>. Pyke RE. Trazodone in Sexual Medicine: Underused and Overdosed? *Sex Med Rev*. 2020 Apr;8(2):206-216; <https://pubmed.ncbi.nlm.nih.gov/30342856/>.

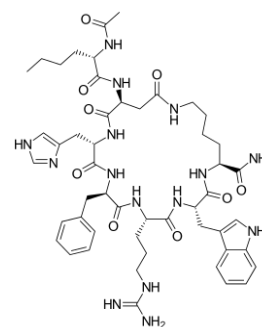
¹⁸⁵ Guay AT, Spark RF, Jacobson J, Murray FT, Geisser ME. Yohimbine treatment of organic erectile dysfunction in a dose-escalation trial. *Int J Impot Res*. 2002 Feb;14(1):25-31; <https://www.medicinacomplementar.com.br/biblioteca/pdfs/Doencas/do-1931.pdf>.

¹⁸⁶ Argiolas A, Argiolas FM, Argiolas G, Melis MR. Erectile Dysfunction: Treatments, Advances and New Therapeutic Strategies. *Brain Sci*. 2023 May 15;13(5):802; <https://www.ncbi.nlm.nih.gov/pmc/articles/PMC10216368/pdf>.

4.9.1 Melanocortin Receptor Agonists

The melanocortins¹⁸⁷ are a family of neuropeptide hormones which are the ligands of the melanocortin receptors.¹⁸⁸ Melanocortin receptors are involved in various physiological functions including skin pigmentation, appetite control, and sexual function – including inducing erections. Melanocortin agonists¹⁸⁹ act on the central nervous system by binding to melanocortin receptors, especially MC4 (expressed in the hypothalamus)¹⁹⁰ which plays a role in sexual arousal and response.¹⁹¹ The activation of these receptors can lead to sexual arousal and facilitate erections primarily through neuronal pathways including neurons in the paraventricular nucleus of the hypothalamus¹⁹² and the release of dopamine¹⁹³ (a neurotransmitter associated with pleasure and reward mechanisms) from the nucleus accumbens¹⁹⁴ and dorsal striatum,¹⁹⁵ enhancing sexual motivation and arousal. The agonist drug does not directly influence the release of nitric oxide in the penis, but the increase in sexual arousal can activate downstream effects that involve the NO pathway, whereupon signals from the CNS may prompt the release of nitric oxide from the endothelial cells and nerve endings in the penis. Administering an agonist that activates these receptors essentially acts as a substitute for external sexual arousal but will fail to produce an erection if the nitric oxide-cGMP pathway (Section 2.3) is compromised (as can occur due to vascular diseases, diabetes, or other conditions affecting endothelial function).

One example of a melanocortin receptor agonist drug is melanotan II (image, right)¹⁹⁶ which has been studied in the context of skin tanning, weight loss, and sexual arousal. This drug can stimulate melanin



¹⁸⁷ <https://en.wikipedia.org/wiki/Melanocortin>.

¹⁸⁸ Martin WJ, MacIntyre DE. Melanocortin receptors and erectile function. Eur Urol. 2004 Jun;45(6):706-13; <https://pubmed.ncbi.nlm.nih.gov/15149741/>.

¹⁸⁹ A substance which initiates a physiological response when combined with a receptor; <https://en.wikipedia.org/wiki/Agonist>.

¹⁹⁰ Sharma S, Garfield AS, Shah B, Kleyn P, Ichetovkin I, Moeller IH, Mowrey WR, Van der Ploeg LHT. Current Mechanistic and Pharmacodynamic Understanding of Melanocortin-4 Receptor Activation. Molecules. 2019 May 16;24(10):1892; <https://www.ncbi.nlm.nih.gov/pmc/articles/PMC6572030/pdf>.

¹⁹¹ Siljee-Wong JE. Melanocortin MC₄ receptor expression sites and local function. Eur J Pharmacol. 2011 Jun 11;660(1):234-40; <https://pubmed.ncbi.nlm.nih.gov/21199645/>.

¹⁹² This is integral to the regulation of sexual behavior and is connected to other brain regions that control arousal and motivational aspects of sexual behavior; https://en.wikipedia.org/wiki/Paraventricular_nucleus_of_hypothalamus.

¹⁹³ <https://en.wikipedia.org/wiki/Dopamine>.

¹⁹⁴ https://en.wikipedia.org/wiki/Nucleus_accumbens#Reward_and_reinforcement.

¹⁹⁵ <https://en.wikipedia.org/wiki/Striatum>.

¹⁹⁶ https://en.wikipedia.org/wiki/Melanotan_II.

production, leading to tanned skin without exposure to UV radiation, and can affect appetite and libido, prompting some¹⁹⁷ to call it the “Barbie drug” because its effects are somewhat characteristic of the Barbie doll: tanned skin, slim physique, and enhanced sexual confidence. The drug¹⁹⁸ is typically administered as subcutaneous injections (e.g., 0.025 mg/kg dosage)¹⁹⁹ and is not available as an oral medication. The injectable form is chosen because of the peptide’s poor absorption and rapid degradation when taken orally. The subcutaneous route allows the drug to be absorbed more slowly and steadily into the bloodstream, ensuring that it can exert its effects more effectively. Unfortunately, severe nausea is a common side effect²⁰⁰ and questions have been raised as to the safety of melanocortin II.²⁰¹

Another agonist drug is bremelanotide (aka. Vyleesi, formerly PT-141),²⁰² which has been FDA approved to treat hypoactive sexual desire disorder in premenopausal women.²⁰³ The drug has also shown efficacy in producing erections in males when delivered intranasally using a disposable, single-use, metered dose delivery device. In one Phase 2A study,²⁰⁴ administration of a 20 mg dose led to penile base rigidity $\geq 80\%$ compared to placebo, with a mean duration of base

¹⁹⁷ Langan EA, Nie Z, Rhodes LE. Melanotropic peptides: more than just Barbie drugs and sun-tan jabs? *Br J Dermatol*. 2010 Sep;163(3):451-5; <https://pubmed.ncbi.nlm.nih.gov/20545686/>.

¹⁹⁸ Ückert S, Bannowsky A, Albrecht K, Kuczyk MA. Melanocortin receptor agonists in the treatment of male and female sexual dysfunctions: results from basic research and clinical studies. *Expert Opin Investig Drugs*. 2014 Nov;23(11):1477-83; <https://pubmed.ncbi.nlm.nih.gov/25096243/>.

¹⁹⁹ Dorr RT, Lines R, Levine N, Brooks C, Xiang L, Hruby VJ, Hadley ME. Evaluation of melanotan-II, a superpotent cyclic melanotropic peptide in a pilot phase-I clinical study. *Life Sci*. 1996;58(20):1777-84; <https://pubmed.ncbi.nlm.nih.gov/8637402/>. Wessells H, Levine N, Hadley ME, Dorr R, Hruby V. Melanocortin receptor agonists, penile erection, and sexual motivation: human studies with Melanotan II. *Int J Impot Res*. 2000 Oct;12 Suppl 4:S74-9; <https://pubmed.ncbi.nlm.nih.gov/11035391/>.

²⁰⁰ Wessells H, Levine N, Hadley ME, Dorr R, Hruby V. Melanocortin receptor agonists, penile erection, and sexual motivation: human studies with Melanotan II. *Int J Impot Res*. 2000 Oct;12 Suppl 4:S74-9; <https://pubmed.ncbi.nlm.nih.gov/11035391/>.

²⁰¹ Habbema L, Halk AB, Neumann M, Bergman W. Risks of unregulated use of alpha-melanocyte-stimulating hormone analogues: a review. *Int J Dermatol*. 2017 Oct;56(10):975-980; <https://pubmed.ncbi.nlm.nih.gov/28266027/>. Dreyer BA, Amer T, Fraser M. Melanotan-induced priapism: a hard-earned tan. *BMJ Case Rep*. 2019 Feb 21;12(2):e227644; <https://www.ncbi.nlm.nih.gov/pmc/articles/PMC6388891/pdf>. Peters B, Hadimeri H, Wahlberg R, Afghahi H. Melanotan II: a possible cause of renal infarction: review of the literature and case report. *CEN Case Rep*. 2020 May;9(2):159-161; <https://www.ncbi.nlm.nih.gov/pmc/articles/PMC7148395/pdf>.

²⁰² <https://en.wikipedia.org/wiki/Bremelanotide>.

²⁰³ Dhillon S, Keam SJ. Bremelanotide: First Approval. *Drugs*. 2019 Sep;79(14):1599-1606.; <https://pubmed.ncbi.nlm.nih.gov/31429064/>.

²⁰⁴ Diamond LE, Earle DC, Rosen RC, Willett MS, Molinoff PB. Double-blind, placebo-controlled evaluation of the safety, pharmacokinetic properties and pharmacodynamic effects of intranasal PT-141, a melanocortin receptor agonist, in healthy males and patients with mild-to-moderate erectile dysfunction. *Int J Impot Res*. 2004 Feb;16(1):51-9; <https://pubmed.ncbi.nlm.nih.gov/14963471/>.

rigidity $\geq 80\%$ of ~24 minutes at 20 mg dose with a duration of onset of ~30 minutes. A related study²⁰⁵ found that the most common adverse effects were flushing, somnolence, nausea, vomiting, headache, diaphoresis, and lower back pain.

4.9.2 Botulinum Neurotoxin A

A Phase 1 study of the intracavernous injection of botulinum neurotoxin, aka. Botox,²⁰⁶ found that the neurotoxin was able to induce penile erection in human males, either when given alone or in association with a PD5 inhibitor.²⁰⁷ The positive effects of the treatment were found to persist for more than three months with no reported collateral effects, and have been confirmed and extended by other studies in patients with different botulinum neurotoxin A formulations and doses.²⁰⁸ The mechanism by which botulinum neurotoxin A facilitates the relaxation of cavernous smooth muscles has not yet been determined, but it likely induces its effect by blocking the release of neurotransmitters that keep cavernous smooth muscles contracted, such as noradrenaline, endothelin, and others.

4.9.3 Stem Cell Therapy

Stem cells²⁰⁹ are clonogenic²¹⁰ self-renewing cells that can undergo proliferation and differentiation into multiple cell phenotypes. Stem cell therapy (SCT)²¹¹ seeks to harness the

²⁰⁵ Rosen RC, Diamond LE, Earle DC, Shadiack AM, Molinoff PB. Evaluation of the safety, pharmacokinetics and pharmacodynamic effects of subcutaneously administered PT-141, a melanocortin receptor agonist, in healthy male subjects and in patients with an inadequate response to Viagra. *Int J Impot Res.* 2004 Apr;16(2):135-42; <https://pubmed.ncbi.nlm.nih.gov/14999221/>.

²⁰⁶ https://en.wikipedia.org/wiki/Botulinum_toxin.

²⁰⁷ El-Shaer W, Ghanem H, Diab T, Abo-Taleb A, Kandeel W. Intra-cavernous injection of BOTOX® (50 and 100 Units) for treatment of vasculogenic erectile dysfunction: Randomized controlled trial. *Andrology.* 2021 Jul;9(4):1166-1175; <https://onlinelibrary.wiley.com/doi/epdf/10.1111/andr.13010>.

²⁰⁸ Giuliano F, Denys P, Joussain C. Effectiveness and Safety of Intracavernosal IncobotulinumtoxinA (Xeomin®) 100 U as an Add-on Therapy to Standard Pharmacological Treatment for Difficult-to-Treat Erectile Dysfunction: A Case Series. *Toxins (Basel).* 2022 Apr 16;14(4):286; <https://www.ncbi.nlm.nih.gov/pmc/articles/PMC9030535/pdf>. Abdelrahman IFS, Raheem AA, Elkhayat Y, Aburahma AA, Abdel-Raheem T, Ghanem H. Safety and efficacy of botulinum neurotoxin in the treatment of erectile dysfunction refractory to phosphodiesterase inhibitors: Results of a randomized controlled trial. *Andrology.* 2022 Feb;10(2):254-261; <https://onlinelibrary.wiley.com/doi/epdf/10.1111/andr.13104>.

²⁰⁹ https://en.wikipedia.org/wiki/Stem_cell.

²¹⁰ Clonogenic refers to the ability of cells to form colonies and proliferate in culture, which is an important characteristic of stem cells and cancer cells.

²¹¹ https://en.wikipedia.org/wiki/Stem-cell_therapy.

regenerative potential of stem cells for the actual repair of injured or damaged tissues.²¹² Tissue injury resulting in erectile dysfunction may include damage to the neurovascular bundle (neuropaxia) during radical prostatectomy; nerve damage, endothelial dysfunction, and oxidative stress associated with diabetes mellitus; or accumulation of fibrous plaque and veno-occlusive ED in Peyronie's disease.²¹³ The perceived value of SCT lies in the transformation, paracrine signaling, and differentiation of stem cells into specialized replacement smooth muscle, epithelial, Schwann, and neuronal cells, even though at present the specific mechanisms that might be useful for SCT are poorly defined and may vary by cell lineage.²¹⁴

Several studies have evaluated the efficacy of SCT for the treatment of erectile dysfunction in humans. In one early study, 15 million human umbilical cord stem cells were infused into both corpus cavernosa of 7 diabetic ED patients, after which six patients regained morning erections by the third month and maintained the capacity for such erections for 6 months, with two patients achieving penetration and orgasm with the addition of PDE5 inhibitors (Section 4.1) prior to intercourse.²¹⁵ A similar case series reported injecting 15 million adipose tissue-derived stem cells (ADSCs) intracavernosally in 6 diabetic ED patients, after which morning erections returned in five of six men by 95 days and continued for more than 4 months, with three patients able to achieve penetrative sex and orgasm with the aid of PDE5 inhibitors for the following 6 months, and with no reported adverse events.²¹⁶ In a phase I open-label single-arm study involving 17 patients suffering from ED after radical prostatectomy who were treated with adipose tissue-derived stem cells found that 8 of the 17 men recovered erectile function and were able to perform sexual intercourse,²¹⁷ and a 2016 study found that placental matrix-derived mesenchymal

²¹² Madl CM, Heilshorn SC, Blau HM. Bioengineering strategies to accelerate stem cell therapeutics. *Nature*. 2018 May;557(7705):335-342; <https://www.ncbi.nlm.nih.gov/pmc/articles/PMC6773426/pdf>.

²¹³ Drury R, Natale C, Hellstrom WJG. Reviewing the evidence for shockwave- and cell-based regenerative therapies in the treatment of erectile dysfunction. *Ther Adv Urol*. 2021 Mar 15;13:17562872211002059; <https://www.ncbi.nlm.nih.gov/pmc/articles/PMC7968013/pdf>.

²¹⁴ Peak TC, Anaissie J, Hellstrom WJ. Current Perspectives on Stem Cell Therapy for Erectile Dysfunction. *Sex Med Rev*. 2016 Jul;4(3):247-256; <https://cdn.mednet.co.il/2017/02/Current-Perspectives-on-Stem-Cell-Therapy-for-Erectile-DysfunctionReview.pdf>. Raheem OA, Natale C, Dick B, Reddy AG, Yousif A, Khera M, Baum N. Novel Treatments of Erectile Dysfunction: Review of the Current Literature. *Sex Med Rev*. 2021 Jan;9(1):123-132; <https://enorm.health/s/Novel-Treatments-of-Erectile-Dysfunction-Review-of-the-Current-Literature-Raheem-2020.pdf>.

²¹⁵ Bahk JY, Jung JH, Han H, Min SK, Lee YS. Treatment of diabetic impotence with umbilical cord blood stem cell intracavernosal transplant: preliminary report of 7 cases. *Exp Clin Transplant*. 2010 Jun;8(2):150-60; <https://theacrm.com/wp-content/uploads/2021/03/Umbilical-SC-in-Diabetic-ED-2010.pdf>.

²¹⁶ Garber M. Intracavernous Administration of Adipose Stem Cells: A New Technique of Treating Erectile Dysfunction in Diabetic Patient, Preliminary Report of 6 Cases. *MOJ Cell Sci Rep*. 2015; 2(1):5-8; <https://www.thepsci.com/pdfs/garber-2015-ed.pdf>.

²¹⁷ Haahr MK, Jensen CH, Toyserkani NM, Andersen DC, Damkier P, Sørensen JA, Lund L, Sheikh SP. Safety and Potential Effect of a Single Intracavernous Injection of Autologous Adipose-Derived Regenerative Cells in Patients with Erectile Dysfunction Following Radical Prostatectomy: An Open-Label Phase I Clinical Trial. *EBioMedicine*. 2016 Jan 19;5:204-10; <https://www.ncbi.nlm.nih.gov/pmc/articles/PMC4816754/pdf>. See also: Haahr MK, Harken Jensen C,

stem cells led to improved erections in ED patients.²¹⁸ Another Phase 1/2 pilot clinical trial utilized bone marrow derived mononuclear cells (BM-MNC) for the treatment of 12 vasculogenic ED patients (following their radical prostatectomy) and reported significantly improved intercourse satisfaction and erectile function.²¹⁹

Despite these early successes, and the results of some later work,²²⁰ the current medical consensus seems to be that “the clinical results are not robust”.²²¹ It remains unclear which varieties of stem cells produce optimal results and which concentrations of stem cells, treatment durations, and dosing schedules are most appropriate, so intracavernosal stem cell therapy must be considered “investigational”²²² and “should be only administered in a clinical research setting.”²²³

Toyserkani NM, Andersen DC, Damkier P, Sørensen JA, Sheikh SP, Lund L. A 12-Month Follow-up After a Single Intracavernous Injection of Autologous Adipose-Derived Regenerative Cells in Patients with Erectile Dysfunction Following Radical Prostatectomy: An Open-Label Phase I Clinical Trial. *Urology*. 2018 Nov;121:203.e6-203.e13; <https://pubmed.ncbi.nlm.nih.gov/29958973/>.

²¹⁸ Levy JA, Marchand M, Iorio L, Cassini W, Zahalsky MP. Determining the Feasibility of Managing Erectile Dysfunction in Humans With Placental-Derived Stem Cells. *J Am Osteopath Assoc*. 2016 Jan;116(1):e1-5; <https://www.degruyter.com/document/doi/10.7556/jaoa.2016.007/pdf>.

²¹⁹ Yiou R, Hamidou L, Birebent B, Bitari D, Lecorvoisier P, Contremoulins I, Khodari M, Rodriguez AM, Augustin D, Roudot-Thoraval F, de la Taille A, Rouard H. Safety of Intracavernous Bone Marrow-Mononuclear Cells for Postradical Prostatectomy Erectile Dysfunction: An Open Dose-Escalation Pilot Study. *Eur Urol*. 2016 Jun;69(6):988-91; <https://pubmed.ncbi.nlm.nih.gov/26439886/>.

²²⁰ Lokeshwar SD, Patel P, Shah SM, Ramasamy R. A Systematic Review of Human Trials Using Stem Cell Therapy for Erectile Dysfunction. *Sex Med Rev*. 2020 Jan;8(1):122-130; <https://pubmed.ncbi.nlm.nih.gov/31640911/>. He M, von Schwarz ER. Stem-cell therapy for erectile dysfunction: a review of clinical outcomes. *Int J Impot Res*. 2021 Apr;33(3):271-277; <https://pubmed.ncbi.nlm.nih.gov/32350455/>.

²²¹ Castiglione F, Cakir OO, Satchi M, Fallara G, Pang KH; European Society for Sexual Medicine Scientific Collaboration and Partnership. The Current Role and Implications of Stem Cell Therapy in Erectile Dysfunction: A Transformation from Caterpillar to Butterfly Is Required. *Eur Urol Focus*. 2023 Jan;9(1):28-31; <https://www.sciencedirect.com/science/article/pii/S2405456922002516>.

²²² Burnett AL, Nehra A, Breau RH, Culkin DJ, Faraday MM, Hakim LS, Heidelbaugh J, Khera M, McVary KT, Miner MM, Nelson CJ, Sadeghi-Nejad H, Seftel AD, Shindel AW. Erectile Dysfunction: AUA Guideline. *J Urol*. 2018 Sep;200(3):633-641; <https://www.auanet.org/documents/Guidelines/PDF/ED-JU.pdf>.

²²³ Pozzi E, Muneer A, Sangster P, Alnajjar HM, Salonia A, Bettocchi C, Castiglione F, Ralph DJ; Trauma, Reconstructive Urology Working Party of the European Association of Urology (EAU) Young Academic Urologists (YAU). Stem-cell regenerative medicine as applied to the penis. *Curr Opin Urol*. 2019 Jul;29(4):443-449; <https://pubmed.ncbi.nlm.nih.gov/31008782/>.

4.9.4 Gene Therapy

Gene therapy²²⁴ is an alternative form of cellular based therapy that would use injections of novel genetic material as another potential future therapy for erectile dysfunction.²²⁵ Gene transfer typically employs a vector such as a virus²²⁶ or a plasmid²²⁷ to import the gene into the cells such that the inserted gene works appropriately. Proposed targets²²⁸ using gene therapy to treat ED include nitric oxide synthase,²²⁹ pigment epithelium-derived factor,²³⁰ and vascular endothelial growth factor,²³¹ and many others.²³² Gene therapy offers the advantage of potentially long-lasting treatment effects due to the low rate of smooth muscle turnover, though at the risk of severe inflammatory reactions.²³³ The external positioning, limited blood flow, and slow cellular turnover of the penis make it an ideal target for gene therapy,²³⁴ but research supporting gene therapy for the treatment of ED remains in its infancy.

Only a relatively few studies on the actual use of gene transfer for ED are available. In animal models, the “Maxi-K” potassium channel gene has been transferred in mesenchymal stem cells for the treatment of diabetes-associated ED in a diabetic rat model, resulting in an improved effect on erectile function of diabetic rats,²³⁵ and “Maxi-K” potassium channel transfer to penile

²²⁴ https://en.wikipedia.org/wiki/Gene_therapy.

²²⁵ Matz EL, Scarberry K, Terlecki R. Platelet-Rich Plasma and Cellular Therapies for Sexual Medicine and Beyond. *Sex Med Rev.* 2022 Jan;10(1):174-179; <https://pubmed.ncbi.nlm.nih.gov/32800771/>.

²²⁶ https://en.wikipedia.org/wiki/Viral_vector.

²²⁷ <https://en.wikipedia.org/wiki/Plasmid>.

²²⁸ Patel DP, Pastuszak AW, Hotaling JM. Emerging Treatments for Erectile Dysfunction: a Review of Novel, Non-surgical Options. *Curr Urol Rep.* 2019 Jun 18;20(8):44; <https://ro-boost.ro/wp-content/uploads/2024/01/MENS-HEALTH-ARTICLE.pdf>.

²²⁹ https://en.wikipedia.org/wiki/Nitric_oxide_synthase.

²³⁰ <https://en.wikipedia.org/wiki/PEDF>.

²³¹ https://en.wikipedia.org/wiki/Vascular_endothelial_growth_factor.

²³² Harraz A, Shindel AW, Lue TF. Emerging gene and stem cell therapies for the treatment of erectile dysfunction. *Nat Rev Urol.* 2010 Mar;7(3):143-52; <https://www.ncbi.nlm.nih.gov/pmc/articles/PMC3927494/pdf>.

²³³ Matz EL, Scarberry K, Terlecki R. Platelet-Rich Plasma and Cellular Therapies for Sexual Medicine and Beyond. *Sex Med Rev.* 2022 Jan;10(1):174-179; <https://pubmed.ncbi.nlm.nih.gov/32800771/>.

²³⁴ Bivalacqua TJ, Hellstrom WJ. Potential application of gene therapy for the treatment of erectile dysfunction. *J Androl.* 2001 Mar-Apr;22(2):183-90; <https://onlinelibrary.wiley.com/doi/pdf/10.1002/j.1939-4640.2001.tb02169.x>.

²³⁵ He Y, He W, Qin G, Luo J, Xiao M. Transplantation KCNMA1 modified bone marrow-mesenchymal stem cell therapy for diabetes mellitus-induced erectile dysfunction. *Andrologia.* 2014 Jun;46(5):479-86; <https://pubmed.ncbi.nlm.nih.gov/23646921/>.

tissue has also been found to increase sexual behavior in atherosclerotic cynomolgus monkeys²³⁶ and to restore erectile function in aged rats.²³⁷ Other gene transfer experiments have demonstrated improved erectile response in diabetic rats and mice.²³⁸ So far the only human Phase 1 trial was published in 2005²³⁹ describing the gene-transfer-assisted upregulation of the “Maxi-K” potassium channel into human penile smooth muscle cells to increase their relaxant properties, in which the data from just a small number of human patients with ED of different etiology showed an improvement in ED without adverse effects.²⁴⁰ More recently, microRNAs (miRNAs) offer new hope for novel miRNA-based therapeutic gene strategies for ED.²⁴¹

²³⁶ Christ GJ, Andersson KE, Williams K, Zhao W, D'Agostino R Jr, Kaplan J, Aboushwareb T, Yoo J, Calenda G, Davies KP, Sellers RS, Melman A. Smooth-muscle-specific gene transfer with the human maxi-k channel improves erectile function and enhances sexual behavior in atherosclerotic cynomolgus monkeys. *Eur Urol*. 2009 Dec;56(6):1055-66; <https://pubmed.ncbi.nlm.nih.gov/19167152/>.

²³⁷ So I, Chae MR, Lee SW. Gene transfer of the K(ATP) channel restores age-related erectile dysfunction in rats. *BJU Int*. 2007 Nov;100(5):1154-60; <https://pubmed.ncbi.nlm.nih.gov/17645416/>.

²³⁸ Shen ZJ, Wang H, Lu YL, Zhou XL, Chen SW, Chen ZD. Gene transfer of vasoactive intestinal polypeptide into the penis improves erectile response in the diabetic rat. *BJU Int*. 2005 Apr;95(6):890-4; <https://pubmed.ncbi.nlm.nih.gov/15794804/>. Pu XY, Hu LQ, Wang HP, Luo YX, Wang XH. Improvement in erectile dysfunction after insulin-like growth factor-1 gene therapy in diabetic rats. *Asian J Androl*. 2007 Jan;9(1):83-91; <https://citeseerx.ist.psu.edu/document?repid=rep1&type=pdf&doi=0ad7367f5848b48d988b0b41f3b467cdfbf70a5f>. Jung JH, Kim BJ, Chae MR, Kam SC, Jeon JH, So I, Chung KH, Lee SW. Gene transfer of TRPC6 (dominant negative) restores erectile function in diabetic rats. *J Sex Med*. 2010 Mar;7(3):1126-38; <https://pubmed.ncbi.nlm.nih.gov/20059667/>. Song KM, Kim WJ, Choi MJ, Limanjaya A, Ghatak K, Minh NN, Ock J, Yin GN, Hong SS, Suh JK, Ryu JK. Intracavernous delivery of Dickkopf3 gene or peptide rescues erectile function through enhanced cavernous angiogenesis in the diabetic mouse. *Andrology*. 2020 Sep;8(5):1387-1397; <https://onlinelibrary.wiley.com/doi/10.1111/andr.12784>. Ock J, Suh JK, Hong SS, Kang JH, Yin GN, Ryu JK. IGFBP5 antisense and short hairpin RNA (shRNA) constructs improve erectile function by inducing cavernosum angiogenesis in diabetic mice. *Andrology*. 2023 Feb;11(2):358-371; <https://www.ncbi.nlm.nih.gov/pmc/articles/PMC10087557/pdf>.

²³⁹ Melman A, Bar-Chama N, McCullough A, Davies K, Christ G. The first human trial for gene transfer therapy for the treatment of erectile dysfunction: preliminary results. *Eur Urol*. 2005 Aug;48(2):314-8; <https://citeseerx.ist.psu.edu/document?repid=rep1&type=pdf&doi=3d09a59f89017349e0092300d124afbb5ea75e5a>.

²⁴⁰ Melman A, Bar-Chama N, McCullough A, Davies K, Christ G. hMaxi-K gene transfer in males with erectile dysfunction: results of the first human trial. *Hum Gene Ther*. 2006 Dec;17(12):1165-76; <https://citeseerx.ist.psu.edu/document?repid=rep1&type=pdf&doi=5485005645c9de1b60bb7bdac40bd19dac46fdc4>. Melman A, Biggs G, Davies K, Zhao W, Tar MT, Christ GJ. Gene transfer with a vector expressing Maxi-K from a smooth muscle-specific promoter restores erectile function in the aging rat. *Gene Ther*. 2008 Mar;15(5):364-70; <https://citeseerx.ist.psu.edu/document?repid=rep1&type=pdf&doi=c6218e5e92ebc11c60d744a1bf838b6cbfdb36a9>.

²⁴¹ Song J, Wang J, Liu K, Xu W, Sun T, Liu J. The role of microRNAs in erectile dysfunction: From pathogenesis to therapeutic potential. *Front Endocrinol (Lausanne)*. 2022 Oct 25;13:1034043; <https://www.ncbi.nlm.nih.gov/pmc/articles/PMC9640492/pdf>.

4.9.5 Penile Transplants

Perhaps the most extreme “conventional” treatment for erectile dysfunction would be to perform a penectomy (amputation of the pathological penis) and then transplant a healthy new penis with full erectile functionality. This has apparently never been proposed as a possible treatment for ED in an otherwise fully intact penis because penile transplantation remains uncommon and has heretofore only been used as a restorative procedure in cases of severe penile trauma.²⁴²

The first penis transplant was attempted in China in 2006.²⁴³ Two weeks after the surgery the new penis “was cut off... because of a severe psychological problem of the recipient and his wife”, although subsequent pathologic examination showed no immunological rejection. The first successful transplant occurred in South Africa in 2014 and again in 2017,²⁴⁴ in both cases resulting in “a fully functional penis” capable of erections that allowed the recipients to “satisfy their own and their partners sexual and relationship needs”.²⁴⁵ The first successful penis transplant in the United States occurred in 2016 at Massachusetts General Hospital.²⁴⁶ The

²⁴² Given the present-day “heroic” and costly nature of penile transplants, which are currently used only in cases of “traumatic or oncological substantial phallus loss”, ethical objections would probably be raised to replacing an otherwise fully intact penis lacking only erectile functionality with a transplant. Ngaage LM, Elegbede A, Sugarman J, Nam AJ, Cooney CM, Cooney DS, Rasko YM, Brandacher G, Redett RJ. The Baltimore Criteria for an ethical approach to penile transplantation: a clinical guideline. *Transpl Int*. 2020 May;33(5):471-482; <https://scholar.archive.org/work/isgyb2z2yjezhguhznadjrjrggu/access/wayback/https://onlinelibrary.wiley.com/doi/pdfdirect/10.1111/tri.13545>. van der Merwe A, Moosa MR, Barsdorf N. Ethical and societal challenges in penis transplantation. *Curr Opin Organ Transplant*. 2020 Dec;25(6):594-600; <https://pubmed.ncbi.nlm.nih.gov/33105200/>. Benjamin H, Celine A, Mounia SM, Barbara H, Jean Paul M. Ethical stakes of penile transplantation: A literature review. *J Plast Reconstr Aesthet Surg*. 2022 May;75(5):1529-1536; <https://pubmed.ncbi.nlm.nih.gov/35221229/>.

²⁴³ Hu W, Lu J, Zhang L, Wu W, Nie H, Zhu Y, Deng Z, Zhao Y, Sheng W, Chao Q, Qiu X, Yang J, Bai Y. A preliminary report of penile transplantation. *Eur Urol*. 2006 Oct;50(4):851-3; <https://pubmed.ncbi.nlm.nih.gov/16930814/>. Hu W, Lu J, Zhang L, Wu W, Nie H, Zhu Y, Deng Z, Zhao Y, Sheng W, Chao Q, Qiu X, Yang J, Bai Y. A preliminary report of penile transplantation: part 2. *Eur Urol*. 2006 Nov;50(5):1115-6; discussion 1116; <https://pubmed.ncbi.nlm.nih.gov/17106949/>.

²⁴⁴ van der Merwe A, Graewe F, Zühlke A, Barsdorf NW, Zarrabi AD, Viljoen JT, Ackermann H, Spies PV, Opondo D, Al-Qaoud T, Bezuidenhout K, Nel JD, Bailey B, Moosa MR. Penile allotransplantation for penis amputation following ritual circumcision: a case report with 24 months of follow-up. *Lancet*. 2017 Sep 9;390(10099):1038-1047; <https://frankgraewe.com/wp-content/uploads/2019/09/Penile-allotransplantation-The-Lancet-1.pdf>.

²⁴⁵ van der Merwe A, Toefy Y, Moosa MR, van Deventer H, Scott CJ. Living with someone elses penis: The lived experiences of two South African penile allograft recipients: A descriptive phenomenological study. *Ann Med Surg (Lond)*. 2021 Sep 4;69:102794; <https://www.ncbi.nlm.nih.gov/pmc/articles/PMC8430241/pdf>.

²⁴⁶ Cetrulo CL Jr., *et al*. Penis Transplantation: First US Experience. *Ann Surg*. 2018 May;267(5):983-988; <https://pubmed.ncbi.nlm.nih.gov/28509699/>.

world's first total penis and scrotum transplant was achieved in 2018²⁴⁷ at the Johns Hopkins University School of Medicine.²⁴⁸ As of 2024, these five procedures were the only penis transplants that had been attempted worldwide.²⁴⁹ At least one research project is exploring the feasibility of penile transplantation for the purpose of gender reassignment surgery.²⁵⁰

Other considerations aside, donor supply is the obvious limitation of this treatment modality for ED. Notes one review:²⁵¹ “The pool of available penile donors remains very small, as VCA [vascularized composite allotransplantation]²⁵² donation requires specific permission that is separate from donor consent as designated by a driver's license or donor authorization card, instead requiring the approval of the deceased donor's authorized representative.²⁵³ From willing organ donors, genitourinary organs are among the least likely to be donated; only 61% of men were willing to donate their penis, versus 81% willing to donate a limb.²⁵⁴ Identifying a donor with a healthy penis who is HLA-matched to the recipient and has a similar skin tone can be challenging, as about 86% of prior VCA donors from the USA²⁵⁵ were white.” For treatment of

²⁴⁷ Redett RJ 3rd, *et al.* Total Penis, Scrotum, and Lower Abdominal Wall Transplantation. *N Engl J Med.* 2019 Nov 7;381(19):1876-1878; <https://www.nejm.org/doi/10.1056/NEJMc1907956>.

²⁴⁸ Time was taken to carefully match donor and patient for age, skin tone and certain immunological and viral parameters; <https://www.hopkinsmedicine.org/news/articles/2018/04/first-ever-penis-and-scrotum-transplant-makes-history-at-johns-hopkins>.

²⁴⁹ Lopez CD, Girard AO, Lake IV, Oh BC, Brandacher G, Cooney DS, Burnett AL, Redett RJ. Lessons learned from the first 15 years of penile transplantation and updates to the Baltimore Criteria. *Nat Rev Urol.* 2023 May;20(5):294-307; <https://www.ncbi.nlm.nih.gov/pmc/articles/PMC9838304/pdf>.

²⁵⁰ <https://reports.mountsinai.org/article/uro2023-07-sex-reassignment-surgery-continues-to-advance>.

²⁵¹ Lopez CD, Girard AO, Lake IV, Oh BC, Brandacher G, Cooney DS, Burnett AL, Redett RJ. Lessons learned from the first 15 years of penile transplantation and updates to the Baltimore Criteria. *Nat Rev Urol.* 2023 May;20(5):294-307; <https://www.ncbi.nlm.nih.gov/pmc/articles/PMC9838304/pdf>.

²⁵² Lake IV, Girard AO, Lopez CD, Cooney DS, Burnett AL, Brandacher G, Oh BC, Redett RJ. Penile Transplantation: Lessons Learned and Technical Considerations. *J Urol.* 2022 May;207(5):960-968; <https://www.auajournals.org/doi/epdf/10.1097/JU.0000000000002504>.

²⁵³ Guidance on optimizing VCA recovery from deceased donors. *Organ Procurement and Transplantation Network*, 2018; <https://optn.transplant.hrsa.gov/policies-bylaws/public-comment/guidance-on-optimizing-vca-recovery-from-deceased-donors/>.

²⁵⁴ Ward S, Boger M, Fleishman A, Shenkel J, Calvo A, Pomahac B, Zwolak R, Krishnan N, Rodrigue JR. Attitudes Toward Organ, Tissue, and Vascularized Composite Allograft (VCA) Donation and Transplantation: A Survey of United States Military Veterans. *Transplantation.* 2021 May 1;105(5):1116-1124; https://drive.google.com/file/d/1mYgVmlmKqLOICGpulWfSOW_cBOKoiyZN/view.

²⁵⁵ Wainright JL, Wholley CL, Rosendale J, Cherikh WS, Di Battista D, Klassen DK. VCA Deceased Donors in the United States. *Transplantation.* 2019 May;103(5):990-997; https://ceadtraining.org/pluginfile.php/397/mod_page/content/7/VCA%20Deceased%20Donors%20in%20the%20United%20States.pdf. Ngaage LM, Elegbede A, Sugarman J, Nam AJ, Cooney CM, Cooney DS, Rasko YM, Brandacher G, Redett RJ. The Baltimore Criteria for an ethical approach to penile transplantation: a clinical guideline. *Transpl Int.* 2020 May;33(5):471-482;

erectile dysfunction, it would also be important to secure a replacement organ from a young donor whose penis was ED-free, thus promising many years of full erectile functionality. An additional difficulty with contemporary penile transplantation is that the recipient would face a lifetime of immunosuppressive medications to prevent rejection of the donor organ, solely to regain erectile function.

Penis donations at time of death for scientific study are more common and typically involve individuals who bequeath their bodies to medical science for educational or research purposes, but these organs are likely not sufficiently functional to warrant transplantation onto a healthy recipient. As of 2024, there are no known or documented cases of illegal sales of human penises by living donors in the illegal organ trade markets. It is believed to be impractical and unlikely for penises to be trafficked in the illegal organ market because a penis transplant is a highly complex procedure that involves not just the organ itself but also the reattachment of nerves and blood vessels to restore both function and sensation, requiring highly specialized surgical skills. The illegal organ trade²⁵⁶ typically focuses on organs that can be transplanted to treat life-threatening conditions, such as kidneys or parts of the liver, where there is a high demand and a corresponding willingness to pay significant sums of money, and where the organs can be removed with the donor still able to live a relatively normal life, making them more viable for illegal trade.

With donor penises in short supply, the traditional alternative to a damaged organ has always been phalloplasty²⁵⁷ – the surgical creation of a penis-like structure.²⁵⁸ As described by one reviewer:²⁵⁹ “Traditional reconstructive options use the principles of free-tissue transfer, which involves taking a patient’s native tissues from another part of their body, harvesting these tissues with a distinct artery and vein to perfuse the entire tissue segment adequately, safely reshaping this tissue segment to appear and function as a neophallus, and using microvascular surgical techniques to connect this newly fashioned penile substitute to recipient arteries, veins, nerves and the urethra for perfusion and functional restoration.”²⁶⁰ These traditional reconstructive

<https://scholar.archive.org/work/isgyb2z2yjezhguhznadjrggu/access/wayback/https://onlinelibrary.wiley.com/doi/pdfdirect/10.1111/tri.13545>.

²⁵⁶ https://en.wikipedia.org/wiki/Organ_trade#Illegal_organ_trade.

²⁵⁷ <https://en.wikipedia.org/wiki/Phalloplasty>.

²⁵⁸ Ottaiano N, Pincus J, Tannenbaum J, Dawood O, Raheem O. Penile reconstruction: An up-to-date review of the literature. *Arab J Urol*. 2021 Jul 26;19(3):353-362; <https://www.ncbi.nlm.nih.gov/pmc/articles/PMC8451639/pdf>.

²⁵⁹ Lopez CD, Girard AO, Lake IV, Oh BC, Brandacher G, Cooney DS, Burnett AL, Redett RJ. Lessons learned from the first 15 years of penile transplantation and updates to the Baltimore Criteria. *Nat Rev Urol*. 2023 May;20(5):294-307; <https://www.ncbi.nlm.nih.gov/pmc/articles/PMC9838304/pdf>.

²⁶⁰ Monstrey S, Hoebeke P, Selvaggi G, Ceulemans P, Van Landuyt K, Blondeel P, Hamdi M, Roche N, Weyers S, De Cuyper G. Penile reconstruction: is the radial forearm flap really the standard technique? *Plast Reconstr Surg*. 2009 Aug;124(2):510-518; http://www.hbrs.no/wp-content/uploads/2019/02/Penile_Reconstruction_Is_the_Radial_Forearm_Flap.22.pdf. Doornaert M, Hoebeke P, Ceulemans P, TSjoen G, Heylens G, Monstrey S. Penile reconstruction with the radial forearm

principles have yielded satisfactory results, but limitations persist, including donor site morbidity, neo-urethral fistulae formation at the neophallus and neo-urethral stricture.²⁶¹ Furthermore, no substitute tissue is capable of truly replacing native penile tissue and its unique properties — reconstructed tissue offers poor erogenous sensation and the unique erectile capacity of penile corpora tissue can only be mimicked using a prosthesis.^{262,} The ultimate goals of phalloplasty do include the creation of an aesthetically penis-like structure with sensation and the ability to have an erection, and in some cases phalloplasty can incorporate native genital tissue to better improve orgasmic function.²⁶³

Another possible solution to the transplantable penis shortage is to employ the emerging technologies of tissue engineering and regenerative medicine to grow or fabricate a new organ from scratch. Tissue engineering might employ synthetic or natural matrices termed scaffolds that can be seeded with living cells created using novel methods of cell culture that allow autologous cells to be grown *ex vivo* from a small sample of a patient's own tissue.²⁶⁴ Bioengineers have initially focused on replacements for the corpus cavernosum, the principal tissue involved in penile erection, using animal models.²⁶⁵ For example, biodegradable 3D printed hydrogel scaffolds seeded with muscle-derived stem cells have revascularized and repaired corpora cavernosa defects in rabbits, recovering penile erectile and ejaculation functions.²⁶⁶ At least one group has announced preparation for a future Phase 1 human clinical

flap: an update. *Handchir Mikrochir Plast Chir.* 2011 Aug;43(4):208-14; <https://www.hbrs.no/wp-content/uploads/2019/02/Monstrey-phalloplasty.pdf>.

²⁶¹ Morrison SD, Shakir A, Vyas KS, Kirby J, Crane CN, Lee GK. Phalloplasty: A Review of Techniques and Outcomes. *Plast Reconstr Surg.* 2016 Sep;138(3):594-615; http://www.hbrs.no/wp-content/uploads/2019/02/Phalloplasty_A_Review_of_Techniques_and_Outcomes.13.pdf.

²⁶² Ma S, Cheng K, Liu Y. Sensibility following innervated free radial forearm flap for penile reconstruction. *Plast Reconstr Surg.* 2011 Jan;127(1):235-241; <https://pubmed.ncbi.nlm.nih.gov/21200218/>.

²⁶³ Sinatti C, Wolff D, Buncamper M, Verla W, Claes K, Lumen N, Waterloos M, Monstrey S, Hoebeke P, Spinoit AF. Phalloplasty in cis-men with penile insufficiency: evaluation of outcomes and surgical complications : Good ability to achieve orgasm, high urinary complication rate. *Int J Impot Res.* 2021 Mar;33(2):178-183; <https://pubmed.ncbi.nlm.nih.gov/33303986/>.

²⁶⁴ Patel MN, Atala A. Tissue engineering of the penis. *ScientificWorldJournal.* 2011;11:2567-78; <https://www.ncbi.nlm.nih.gov/pmc/articles/PMC3253692/pdf>. Elia E, Caneparo C, McMartin C, Chabaud S, Bolduc S. Tissue Engineering for Penile Reconstruction. *Bioengineering (Basel).* 2024 Feb 28;11(3):230; <https://www.ncbi.nlm.nih.gov/pmc/articles/PMC10967839/pdf>.

²⁶⁵ Kwon TG, Yoo JJ, Atala A. Autologous penile corpora cavernosa replacement using tissue engineering techniques. *J Urol.* 2002 Oct;168(4 Pt 2):1754-8; <https://pubmed.ncbi.nlm.nih.gov/12352353/>. Andrew TW, Kanapathy M, Murugesan L, Muneer A, Kalaskar D, Atala A. Towards clinical application of tissue engineering for erectile penile regeneration. *Nat Rev Urol.* 2019 Dec;16(12):734-744; https://discovery.ucl.ac.uk/id/eprint/10087577/1/44952_3_art_0_pyfnrv_Nature%202019.pdf. Chouhan JD, Thakker PU, Terlecki RP. Engineering of erectile tissue: the state and future of corporal restoration. *World J Urol.* 2020 Sep;38(9):2109-2113; <https://pubmed.ncbi.nlm.nih.gov/31069461/>.

²⁶⁶ An G, Guo F, Liu X, Wang Z, Zhu Y, Fan Y, Xuan C, Li Y, Wu H, Shi X, Mao C. Functional reconstruction of injured corpus cavernosa using 3D-printed hydrogel scaffolds seeded with HIF-1 α -

trial to create bioengineered penile tissue constructs to be grafted onto a preexisting penile deformity.²⁶⁷ However, almost all research to date targets the creation of viable tissue for local repair purposes, not complete functional organs, and in animal models, not human patients.

In one report of applying the tissue engineering approach to the creation of a viable rabbit penis at the Wake Forest Institute for Regenerative Medicine in North Carolina,²⁶⁸ a donor rabbit penis was soaked in a mild detergent of enzymes for a couple of weeks to wash away the donor cells, leaving a mostly collagen scaffold – a skeleton that looked and felt just like the organ. The structure was then reseeded with the patient’s own cells taken in a biopsy from salvageable tissue and grown in culture. Smooth muscle cells, which relax during an erection to allow the vessels to dilate and the penis to fill with blood, were introduced first, followed by endothelial cells that line the interior surface of blood and lymphatic vessels, after which the bioengineered penis was ready to be transplanted to the recipient. After the transplantation, the researchers “watched anxiously to see if two rabbits would have sex. The suspense was short-lived: within a minute of being put together, the male mounted the female and successfully mated.” The procedure was performed on 12 rabbits, all of whom mated and four of which produced offspring. As of 2024, transplantation of a complete bioengineered penis had not yet been attempted in humans.

4.10 Lifestyle Changes

Psychosexual counseling is often advocated to address psychological contributors in ED cases, while encouraging lifestyle changes such as weight management, cessation of smoking, and regular exercise²⁶⁹ that might improve overall cardiovascular health and ED outcomes. Kegel exercises²⁷⁰ can improve muscle tone and circulation in the pelvic region while also enhancing the ability to achieve and maintain erections.²⁷¹ Various aphrodisiacs²⁷² (notoriously including cantharidin,²⁷³ aka. Spanish Fly²⁷⁴), pheromones,²⁷⁵ and love potions²⁷⁶ have been alleged to increase sexual desire, but appear to be of dubious effectiveness.

expressing stem cells. Nat Commun. 2020 Jun 1;11(1):2687;
<https://www.ncbi.nlm.nih.gov/pmc/articles/PMC7264263/pdf>.

²⁶⁷ Bioengineered Penile Tissue Constructs for Irreversibly Damaged Penile Corpora;
<https://clinicaltrials.gov/study/NCT03463239>. See also: Chouhan JD, Thakker PU, Terlecki RP.
 Engineering of erectile tissue: the state and future of corporal restoration. World J Urol. 2020
 Sep;38(9):2109-2113; <https://pubmed.ncbi.nlm.nih.gov/31069461/>.

²⁶⁸ <https://www.theguardian.com/education/2014/oct/04/penis-transplants-anthony-atala-interview>.

²⁶⁹ https://en.wikipedia.org/wiki/Kegel_exercise#Men.

²⁷⁰ https://en.wikipedia.org/wiki/Kegel_exercise.

²⁷¹ <https://www.webmd.com/men/best-exercises-erectile-dysfunction-premature-ejaculation>.

²⁷² <https://en.wikipedia.org/wiki/Aphrodisiac>.

²⁷³ https://en.wikipedia.org/wiki/Cantharidin#Aphrodisiac_preparations.

²⁷⁴ https://en.wikipedia.org/wiki/Lytta_vesicatoria.

²⁷⁵ https://en.wikipedia.org/wiki/Pheromone#Human_sex_pheromone_controversies and
https://en.wikipedia.org/wiki/Human_sex_pheromones.

²⁷⁶ https://en.wikipedia.org/wiki/Love_potion.

5. Nanorobotic Treatments for Erectile Dysfunction

The advent of nanofactories will make it possible to comprehensively treat and cure male erectile dysfunction using medical nanorobots generally of the types summarized in [Section 5.1](#), unlike conventional ED treatments ([Section 4](#)) that provide only partial or temporary symptomatic relief.

[Section 5.2](#) describes a range of nanorobotic treatments that would provide actual permanent cures for the underlying problems that are causing the ED, including curative treatments for impaired blood flow ([Section 5.2.1](#)), neurological disorders ([Section 5.2.2](#)), and other ED-related pathologies and co-morbidities of erectile dysfunction ([Section 5.2.3](#)) using fleets of individual medical nanorobots, or using a nanorobotic device called a nanocatheter ([Section 5.2.4](#)) that can be inserted into deep tissues to directly perform similar necessary repairs such as arterial plaque debridement, whole cell transport and implantation, cytosolic intervention in individual cells, and tissue and nerve repair.

Medical nanorobots can also provide symptomatic relief from ED ([Section 5.3](#)) without correcting the underlying organic problem that is causing the condition, because temporarily fixing a symptom can often be easier and quicker than permanently curing multiple underlying diseases. There are several convenient methods by which nanorobots deployed in penile tissues could achieve effective vasodilation sufficient to establish and maintain a normal erection ([Section 5.3.1](#)), supplemented by nanorobots deployed in the brain that can artificially stimulate sexual arousal ([Section 5.3.2](#)) and other nanorobotic systems designed to enhance or extend the orgasmic response ([Section 5.3.3](#)).

Nanorobotic penile prostheses ([Section 5.4](#)) could provide a reliable substitute for erectile functionality without curing or treating the underlying biological pathology of ED. Examples may include a nanomechanical implant ([Section 5.4.1](#)), a nanorobotic condom ([Section 5.4.2](#)), an implanted motorized mesh ([Section 5.4.3](#)), or a utility-fog based condom, implant, or whole-penis transplant ([Section 5.4.4](#)).

[Section 5.5](#) briefly poses (but defers answering) the question of the relevance of physical sex in a future world of “supermen” where people can achieve orgasm simply by an act of will.

5.1 Examples of Medical Nanorobots

The early genesis of the concept of medical nanorobots, manufactured in nanofactories, sprang from the visionary idea that tiny nanomachines could be designed, manufactured, and introduced into the human body to perform cellular repairs at the molecular level. Although the medical application of nanotechnology was championed in the popular writings of Drexler²⁷⁷ in the 1980s and 1990s and in the technical writings of Freitas²⁷⁸ in the 1990s, 2000s, 2010s, and 2020s, the first scientist to voice the possibility was the late Nobel physicist Richard P. Feynman, who worked on the Manhattan Project at Los Alamos during World War II and later taught at Caltech for most of his professorial career.

In his prescient 1959 talk “There’s Plenty of Room at the Bottom,” Feynman proposed employing machine tools to make smaller machine tools, these to be used in turn to make still smaller machine tools, and so on all the way down to the atomic level.²⁷⁹ He prophetically concluded that this is “a development which I think cannot be avoided.” After discussing his ideas with a colleague, Feynman offered the first known proposal for a medical nanorobotic procedure of any kind – in this instance, to cure heart disease: “A friend of mine (Albert R. Hibbs) suggests a very interesting possibility for relatively small machines. He says that, although it is a very wild idea, it would be interesting in surgery if you could swallow the surgeon. You put the mechanical surgeon inside the blood vessel and it goes into the heart and looks around. (Of course the information has to be fed out.) It finds out which valve is the faulty one and takes a little knife and slices it out. Other small machines might be permanently incorporated in the body to assist some inadequately functioning organ.” Later in his historic 1959 lecture, Feynman urges us to consider the possibility, in connection with microscopic biological cells, “that we can manufacture an object that maneuvers at that level!” The field had progressed far enough by 2007, half a century after Feynman’s speculations, to allow Martin Moskovits, Professor of Chemistry and Dean of Physical Science at UC Santa Barbara, to write²⁸⁰ that “the notion of an ultra-small robot that can, for example, navigate the bloodstream performing microsurgery or

²⁷⁷ Drexler KE. *Engines of Creation: The Coming Era of Nanotechnology*. Anchor Press/Doubleday, New York, 1986, Chapter 7 “Engines of Healing”; https://web.archive.org/web/20180722191948/http://e-drexler.com/d/06/00/EOC/EOC_Chapter_7.html. Drexler KE, Peterson C, Pergamit G. *Unbounding the Future: The Nanotechnology Revolution*. William Morrow/Quill Books, New York, 1991, Chapter 10 “Nanomedicine”; https://web.archive.org/web/20100302193412/http://www.foresight.org/UTF/Unbound_LBW/chapt_10.html.

²⁷⁸ Freitas RA Jr. *Nanomedicine, Volume I: Basic Capabilities*. Landes Bioscience, Georgetown, TX, 1999; <http://www.nanomedicine.com/NMI.htm>. Freitas RA Jr. *Nanomedicine, Volume IIA: Biocompatibility*. Landes Bioscience, Georgetown, TX, 2003; <http://www.nanomedicine.com/NMIIA.htm>. Freitas RA Jr. “Technical Analyses of Types of Diamondoid Medical Nanorobots,” <http://www.nanomedicine.com/#NanorobotAnalyses>. See also: <http://www.rfreitas.com/NanoPubls.htm>.

²⁷⁹ Feynman RP. There’s plenty of room at the bottom. *Eng Sci (CalTech)* 1960;23:22-36; <http://www.zyvex.com/nanotech/feynman.html>.

²⁸⁰ Moskovits M. Nanoassemblers: A likely threat? *Nanotech. Law & Bus.* 2007;4:187-195; https://heinonline.org/hol/cgi-bin/get_pdf.cgi?handle=hein.journals/nantechlb4§ion=29.

activating neurons so as to restore muscular activity, is not an unreasonable goal, and one that may be realized in the near future.”

Many questions arise when one first encounters the idea of micron-scale nanorobots, constructed of nanoscale components and operating inside the human body. At the most fundamental level, technical questions about the influence of quantum effects on molecular structures, friction and wear among nanomechanical components, radiation damage, other failure mechanisms, the influence of thermal noise on reliability, and the effects of Brownian bombardment on nanomachines have all been extensively discussed and resolved in the literature.²⁸¹ Self-assembled molecular motors consisting of just 50-100 atoms have been demonstrated experimentally since the late 1990s.²⁸² Published discussions of technical issues of specific relevance to medical nanorobots include proposed methods for recognizing, sorting and pumping individual molecules;²⁸³ theoretical designs for mechanical nanorobot sensors;²⁸⁴ flexible nanorobot hull surfaces,²⁸⁵ power sources,²⁸⁶ communications²⁸⁷ and navigation²⁸⁸ systems, and

²⁸¹ Drexler KE. *Nanosystems: Molecular Machinery, Manufacturing, and Computation*. John Wiley & Sons, New York, 1992; <https://www.amazon.com/dp/0471575186/>. Freitas RA Jr. *Nanomedicine, Volume I: Basic Capabilities*. Landes Bioscience, Georgetown, TX, 1999; <http://www.nanomedicine.com/NMI/2.1.htm>.

²⁸² Kelly TR, De Silva H, Silva RA. Unidirectional rotary motion in a molecular system. *Nature*. 1999 Sep 9;401:150-152; <https://www.bostoncollege.org/content/dam/bc1/schools/mcas/Chemistry/news-and-notes/pdf/3.pdf>. Koumura N, Zijlstra RW, van Delden RA, Harada N, Feringa BL. Light-driven monodirectional molecular rotor. *Nature* 1999 Sep 9;401:152-155; <https://core.ac.uk/download/pdf/148148838.pdf>. Huang TJ, Lu W, Tseng HR, *et al.* Molecular shuttle switching in closely packed Langmuir films, 11th Foresight Conf. Mol. Nanotech., San Francisco CA, 10-12 Oct 2003. Leigh DA, Wong JKY, Dehez F, Zerbetto F. Unidirectional rotation in a mechanically interlocked molecular rotor. *Nature*. 2003 Jul 10;424(6945):174-179; <http://biotheory.phys.cwru.edu/phys414/nature01758.pdf>. Browne WR, Feringa BL. Making molecular machines work. *Nat Nanotechnol*. 2006 Oct;1(1):25-35; <https://www.rug.nl/research/portal/files/6702682/2006NatureNanotechBrowne.pdf>. Kay ER, Leigh DA, Zerbetto F. Synthetic molecular motors and mechanical machines. *Angew Chem Int Ed* 2007;46(1-2):72-191; <https://pubmed.ncbi.nlm.nih.gov/17133632/>.

²⁸³ Drexler KE. *Nanosystems: Molecular Machinery, Manufacturing, and Computation*. John Wiley & Sons, New York, 1992, Section 13.2; <https://www.amazon.com/dp/0471575186/>. Freitas RA Jr. *Nanomedicine, Volume I: Basic Capabilities*. Landes Bioscience, Georgetown, TX, 1999, Chapter 3, “Molecular Transport and Sortation”; <http://www.nanomedicine.com/NMI/3.1.htm>.

²⁸⁴ Freitas RA Jr. *Nanomedicine, Volume I: Basic Capabilities*. Landes Bioscience, Georgetown, TX, 1999, Chapter 4, “Nanosensors and Nanoscale Sensing”; <http://www.nanomedicine.com/NMI/4.1.htm>.

²⁸⁵ Freitas RA Jr. *Nanomedicine, Volume I: Basic Capabilities*. Landes Bioscience, Georgetown, TX, 1999, Chapter 5, “Shapes and Metamorphic Surfaces”; <http://www.nanomedicine.com/NMI/5.1.htm>. Hogg T. Energy dissipation by metamorphic micro-robots in viscous fluids. *J Micro-Bio Robotics* 2016; 11(1-4):85-95; <https://arxiv.org/pdf/1507.01145>.

²⁸⁶ Freitas RA Jr. *Nanomedicine, Volume I: Basic Capabilities*. Landes Bioscience, Georgetown, TX, 1999, Chapter 6, “Power”; <http://www.nanomedicine.com/NMI/6.1.htm>. Hogg T, Freitas RA Jr. Chemical power for microscopic robots in capillaries. *Nanomedicine*. 2010 Apr;6(2):298-317; <https://arxiv.org/pdf/0906.5022>.

manipulator mechanisms;²⁸⁹ nanorobot mobility mechanisms for travel through bloodstream, tissues and cells,²⁹⁰ and for penetration of the blood-brain barrier;²⁹¹ onboard clocks²⁹² and nanocomputers;²⁹³ and the full panoply of nanorobot biocompatibility issues.²⁹⁴

The idea of placing semi-autonomous self-powered nanorobots inside of us might seem a bit odd, but the human body already teems with similar natural nanodevices. More than 40 trillion single-celled microbes swim through our colon, outnumbering our tissue cells almost ten to one.²⁹⁵ Many bacteria move by whipping around a tiny tail, or flagellum, that is driven by a 30-nanometer biological ionic nanomotor powered by pH differences between the inside and the outside of the bacterium. Our bodies also maintain a population of more than a trillion motile biological nanodevices called fibroblasts and white cells such as neutrophils and lymphocytes,

²⁸⁷ Freitas RA Jr. Nanomedicine, Volume I: Basic Capabilities. Landes Bioscience, Georgetown, TX, 1999, Chapter 7, “Communication”; <http://www.nanomedicine.com/NMI/7.1.htm>. Hogg T, Freitas RA Jr. Acoustic communication for medical nanorobots. Nano Commun Networks 2012; 3(2):83-102; <https://arxiv.org/pdf/1202.0568>.

²⁸⁸ Freitas RA Jr. Nanomedicine, Volume I: Basic Capabilities. Landes Bioscience, Georgetown, TX, 1999, Chapter 8, “Navigation”; <http://www.nanomedicine.com/NMI/8.1.htm>.

²⁸⁹ Freitas RA Jr. Nanomedicine, Volume I: Basic Capabilities. Landes Bioscience, Georgetown, TX, 1999, Section 9.3, “Nanomanipulators”; <http://www.nanomedicine.com/NMI/9.3.htm>.

²⁹⁰ Freitas RA Jr. Nanomedicine, Volume I: Basic Capabilities. Landes Bioscience, Georgetown, TX, 1999, Section 9.4, “*In Vivo* Locomotion”; <http://www.nanomedicine.com/NMI/9.4.htm>. Hogg T. Using surface-motions for locomotion of microscopic robots in viscous fluids. J Micro-Bio Robotics. 2014; 9(3-4):61-77; <https://arxiv.org/pdf/1311.0801>.

²⁹¹ Freitas RA Jr. The Alzheimer Protocols: A Nanorobotic Cure for Alzheimer’s Disease and Related Neurodegenerative Conditions. IMM Report No. 48, June 2016; Section 4.3 “Medical Nanorobots: Ingress to, and Egress from, the Brain”; <http://www.imm.org/Reports/rep048.pdf>. Freitas RA Jr. Nanomedicine, Volume IIA: Biocompatibility. Landes Bioscience, Georgetown, TX, 2003; Section 15.3.6.5, “Biocompatibility with Neural Cells”; <http://www.nanomedicine.com/NMIIA/15.3.6.5.htm#p8>.

²⁹² Freitas RA Jr. Nanomedicine, Volume I: Basic Capabilities. Landes Bioscience, Georgetown, TX, 1999, Section 10.1, “Nanochronometry”; <http://www.nanomedicine.com/NMI/10.1.htm>.

²⁹³ Drexler KE. Nanosystems: Molecular Machinery, Manufacturing, and Computation. John Wiley & Sons, New York, 1992, Chapter 12; <https://www.amazon.com/dp/0471575186/>. Freitas RA Jr. Nanomedicine, Volume I: Basic Capabilities. Landes Bioscience, Georgetown, TX, 1999, Section 10.2, “Nanocomputers”; <http://www.nanomedicine.com/NMI/10.2.htm>.

²⁹⁴ Freitas RA Jr. Nanomedicine, Volume IIA: Biocompatibility. Landes Bioscience, Georgetown, TX, 2003; <http://www.nanomedicine.com/NMIIA.htm>.

²⁹⁵ Freitas RA Jr. Nanomedicine, Volume I: Basic Capabilities. Landes Bioscience, Georgetown, TX, 1999, Section 8.5.1, “Cytometrics”; <http://www.nanomedicine.com/NMI/8.5.1.htm>.

each measuring up to $\sim 10\ \mu\text{m}$ in size.²⁹⁶ These beneficial natural nanorobots are constantly crawling around inside us, repairing damaged tissues, attacking invading microbes, and gathering up foreign particles and transporting them to various organs for disposal from the body.²⁹⁷

The greatest power of nanomedicine will emerge as we learn to design and construct complete artificial nanorobots using nanometer-scale parts and subsystems such as diamondoid bearings and gears, nanomotors and molecular pumps, nanomanipulators, nanosensors, nanobatteries, and nanocomputers.

In this Section we briefly describe three major classes of hypothetical medical nanorobots, listed in order of increasing capacity and sophistication:

- (1) **free-floating nonmotile nanorobots** (e.g., respirocytes; [Section 5.1.1](#)),
- (2) **motile nanorobots** (e.g., microbivores; [Section 5.1.2](#)), and
- (3) **cell repair nanorobots** (e.g., chromalloyocytes; [Section 5.1.3](#)).

Much of the following material is drawn from a previously published summary²⁹⁸ which also included a discussion of the forthcoming development of nanofactories that can fabricate the atomically precise nanorobots that would be used in the treatments described elsewhere in this paper.

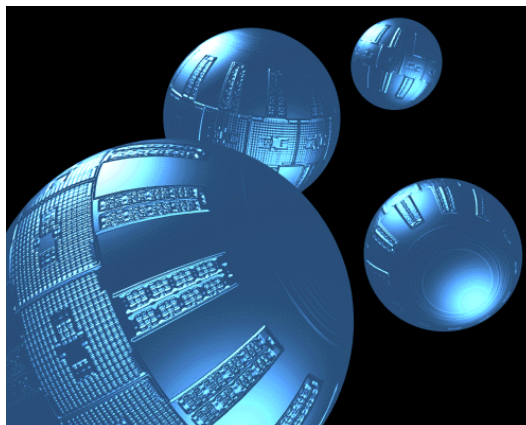
²⁹⁶ Freitas RA Jr. Nanomedicine, Volume I: Basic Capabilities. Landes Bioscience, Georgetown, TX, 1999, Section 8.5.1, “Cytometrics”; <http://www.nanomedicine.com/NMI/8.5.1.htm>.

²⁹⁷ Freitas RA Jr. Nanomedicine, Volume IIA: Biocompatibility. Landes Bioscience, Georgetown, TX, 2003; Section 15.4.3.1, “Phagocytes, Phagocytosis, and the RES”; <http://www.nanomedicine.com/NMIIA/15.4.3.1.htm>.

²⁹⁸ Freitas RA Jr. Cryostasis Revival: The Recovery of Cryonics Patients through Nanomedicine. Alcor Life Extension Foundation, Scottsdale AZ, 2022; Section 1.2 “Medical Nanorobotics” and Section 1.3 “Atomically Precise Manufacturing of Medical Nanorobots”; <https://www.alcor.org/cryostasis-revival/>.

5.1.1 Respirocyte-Class Nanorobots

The first theoretical design study of a medical nanorobot ever published in a peer-reviewed medical journal (by Freitas in 1998)²⁹⁹ described an artificial mechanical red blood cell or “respirocyte” to be made of 18 billion precisely arranged atoms. The device was to be a bloodborne spherical 1- μm diameter diamondoid 1000-atmosphere pressure vessel³⁰⁰ with active pumping³⁰¹ powered by the oxidation of endogenous serum glucose,³⁰² able to deliver 236 times more oxygen to the tissues per unit volume than natural red cells and to manage acidity caused by carbonic acid formation, all controlled by gas concentration sensors³⁰³ and an onboard nanocomputer.³⁰⁴



The basic operation of respirocytes (image, above; artwork by Forrest Bishop)³⁰⁵ is straightforward. These nanorobots would mimic the action of the natural hemoglobin-filled red blood cells, while operating at 1000 atm vs. only 0.1-0.5 atm equivalent for natural Hb. In the tissues, oxygen will be pumped out of the device by the molecular sorting rotors on one side. Carbon dioxide will be pumped into the device by molecular sorting rotors on the other side, one

²⁹⁹ Freitas RA Jr. Exploratory design in medical nanotechnology: a mechanical artificial red cell. *Artif Cells Blood Substit Immobil Biotechnol.* 1998 Jul;26(4):411-30; <https://www.tandfonline.com/doi/pdf/10.3109/10731199809117682>. A longer version of this paper appears at:

<https://web.archive.org/web/20100420085137/http://www.foresight.org/Nanomedicine/Respirocytes.html>.

³⁰⁰ Freitas RA Jr. *Nanomedicine, Volume I: Basic Capabilities*. Landes Bioscience, Georgetown, TX, 1999, Section 10.3, “Pressure Storage and Ballasting”; <http://www.nanomedicine.com/NMI/10.3.htm>.

³⁰¹ Freitas RA Jr. *Nanomedicine, Volume I: Basic Capabilities*. Landes Bioscience, Georgetown, TX, 1999, Section 3.4.2, “Sorting Rotors”; <http://www.nanomedicine.com/NMI/3.4.2.htm>.

³⁰² Freitas RA Jr. *Nanomedicine, Volume I: Basic Capabilities*. Landes Bioscience, Georgetown, TX, 1999, Section 6.3.4, “Chemical Energy Conversion Processes”; <http://www.nanomedicine.com/NMI/6.3.4.htm>.

³⁰³ Freitas RA Jr. *Nanomedicine, Volume I: Basic Capabilities*. Landes Bioscience, Georgetown, TX, 1999, Section 4.2.1, “Broadband Receptor Arrays”; <http://www.nanomedicine.com/NMI/4.2.1.htm>.

³⁰⁴ Drexler KE. *Nanosystems: Molecular Machinery, Manufacturing, and Computation*. John Wiley & Sons, New York, 1992, Chapter 12; <https://www.amazon.com/dp/0471575186/>. Freitas RA Jr. *Nanomedicine, Volume I: Basic Capabilities*. Landes Bioscience, Georgetown, TX, 1999, Section 10.2, “Nanocomputers”; <http://www.nanomedicine.com/NMI/10.2.htm>.

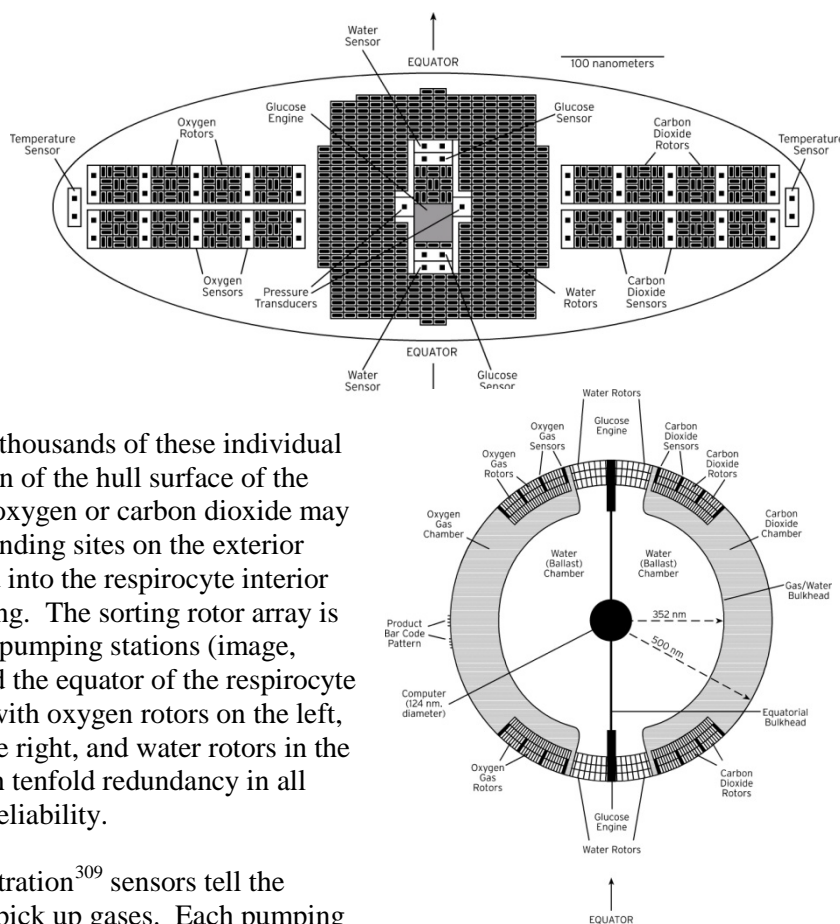
³⁰⁵

<https://web.archive.org/web/20160325053612/https://foresight.org/Nanomedicine/Gallery/Captions/Image139.html>.

molecule at a time. Half a minute later, when the respirocyte reaches the patient's lungs in the normal course of the circulation of the blood, these same rotors reverse their direction of rotation, recharging the device with fresh oxygen and dumping the stored CO₂, which diffuses into the lungs and can then be exhaled by the patient. Each rotor requires very little power, only ~0.03 pW to pump ~10⁶ molecules/sec in continuous operation.

In the exemplar respirocyte design,³⁰⁶ onboard pressure tanks can hold up to 3 billion oxygen (O₂) or carbon dioxide (CO₂) molecules. Molecular sorting rotors³⁰⁷ are arranged on the surface to load and unload gases from the pressurized tanks. Tens of thousands of these individual pumps cover a large fraction of the hull surface of the respirocyte. Molecules of oxygen or carbon dioxide may drift into their respective binding sites on the exterior rotor surface and be carried into the respirocyte interior as the rotor turns in its casing. The sorting rotor array is organized into 12 identical pumping stations (image, above right) laid out around the equator of the respirocyte (cutaway image, at right), with oxygen rotors on the left, carbon dioxide rotors on the right, and water rotors in the middle of each station, with tenfold redundancy in all components for enhanced reliability.

Temperature³⁰⁸ and concentration³⁰⁹ sensors tell the devices when to release or pick up gases. Each pumping



³⁰⁶ Freitas RA Jr. Exploratory design in medical nanotechnology: a mechanical artificial red cell. *Artif Cells Blood Substit Immobil Biotechnol.* 1998 Jul;26(4):411-30; <https://www.tandfonline.com/doi/pdf/10.3109/10731199809117682>. A longer version of this paper appears at: <https://web.archive.org/web/20100420085137/http://www.foresight.org/Nanomedicine/Respirocytes.html>.

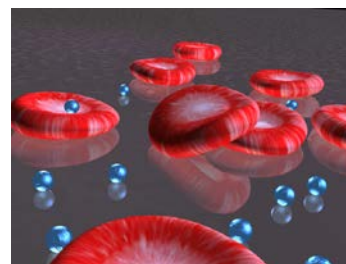
³⁰⁷ Drexler KE. *Nanosystems: Molecular Machinery, Manufacturing, and Computation*. John Wiley & Sons, New York, 1992, Section 13.2; <https://www.amazon.com/dp/0471575186/>. Freitas RA Jr. *Nanomedicine, Volume I: Basic Capabilities*. Landes Bioscience, Georgetown, TX, 1999, Section 3.4.2, "Sorting Rotors"; <http://www.nanomedicine.com/NMI/3.4.2.htm>.

³⁰⁸ Freitas RA Jr. *Nanomedicine, Volume I: Basic Capabilities*. Landes Bioscience, Georgetown, TX, 1999, Section 4.6, "Thermal Nanosensors"; <http://www.nanomedicine.com/NMI/4.6.htm>.

³⁰⁹ Freitas RA Jr. *Nanomedicine, Volume I: Basic Capabilities*. Landes Bioscience, Georgetown, TX, 1999, Section 4.2, "Chemical and Molecular Nanosensors"; <http://www.nanomedicine.com/NMI/4.2.htm>.

station will have special pressure sensors³¹⁰ to receive ultrasonic acoustic messages³¹¹ so the physician can (a) tell the devices to turn on or off, or (b) change the operating parameters of the devices, while the nanorobots are inside a patient. The onboard nanocomputer enables complex device behaviors also remotely reprogrammable by the physician via externally applied ultrasound acoustic signals. Internal power will be transmitted mechanically or hydraulically using an appropriate working fluid, and can be distributed as required using rods and gear trains³¹² or using pipes and mechanically operated valves, controlled by the nanocomputer. There is also a large internal void surrounding the nanocomputer which can be a vacuum, or can be filled with (or emptied of) up to 6 billion molecules of water. This will allow the device to control its buoyancy very precisely and provides a crude but simple method for removing respirocytes from the body using a blood centrifuge,³¹³ a future procedure that has been termed “nanapheresis”.³¹⁴

A 5 cc therapeutic dose of 50% respirocyte saline suspension containing 5 trillion nanorobots would exactly replace the gas carrying capacity of the patients entire 5.4 liters of blood. Each device stores enough onboard glucose/O₂ to provide power for at least one circulation time (60 sec), and can also store the CO₂.³¹⁵ If up to 1 liter of respirocyte suspension could safely be added to the human bloodstream,³¹⁶ this would keep a patient’s tissues oxygenated for up to an hour even if a heart attack caused the heart to stop beating, or if there was a complete absence of respiration or no external availability of oxygen. Primary medical applications of respirocytes (image, above; artwork by Forrest



³¹⁰ Freitas RA Jr. Nanomedicine, Volume I: Basic Capabilities. Landes Bioscience, Georgetown, TX, 1999, Section 4.5, “Pressure Sensing”; <http://www.nanomedicine.com/NMI/4.5.htm>.

³¹¹ Freitas RA Jr. Nanomedicine, Volume I: Basic Capabilities. Landes Bioscience, Georgetown, TX, 1999, Section 7.2.2, “Acoustic Broadcast Communication”; <http://www.nanomedicine.com/NMI/7.2.2.htm>.

³¹² Freitas RA Jr. Nanomedicine, Volume I: Basic Capabilities. Landes Bioscience, Georgetown, TX, 1999, Section 6.4.3.4, “Gear Trains and Mechanical Tethers”; <http://www.nanomedicine.com/NMI/6.4.3.4.htm>.

³¹³ Freitas RA Jr. Cryostasis Revival: The Recovery of Cryonics Patients through Nanomedicine. Alcor Life Extension Foundation, Scottsdale AZ, 2022; Appendix M, “Nanorobot Extraction from the Body”; <https://www.alcor.org/cryostasis-revival/>.

³¹⁴ Freitas RA Jr. Nanomedicine, Volume I: Basic Capabilities. Landes Bioscience, Georgetown, TX, 1999, Section 10.3.6, “Buoyancy Control and Nanapheresis”; <http://www.nanomedicine.com/NMI/10.3.6.htm>.

³¹⁵ Aqueous conversion of CO₂ to carbonic acid is slow, a significant fraction of a second, while the reverse takes ~300 nsec at neutral pH, hence this equilibrium reaction shouldn’t interfere with the respirocyte sorting rotor CO₂ molecule identification and removal process from plasma water. Personal communication from Brian Wowk to Robert Freitas, 30 Sep 2021.

³¹⁶ Freitas RA Jr. Nanomedicine Vol. IIA: Biocompatibility. Landes Bioscience, Georgetown, TX, 2003, Section 15.6.2, “Bloodstream Intrusiveness”; <http://www.nanomedicine.com/NMI/15.6.2.htm>.

Bishop)³¹⁷ might include emergency revival of victims of carbon monoxide suffocation at the scene of a fire, rescue of drowning victims, and transfusable pre-oxygenated blood substitution. Respirocytes could serve as “instant blood” at an accident scene with no need for blood typing, and, thanks to the dramatically higher gas-transport efficiency of respirocytes over natural red cells, a mere 1 cm³ infusion of the devices would provide the oxygen-carrying ability of a full liter of ordinary blood, possibly saving lives even in cases of moderate hypovolemia (lost blood fluid volume) that might otherwise lead to hemorrhagic shock.³¹⁸

Larger doses of respirocytes could also: (1) be used as a temporary treatment for anemia and various lung and perinatal/neonatal disorders, (2) enhance tumor therapies and diagnostics and improve outcomes for cardiovascular, neurovascular, or other surgical procedures, (3) help prevent asphyxia and permit artificial breathing (e.g., underwater, high altitude, etc.), and (4) have many additional applications in sports, veterinary medicine, military science, and space exploration.

³¹⁷

<https://web.archive.org/web/20210508220644/https://foresight.org/Nanomedicine/Gallery/Captions/Image140.html>.

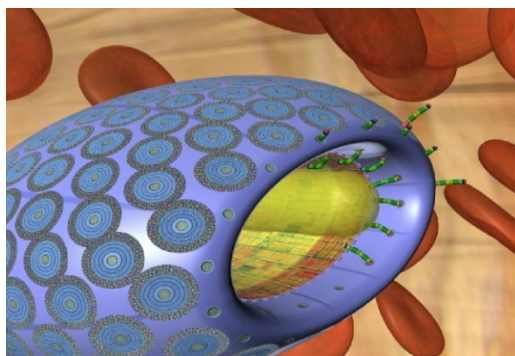
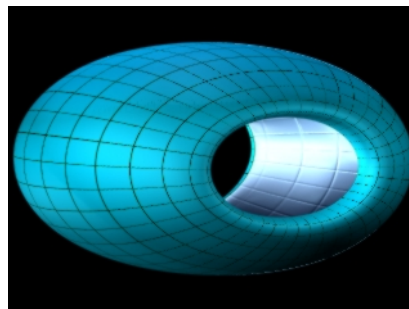
³¹⁸ Takasu A, Prueckner S, Tisherman SA, Stezoski SW, Stezoski J, Safar P. Effects of increased oxygen breathing in a volume controlled hemorrhagic shock outcome model in rats. *Resuscitation*. 2000 Aug 1;45(3):209-20; <https://www.sciencedirect.com/science/article/abs/pii/S0300957200001830>. Dyson A, Stidwill R, Taylor V, Singer M. The impact of inspired oxygen concentration on tissue oxygenation during progressive haemorrhage. *Intensive Care Med*. 2009 Oct;35(10):1783-91; <https://pubmed.ncbi.nlm.nih.gov/19618165/>.

5.1.2 Microbivore-Class Nanorobots

Perhaps the most widely recognized form of disease is an attack on the human body by invading viruses, bacteria, protozoa, or other microscopic parasites. One general class of medical nanorobot could serve as the first-line nanomedical treatment for pathogen-related disease.

Called a “microbivore”, this artificial nanorobotic white cell substitute, made of diamond and sapphire, would seek out and harmlessly digest unwanted bloodborne pathogens.³¹⁹ One main task of natural white cells is to phagocytose and kill microbial invaders in the

bloodstream. Microbivore nanorobots would also perform the equivalent of phagocytosis and microbial killing, but would operate much faster, more reliably, and under human control.



The baseline microbivore (image, left; hull design image, above; all microbivore artwork by Forrest Bishop)³²⁰ is designed as an oblate spheroidal nanomedical device measuring 3.4 μm in diameter along its major axis and 2.0 μm in diameter along its minor axis, consisting of 610 billion precisely arranged structural atoms in a gross geometric volume of 12.1 μm^3 and a dry mass of 12.2 picograms. This size helps to ensure that the nanorobot can safely pass through or avoid even the narrowest of human capillaries and other tight spots

in the spleen (e.g., the interendothelial splenofenestral slits)³²¹ and elsewhere in the human body,³²² given device motility. The microbivore has a mouth with an iris-like door, called the ingestion port, where microbes are fed in to be digested. This port is large enough to internalize a single microbe from virtually any major bacteremic species in a single gulp. The microbivore also has a rear end, or exhaust port, where the completely digested remains of the pathogen are harmlessly expelled from the device. The rear door opens between the main body of the

³¹⁹ Freitas RA Jr. Microbivores: Artificial mechanical phagocytes using digest and discharge protocol. *J Evol Technol* 2005;14:1-52; <http://www.jetpress.org/volume14/freitas.html>.

³²⁰

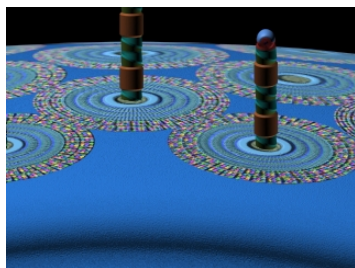
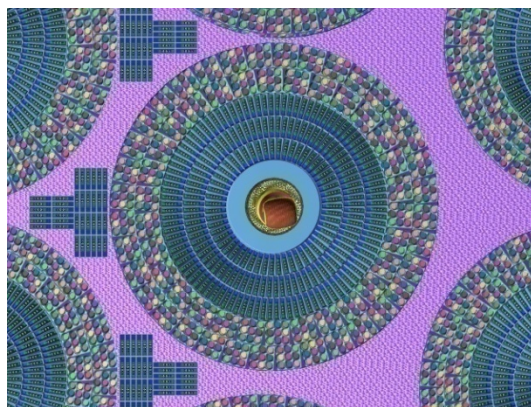
<https://web.archive.org/web/20160827082558/https://foresight.org/Nanomedicine/Gallery/Captions/Image197.html>.

³²¹ Freitas RA Jr. *Nanomedicine Vol. IIA: Biocompatibility*. Landes Bioscience, Georgetown, TX, 2003, Section 15.4.2.3, “Geometrical Trapping in Spleen Vasculature”; <http://www.nanomedicine.com/NMI/15.4.2.3.htm>.

³²² Freitas RA Jr. *Nanomedicine Vol. IIA: Biocompatibility*. Landes Bioscience, Georgetown, TX, 2003, Section 15.4.2, “Geometrical Trapping of Bloodborne Medical Nanorobots”; <http://www.nanomedicine.com/NMI/15.4.2.htm>.

microbivore and a tail-cone structure. According to the scaling study by Freitas,³²³ the device may consume up to 200 pW of continuous power (using bloodstream glucose and oxygen for energy) while completely digesting trapped microbes at a maximum throughput of $2 \mu\text{m}^3$ of organic material per 30-second cycle. This “digest and discharge” protocol³²⁴ is conceptually similar to the internalization and digestion process practiced by natural phagocytes, except that the artificial process should be a hundred-fold faster and also cleaner. For example, it is well-known that macrophages release biologically active compounds during bacteriophagy,³²⁵ whereas well-designed microbivores need only release biologically inactive effluent.

The first task for the bloodborne microbivore is to reliably acquire a pathogen to be digested. If the correct bacterium bumps into the nanorobot surface, reversible species-specific binding sites on the microbivore hull can recognize and weakly bind to the bacterium. A set of 9 distinct antigenic markers should be specific enough,³²⁶ since all 9 must register a positive binding event to confirm that a targeted microbe has been caught. There are 20,000 copies of these 9-marker receptor sets, distributed in 275 disk-shaped regions across the microbivore surface (image, right). Inside each receptor ring are more rotors to absorb ambient glucose and oxygen from the bloodstream to provide nanorobot power.



At the center of each 150-nm diameter receptor disk is a grapple silo (image, left). Once a bacterium has been captured by the reversible receptors, telescoping robotic grapples³²⁷ rise up out of the microbivore surface and attach to the trapped bacterium, establishing secure anchorage to the microbe's cell wall, capsid, or plasma membrane. The microbivore grapple arms are about 100 nanometers long and have various rotating and telescoping

³²³ Freitas RA Jr. Microbivores: Artificial mechanical phagocytes using digest and discharge protocol. J Evol Technol 2005;14:1-52; <http://www.jetpress.org/volume14/freitas.html>.

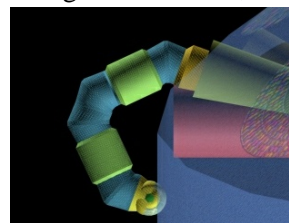
³²⁴ Freitas RA Jr. Nanomedicine, Volume I: Basic Capabilities. Landes Bioscience, Georgetown, TX, 1999, Section 10.4.2.4.2, “Digest and Discharge (DD)”;
<http://www.nanomedicine.com/NMI/10.4.2.4.2.htm>.

³²⁵ Fincher EF 4th, Johannsen L, Kapás L, Takahashi S, Krueger JM. Microglia digest *Staphylococcus aureus* into low molecular weight biologically active compounds. Am J Physiol. 1996 Jul;271(1 Pt 2):R149-56; <http://www.ncbi.nlm.nih.gov/pubmed/8760216>.

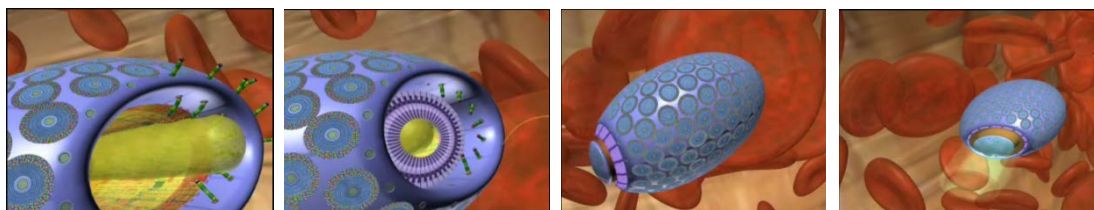
³²⁶ Freitas RA Jr. Nanomedicine, Volume I: Basic Capabilities. Landes Bioscience, Georgetown, TX, 1999, Section 8.5.2.2, “Identification of Cell Type”; <http://www.nanomedicine.com/NMI/8.5.2.2.htm>.

³²⁷ Freitas RA Jr. Nanomedicine, Volume I: Basic Capabilities. Landes Bioscience, Georgetown, TX, 1999, Section 9.3.1.4, “Telescoping Manipulators”; <http://www.nanomedicine.com/NMI/9.3.1.4.htm>.

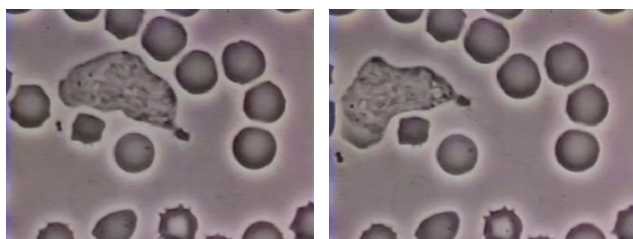
joints that allow them to change their position, angle, and length. After rising out of its silo, a grapple arm could execute complex twisting motions (image, right), and adjacent grapple arms can physically reach each other, allowing them to hand off bound objects as small as a virus particle. Grapple handoff motions could transport a large rod-shaped bacterium from its original capture site forward to the ingestion port at the front of the device. The captive organism would be rotated into the proper orientation as it approaches the open microbivore mouth. There the pathogen is internalized into a $2\ \mu\text{m}^3$ morcellation chamber under continuous control of mouth grapples and an internal mooring mechanism.



There are two concentric cylinders inside the microbivore. The bacterium will be minced into nanoscale pieces in the morcellation chamber (the smaller inner cylinder),³²⁸ then the remains are pistoned into a separate $2\ \mu\text{m}^3$ digestion chamber (the larger outer cylinder). In a preprogrammed sequence, ~40 different engineered digestive enzymes will be successively injected and extracted six times during a single digestion cycle, progressively reducing the morcellate to amino acids, mononucleotides, glycerol, free fatty acids and simple sugars, using an appropriate array of molecular sorting rotors. These basic end-product molecules are then harmlessly discharged back into the bloodstream through the exhaust port at the rear of the device, completing the 30-second digestion cycle (images, below; artwork by Forrest Bishop). When treatment is finished, the doctor may transmit an ultrasound signal to tell the circulating microbivores that their work is done. These motile nanorobots may then exit the body through the kidneys by various means and be excreted with the urine in due course.



A human neutrophil, the most common type of leukocyte or white cell, can capture and engulf a microbe in a minute or less (images, below), but complete digestion and excretion of the microbe's remains can take an hour or longer. Our natural white cells – even when aided by antibiotics – can sometimes take weeks or months to completely clear bacteria from the



bloodstream. By comparison, a single terabot (10^{12} -nanorobot) dose of microbivores should be able to fully eliminate bloodborne pathogens in just minutes, or hours in the case of locally dense infections. This is accomplished without increasing the risk of sepsis or septic shock because all bacterial

³²⁸ Freitas RA Jr. Nanomedicine, Volume I: Basic Capabilities. Landes Bioscience, Georgetown, TX, 1999, Section 9.3.5.1, "Morcellation and Mincing"; <http://www.nanomedicine.com/NMI/9.3.5.1.htm>.

components (including all cell-wall lipopolysaccharide) will be internalized and fully digested into harmless non-antigenic molecules prior to discharge from the microbivore device.

And no matter that a bacterium has acquired multiple drug resistance to antibiotics or to any other traditional treatment – the microbivore will eat it anyway. Microbivores would be up to ~1000 times faster-acting than antibiotic-based cures which often need weeks or months to work. The nanorobots would digest ~100 times more microbial material than an equal volume of natural white cells could digest in any given time period, and would have far greater maximum lifetime capacity for phagocytosis than natural white blood cells.

5.1.3 Chromalloyte-Class Nanorobots

The chromalloyte³²⁹ is a mobile cell-repair nanorobot whose primary function is to perform chromosome replacement therapy (CRT). In CRT, the entire chromatin content of the nucleus in a living cell is extracted and promptly replaced with a new set of prefabricated chromosomes that have been artificially manufactured as defect-free copies of the originals.



The chromalloyte (images, left; artwork by Stimulacra) will be capable of limited vascular surface travel into the capillary bed of the targeted tissue or organ, followed by diapedesis (exiting a blood vessel into the tissues),³³⁰ histonatonation (locomotion through tissues),³³¹ cytopenetration (entry into the cell

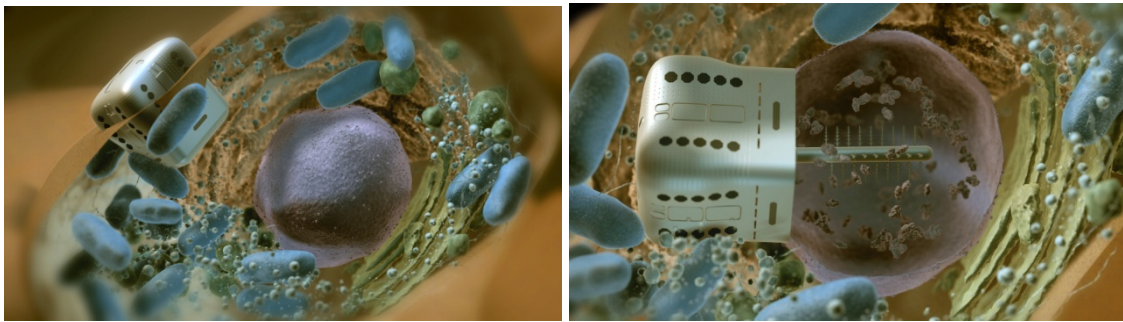
interior; see nanorobot images, below, by E-spaces),³³² and complete chromatin replacement in the nucleus of the target cell. The CRT mission ends with a return to the vasculature and subsequent extraction of the nanodevices from the body at the original infusion site.

³²⁹ Freitas RA Jr. The ideal gene delivery vector: Chromalloytes, cell repair nanorobots for chromosome replacement therapy. J Evol Technol 2007;16:1-97; <http://jetpress.org/v16/freitas.pdf>.

³³⁰ Freitas RA Jr. Nanomedicine, Volume I: Basic Capabilities. Landes Bioscience, Georgetown, TX, 1999, Section 9.4.4.1, “Nanorobot Diapedesis”; <http://www.nanomedicine.com/NMI/9.4.4.1.htm>.

³³¹ Freitas RA Jr. Nanomedicine, Volume I: Basic Capabilities. Landes Bioscience, Georgetown, TX, 1999, Section 9.4.4, “Histonatonation”; <http://www.nanomedicine.com/NMI/9.4.4.htm>.

³³² Freitas RA Jr. Nanomedicine, Volume I: Basic Capabilities. Landes Bioscience, Georgetown, TX, 1999, Section 9.4.5, “Cytopenetration”; <http://www.nanomedicine.com/NMI/9.4.5.htm>.



This ~3 hour chromosome replacement process is expected to involve a 26-step sequence of distinct semi-autonomous sensor-driven activities which are described at length in a comprehensive published technical paper on the subject by Freitas³³³ and in summary below, including: (1) injection, (2) extravasation, (3) ECM immigration, (4) cytopenetration (image above, left), (5) inhibition of mechanotransduction (to avoid nanorobot mechanical actions triggering unwanted cell responses), (6) nuclear localization, (7) nucleopenetration, (8) blockade of apoptosis (to prevent misinterpretation of CRT processes as damage demanding cell suicide), (9) arrest of DNA repair (to prevent misinterpretation of CRT processes as damage demanding repair), (10) blockade of inflammatory signals, (11) deactivation of transcription, (12) detachment of chromatin from inner nuclear wall lamins (cortex proteins), (13) extension of the “proboscis” into the cell nucleus (image above, right), (14) rotation of the proboscis, (15) deployment of the chromosomal collection funnel, (16) digestion of stray chromatin, (17) dispensation of new chromatin, (18) decondensation of the new chromatin, (19) re-anchoring of the dispensed chromatin to inner nuclear wall lamins, (20) reactivation of transcription, (21) reactivation of DNA repair and other DNA-related maintenance and usage processes, (22) nuclear emigration, (23) cellular emigration, (24) ECM emigration, (25) return to original point of entry into the body, and (26) removal from the body. Treatment of an entire large human organ such as a liver, involving simultaneous CRT on all 250 billion hepatic tissue cells, might require the localized infusion of a ~1 terabot (10^{12} devices) or ~69 cm³ chromalloyocyte dose in a 1-liter (7% v/v nanorobots) saline suspension during a ~7 hour course of therapy. This nanodevice population draws 100-200 watts which lies within estimated nanorobot thermogenic limits consistent with maintenance of constant human body temperature.³³⁴

³³³ Freitas RA Jr. The ideal gene delivery vector: Chromalloyocytes, cell repair nanorobots for chromosome replacement therapy. J Evol Technol 2007;16:1-97; <http://jetpress.org/v16/freitas.pdf>.

³³⁴ Freitas RA Jr. Nanomedicine, Volume I: Basic Capabilities. Landes Bioscience, Georgetown, TX, 1999, Section 6.5.2, “Thermogenic Limits *in vivo*”; <http://www.nanomedicine.com/NMI/6.5.2.htm>. Freitas RA Jr. The ideal gene delivery vector: Chromalloyocytes, cell repair nanorobots for chromosome replacement therapy. J Evol Technol 2007;16:1-97, Section 3.6, “Power Supply”; <http://jetpress.org/v16/freitas.pdf>.

Replacement chromosome sets would be manufactured³³⁵ in a desktop *ex vivo* chromosome sequencing and manufacturing facility (conceptual image, right),³³⁶ then loaded into the nanorobots for delivery to specific targeted cells during CRT. The new DNA is manufactured to incorporate proper methylation for the target cell type and other post-translational modifications constituting the “histone code” used by the cell to encode various chromatin conformations and gene expression states.³³⁷



A single fully-loaded lozenge-shaped $69 \mu\text{m}^3$ chromallocyte can measure $4.18 \mu\text{m}$ and $3.28 \mu\text{m}$ along cross-sectional diameters and $5.05 \mu\text{m}$ in length, typically consuming 50-200 pW of power in normal operation and a maximum of 1000 pW in bursts during outmessaging, the most energy-intensive task. Onboard power can be provided acoustically from the outside in an operating-table scenario (image, left) in which the patient is well-coupled to a medically-safe 1000 W/m^2 0.5 MHz ultrasound transverse-plane-wave transmitter throughout the procedure. The American Institute of Ultrasound in Medicine (AIUM) deems 10,000-sec exposures to 1000 W/m^2 ultrasound to be safe.³³⁸



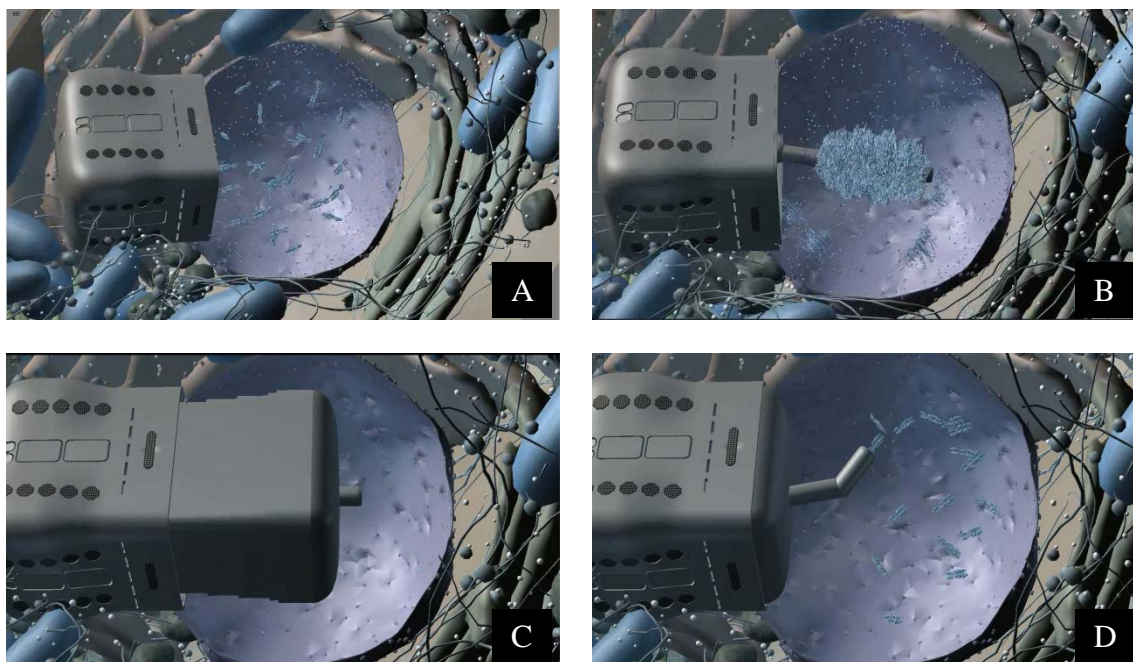
The chromallocyte design includes an extensible primary manipulator $4 \mu\text{m}$ long and $0.55 \mu\text{m}$ in diameter called the proboscis that is used to spool up chromatin strands via slow rotation when inserted into the cell nucleus (image sequence, below; images by E-spaces). After spooling (images A and B), a segmented funnel assembly is extended around the spooled bolus of DNA, fully enclosing and sequestering the old genetic material (image C). The new genetic material can then be discharged into the nucleus through the center of the proboscis by pistoning from internal storage vaults (image D), while the old chromatin that is sequestered inside the sealed leakproof funnel assembly is forced into the storage vaults as space is vacated by the new chromatin that is simultaneously being pumped out.

³³⁵ Strickland E. DNA manufacturing enters the age of mass production. IEEE Spectrum, 23 Dec 2015; <http://spectrum.ieee.org/biomedical/devices/dna-manufacturing-enters-the-age-of-mass-production>.

³³⁶ Freitas RA Jr. The ideal gene delivery vector: Chromallocytes, cell repair nanorobots for chromosome replacement therapy. J Evol Technol 2007;16:1-97, Section 4, “*Ex Vivo* Chromosome Sequencing and Manufacturing Facility”; <http://jetpress.org/v16/freitas.pdf>.

³³⁷ Villar-Garea A, Imhof A. The analysis of histone modifications. Biochim Biophys Acta. 2006 Dec;1764(12):1932-9; <http://www.ncbi.nlm.nih.gov/pubmed/17015046>.

³³⁸ Freitas RA Jr. Nanomedicine, Volume I: Basic Capabilities. Landes Bioscience, Georgetown, TX, 1999, Section 6.4.1, “Acoustic Power Transmission”; <http://www.nanomedicine.com/NMI/6.4.1.htm>.



The chromalloy cell can employ a mobility system similar to the microbivore grapple system, possibly including a solvation wave drive³³⁹ to help ensure smooth passage through cell plasma membrane and nuclear membrane.

Chromalloy cells should be regarded as prototype cell repair machines. They can selectively insert, extract, or replace specific cellular components on a cell-by-cell basis, on any accessible cell or tissue in the body.

³³⁹ Freitas RA Jr. Nanomedicine, Volume I: Basic Capabilities. Landes Bioscience, Georgetown, TX, 1999, Section 9.4.5.3, "Solvation Wave Drive"; <http://www.nanomedicine.com/NMI/9.4.5.3.htm>.

5.2 Nanorobotic Curative Treatments for ED

Almost all of the conventional treatments for erectile dysfunction mentioned in [Section 4](#) provide only partial or temporary symptomatic relief. This Section describes a range of nanorobotic treatments that would provide actual permanent cures for the underlying problems that are causing the ED, including: (1) treatments for impaired blood flow ([Section 5.2.1](#)), which may involve removing arterial obstructions ([Section 5.2.1.1](#)) or eliminating venous leakage ([Section 5.2.1.2](#)); treatments for neurological disorders ([Section 5.2.2](#)) such as damage to nerves in the pelvis, spinal column, or brain; and treatments for other ED-related pathologies ([Section 5.2.3](#)) such as hormone imbalances, enzymatic abnormalities, and other co-morbidities of erectile dysfunction.

Besides individual nanorobots, a nanorobotic mechanism called a nanocatheter ([Section 5.2.4](#)) can be inserted into deep tissues to directly perform necessary repairs involving vascular plaque debridement ([Section 5.2.4.2](#)), whole cell transport ([Section 5.2.4.3](#)), cytosolic intervention in individual cells ([Section 5.2.4.4](#)), and tissue and nerve repair ([Section 5.2.4.5](#)), while avoiding pain for the patient during treatment ([Section 5.2.4.1](#)).

Individual nanorobots can also be employed to provide purely symptomatic relief from ED ([Section 5.3](#)).

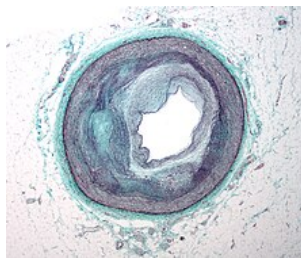
5.2.1 Nanorobotic Cure for ED-Related Impaired Blood Flow

To organically correct impaired blood flow will require repairing any damage to blood vessels caused by atherosclerosis ([Section 5.2.1.1](#)) or any venous leakage ([Section 5.2.1.2](#)) that might have developed. Diagnostic nanorobots will determine which of the above repairs are needed, along with the extent and location of the vascular damage in each case, allowing the attending physician to plan and execute the required nanorobotic reparative procedures.

5.2.1.1 Arterial Obstruction

Atherosclerotic damage to blood vessels would include any vascular wall lesions or plaques (fatty deposits) that have accumulated in the internal pudendal arteries,³⁴⁰ the penile arteries,³⁴¹ or the cavernous arteries³⁴² of the penis, narrowing the internal diameter of these vessels³⁴³ thus preventing the sufficient filling of the corpora cavernosa that is essential for an erection.

Atherosclerotic lesions or plaques typically do not occur directly within the corpora cavernosa, but primarily affect only the arteries that supply blood to these tissues rather than the tissues



themselves. The incidence of atherosclerosis³⁴⁴ is typically associated with, among other things, diabetes,³⁴⁵ obesity,³⁴⁶ Western pattern diet,³⁴⁷ hypertension,³⁴⁸ and smoking.³⁴⁹

The image at left shows a micrograph of a cardiac artery with significant atherosclerosis and marked luminal narrowing.³⁵⁰ The detailed illustration below³⁵¹ shows the typical progression of atherosclerosis in which the endothelial cell-lined artery wall becomes

³⁴⁰ https://en.wikipedia.org/wiki/Internal_pudendal_artery.

³⁴¹ https://en.wikipedia.org/wiki/Penile_artery.

³⁴² Caretta N, Feltrin G, Tarantini G, D'Agostino C, Tona F, Schipilliti M, Selice R, Minicuci N, Gerosa G, Foresta C. Erectile dysfunction, penile atherosclerosis, and coronary artery vasculopathy in heart transplant recipients. J Sex Med. 2013 Sep;10(9):2295-302; <https://pubmed.ncbi.nlm.nih.gov/23809661/>.

³⁴³ Prezioso D, Iacono F, Russo U, Romeo G, Ruffo A, Russo N, Illiano E. Evaluation of penile cavernosal artery intima-media thickness in patients with erectile dysfunction. A new parameter in the diagnosis of vascular erectile dysfunction. Our experience on 59 cases. Arch Ital Urol Androl. 2014 Mar 28;86(1):9-14; <https://pdfs.semanticscholar.org/89d3/70debf1ed557ad43b8785fae8703b0caa09c.pdf>.

³⁴⁴ <https://en.wikipedia.org/wiki/Atherosclerosis>.

³⁴⁵ <https://en.wikipedia.org/wiki/Diabetes>.

³⁴⁶ https://en.wikipedia.org/wiki/Abdominal_obesity.

³⁴⁷ https://en.wikipedia.org/wiki/Western_pattern_diet.

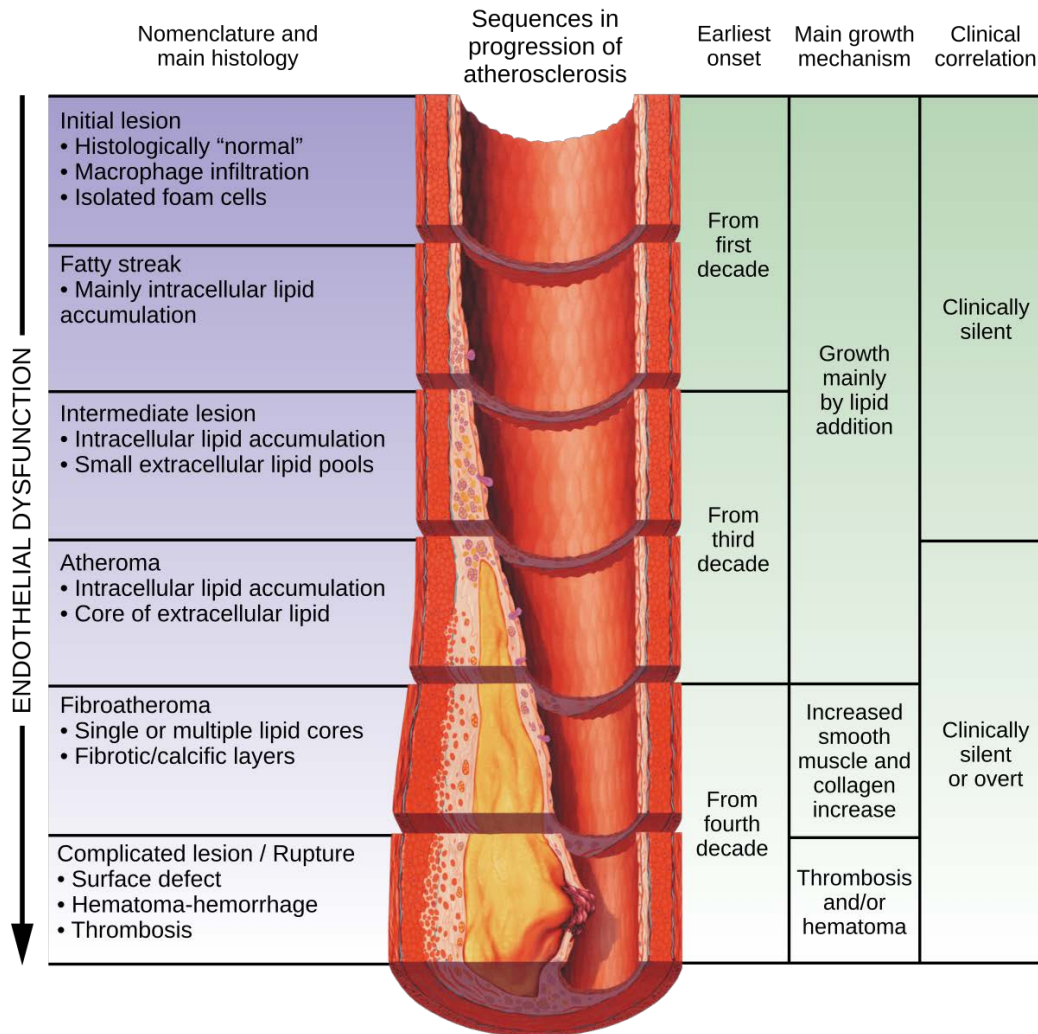
³⁴⁸ <https://en.wikipedia.org/wiki/Hypertension>.

³⁴⁹ https://en.wikipedia.org/wiki/Tobacco_smoking.

³⁵⁰ https://en.wikipedia.org/wiki/File:RCA_atherosclerosis.jpg.

³⁵¹ https://en.wikipedia.org/wiki/Atherosclerosis#/media/File:Atherosclerosis_timeline_-_endothelial_dysfunction.svg.

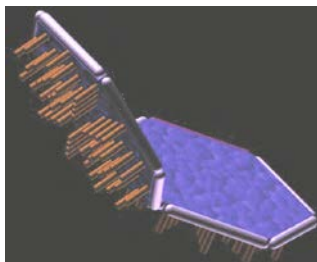
thicker and less elastic due to the presence of fatty-material-accumulating white cells under the inner lining of the arterial wall, creating a deposit called an atheroma.³⁵² As the atheromas grow, the arterial lumens narrow. In time, the atheromas may collect calcium deposits, become brittle, and rupture, spilling their fatty contents and triggering the formation of a blood clot. The clot can further narrow or even occlude the artery, possibly leading to heart attack, or it may detach and float downstream, producing a vascular embolism.



As previously described elsewhere for the treatment of vascular and heart disease,³⁵³ a medical nanorobot called a "vasculocyte" (image below)³⁵⁴ may be the nanorobotic treatment of choice

³⁵² <https://en.wikipedia.org/wiki/Atheroma>.

³⁵³ Freitas RA Jr. Chapter 23. Comprehensive Nanorobotic Control of Human Morbidity and Aging. In: Fahy GM, West MD, Coles LS, Harris SB, eds, The Future of Aging: Pathways to Human Life Extension, Springer, New York, 2010; Section 23.6.2.3, "Heart and Vascular Disease"; <http://www.nanomedicine.com/Papers/Aging.pdf>.



for the limited vascular repair of primarily intimal arteriosclerotic lesions prior to complete arterial occlusion.³⁵⁵ The device is designed as a squat, hexagonal-shaped nanorobot with rounded corners, measuring $\sim 2.7 \mu\text{m}$ across and $1 \mu\text{m}$ tall,³⁵⁶ that walks the inside surface of blood vessels atop telescoping appendages arranged on its underbelly. Its 400-billion atom structure would weigh about 8 picograms, probably consuming up to $\sim 200 \text{ pW}$ of power. The machine is scaled so that its longest cross-body diagonal³⁵⁷ is shorter than $4 \mu\text{m}$, the diameter of the narrowest capillaries in the human body.³⁵⁸ The slightly-curved topmost surface will be almost completely tiled with 174,000 molecular sorting rotors³⁵⁹ to allow rapid exchange of specific molecules between the interior of the nanorobot and the patient's bloodstream.

On its six side walls the vasculocyte will be enveloped by an extensible “bumper” surface³⁶⁰ which cycles between 100 nm and 300 nm of thickness as internally-stored piston-pumped ballast fluid inflates and deflates the surface about once every second.³⁶¹ This cycling will allow a nanorobot situated on an arterial wall to continuously adjust its girth by up to 15% to match the regular distensions of arterial wall circumference that occur during each systolic pulse of the

³⁵⁴ Artist credit: Forrest Bishop;
<https://web.archive.org/web/20210505235054/https://foresight.org/Nanomedicine/Gallery/Artist/Bishop.html>.

³⁵⁵ Freitas RA Jr. The end of heart disease. Institute for Molecular Manufacturing, unpublished internal design study, 1996.

³⁵⁶ These dimensions ensure that the device's longest cross-body diagonal is $<4 \mu\text{m}$, below the diameter of the narrowest capillaries in the human body.

³⁵⁷ Freitas RA Jr. Nanomedicine, Volume I: Basic Capabilities, Landes Bioscience, Georgetown TX, 1999; Section 5.2.1, “Free-Floating Solitary Nanodevices”; <http://www.nanomedicine.com/NMI/5.2.1.htm>.

³⁵⁸ Freitas RA Jr. Nanomedicine, Volume I: Basic Capabilities, Landes Bioscience, Georgetown TX, 1999; Section 8.2.1.2, “Arteriovenous Microcirculation”; <http://www.nanomedicine.com/NMI/8.2.1.2.htm>.

³⁵⁹ Drexler KE. Nanosystems: Molecular Machinery, Manufacturing, and Computation, John Wiley & Sons, New York, 1992, Section 13.2.1(a) “Modulated receptors for selective transport: Basic concepts”; <https://www.amazon.com/dp/0471575186/>. Freitas RA Jr. Nanomedicine, Volume I: Basic Capabilities, Landes Bioscience, Georgetown, TX, 1999; Section 3.4.2, “Sorting Rotors”; <http://www.nanomedicine.com/NMI/3.4.2.htm>.

³⁶⁰ Freitas RA Jr. Nanomedicine, Volume I: Basic Capabilities, Landes Bioscience, Georgetown TX, 1999; Section 5.4, “Metamorphic Bumpers”; <http://www.nanomedicine.com/NMI/5.4.htm>.

³⁶¹ Freitas RA Jr. Nanomedicine, Volume I: Basic Capabilities, Landes Bioscience, Georgetown TX, 1999; Section 5.3.3, “Metamorphic Power and Control”; <http://www.nanomedicine.com/NMI/5.3.3.htm>.

heart,³⁶² thus maintaining watertight contact with similarly-cycling neighboring devices all of which are stationkeeping over a particular section of vascular tissue.

On its bottom face the vasculocyte will have hundreds of stubby telescoping appendages,³⁶³ each capable of 1 cm/sec movements. The appendages are roughly similar to the 250 nm long grapples employed in the microbivore.³⁶⁴ These are spaced out along a regular grid about 100 nm apart, with only 10% of them used at any one time both to preserve tenfold redundancy and to avoid any possibility of leg-leg collisions. Each leg walks on a “footpad” tool tip³⁶⁵ that is ~10 nm in diameter. Acting like a snowshoe, the footpad will distribute leg motion forces widely enough to avoid disrupting cell membranes.³⁶⁶ However, the appendages should be capable of telescoping out to at least twice the normal length of a microbivore grapple to accommodate the varying 200-500 nm thickness of the endothelial glycocalyx³⁶⁷ and microvilli.³⁶⁸ The mechanocompatibility of legged nanorobots walking on living biological surfaces has been discussed elsewhere.³⁶⁹

Many different tool tips³⁷⁰ might be deployed up through the interior hollows of the many nanorobotic limbs. Appendages on the underbelly may be used as manipulator arms for blood clot and foam cell disassembly, endothelial cell herding, adhesive glycoprotein removal, and so forth. Syringe tips will allow suction or drug injection by penetrating the 10-nm thick cellular

³⁶² Freitas RA Jr. Nanomedicine, Volume I: Basic Capabilities, Landes Bioscience, Georgetown TX, 1999; Section 5.2.4.2, “Tiling Deforming Surfaces”; <http://www.nanomedicine.com/NMI/5.2.4.2.htm>.

³⁶³ Drexler KE. Nanosystems: Molecular Machinery, Manufacturing, and Computation, John Wiley & Sons, New York, 1992; Section 13.4.1(f), “Speed, productivity, and magnitude of power dissipation”; http://e-drexler.com/d/09/00/Drexler_MIT_dissertation.pdf. Freitas RA Jr. Nanomedicine, Volume I: Basic Capabilities, Landes Bioscience, Georgetown TX, 1999; Section 9.3.1.4, “Telescoping Manipulators”; <http://www.nanomedicine.com/NMI/9.3.1.4.htm>.

³⁶⁴ Freitas RA Jr. Microbivores: Artificial Mechanical Phagocytes using Digest and Discharge Protocol. J Evol Technol. 2005 Apr;14:55-106; <http://www.jetpress.org/volume14/freitas.pdf>.

³⁶⁵ Freitas RA Jr. Nanomedicine, Volume I: Basic Capabilities, Landes Bioscience, Georgetown TX, 1999; Section 9.4.3, “Cytoambulation”; <http://www.nanomedicine.com/NMI/9.4.3.htm>.

³⁶⁶ Freitas RA Jr. Nanomedicine, Volume I: Basic Capabilities, Landes Bioscience, Georgetown TX, 1999; Section 9.4.3.2, “Cell Plasma Membrane Elasticity”; <http://www.nanomedicine.com/NMI/9.4.3.2.htm>.

³⁶⁷ Reitsma S, Slaaf DW, Vink H, van Zandvoort MA, oude Egbrink MG. The endothelial glycocalyx: composition, functions, and visualization. Pflugers Arch. 2007 Jun;454(3):345-59; <https://www.ncbi.nlm.nih.gov/pmc/articles/PMC1915585/pdf>.

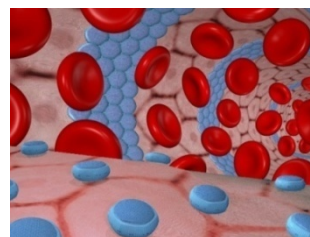
³⁶⁸ <https://en.wikipedia.org/wiki/Microvillus>.

³⁶⁹ Freitas RA Jr. Nanomedicine, Volume IIA: Biocompatibility, Landes Bioscience, Georgetown, TX, 2003; Chapter 15.5, “Nanorobot Mechanocompatibility”; <http://www.nanomedicine.com/NMIIA/15.5.htm>.

³⁷⁰ Freitas RA Jr. Nanomedicine, Volume I: Basic Capabilities, Landes Bioscience, Georgetown TX, 1999; Section 9.3.2, “Nanoscale End-Effectors and Tool Tips”; <http://www.nanomedicine.com/NMI/9.3.2.htm>.

membranes over which the device is walking. Other specialized tips will be used for bulk tissue disposal (e.g., a rotating cutting annulus), molecular absorption (e.g., using binding sites keyed to the molecules that make up plaque), cell peeling (e.g., specialized grippers), and as sensors for biomarker detection, chemotactic mapping, and other physical measurements.

In a whole-body vascular surveillance scenario, after injection into the bloodstream the vasculocytes would circulate freely in the patient's bloodstream for a few minutes, finally dropping out onto a capillary wall and beginning to crawl upstream (or downstream, if in the pulmonary bed) along the vessel surface. Each device moves past the precapillary sphincters, through the metarterioles to the wide end of the terminal arterioles, then up the terminal arterial branches (150 μm in diameter) and into the arteries, where it joins up with others, forming into traveling circumferential scanning rings consisting of millions of individual nanorobots walking side by side (image, right).³⁷¹ Eventually these traveling bands³⁷² will enter the 25,000-micron diameter aorta, leading, ultimately, to the heart. Upon reaching the heart uneventfully, each device would release its grip on the arterial wall and return to the bloodstream, allowing removal from the body either by nanapheresis centrifugation³⁷³ or by excretion through the kidneys (Section 5.3.1.6).³⁷⁴ Ambulating along the arterial tree at speeds up to $v_{\text{vasculo}} \sim 1 \text{ cm/sec}$,³⁷⁵ much slower than typical 10-60 cm/sec arterial blood velocities, a vasculocyte ringset could travel the 70 cm mean distance from capillaries to aorta heart in $\sim 70 \text{ sec}$ ($\sim 1.2 \text{ min}$) if uninterrupted. Note that the peak wall shear stress in the aorta (where blood velocity is highest) is $\sigma_{\text{aorta}} \sim 5 \text{ N/m}^2$,³⁷⁶ creating a dislodgement force of $\sigma_{\text{aorta}} V_{\text{nanorobot}}^{2/3} \sim 23 \text{ pN}$ that is easily resisted by the multiple 100-pN footpad anchors on the feet of legged medical nanorobots.³⁷⁷



³⁷¹ Artist credit: Tim Fonseca;

<https://web.archive.org/web/20210228002635/https://foresight.org/Nanomedicine/Gallery/Artist/Fonseca.html>.

³⁷² Lapidus IR, Schiller R. A model for traveling bands of chemotactic bacteria. *Biophys J*. 1978 Apr;22(1):1-13; <https://www.ncbi.nlm.nih.gov/pmc/articles/PMC1473406/pdf>.

³⁷³ Freitas RA Jr. *Nanomedicine, Volume I: Basic Capabilities*, Landes Bioscience, Georgetown TX, 1999; Section 10.3.6, "Buoyancy Control and Nanapheresis"; <http://www.nanomedicine.com/NMI/10.3.6.htm>.

³⁷⁴ Weatherbee CW, Freitas RA Jr. The structure of the human kidney as applicable to nanoscale robot navigation. Unpublished manuscript, 2010.

³⁷⁵ Freitas RA Jr. *Nanomedicine, Volume I: Basic Capabilities*, Landes Bioscience, Georgetown TX, 1999; Section 9.4.3.5, "Legged Ambulation"; <http://www.nanomedicine.com/NMI/9.4.3.5.htm>.

³⁷⁶ Oshinski JN, Ku DN, Mukundan S Jr, Loth F, Pettigrew RI. Determination of wall shear stress in the aorta with the use of MR phase velocity mapping. *J Magn Reson Imaging*. 1995 Nov-Dec;5(6):640-7; <https://pubmed.ncbi.nlm.nih.gov/8748480/>.

³⁷⁷ Freitas RA Jr. *Nanomedicine, Volume I: Basic Capabilities*, Landes Bioscience, Georgetown TX, 1999; Section 9.4.3.3, "Anchoring and Dislodgement Forces"; <http://www.nanomedicine.com/NMI/9.4.3.3.htm>.

However, if disease is present the nanorobots will detect sclerotic tissue based on surface plaque temperature heterogeneity,³⁷⁸ directly sampled tissue biomarkers,³⁷⁹ observation of ultrastructural alterations in endothelial cell morphology,³⁸⁰ thinning of endothelial glycocalyx³⁸¹ or other evidence of endothelial dysfunction,³⁸² and circumferential vasculometric variations. Upon such detection, enough vasculocytes would collect over the affected area to entirely cover the lesion. The nanorobots aggregate into a watertight arterial “bandage” by locking themselves together side by side through their inflatable bumpers, then establish mutual communications links³⁸³ and anchor themselves securely to the underlying tissue to begin repair operations which may be externally supervised and directed by the physician in real time.

In an erectile dysfunction treatment scenario, the vasculocytes can be directed to confine their most focused activities on the penile arterial system. The arterial system of the penis includes two **internal pudendal arteries**,³⁸⁴ each $D_{ipa} \sim 2\text{--}3\text{ mm}$ in diameter and $L_{ipa} \sim 4\text{--}6\text{ cm}$ in length, giving a total intimal surface area of $A_{ipa} = 2\pi D_{ipa} L_{ipa} \sim 7.5\text{ cm}^2$ (range $5.0\text{--}11.3\text{ cm}^2$) for both arteries. The internal pudendal arteries branch into four penile arteries, including two **dorsal**

³⁷⁸ Stefanadis C, Diamantopoulos L, Vlachopoulos C, Tsiamis E, Dernellis J, Toutouzas K, Stefanadi E, Toutouzas P. Thermal heterogeneity within human atherosclerotic coronary arteries detected *in vivo*: A new method of detection by application of a special thermography catheter. *Circulation* 1999 Apr 20;99(15):1965-1971;

<https://citeseerx.ist.psu.edu/document?repid=rep1&type=pdf&doi=e8a2131faa35a0e0b8471ec397526079bd9e8d67>.

³⁷⁹ Schönbeck U, Libby P. CD40 signaling and plaque instability. *Circ Res*. 2001 Dec 7;89(12):1092-103; <https://www.ahajournals.org/doi/full/10.1161/hh2401.101272>. Lipinski MJ, Fuster V, Fisher EA, Fayad ZA. Technology insight: targeting of biological molecules for evaluation of high-risk atherosclerotic plaques with magnetic resonance imaging. *Nat Clin Pract Cardiovasc Med*. 2004 Nov;1(1):48-55; <https://citeseerx.ist.psu.edu/document?repid=rep1&type=pdf&doi=b92398c9d283bb97f2a53f69391063785e79319e>. Koenig W, Khuseynova N. Biomarkers of atherosclerotic plaque instability and rupture. *Arterioscler Thromb Vasc Biol*. 2007 Jan;27(1):15-26; <https://www.ahajournals.org/doi/full/10.1161/01.atv.0000251503.35795.4f>.

³⁸⁰ Walski M, Chlopicki S, Celary-Walska R, Frontczak-Baniewicz M. Ultrastructural alterations of endothelium covering advanced atherosclerotic plaque in human carotid artery visualised by scanning electron microscope. *J Physiol Pharmacol*. 2002 Dec;53(4 Pt 1):713-23; https://www.jpp.krakow.pl/journal/archive/12_02/pdf/713_12_02_article.pdf.

³⁸¹ Gouverneur M, Berg B, Nieuwdorp M, Stroes E, Vink H. Vasculoprotective properties of the endothelial glycocalyx: effects of fluid shear stress. *J Intern Med*. 2006 Apr;259(4):393-400; <https://onlinelibrary.wiley.com/doi/epdf/10.1111/j.1365-2796.2006.01625.x>.

³⁸² Hadi HA, Carr CS, Al Suwaidi J. Endothelial dysfunction: cardiovascular risk factors, therapy, and outcome. *Vasc Health Risk Manag*. 2005;1(3):183-98; <https://www.ncbi.nlm.nih.gov/pmc/articles/PMC1993955/pdf>.

³⁸³ Freitas RA Jr. *Nanomedicine, Volume I: Basic Capabilities*, Landes Bioscience, Georgetown TX, 1999; Section 5.4.2, “Transbumper Communication”; <http://www.nanomedicine.com/NMI/5.4.2.htm>.

³⁸⁴ https://en.wikipedia.org/wiki/Internal_pudendal_artery.

arteries,³⁸⁵ $D_{da} \sim 1\text{-}2$ mm in diameter and $L_{da} \sim 10\text{-}15$ cm long, and two **bulbourethral arteries**,³⁸⁶ $D_{ba} \sim 1$ mm in diameter and $L_{ba} \sim 5\text{-}7$ cm long, giving a surface area of $A_{pa} = 2\pi (D_{da} L_{da} + D_{ba} L_{ba}) \sim 14.8$ cm² (range 9.4-23.3 cm²) for all four arteries, and also two **cavernosal arteries**,³⁸⁷ $D_{ca} \sim 1\text{-}2$ mm in diameter and $L_{ca} \sim 10\text{-}15$ cm long, giving a surface area of $A_{ca} = 2\pi D_{ca} L_{ca} \sim 10.9$ cm² (range 6.3-18.9 cm²) for both arteries and a total penile arterial luminal surface area for all eight arteries of $A_{penart} = A_{ipa} + A_{pa} + A_{ca} \sim 33.2$ cm² (range 20.7-53.4 cm²) and total length $L_{penart} = 2L_{ipa} + 2L_{da} + 2L_{ba} + 2L_{ca} \sim 71$ cm (range 58-86 cm) that must be swept for atherosclerotic lesions and plaque by the vasculocytes. If each nanorobot covers $A_{vasculocyte} \sim 6.3$ μm² of vascular surface when close-packed into traveling bands,³⁸⁸ then $N_{vasculocytes} = A_{penart} / A_{vasculocyte} \sim 400$ million robots (~ 3 mm³ total device volume, taking $V_{vasculocyte} \sim 8.3$ μm³) would be sufficient to overlay the entire surface area of the penile large arterial tree with reparative vasculocytes, a fleet that would consume at most ~ 0.1 watts of power during periods of maximum activity. Note that atherosclerosis rarely affects the smaller helicine arteries that are fed from the cavernosal arteries and provide blood directly to the sinusoids of the corpora cavernosa.

After the surveillance is completed and the results are outmessaged³⁸⁹ to external computers in the operating theater, the attending physician selects a specific series of treatment actions and then inmessages³⁹⁰ these instructions back to the *in vivo* nanorobots already stationed in the penile arterial system as described earlier. One primary activity will be to excise and digest all extracellular lipid deposits, fibrotic and calcific layers, dead cells, complex thrombotic lesions, and (if present) a fibrous cap made of migrated smooth muscle cells and collagen, that may compose a plaque overlaying the endothelial cell lining of the penile arterial vasculature. In a case of severe ED where all arteries are $f_{occlude} \sim 30\%$ volumetrically occluded by plaque,³⁹¹ the volume of plaque to be removed would be $V_{plaque} = 2(\pi/4) f_{occlude} (D_{ipa}^2 L_{ipa} + D_{da}^2 L_{da} + D_{ba}^2 L_{ba} + D_{ca}^2 L_{ca}) \sim 0.4$ cm³ (range 0.2-0.8 cm³). A microbivore (Section 5.1.2) of volume $V_{microbivore} = 12.1$ μm³ can digest $V_{digest} \sim 2$ μm³ of biological material in $t_{digest} \sim 30$ sec, discharging only biocompatible effluents into the bloodstream, hence a vasculocyte configured as a microbivore might achieve a digestion rate of $\beta_{digest} = (V_{vasculocyte} / V_{microbivore}) (V_{digest} / t_{digest}) \sim 0.046$ μm³/robot-sec of ingested plaque material. In that case, the time to digest the plaque from all penile arteries in cases of severe ED would be $t_{plaque} \sim V_{plaque} / \beta_{digest} N_{vasculocytes} \sim 21,700$ sec (~ 6

³⁸⁵ https://en.wikipedia.org/wiki/Dorsal_artery_of_the_penis.

³⁸⁶ https://en.wikipedia.org/wiki/Artery_of_bulb_of_penis.

³⁸⁷ https://en.wikipedia.org/wiki/Deep_artery_of_the_penis.

³⁸⁸ A hexagonal nanorobot of width $w = 2.7$ μm + (0.2-0.6 μm bumper extensions) ~ 3.1 μm (range 2.9-3.3 μm) and height $h = 1$ μm has side length $s = w / 3^{1/2} \sim 1.79$ μm (1.67-1.91 μm), top facial surface area $A_{vasculocyte} = (3/2) 3^{1/2} s^2 \sim 8.3$ μm² (7.2-9.5 μm²) and volume $V_{vasculocyte} = h A_{vasculocyte} \sim 8.3$ μm³.

³⁸⁹ Freitas RA Jr. Nanomedicine, Volume I: Basic Capabilities, Landes Bioscience, Georgetown TX, 1999; Section 7.4.7, "Outmessaging to External Receivers"; <http://www.nanomedicine.com/NMI/7.4.7.htm>.

³⁹⁰ Freitas RA Jr. Nanomedicine, Volume I: Basic Capabilities, Landes Bioscience, Georgetown TX, 1999; Section 7.4.1, "Inmessaging from External Sources"; <http://www.nanomedicine.com/NMI/7.4.1.htm>.

³⁹¹ If $\sim 20\%$ of vessel length is 60-70% volumetrically occluded by focal plaques in severe ED and $\sim 80\%$ of vessel length is only $\sim 20\%$ volumetrically occluded by diffuse plaques, then the overall plaque volume across all penile arteries is $\sim 30\%$.

hrs). This is much faster than natural hemangioblast precursor cells derived from human stem cells that show robust reparative function of damaged rat/mouse vasculature in 24-48 hours.³⁹² Note that a similar function could be performed via nanocatheter insertion ([Section 5.2.4.2](#)).

Removing arterial plaques is a major step in restoring vascular health, but atherosclerotic arteries may also exhibit increased stiffness and loss of elasticity due to several additional changes within the arterial wall that can be addressed by nanorobot variants specialized for the purpose. Some additional arterial pathological changes requiring repair may include:

(1) **Endothelial Dysfunction.** Atherosclerotic endothelial cells may partially or entirely lose their ability to produce nitric oxide (NO) – a critical molecule for vasodilation – diminishing the vessel's ability to respond to changes in blood flow and pressure, contributing to stiffness. Increased oxidative stress can exacerbate the loss of elasticity by promoting inflammation and contributing to the breakdown of the normal, flexible structure of the arterial wall. In cases of light to moderate damage, vasculocytes specialized for cell repair³⁹³ could perform a diagnostic and repair function by making biochemical adjustments to the endothelial cytosol or nucleus to restore normal NO production. In cases of more severe damage, irreparable cells can be excised and digested, and replacement endothelial cells can be manufactured exogenously³⁹⁴ and transported to active repair sites for transplantation as required. Large-artery penile endothelial cells typically measure 10-20 μm (width) x 20-40 μm (length) x 1-2 μm (thickness) with a representative volume of $V_{\text{EC}} \sim 570 \mu\text{m}^3$ (range 200-1600 μm^3). Even if dehydrated, these cells would be too large for delivery by a bloodborne medical nanorobot, so they must be transported to the repair site via nanocatheter insertion ([Section 5.2.4.3](#)).

(2) **Sub-Endothelial Extracellular Matrix (ECM) Alterations.** In response to endothelial injury and chronic inflammation, there is often an increase in the production of extracellular matrix components, such as collagen and elastin, beneath the endothelial layer. However, the collagen produced in response to injury is often disorganized and stiffer, leading to fibrosis that rigidifies the arterial wall and reduces its ability to expand and contract. The ECM can also suffer elastin degradation. The normal elastic properties of arteries are largely due to elastin, a protein that allows the vessel to stretch and recoil. In atherosclerosis, elastin can be degraded by enzymes such as matrix metalloproteinases (MMPs) which are upregulated in response to chronic inflammation. The loss of elastin and its replacement by stiffer collagen contributes to the loss of arterial elasticity. The ECM can be repaired by long-reach vasculocytes equipped with telescoping probes perhaps 3-5 μm in extensible length that can be passed through the relatively thin endothelial cells into the ECM lying below. These probes can incorporate chemical and mechanical force sensors capable of detecting an abnormally stiff ECM,

³⁹² Lu SJ, Feng Q, Caballero S, Chen Y, Moore MA, Grant MB, Lanza R. Generation of functional hemangioblasts from human embryonic stem cells. *Nat Methods*. 2007 Jun;4(6):501-9; <https://www.ncbi.nlm.nih.gov/pmc/articles/PMC3766360/pdf>.

³⁹³ Freitas RA Jr. The ideal gene delivery vector: Chromalloyocytes, cell repair nanorobots for chromosome replacement therapy. *J Evol Technol* 2007;16:1-97; <http://jetpress.org/v16/freitas.pdf>.

³⁹⁴ Freitas RA Jr. Cell Mills: Nanofactory Manufacture of Biological Components. IMM Report No. 53, 15 June 2024; <http://www.imm.org/Reports/rep053.pdf>.

determining its cause, then injecting carefully targeted and metered doses of enzymes or other biochemicals designed to break down elastin and collagen, or to rebuild elastin, as required.

(3) **Phenotypic Switching of Smooth Muscle Cells.** Smooth muscle cells in the arterial wall can switch from a contractile phenotype to a synthetic phenotype³⁹⁵ in response to atherosclerotic changes – in particular, by immune cells such as macrophages and T cells that release cytokines and growth factors such as transforming growth factor-beta (TGF- β) and platelet-derived growth factor (PDGF). In their synthetic state, these smooth muscle cells produce more extracellular matrix, including collagen, and contribute to the thickening and stiffening of the arterial wall. This switched state should be reversible by the insertion of appropriate biochemical agents³⁹⁶ into the cytosol of the misbehaving cells using nanorobotic instrumentalities. Note that the arterial wall includes (A) the **tunica intima**, a 1-2 μm monolayer of endothelial cells underlain by a 1-2 μm layer of extracellular matrix which includes a basement membrane and some connective tissue primarily composed of collagen and elastin, and (B) the 100-300 μm thick **tunica media**, which contains the smooth muscle cells responsible for the contractility and structural integrity of the artery, mostly evenly distributed. Delivery of cytosolic modification agents to these cells will require either a nanorobot capable of histonation³⁹⁷ including diapedesis, ECM brachiation, intercellular passage, and post-mission withdrawal, or alternately may be accomplished via nanocatheter insertion (Section 5.2.4.4). Nanorobotic treatment devices likely also require a limited ability to digest calcified tissues, since the aforementioned switched smooth muscle cells can also undergo osteogenic differentiation, contributing to the calcification of the arterial wall and further increasing vascular stiffness.

(4) **Inflammation and Immune Response.** Atherosclerosis is associated with chronic low-grade inflammation within the arterial wall. This inflammation not only drives the formation of plaques but also contributes to the stiffening of the vessel by recruiting immune cells that release cytokines and growth factors, promoting fibrosis and calcification. The inflammatory process begins in the tunica intima, the innermost layer of the artery. Then, as atherosclerosis

³⁹⁵ aka. “synthetic SMCs”, “proliferative SMCs”, “dedifferentiated SMCs”, “secretory phenotype”, or “phenotypically modulated SMCs”.

³⁹⁶ Biochemical substances that may be capable of reverting smooth muscle cells back to the contractile phenotype upon injection into the cytosol of affected cells using medical nanorobots may include: (1) pharmaceutical agents such as statins, anti-inflammatory drugs, or angiotensin-converting enzyme (ACE) inhibitors; (2) signaling molecules and growth factors such as retinoic acid (which promotes the contractile phenotype by activating specific nuclear receptors that regulate gene expression associated with SMC differentiation) or microRNAs (miRNAs) such as miR-143 and miR-145 (which promote the contractile phenotype by regulating genes involved in SMC differentiation); and (3) gene therapy and molecular interventions such as introducing genes that code for contractile proteins (like smooth muscle α -actin or myosin heavy chain) that lead to the overexpression of contractile proteins and can encourage SMCs to revert to the contractile phenotype, or introducing transcription factors such as myocardin (which promotes the expression of contractile genes and may induce the switch back to the contractile state), using chromalloyocytes.

³⁹⁷ aka. “swimming through tissue”; Freitas RA Jr. Nanomedicine, Volume I: Basic Capabilities, Landes Bioscience, Georgetown TX, 1999; Section 9.4.4, “Histonation”; <http://www.nanomedicine.com/NMI/9.4.4.htm>.

progresses, the inflammation sometimes extends deeper into the tunica media in the most serious cases, slowly eating away at the vessel walls from the inside out. Performing the nanorobotic repair operations described earlier in [Section 5.2.1.1](#) should quell the inflammatory response, allowing arterial repair to proceed to a complete and stable conclusion.

5.2.1.2 Venous Leakage

Venous leak,³⁹⁸ also known as venogenic erectile dysfunction, penile venous insufficiency, or veno-occlusive dysfunction, refers to a condition in which the veins of the penis are unable to properly restrict the outflow of blood during an erection in order to trap blood within the penile corpora cavernosa, despite the presence of sufficient arterial blood flow through the cavernosal arteries of the penis.³⁹⁹ This allows excessive drainage of veins in the cavernosal tissue of the penis, undermining the normal erectile function.

One possible cause for this condition is the failure of smooth muscle to relax: If the smooth muscle within the corpora cavernosa fails to relax fully,⁴⁰⁰ the pressure needed to compress the subtunical venular plexuses adequately might not be achieved. Structural abnormalities could be another cause: The connective tissue of the tunica albuginea⁴⁰¹ might be defective or damaged, which can prevent it from adequately compressing the venous plexuses, most importantly the deep dorsal vein of the penis, the pair of cavernosal veins, and two pairs of para-arterial veins between the Buck's fascia and the tunica albuginea. Correcting these defects, or correcting increased fibrosis of the corpora cavernosa, will require some tissue remodeling using either (1) a cell repair nanorobot⁴⁰² capable of histonation⁴⁰³ including diapedesis, ECM brachiation, intercellular passage, and post-mission withdrawal, roughly analogous to the fibroblast,⁴⁰⁴ or (2)

³⁹⁸ https://en.wikipedia.org/wiki/Venous_leak.

³⁹⁹ Kaba R, Pearce I. Venous leak and erectile dysfunction – an important differential. J Clin Urology 2020; 13(1):33-39; <https://journals.sagepub.com/eprint/DJFPN9QYWVYFWWDKKHG4/full>.

⁴⁰⁰ Plaque formation generally does not occur in the corpora cavernosa of the penis. However, chronic ischemia (inadequate blood supply) can lead to cavernosal fibrosis in which the normal smooth muscle tissue is replaced by scar tissue. This reduces the elasticity and functionality of the corpora cavernosa, making it harder to achieve a rigid erection. The ability of the corpora cavernosa to trap blood during an erection can be impaired (veno-occlusive dysfunction) if the tissues become fibrotic or if the smooth muscle loses its normal function, leading to difficulties in maintaining an erection.

⁴⁰¹ The tunica albuginea is the fibrous envelope that extends the length of the corpus cavernosum and the corpus spongiosum in the penis; [https://en.wikipedia.org/wiki/Tunica_albuginea_\(penis\)](https://en.wikipedia.org/wiki/Tunica_albuginea_(penis)).

⁴⁰² Freitas RA Jr. The ideal gene delivery vector: Chromalloyocytes, cell repair nanorobots for chromosome replacement therapy. J Evol Technol 2007;16:1-97; <http://jetpress.org/v16/freitas.pdf>.

⁴⁰³ Freitas RA Jr. Nanomedicine, Volume I: Basic Capabilities, Landes Bioscience, Georgetown TX, 1999; Section 9.4.4, "Histonation"; <http://www.nanomedicine.com/NMI/9.4.4.htm>.

⁴⁰⁴ <https://en.wikipedia.org/wiki/Fibroblast>.

an alternative nanocatheter approach to address smooth muscle cell ([Section 5.2.4.4](#)) or connective tissue ([Section 5.2.4.5](#)) defects.

The condition might also be caused by anomalies in the venous anatomy itself, such as the presence of excessive or aberrant venous channels that should not be there, that could also prevent proper venous occlusion. To correct such venous structural defects, bloodborne nanorobots can perform temporary⁴⁰⁵ or permanent vascular occlusion functionally analogous to the contemporary techniques of surgical ablation,⁴⁰⁶ embolization,⁴⁰⁷ or multi-vessel ligation⁴⁰⁸ of the leaking veins.

⁴⁰⁵ Freitas RA Jr. Chapter 23. Comprehensive Nanorobotic Control of Human Morbidity and Aging. In: Fahy GM, West MD, Coles LS, Harris SB, eds, *The Future of Aging: Pathways to Human Life Extension*, Springer, New York, 2010; Section 23.6.3.5.1, “Vascular Gates”; <http://www.nanomedicine.com/Papers/Aging.pdf>.

⁴⁰⁶ Schild HH, Müller SC, Mildenerberger P, Strunk H, Kaltenborn H, Kersjes W, Fritz T, Thelen M. Percutaneous penile venoablation for treatment of impotence. *Cardiovasc Intervent Radiol*. 1993 Sep-Oct;16(5):280-6; <https://pubmed.ncbi.nlm.nih.gov/8269423/>. Nakata M, Takashima S, Kaminou T, Koda Y, Morimoto A, Hamuro M, Matsuoka T, Yasumoto R, Nakamura K, Yamada R. Embolotherapy for venous impotence: use of ethanol. *J Vasc Interv Radiol*. 2000 Sep;11(8):1053-7; <https://pubmed.ncbi.nlm.nih.gov/10997470/>. Herwig R, Sansalone S. Venous leakage treatment revisited: pelvic venoablation using aethoxysclerol under air block technique and Valsalva maneuver. *Arch Ital Urol Androl*. 2015 Mar 31;87(1):1-4; <https://www.pagepressjournals.org/aiua/article/view/aiua.2015.1.1/4563>.

⁴⁰⁷ Peşkırcioğlu L, Tekin I, Boyvat F, Karabulut A, Ozkardeş H. Embolization of the deep dorsal vein for the treatment of erectile impotence due to veno-occlusive dysfunction. *J Urol*. 2000 Feb;163(2):472-5; <https://pubmed.ncbi.nlm.nih.gov/10647658/>. Rebonato A, Auci A, Sanguinetti F, Maiettini D, Rossi M, Brunese L, Carrafiello G, Torri T. Embolization of the periprostatic venous plexus for erectile dysfunction resulting from venous leakage. *J Vasc Interv Radiol*. 2014 Jun;25(6):866-72; <https://pubmed.ncbi.nlm.nih.gov/24613267/>. Diehm N, Pelz S, Kalka C, Keo HH, Mohan V, Schumacher MC, Do DD, Hoppe H. Venous Leak Embolization in Patients with Venogenic Erectile Dysfunction via Deep Dorsal Penile Vein Access: Safety and Early Efficacy. *Cardiovasc Intervent Radiol*. 2023 May;46(5):610-616; <https://www.ncbi.nlm.nih.gov/pmc/articles/PMC10156837/pdf>.

⁴⁰⁸ Freedman AL, Costa Neto F, Mehringer CM, Rajfer J. Long-term results of penile vein ligation for impotence from venous leakage. *J Urol*. 1993 May;149(5 Pt 2):1301-3; <https://pubmed.ncbi.nlm.nih.gov/8479020/>. Hwang TI, Yang CR. Penile vein ligation for venogenic impotence. *Eur Urol*. 1994;26(1):46-51; <https://pubmed.ncbi.nlm.nih.gov/7925529/>. Popken G, Katzenwadel A, Wetterauer U. Long-term results of dorsal penile vein ligation for symptomatic treatment of erectile dysfunction. *Andrologia*. 1999;31 Suppl 1:77-82; <https://pubmed.ncbi.nlm.nih.gov/10643523/>. Lue TF. Surgery for crural venous leakage. *Urology*. 1999 Oct;54(4):739-41; <https://pubmed.ncbi.nlm.nih.gov/10510940/>. Rahman NU, Dean RC, Carrion R, Bochinski D, Lue TF. Crural ligation for primary erectile dysfunction: a case series. *J Urol*. 2005 Jun;173(6):2064-6; <https://pubmed.ncbi.nlm.nih.gov/15879835/>.

5.2.2 Nanorobotic Cure for ED-Related Neurological Disorders

Normal erectile function requires an intact neural pathway from the brain and spinal cord to the penile tissues. Neurological disorders such as Parkinson's disease, multiple sclerosis (MS), stroke, and spinal cord injuries can interrupt these pathways, causing damage or degeneration of nerves that transmit signals necessary to initiate the release of nitric oxide, thus preventing the relaxation of smooth muscle in the corpora cavernosa.

Nerves affected by these disorders include (1) the parasympathetic pelvic splanchnic nerves that travel to the penis via the sacral spinal cord region (S2-S4), that transmit signals necessary to initiate the release of nitric oxide which triggers the relaxation of smooth muscle in the corpora cavernosa [Parkinson's, MS] in the **pelvis**; (2) the sacral spinal cord (S2-S4) for parasympathetic control, and the thoracolumbar spinal cord (T11-L2) for sympathetic control [MS, spinal], in the **spinal column**; and (3) dopaminergic pathways involving the substantia nigra⁴⁰⁹ and its projections, cerebral cortical areas involved in sexual function such as the medial prefrontal cortex and the paracentral lobule, and brainstem autonomic centers such as the paraventricular nucleus of the hypothalamus and their descending pathways that control erection [Parkinson's, stroke], in the **brain**. General nanorobotic cellular and tissue repairs to the brain and spine have been briefly reviewed elsewhere.⁴¹⁰

Considering only the specific pelvic nerves directly involved in erection: (1) the **pelvic splanchnic nerves** transmit from the brain and spinal cord the signals necessary to initiate the release of nitric oxide which triggers the relaxation of smooth muscle in the corpora cavernosa, (2) the **cavernous nerves** arising from the pelvic plexus proximately innervate the penile tissue and are directly responsible for the relaxation of smooth muscle in the corpora cavernosa, and (3) the **pudendal nerves** control the sensory feedback from the penis and the motor functions of the pelvic floor muscles (e.g., the ischiocavernosus and bulbospongiosus muscles) that contribute to the maintenance of an erection by increasing penile rigidity, and are also involved in ejaculation. These nerves can be damaged by demyelination [MS],⁴¹¹ degeneration [diabetic neuropathy],⁴¹² compression⁴¹³ or entrapment,⁴¹⁴ or by direct trauma⁴¹⁵ or surgical injury [prostate surgery].⁴¹⁶

⁴⁰⁹ https://en.wikipedia.org/wiki/Substantia_nigra.

⁴¹⁰ Freitas RA Jr. The Alzheimer Protocols: A Nanorobotic Cure for Alzheimer's Disease and Related Neurodegenerative Conditions. IMM Report No. 48, June 2016; <http://www.imm.org/Reports/rep048.pdf>.

⁴¹¹ https://en.wikipedia.org/wiki/Demyelinating_disease.

⁴¹² Degenerated nerves lose their ability to conduct electrical impulses effectively, leading to impaired function in the penile tissues they innervate (in this case, the penile tissues). Degeneration of the pelvic splanchnic nerves in diabetic patients is primarily caused by chronic hyperglycemia, leading to a cascade of harmful effects including oxidative stress, ischemia, inflammation, and demyelination.

⁴¹³ Compression can physically damage the nerve fibers (axons) or disrupt the blood supply to the nerve (ischemia), leading to impaired signal transmission. Prolonged compression can lead to degeneration of the nerve fibers, resulting in permanent damage if not relieved. Compression can occur from mechanical pressure (e.g., squeezing a nerve between two structures such as bone and muscle, or tumor and pelvic wall), inflammation and edema (increasing the volume of non-penile pelvic tissues, which can press against

Correcting these neuronal defects will require tissue remodeling using either a cell repair nanorobot⁴¹⁷ capable of histonataion⁴¹⁸ including diapedesis, ECM brachiation, intercellular passage, and post-mission withdrawal, or an alternative nanocatheter approach ([Section 5.2.4.5](#)).

For example, consider the nanorobotic repair of normally myelinated **pelvic splanchnic nerves** that have become demyelinated. In severe cases of demyelination, such as those seen in advanced diabetic neuropathy, multiple sclerosis, or other neurodegenerative diseases, it is common for 50-80% of the original myelin to be damaged or missing, but even moderate demyelination in the 20-50% range can produce slowed or disrupted nerve signaling, contributing to erectile dysfunction. Typically there are three pairs of myelinated pelvic splanchnic nerves, with each nerve 5-15 cm in length and 1-3 mm in diameter, which enter the pelvic plexus or inferior hypogastric plexus. Thus the total myelinated surface area is $A_{\text{mye}} \sim 40 \text{ cm}^2$, and the total myelination volume is $V_{\text{mye}} \sim A_{\text{mye}} x_{\text{mye}} \sim 4 \text{ mm}^3$, assuming a $x_{\text{mye}} \sim 1 \mu\text{m}$ myelin coat thickness. If a histonataing nanorobot that is $A_{\text{robot}} \sim 10 \mu\text{m}^2$ in areal extent can move an $A_{\text{myescanner}} \sim 1 \mu\text{m}^2$ scanning sensor across the surface of a pelvic splanchnic nerve at a scan speed of $v_{\text{scan}} \sim 1 \mu\text{m}/\text{sec}$, then $N_{\text{robots}} = 4$ million robots could inspect all nerve surfaces for evidence of demyelination in $t_{\text{myescan}} \sim A_{\text{mye}} A_{\text{myescanner}}^{1/2} / A_{\text{myescanner}} v_{\text{scan}} N_{\text{robots}} \sim 1000 \text{ sec}$, with the nanorobots occupying $A_{\text{robot}} N_{\text{robots}} / A_{\text{mye}} \sim 1\%$ of the nerve surface area at any one time. If each nanorobot carries $V_{\text{myepatch}} \sim 10 \mu\text{m}^3$ of replacement myelin, then the fleet has enough patch material to replace $V_{\text{myepatch}} N_{\text{robots}} / V_{\text{mye}} \sim 1\%$ of missing myelin every $t_{\text{myescan}} \sim 1000 \text{ sec}$ assuming the robots can apply patch material at the same v_{scan} speed. All repairs could be completed in 20,000-80,000 sec (6-22 hrs) assuming 20%-80% of the original myelin volume is replaced or repaired, or the number of nanorobots could be increased to shorten the repair time,

the nerves), or fibrosis and scarring which can encase or squeeze the nerve, reducing its ability to transmit signals.

⁴¹⁴ Entrapment of the pudendal nerves, aka. pudendal neuralgia, occurs when the nerve becomes compressed or trapped by surrounding tissues, leading to pain, sensory disturbances, and motor dysfunction. The pudendal nerve passes through several anatomical structures, including the Alcock' canal (a fascial tunnel formed by the obturator internus muscle) and the sacrospinous ligament near the ischial spine, both of which can become narrowed due to fibrosis or scar tissue, muscle hypertrophy or spasm, or ligament thickening or abnormal tensioning. Overactivity or dysfunction in the pelvic floor muscles can also lead to increased pressure on the pudendal nerve as it passes through the pelvic region.

⁴¹⁵ A direct injury to the pelvis, such as from a fracture, can cause structural changes or swelling that compress the pudendal nerve. Activities that place prolonged pressure on the perineal area, such as long-distance cycling, horseback riding, or certain sitting postures, can lead to entrapment of the pudendal nerve.

⁴¹⁶ https://en.wikipedia.org/wiki/Prostatectomy#Erectile_dysfunction.

⁴¹⁷ Freitas RA Jr. The ideal gene delivery vector: Chromalloyocytes, cell repair nanorobots for chromosome replacement therapy. J Evol Technol 2007;16:1-97; <http://jetpress.org/v16/freitas.pdf>.

⁴¹⁸ Freitas RA Jr. Nanomedicine, Volume I: Basic Capabilities, Landes Bioscience, Georgetown TX, 1999; Section 9.4.4, "Histonataion"; <http://www.nanomedicine.com/NMI/9.4.4.htm>.

e.g., 40 million robots working for 2000-8000 sec (1-2 hrs). The **pudendal nerves** can similarly be remyelinated.⁴¹⁹

Note that these nanorobots, as specified, are ~10,000 times more productive than natural biological oligodendrocyte neuroglial cells⁴²⁰ that remyelinate⁴²¹ denuded neural axons in the human body – which is not surprising since the robots need only dispense myelin repair material from onboard storage whereas the oligodendrocytes must synthesize the lipid-rich substance⁴²² from scratch. Specifically, based on observations of myelin sheath thickness (0.1-2 μm) and the rate of forward progress at which oligodendrocytes extend their processes to wrap around axons (several $\mu\text{m}/\text{day}$), these 500-1000 μm^3 mobile neuroglial cells may synthesize and deploy 0.01-0.1 $\mu\text{m}^3/\text{hr}$ of new myelin sheath, giving them a volumetric productivity of **$0.1\text{-}1 \times 10^{-4} \mu\text{m}^3/\mu\text{m}^3\text{-hr}$** . By contrast, the nanorobots have a volume of ~32 μm^3 and are specified to dispense 10 μm^3 of myelin every 1000 sec, giving them a volumetric productivity of **$\sim 1 \mu\text{m}^3/\mu\text{m}^3\text{-hr}$** .

The unmyelinated **cavernous nerve** fibers emanate from the pelvic plexus. There are two greater cavernous nerves, one on either side of the penis, each typically about 5-10 cm in length and 1-2 mm in diameter. These nerves give rise to several lesser cavernous nerves on each side, measuring 3-7 cm in length and 0.5-1 mm in diameter. Each of these nerves then branches into several thousand tiny individual nerve fibers, generally 3-10 cm long and 1-5 μm in diameter, perhaps with a total fiber length of $L_{\text{fiber}} \sim 100 \text{ m}$, innervating the entire length and breadth of the corpora cavernosa and surrounding structures, and giving a total repair surface of $\sim 10 \text{ cm}^2$. If histonating nanorobots can survey and repair these tiny nerve fibers at a very conservative speed of $v_{\text{fiber}} \sim v_{\text{scan}} / 100 = 0.01 \mu\text{m}/\text{sec}$, then a fleet of $N_{\text{robots}} = 4$ million robots could repair all the penile nerve fibers in $t_{\text{fiber}} \sim L_{\text{fiber}} / v_{\text{fiber}} N_{\text{robots}} \sim 2500 \text{ sec}$.

5.2.3 Nanorobotic Cure for Other ED-Related Pathologies

The principal ED-related **hormone imbalance** ([Section 3.3](#)) is a low bloodstream level of testosterone in the human male, typically due to hypogonadism which can have a multitude of causes.⁴²³ Testosterone replacement therapy ([Section 4.3](#)) is a convenient and widely-used symptomatic treatment to elevate blood concentrations back to normal levels. Another symptomatic treatment for hypogonadism is administration of human chorionic gonadotropin (hCG),⁴²⁴ which stimulates the LH receptor⁴²⁵ and elicits testosterone synthesis – though this is

⁴¹⁹ There are two myelinated pudendal nerves that emerge from the sacral plexus, 10-15 cm long and 2-5 mm wide, with each nerve splitting into three branches, one of which the dorsal nerve of the penis. The pudendal nerve is a mixed nerve containing heavily myelinated motor and sensory fibers.

⁴²⁰ <https://en.wikipedia.org/wiki/Oligodendrocyte>.

⁴²¹ <https://en.wikipedia.org/wiki/Remyelination>.

⁴²² <https://en.wikipedia.org/wiki/Myelin#Composition>.

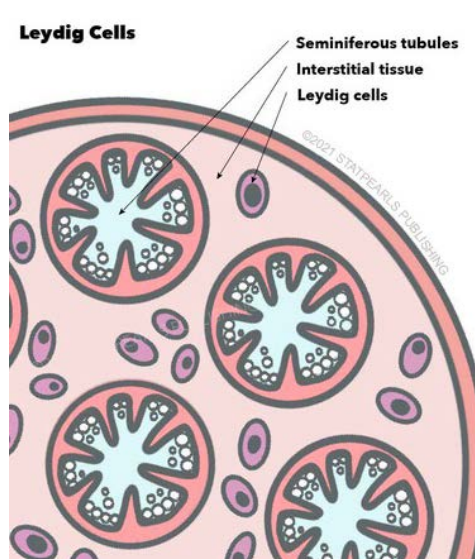
⁴²³ <https://en.wikipedia.org/wiki/Hypogonadism#Classification>.

⁴²⁴ Chudnovsky A, Niederberger CS. Gonadotropin therapy for infertile men with hypogonadotropic hypogonadism. J Androl. 2007 Sep-Oct;28(5):644-6;
<https://onlinelibrary.wiley.com/doi/pdfdirect/10.2164/jandrol.107.003400>.

⁴²⁵ https://en.wikipedia.org/wiki/Luteinizing_hormone/choriogonadotropin_receptor.

ineffective in men with primary hypogonadism whose testes can no longer synthesize testosterone.

A curative treatment for primary hypogonadism that permanently restores normal testosterone production in the testes requires correcting the organic problem that is causing the hypogonadism. In most cases of primary hypogonadism, the inability of the testes to synthesize and release testosterone into the bloodstream is mostly due to damage or dysfunction in the Leydig cells⁴²⁶ (image, right)⁴²⁷ of the testes, which are responsible for producing testosterone. Various cellular pathologies of the Leydig cells – including (1) nucleus DNA damage, (2) genetic mutations, (3) damaged mitochondrial DNA, (4) cytosolic misfolded proteins due to endoplasmic reticulum stress, (5) oxidative damage to proteins, lipids, or DNA caused by high levels of reactive oxygen species, and even (6) cellular senescence – can be reversed by cell repair nanorobots⁴²⁸ that can diagnose the particular cellular pathology and then exchange pristine new molecules or whole organelles for the damaged old ones in every Leydig cell. Cell mills⁴²⁹ can readily manufacture atomically-precise autologous whole replacement cells which could be inserted into the testes as the old ones are removed, probably using a nanocatheter approach (Section 5.2.4.3) given the size of the cells.⁴³⁰ Alternatively, entire autologous replacement testes could be fabricated in an organ mill⁴³¹ and transplanted into the patient's scrotum.⁴³²



The principal ED-related **enzymatic abnormality** (Section 3.4) is the over-expression of the phosphodiesterase type 5 (PDE5)⁴³³ enzyme by smooth muscle cells in the corpora cavernosa.

⁴²⁶ https://en.wikipedia.org/wiki/Leydig_cell.

⁴²⁷ Aladamat N, Tadi P. Histology, Leydig Cells. StatPearls [Internet], 14 Nov 2022; <https://www.ncbi.nlm.nih.gov/books/NBK556007/>.

⁴²⁸ Freitas RA Jr. The ideal gene delivery vector: Chromalloyocytes, cell repair nanorobots for chromosome replacement therapy. J Evol Technol 2007;16:1-97; <http://jetpress.org/v16/freitas.pdf>.

⁴²⁹ Freitas RA Jr. Cell Mills: Nanofactory Manufacture of Biological Components. IMM Report No. 53, 15 June 2024; <http://www.imm.org/Reports/rep053.pdf>.

⁴³⁰ Leydig cells are 15-20 µm in diameter and number approximately 200-700 million in each testicle.

⁴³¹ Freitas RA Jr. Cell Mills: Nanofactory Manufacture of Biological Components. IMM Report No. 53, 15 June 2024; Section 5, "Tissue Mills"; <http://www.imm.org/Reports/rep053.pdf>.

⁴³² <https://en.wikipedia.org/wiki/Scrotum>.

⁴³³ https://en.wikipedia.org/wiki/CGMP-specific_phosphodiesterase_type_5.

PDE5 degrades cGMP, a second messenger molecule that activates and maintains vasodilation, and its over-expression reduces the ability of these cells to relax, thus preventing adequate penile engorgement. Chronic conditions like diabetes, hypertension, and atherosclerosis induce endothelial dysfunction, oxidative stress, and inflammatory changes that can induce PDE5 overexpression.

More specifically, chronic hyperglycemia in diabetes, the elevated blood pressure in hypertension, and the formation of plaques on endothelial cells in atherosclerosis lead to an increase in reactive oxygen species (ROS) which can reduce NO availability by directly reacting with NO to form peroxynitrite, a reactive nitrogen species that is damaging to cells. Reduced NO levels lead to decreased cGMP production because NO is the primary activator of guanylate cyclase. The combination of oxidative stress, reduced NO, and chronic inflammation activates several intracellular signaling pathways, including protein kinase C (PKC), mitogen-activated protein kinases (MAPKs), and the NF- κ B pathway. These pathways can converge on the transcriptional regulation of PDE5. These signaling pathways can lead to the activation of transcription factors that bind to the promoter regions of the PDE5 gene, increasing its transcription. For example, oxidative stress and inflammatory signaling can upregulate transcription factors such as AP-1, Sp1, or NF- κ B, which may enhance PDE5 gene expression, exacerbating the symptoms of erectile dysfunction.

As noted earlier in connection with nanorobotic treatments to address phenotypic switching of smooth muscle cells ([Section 5.2.1.1 \(3\)](#)), the delivery of cytosolic modification agents⁴³⁴ or nanomachine instrumentalities into these cells will require either a cell repair nanorobot capable of histonation⁴³⁵ including diapedesis, ECM brachiation, intercellular passage, and post-mission withdrawal, or alternately may be accomplished via nanocatheter injection or insertion ([Section 5.2.4.4](#)). Afterwards, the root causes of the pre-existing diabetes or hypertension conditions must also be addressed to prevent a future recurrence of the PDE5 overexpression pathology.

There are also a large number of ED-related **co-morbidities** that either cause or aggravate erectile dysfunction, including cardiovascular disease, diabetes, obesity, neurological disorders, enlarged prostate, chronic liver or kidney disease, and sleep disorders ([Section 3.7](#)), and ED-related male disorders including anorgasmia,⁴³⁶ delayed ejaculation,⁴³⁷ premature ejaculation,⁴³⁸ and retrograde ejaculation.⁴³⁹ Nanorobotic cures are required for all of these primary pathologies and

⁴³⁴ Reducing PDE5 overexpression in smooth muscle cells could be achieved using RNA-based strategies (siRNA, shRNA, or antisense oligonucleotides, aka. ASOs), introducing regulatory molecules like miRNA or small molecules that suppress PDE5 expression, or gene-editing of individual cells. Each of these approaches needs the precise delivery into individual cells that would be provided by chromalloyocytes.

⁴³⁵ aka. "swimming through tissue"; Freitas RA Jr. Nanomedicine, Volume I: Basic Capabilities, Landes Bioscience, Georgetown TX, 1999; Section 9.4.4, "Histonation"; <http://www.nanomedicine.com/NMI/9.4.4.htm>.

⁴³⁶ <https://en.wikipedia.org/wiki/Anorgasmia>.

⁴³⁷ https://en.wikipedia.org/wiki/Delayed_ejaculation.

⁴³⁸ https://en.wikipedia.org/wiki/Premature_ejaculation.

⁴³⁹ https://en.wikipedia.org/wiki/Retrograde_ejaculation.

a few have been described elsewhere at length,⁴⁴⁰ but a comprehensive discussion is beyond the scope of this paper.

5.2.4 Nanocatheter-Based Interventions

As the era of surgical nanorobotics arrives,⁴⁴¹ today's smallest millimeter-diameter flexible catheters will shrink to micron-diameter mechanical fibers that can be steered⁴⁴² through the tiniest blood vessels (including capillaries). Tactile,⁴⁴³ haptic,⁴⁴⁴ and other sensory feedback will allow surgical practitioners to maneuver the nanocatheter into a patient to either emplace or remove materials from inside tissues, then to withdraw bloodlessly from the body. The nanosurgeon may control the procedure via hand-guided interfaces similar to various medical exoskeletal appliances,⁴⁴⁵ instrumented gloves⁴⁴⁶ and hand-held surgical robots⁴⁴⁷ that have been

⁴⁴⁰ Freitas RA Jr. Chapter 23. Comprehensive Nanorobotic Control of Human Morbidity and Aging. In: Fahy GM, West MD, Coles LS, Harris SB, eds, *The Future of Aging: Pathways to Human Life Extension*, Springer, New York, 2010; <http://www.nanomedicine.com/Papers/Aging.pdf>. Freitas RA Jr. The Alzheimer Protocols: A Nanorobotic Cure for Alzheimer's Disease and Related Neurodegenerative Conditions. IMM Report No. 48, June 2016, 433 pp; <http://www.imm.org/Reports/rep048.pdf>. Freitas RA Jr. Cryostasis Revival: The Recovery of Cryonics Patients through Nanomedicine. Alcor Life Extension Foundation, Scottsdale AZ, 2022; <https://www.alcor.org/cryostasis-revival/>.

⁴⁴¹ Freitas RA Jr. Chapter 23. Comprehensive Nanorobotic Control of Human Morbidity and Aging. In: Fahy GM, West MD, Coles LS, Harris SB, eds, *The Future of Aging: Pathways to Human Life Extension*, Springer, New York, 2010; Section 6.3.5.3, "Endoscopic Nanosurgery and Surgical Nanorobots"; <http://www.nanomedicine.com/Papers/Aging.pdf>.

⁴⁴² Glozman D, Shoham M. Flexible needle steering for percutaneous therapies. *Comput Aided Surg* 2006 Jul; 11(4):194-201; <http://www.ncbi.nlm.nih.gov/pubmed/17060077>.

⁴⁴³ Ku J, Mraz R, Baker N, Zakzanis KK, Lee JH, Kim IY, Kim SI, Graham SJ. A data glove with tactile feedback for FMRI of virtual reality experiments. *Cyberpsychol Behav*. 2003 Oct;6(5):497-508; <http://www.ncbi.nlm.nih.gov/pubmed/14583125>. Winter SH, Bouzit M. Use of magnetorheological fluid in a force feedback glove. *IEEE Trans Neural Syst Rehabil Eng* 2007 Mar;15(1):2-8; <http://www.ncbi.nlm.nih.gov/pubmed/17436869>.

⁴⁴⁴ McColl R, Brown I, Seligman C, Lim F, Alsaraira A. Haptic rendering for VR laparoscopic surgery simulation. *Australas Phys Eng Sci Med* 2006;29:73-78; <http://dspace2.flinders.edu.au/xmlui/bitstream/handle/2328/9552/2006017101.pdf?sequence=1>. De Rossi D, Carpi F, Carbonaro N, Tognetti A, Scilingo EP. Electroactive polymer patches for wearable haptic interfaces. *Conf Proc IEEE Eng Med Biol Soc*. 2011;2011:8369-72; <http://www.ncbi.nlm.nih.gov/pubmed/22256288>.

⁴⁴⁵ Fleischer C, Wege A, Kondak K, Hommel G. Application of EMG signals for controlling exoskeleton robots. *Biomed Tech (Berl)* 2006 Dec;51(5-6):314-319; <http://pdv.cs.tu-berlin.de/ExoSkeleton/Paper/bmte.51.5-6.314.pdf>. Cavallaro EE, Rosen J, Perry JC, Burns S. Real-time myoprocessors for a neural controlled powered exoskeleton arm. *IEEE Trans Biomed Eng* 2006 Nov;53(11):2387-2396; http://bionics.seas.ucla.edu/publications/JP_12.pdf. Gordon KE, Ferris DP. Learning to walk with a robotic ankle exoskeleton. *J Biomech* 2007;40(12):2636-2644; <http://www.ncbi.nlm.nih.gov/pubmed/17275829>. Ben-Tzvi P, Ma Z. Sensing and Force-Feedback

under development for several decades, and may include multisensory interfaces with individual cells.⁴⁴⁸ This Section extends previous discussions of the nanocatheter concept published in 2003,⁴⁴⁹ 2005,⁴⁵⁰ 2010,⁴⁵¹ 2016,⁴⁵² and 2022.⁴⁵³

Exoskeleton (SAFE) Robotic Glove. IEEE Trans Neural Syst Rehabil Eng. 2015 Nov;23(6):992-1002; <http://www.ncbi.nlm.nih.gov/pubmed/25494512>.

⁴⁴⁶ Castro MC, Cliquet A. A low-cost instrumented glove for monitoring forces during object manipulation. IEEE Trans Rehabil Eng 1997 Jun;5(2):140-147; <http://www.ncbi.nlm.nih.gov/pubmed/9184900>. Yun MH, Cannon D, Freivalds A, Thomas G. An instrumented glove for grasp specification in virtual-reality-based point-and-direct telerobotics. IEEE Trans Syst Man Cybern B Cybern 1997 Oct;27(5):835-846; <http://groklab.org/files/2007/02/An-instrumented-glove-for-grasp-specification-in-virtual-reality-based-point-and-direct-telerobotics.pdf>. Skinner A, Lathan C. Assessment of laparoscopic surgical skill acquisition and retention. Stud Health Technol Inform. 2012;173:478-82; <http://www.ncbi.nlm.nih.gov/pubmed/22357040>. Saggio G, Lazzaro A, Sbernini L, Carrano FM, Passi D, Corona A, Panetta V, Gaspari AL, Di Lorenzo N. Objective Surgical Skill Assessment: An Initial Experience by Means of a Sensory Glove Paving the Way to Open Surgery Simulation? J Surg Educ. 2015 Sep-Oct;72(5):910-7; <http://www.ncbi.nlm.nih.gov/pubmed/26089159>.

⁴⁴⁷ Tonet O, Focacci F, Piccigallo M, Cavallo F, Uematsu M, Megali G, Dario P. Comparison of control modes of a hand-held robot for laparoscopic surgery. Med Image Comput Comput Assist Interv. 2006;9(Pt 1):429-36; https://www.researchgate.net/profile/Oliver_Tonet/publication/6452106_Comparison_of_control_modes_of_a_hand-held_robot_for_laparoscopic_surgery/links/09e4150e5adb7137c1000000.pdf.

⁴⁴⁸ Koerner M, Wait E, Winter M, Bjornsson C, Kokovay E, Wang Y, Goderie SK, Temple S, Cohen AR. Multisensory interface for 5D stem cell image volumes. Conf Proc IEEE Eng Med Biol Soc. 2014;2014:1178-81; <http://www.ncbi.nlm.nih.gov/pmc/articles/PMC4321857/>

⁴⁴⁹ Freitas RA Jr. Nanomedicine, Volume IIA: Biocompatibility, Landes Bioscience, Georgetown, TX, 2003; Section 15.5.1.2, "Epidermalgia and Allodynia"; <http://www.nanomedicine.com/NMIIA/15.5.1.2.htm>.

⁴⁵⁰ Freitas RA Jr. Nanotechnology, nanomedicine and nanosurgery. Int J Surg. 2005;3(4):243-6; <https://www.sciencedirect.com/science/article/pii/S1743919105001299>.

⁴⁵¹ Freitas RA Jr. Chapter 23. Comprehensive Nanorobotic Control of Human Morbidity and Aging. In: Fahy GM, West MD, Coles LS, Harris SB, eds, The Future of Aging: Pathways to Human Life Extension, Springer, New York, 2010; Section 23.6.2.2, "Cancer"; Section 23.6.3.5.3, "Endoscopic Nanosurgery and Surgical Nanorobots"; Section 23.6.3.5.4, "Nanosyringoscopy"; Section 23.7.1.4, "Restoring Essential Lost or Atrophied Cells"; and Section 23.7.2(5)(d), "Rebuild neural tissue"; <http://www.nanomedicine.com/Papers/Aging.pdf>.

⁴⁵² Freitas RA Jr. The Alzheimer Protocols: A Nanorobotic Cure for Alzheimer's Disease and Related Neurodegenerative Conditions. IMM Report No. 48, June 2016; Section 4.3.5, "Nanocatheter Transport into the Brain"; Section 5.2.5, "Repair or Eliminate Toxic, Dysfunctional, and Senescent Cells"; Section 5.2.6, "Restore Essential Lost or Atrophied Cells"; Section 5.3.2.1, "Replacement Cell Manufacture"; Section 5.3.2.2., "Intracranial Debridement"; Section 5.3.2.3, "Cell Insertion and Emplacement"; <http://www.imm.org/Reports/rep048.pdf>.

⁴⁵³ Freitas RA Jr. Cryostasis Revival: The Recovery of Cryonics Patients through Nanomedicine. Alcor Life Extension Foundation, Scottsdale AZ, 2022; Section 4.12.1.6, "Cancer Cells"; Section 4.12.2.8,

The **nanocatheter** is a specialized fiber-like nanomechanical probe instrument with nanorobotic mechanisms embedded in its external surfaces to assist in actively propelling the telescoping apparatus gently through the tissues.⁴⁵⁴ Using external sensors the probe samples the chemical environment (e.g., concentrations of oxygen, glucose, hormones, cytokines) during insertion⁴⁵⁵ and provides a torrent of mechanical and optical sensory feedback together with precision positional metrology to allow the surgeon to know exactly where his tools are at all times, and also where his “virtual presence” is in relation to his targets, in cases of manually-guided procedures. Internal hollow spaces within the nanocatheter can be used to transport tools, sensors, fluids, drugs, nanorobots, replacement cells, or debridement detritus between patient and physician. The tip of the nanocatheter may include a working toolhead with thousands of independent manipulators and sensors branching outward from the central trunk on retractile stalks, from which data can be encoded in real time and passed to external computers in the operating theater along an optical data bus located inside each nanocatheter. Surgeons will gain the ability to easily control many more than one active surgical instrument or surgical task at a time.⁴⁵⁶ The multitasking by endoscopic nanosurgeons ultimately may extend to many thousands of nanocatheters and millions of simultaneously occurring mechanical and chemical processes during a single manually-guided and automation-assisted surgical procedure.

As an extension of today’s surgical microrobotics (a young but thriving field of experimental research),⁴⁵⁷ populations of individual surgical nanorobots could be introduced into the body from

“Whole-Cell Replacement Option”; Section 4.12.3.1, “Foreign Object Extraction and Avulsion Wound Repair”; Section 4.12.3.2, “Residual Vascular Repair”; and Section 4.12.4.3, “Missing Brain Tissue”; <https://www.alcor.org/cryostasis-revival/>

⁴⁵⁴ Freitas RA Jr. Nanomedicine, Volume I: Basic Capabilities. Landes Bioscience, Georgetown, TX, 1999; Section 9.4.4, “Histonatation”; <http://www.nanomedicine.com/NMI.htm>.

⁴⁵⁵ Freitas RA Jr. Nanomedicine, Volume I: Basic Capabilities. Landes Bioscience, Georgetown, TX, 1999; Chapter 4, “Nanosensors and nanoscale Sensing”; <http://www.nanomedicine.com/NMI.htm>.

⁴⁵⁶ Zhijiang D, Zhiheng J, Minxiu K. Virtual reality-based telesurgery via teleprogramming scheme combined with semi-autonomous control. Conf Proc IEEE Eng Med Biol Soc 2005;2:2153-2156; <http://www.ncbi.nlm.nih.gov/pubmed/17282656>.

⁴⁵⁷ Nelson BJ, Kaliakatsos IK, Abbott JJ. Microrobots for minimally invasive medicine. Annu Rev Biomed Eng. 2010 Aug 15;12:55-85; http://www.msrlpublications.ch/btw/files/Nelson_ARBE.pdf. Olamaei N, Cheriet F, Beaudoin G, Martel S. MRI visualization of a single 15 μ m navigable imaging agent and future microrobot. Conf Proc IEEE Eng Med Biol Soc. 2010;2010:4355-8; <http://www.ncbi.nlm.nih.gov/pubmed/21096004>. Ullrich F, Bergeles C, Pokki J, Ergeneman O, Erni S, Chatzipirpiridis G, Pané S, Framme C, Nelson BJ. Mobility experiments with microrobots for minimally invasive intraocular surgery. Invest Ophthalmol Vis Sci. 2013 Apr 23;54(4):2853-63; http://www.msrlpublications.ch/btw/files/Ullrich_IOVS_2013.pdf. Ceylan H, Giltinan J, Kozielski K, Sitti M. Mobile microrobots for bioengineering applications. Lab Chip. 2017 May 16;17(10):1705-1724; <https://pdfs.semanticscholar.org/9ad6/a7409b3711e9919b2c33c527cef783d983f9.pdf>. Hu M, Ge X, Chen X, Mao W, Qian X, Yuan WE. Micro/Nanorobot: A Promising Targeted Drug Delivery System. Pharmaceutics. 2020 Jul 15;12(7):665; <https://www.ncbi.nlm.nih.gov/pmc/articles/PMC7407549/pdf>. Soto F, Wang J, Ahmed R, Demirci U. Medical Micro/Nanorobots in Precision Medicine. Adv Sci (Weinh). 2020 Oct 4;7(21):2002203; <https://www.ncbi.nlm.nih.gov/pmc/articles/PMC7610261/pdf>. Sun B, Wood

the ends of nanocatheters into various vessels and other cavities within the body, and later retrieved when their job is done. A future surgical nanorobot, programmed or guided by a human surgeon, could act as a semi-autonomous on-site surgeon inside the human body, assisting activities occurring near the tip of the nanocatheter and coordinated by an onboard computer while maintaining contact with the supervising surgeon via coded ultrasound signals.

Insertion of the nanocatheter, even through brain tissue, should not create any significant damage if done slowly and carefully enough.⁴⁵⁸ Active nanocatheter tips festooned with sensors and manipulators will permit the nanosurgeon to steer the nanocatheter exclusively through tissue while avoiding bone and vascular puncture events. For example, cryobiologists have found that neurons and nerve processes are not torn apart when ice forms in the brain even at low temperatures in the presence of cryoprotectants.⁴⁵⁹ This supports the idea that the extracellular space can be significantly locally expanded without lasting harm. The migration of newly-generated neurons through the brain provides additional evidence that the organ can tolerate significant local distortion of the extracellular space. Migration of neurons or their precursors out of the hippocampus over large distances to other parts of the brain during neurogenesis⁴⁶⁰ is a mechanical process that is normal and apparently well tolerated. The passage of a sensor-guided tip-mobile nanocatheter should likewise produce minimal tissue damage during device insertion and retraction. Non-brain organs and tissues should be even less sensitive to such damage.

Might a long skinny nanocatheter buckle when pushed through the brain? If the force required to coaxially push a nanocatheter cylinder of length L_{cath} and radius R_{cath} at a velocity v_{cath} through brain tissue of viscosity η_{brain} is $F_{\text{push}} = (4\pi \eta_{\text{brain}} L_{\text{cath}} v_{\text{cath}}) / (1 + \ln(L_{\text{cath}}^2/R_{\text{cath}}^2))$,⁴⁶¹ and if the Euler buckling force $F_{\text{buckle}} = \pi^3 E_{\text{cath}} (R_{\text{cath}}^4 - r_{\text{cath}}^4) / (4 L_{\text{cath}}^2)$ for a hollow nanocatheter of inside

G, Miyashita S. Milestones for autonomous *in vivo* microrobots in medical applications. *Surgery*. 2021 Apr;169(4):755-758; <https://eprints.whiterose.ac.uk/170891/1/surgery%20manuscript%20V2-7.pdf>.
 Bramhe S, Pathak SS. Robotic Surgery: A Narrative Review. *Cureus*. 2022 Sep 15;14(9):e29179; <https://www.ncbi.nlm.nih.gov/pmc/articles/PMC9573327/pdf>.
 Lee JG, Raj RR, Day NB, Shields CW 4th. Microrobots for Biomedicine: Unsolved Challenges and Opportunities for Translation. *ACS Nano*. 2023 Aug 8;17(15):14196-14204; <https://www.ncbi.nlm.nih.gov/pmc/articles/PMC10928690/pdf>.
 Sun T, Chen J, Zhang J, Zhao Z, Zhao Y, Sun J, Chang H. Application of micro/nanorobot in medicine. *Front Bioeng Biotechnol*. 2024 Jan 25;12:1347312; <https://www.ncbi.nlm.nih.gov/pmc/articles/PMC10850249/pdf>.
 Lu L, Zhao H, Lu Y, Zhang Y, Wang X, Fan C, Li Z, Wu Z. Design and Control of the Magnetically Actuated Micro/Nanorobot Swarm toward Biomedical Applications. *Adv Healthc Mater*. 2024 Jun;13(15):e2400414; <https://pubmed.ncbi.nlm.nih.gov/38412402/>.
 Iacovacci V, Diller E, Ahmed D, Menciassi A. Medical Microrobots. *Annu Rev Biomed Eng*. 2024 Jul;26(1):561-591; <https://www.annualreviews.org/content/journals/10.1146/annurev-bioeng-081523-033131>.

⁴⁵⁸ Freitas RA Jr. *Nanomedicine, Volume IIA: Biocompatibility*, Landes Bioscience, Georgetown, TX, 2003; Chapter 15.5, “Nanorobot Mechanocompatibility”; <http://www.nanomedicine.com/NMIIA/15.5.htm>.

⁴⁵⁹ Fahy G. Personal communication to R. Freitas, 2008.

⁴⁶⁰ Ehninger D, Kempermann G. Neurogenesis in the adult hippocampus. *Cell Tissue Res*. 2008 Jan;331(1):243-50; <http://www.ncbi.nlm.nih.gov/pubmed/17938969>.

⁴⁶¹ Freitas RA Jr. *Nanomedicine, Volume I: Basic Capabilities*. Landes Bioscience, Georgetown, TX, 1999; Section 9.4.2.4, “Force and Power Requirements”; <http://www.nanomedicine.com/NMI/9.4.2.4.htm>.

radius r_{cath} composed of material with Young's modulus E_{cath} ,⁴⁶² and ignoring bony skull penetration (which may be accomplished by conventional surgery), then the maximum velocity at which a nanocatheter can be pushed through brain tissue without buckling would occur when the pushing force F_{push} equals the buckling force F_{buckle} , or $v_{\text{cathMAX}} = \mathbf{2.3 \text{ mm/sec}}$, taking $R_{\text{cath}} = 50 \text{ }\mu\text{m}$, $r_{\text{cath}} = 47.5 \text{ }\mu\text{m}$ (i.e., $2.5 \text{ }\mu\text{m}$ nanocatheter wall thickness), $L_{\text{cath}} \sim V_{\text{brain}}^{1/3} = 11.5 \text{ cm}$ where adult male human brain volume $V_{\text{brain}} = 1510 \text{ cm}^3$,⁴⁶³ $E_{\text{cath}} = 10^{12} \text{ N/m}^2$ for diamond, and a shear viscosity of human brain tissue at 25-50 Hz of $\eta_{\text{brain}} \sim 3.4 \text{ Pa-sec}$.⁴⁶⁴ The shear viscosities of soft tissues inside the human body generally range from 1-100 Pa-sec, suggesting a pushing speed range of $v_{\text{cathMAX}} = \mathbf{0.07-7 \text{ mm/sec}}$ for buckle-free nanocatheter insertion.

Of course, the speed at which a nanocatheter can advance through tissue is not limited solely by buckling force if the toolhead and exterior surfaces of the device include tractor mechanisms similar to those previously described for nanorobot diapedesis,⁴⁶⁵ ECM brachiation,⁴⁶⁶ intercellular transit,⁴⁶⁷ and plasma membrane penetration.⁴⁶⁸ Rather than just relying on pushing, these tractor mechanisms could help safely pull the entire nanocatheter through the tissue at higher speeds, guided by onboard sensors and various external⁴⁶⁹ and onboard⁴⁷⁰ navigational aids to allow precise progression to the intended target at a speed of $v_{\text{cath}} \sim \mathbf{1 \text{ mm/sec}}$. A

⁴⁶² Freitas RA Jr. Nanomedicine, Volume I: Basic Capabilities. Landes Bioscience, Georgetown, TX, 1999; Section 9.3.1.2, "Nanocilium Manipulators"; <http://www.nanomedicine.com/NMI/9.3.1.2.htm>.

⁴⁶³ Lüders E, Steinmetz H, Jäncke L. Brain size and grey matter volume in the healthy human brain. Neuroreport. 2002 Dec 3;13(17):2371-4; <http://www.genling.nw.ru/Staff/Psycholinguistics/Brain%20Size.pdf>.

⁴⁶⁴ Sack I, Beierbach B, Hamhaber U, Klatt D, Braun J. Non-invasive measurement of brain viscoelasticity using magnetic resonance elastography. NMR Biomed. 2008 Mar;21(3):265-71; <http://www.ncbi.nlm.nih.gov/pubmed/17614101>.

⁴⁶⁵ Freitas RA Jr. Nanomedicine, Volume I: Basic Capabilities. Landes Bioscience, Georgetown, TX, 1999; Section 9.4.4.1, "Nanorobot Diapedesis"; <http://www.nanomedicine.com/NMI/9.4.4.1.htm>.

⁴⁶⁶ Freitas RA Jr. Nanomedicine, Volume I: Basic Capabilities. Landes Bioscience, Georgetown, TX, 1999; Section 9.4.4.2, "ECM Brachiation"; <http://www.nanomedicine.com/NMI/9.4.4.2.htm>.

⁴⁶⁷ Freitas RA Jr. Nanomedicine, Volume I: Basic Capabilities. Landes Bioscience, Georgetown, TX, 1999; Section 9.4.4.3, "Intercellular Passage"; <http://www.nanomedicine.com/NMI/9.4.4.3.htm>.

⁴⁶⁸ Freitas RA Jr. Nanomedicine, Volume I: Basic Capabilities. Landes Bioscience, Georgetown, TX, 1999; Section 9.4.5.2, "Metamorphic Screw Drive"; <http://www.nanomedicine.com/NMI/9.4.5.2.htm>; and Section 9.4.5.3, "Solvation Wave Drive"; <http://www.nanomedicine.com/NMI/9.4.5.3.htm>.

⁴⁶⁹ Freitas RA Jr. Nanomedicine, Volume I: Basic Capabilities. Landes Bioscience, Georgetown, TX, 1999; Section 8.3, "Positional Navigation"; <http://www.nanomedicine.com/NMI/8.3.htm>.

⁴⁷⁰ Freitas RA Jr. Nanomedicine, Volume I: Basic Capabilities. Landes Bioscience, Georgetown, TX, 1999; Section 8.4, "Functional Navigation"; <http://www.nanomedicine.com/NMI/8.4.htm>.

preliminary discussion of biocompatibility issues surrounding histopenetration by nanorobotic devices is published elsewhere.⁴⁷¹

If we assume that the outermost $x_{\text{tractor}} \sim 0.5 \mu\text{m}$ of the nanocatheter's external surface incorporates guided tractor nanomachinery capable of dragging the nanocatheter forward through tissue along its entire length, then the maximum required towing force to overcome friction may be approximated as $F_{\text{NCtowing}} \sim \mu_{\text{cath}} A_{\text{NCtowing}} p_{\text{cath}} = \mathbf{0.3-94 \text{ mN}}$ (milli-Newtons) with a maximum required towing power of $P_{\text{NCtowing}} \sim v_{\text{cath}} F_{\text{NCtowing}} = 0.3-94 \mu\text{W}$, taking the maximum tissue-contacting length of the nanocatheter $L_{\text{cath}} \sim 10 \text{ cm}$, nanocatheter radius $R_{\text{cath}} = 50 \mu\text{m}$, the maximum contact area $A_{\text{NCtowing}} = 2\pi R_{\text{cath}} L_{\text{cath}} = 3.14 \times 10^{-5} \text{ m}^2$, the coefficient of friction in human soft tissue $\mu_{\text{cath}} = 0.1-0.3$,⁴⁷² the pressure exerted by the tissue on the nanocatheter $p_{\text{cath}} = 10^2-10^4 \text{ Pa}$,⁴⁷³ and the dragging velocity $v_{\text{cath}} = 1 \text{ mm/sec}$. The tractor nanomachinery then requires an operating power density of $P_D \sim P_{\text{NCtowing}} / A_{\text{NCtowing}} x_{\text{tractor}} \sim 0.00002-0.006 \text{ MW/L}$, well within the typical $10^{-5} - 10^{-1} \text{ MW/L}$ power densities estimated for mature nanomachine systems ranging from microscale medical nanorobots to macroscale nanofactories.⁴⁷⁴ Note that the towing force F_{NCtowing} estimated above is ~ 100 times larger than the force required to

⁴⁷¹ Freitas RA Jr. Nanomedicine, Volume IIA: Biocompatibility, Landes Bioscience, Georgetown, TX, 2003; Section 15.5.2, "Histopenetration and Perforation"; <http://www.nanomedicine.com/NMIIA/15.5.2.htm>; and Section 15.5.4, "Mechanocompatibility with Extracellular Matrix and Tissue Cells"; <http://www.nanomedicine.com/NMIIA/15.5.4.htm>.

⁴⁷² Hu Y, Li M, Lei Y. Friction analysis in needle insertion into soft tissue. ASME 2021 16th International Manufacturing Science and Engineering Conference, Paper No: MSEC2021-63715, 21-25 Jun 2021; <https://asmedigitalcollection.asme.org/MSEC/proceedings-abstract/MSEC2021/85062/V001T03A008/1115413>.

⁴⁷³ The range of likely tissue pressures was estimated by reference to several benchmarks, including: intra-abdominal pressures of 5-15 mmHg (700-2000 Pa) under normal conditions; tissue compression due to muscle contractions that can reach $\sim 10^4 \text{ Pa}$ in active or mechanically stressed tissues; and venous (8-12 mmHg, 1100-1600 Pa) and arterial (120-160 mmHg, 16,000-21,000 Pa) blood pressures. Additionally, the Young's modulus for soft tissues has been reported* as 100-1000 Pa for brain, 3000-5000 Pa for spleen and pancreas, 1000-10,000 Pa for skin, 8000-17,000 Pa for glands and muscle, and 30,000-50,000 for tendon; assuming a maximum 10% tissue strain under typical physiological conditions, the range of tissue pressures assuming the highest modulus in each case would be 100-5000 Pa.

* Liu J, Zheng H, Poh PS, Machens HG, Schilling AF. Hydrogels for Engineering of Perfusable Vascular Networks. Int J Mol Sci. 2015 Jul 14;16(7):15997-6016; <https://www.ncbi.nlm.nih.gov/pmc/articles/PMC4519935/pdf>.

⁴⁷⁴ Freitas RA Jr. Energy Density. IMM Report No. 50, 25 June 2019, 516 pp; <http://www.imm.org/Reports/rep050.pdf>.

overcome viscous dragging,⁴⁷⁵ which is $F_{NCviscous} \sim 4\pi \eta_{tissue} L_{cath} v_{cath} / (1 + \ln (L_{cath}^2/R_{cath}^2)) = 0.00008-0.8 \text{ mN}$, taking dynamic viscosity $\eta_{tissue} = 10^{-3}-10^1 \text{ Pa-sec}$ for soft tissues.⁴⁷⁶

5.2.4.1 Nanocatheter Pain Avoidance

Another practical consideration when using nanocatheters extensively for medical procedures inside the human body is the question of pain. This is not a concern if the patient receiving a nanocatheter-based surgical treatment is fully anesthetized and unconscious. But could such procedures be performed without pain or uncomfortable sensation while the patient is fully awake?

While it is often noted that skin penetration by 50-150 μm diameter microneedles can be both non-damaging⁴⁷⁷ and painless,⁴⁷⁸ such needles are typically designed to penetrate only the outermost layer of the skin (stratum corneum) or just slightly into the epidermis. A microneedle that only penetrates shallowly (e.g., $<200 \mu\text{m}$) is unlikely to cause sensation because it doesn't reach the dermis where pain receptors (nociceptors) are located. But if it penetrates beyond the epidermis into the dermis, it can trigger these receptors, potentially causing pain or other sensations. Besides the dermis, deeper structures such as liver, kidney, and penis are richly supplied with nerves, as are muscles and bones. Subcutaneous fat areas also contain some nerve endings. Brain tissue lacks pain receptors, but the surrounding meninges and skull are innervated. Nanocatheters in the 1-5 μm diameter range that were inserted extremely slowly (e.g., 1-10 $\mu\text{m/sec}$) might produce fewer pain sensations, but broadly useful nanocatheters may demand somewhat larger diameters and higher insertion velocities for practical use.

Pain-free operation of nanocatheters on unanesthetized patients may require using a nanorobot-based regional nerve-blocking system or a localized anesthetic deployment system that releases anesthetic drug molecules from the toolhead of the nanocatheter as it advances through the tissue, much like dentists' common injection technique⁴⁷⁹ of minimizing discomfort by gradually

⁴⁷⁵ Freitas RA Jr. Nanomedicine, Volume I: Basic Capabilities. Landes Bioscience, Georgetown, TX, 1999; Section 9.4.2.4, "Force and Power Requirements", Eqn. 9.75; <http://www.nanomedicine.com/NMI/9.4.2.4.htm>.

⁴⁷⁶ The range of likely tissue dynamic viscosities was estimated by reference to several benchmarks, including: $3-4 \times 10^{-3} \text{ Pa-sec}$ for blood, $10^{-3}-10^{-2} \text{ Pa-sec}$ for extracellular matrix or interstitial fluid, $10^{-2}-10^{-1} \text{ Pa-sec}$ for adipose (fatty) tissue, $10^{-1}-10^1 \text{ Pa-sec}$ for muscle tissue, and 10^0-10^1 Pa-sec for brain.

⁴⁷⁷ Chua JY, Pendharkar AV, Wang N, Choi R, Andres RH, Gaeta X, Zhang J, Moseley ME, Guzman R. Intra-arterial injection of neural stem cells using a microneedle technique does not cause microembolic strokes. *J Cereb Blood Flow Metab.* 2011 May;31(5):1263-71; <http://www.ncbi.nlm.nih.gov/pmc/articles/PMC3099630/>.

⁴⁷⁸ Roxhed N, Samel B, Nordquist L, Griss P, Stemme G. Painless drug delivery through microneedle-based transdermal patches featuring active infusion. *IEEE Trans Biomed Eng.* 2008 Mar;55(3):1063-71; <http://www.ncbi.nlm.nih.gov/pubmed/18334398>.

⁴⁷⁹ This technique is commonly referred to as "progressive injection", "incremental injection", "stepwise injection", or "tissue-friendly injection".

anesthetizing the tissue as the needle advances. By injecting small amounts of anesthetic and waiting for it to take effect before moving the needle deeper, the dentist ensures that most of the injection process occurs in tissue that is already numbed.

Another possible pain-free method for using nanocatheters on unanesthetized patients would be to send histonating⁴⁸⁰ nanorobots to each nociceptor⁴⁸¹ along the expected path through soft tissue that will subsequently be traveled by the nanocatheter, and numb each cell via anesthetic drug injection or some other means prior to the arrival of the nanocatheter. Most nociceptors are free nerve endings representing the terminal part of the single axon from the cell body of a sensory neuron located in the dorsal root ganglia. If the cell bodies servicing the target nociceptors can be located,⁴⁸² a nanorobot could be dispatched to each one of them to deliver, for example, a $\sim 0.2 \mu\text{m}^3$ bupivacaine injection sufficient to provide several hours of nociceptor unresponsiveness.⁴⁸³

How many nanorobots would we need? There are perhaps 200-300 nociceptors/ mm^3 in the skin but only $\rho_{\text{noci}} \sim 50\text{-}100$ nociceptors/ mm^3 in the deeper soft tissues (e.g., muscle and connective tissue), so an $L_{\text{cath}} = 10$ cm long nanocatheter of radius $R_{\text{cath}} = 50 \mu\text{m}$ inserted into soft tissue should encounter $N_{\text{Ncoci}} = 2\pi R_{\text{cath}} L_{\text{cath}} x_{\text{noci}} \rho_{\text{noci}} \sim 16$ nociceptors within $x_{\text{noci}} \sim 10 \mu\text{m}$ of its external surface (the cells' approximate range of mechanical sensitivity), requiring only 16 nanorobots to perform this task. Such small numbers of free-swimming robots could be readily dispensed from the tip of the nanocatheter as it snakes forward into the tissue. The nanorobots

⁴⁸⁰ Freitas RA Jr. Nanomedicine, Volume I: Basic Capabilities, Landes Bioscience, Georgetown TX, 1999; Section 9.4.4, "Histonation"; <http://www.nanomedicine.com/NMI/9.4.4.htm>.

⁴⁸¹ <https://en.wikipedia.org/wiki/Nociceptor>.

⁴⁸² Based on standard anatomical maps, it should be possible to locate the spinal location of the dorsal root ganglia for the nociceptors of interest along the intended nanocatheter path (e.g., S2, S3 and S4 in the case of the penis) without having to perform a comprehensive cell survey of the entire tissue volume being transited.

⁴⁸³ Sensory neuron cell bodies are typically 15-50 μm in diameter, perhaps $\sim 10,000 \mu\text{m}^3$ in volume. Temporary cell anesthesia can be provided most volume-efficiently by tetrodotoxin (TTX) [<https://en.wikipedia.org/wiki/Tetrodotoxin>] or ω -conotoxin [<https://en.wikipedia.org/wiki/Conotoxin>] which block voltage-gated sodium or calcium channels, respectively, at concentrations of ~ 1 nM or $\sim 10^{-20}$ moles/cell body volume. TTX is 319 gm/mole and ~ 2.8 gm/ cm^3 , giving an **$\sim 1100 \text{ nm}^3$** cell-body dose, whereas ω -conotoxin is ~ 3000 gm/mole and ~ 1.5 gm/ cm^3 , giving a **$\sim 20,000 \text{ nm}^3$** cell-body dose, but both are potent neurotoxins with narrow safety margins for reversibility and high risk of permanent damage. Bupivacaine [<https://en.wikipedia.org/wiki/Bupivacaine>] also blocks voltage-gated sodium channels but has much wider dosage safety margins, effective at 10-100 μM or 10^{-16} - 10^{-15} moles/cell body volume; bupivacaine is 288 gm/mole and ~ 1.5 gm/ cm^3 ,* giving a **$0.02\text{-}0.2 \mu\text{m}^3$** cell-body dose.

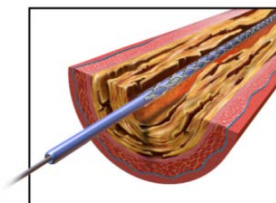
* Williams DL, Nuwayser ES, Kerrigan JH, Creeden DE, Nucefora WA, Gay MH. Local Anesthetic Microencapsulation: Final Report, Report No. BIOTEK 2111-F, DTIC, 4 Nov 1983, Section G. Microcapsule surface drug concentrations, p. 80; <https://apps.dtic.mil/sti/tr/pdf/ADA166796.pdf>.

would have to travel slowly enough, and apply small enough locomotive forces,⁴⁸⁴ to avoid activating any nociceptor pain responses en route to the targeted sensory neuron cell bodies.

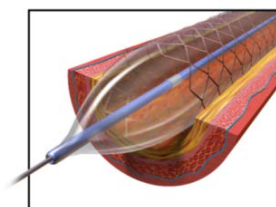
Without such methods, it seems unlikely that a tissue-penetrating $\sim 100\ \mu\text{m}$ diameter nanocatheter could be threaded past all tissue nociceptors to avoid triggering pain. Each nociceptor follows a highly sinuous pathway through their $\rho_{\text{noc}}^{-1} \sim 0.01\text{-}0.02\ \text{mm}^3$ patrol volume, usually branching into a network or tree-like structure throughout the tiny block of tissue it surveils. Nociceptor free nerve endings are $\sim 1\ \mu\text{m}$ in diameter with a total length of perhaps $100\text{-}500\ \mu\text{m}$ summing all branches, but the average gap between adjacent fibers would likely be in the $10\text{-}30\ \mu\text{m}$ range, with gaps as small as $1\text{-}5\ \mu\text{m}$ in regions where fibers are densely packed or closely follow one another and gaps as large as $50\text{-}100\ \mu\text{m}$ in less densely innervated regions or where branches are more spread out. These gaps are too small to ensure that a large nanocatheter would avoid contacting a nociceptor during tissue penetration, and probably too small to allow practical sinuous path evasions by even a tenfold-narrower and extremely flexible nanocatheter.

5.2.4.2 Plaque Debridement

A nanocatheter instrument could be threaded into the penile arteries to remove atherosclerotic lesions. As noted earlier ([Section 5.2.1.1](#)), there are four pairs of penile arteries that receive blood from the two internal iliac arteries and feed blood into the smaller helicine arteries that directly supply the sinusoids of the corpora cavernosa to create and maintain an erection: the internal pudendal arteries (diameter **2000-3000 μm**), the dorsal arteries (diameter **1000-2000 μm**), the bulbourethral arteries (diameter **$\sim 1000\ \mu\text{m}$**), and the cavernosal arteries (diameter **1000-2000 μm**) which are most prone to the typical processes of atherosclerosis such as endothelial injury, lipid deposition, and plaque formation. These arteries are large enough to easily accommodate the intrusion of a **100 μm** diameter nanocatheter device.



Contemporary medicine commonly employs two catheter-based “minimally invasive” techniques for dealing with arterial atherosclerotic plaques. The first is called balloon **angioplasty**,⁴⁸⁵ in which a catheter is threaded through the affected artery to position a balloon segment inside the plaque (images, right).⁴⁸⁶ The balloon is inflated, crushing the soft plaque material into the arterial wall and creating a larger bore through which blood can more freely pass. This method doesn’t actually remove the plaque but just redistributes it, which is why it is often combined with the insertion of a rigid stent that can help hold the enlarged segment open after the balloon is deflated and the catheter is removed. The second technique is called **atherectomy**,⁴⁸⁷

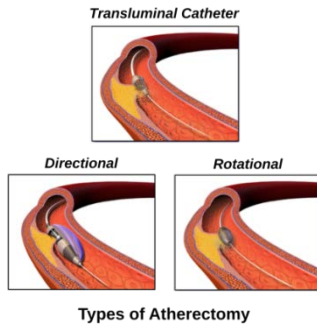


⁴⁸⁴ Freitas RA Jr. Nanomedicine, Volume IIA: Biocompatibility, Landes Bioscience, Georgetown, TX, 2003; Section 15.5.4.3, “Size and Force Threshold for Perceptible Histonatation”; <http://www.nanomedicine.com/NMIIA/15.5.4.3.htm>

⁴⁸⁵ <https://en.wikipedia.org/wiki/Angioplasty>.

⁴⁸⁶ https://en.wikipedia.org/wiki/Angioplasty#/media/File:Angioplasty_-_Balloon_Inflated_with_Stent.png.

⁴⁸⁷ <https://en.wikipedia.org/wiki/Atherectomy>.



in which a catheter inserts a cutting device to progressively excise the plaque material (images, left).⁴⁸⁸ The principal types of cutting devices most commonly used are orbital (a diamond-coated crown or burr on a rotating catheter tip that slowly sands away the plaque using an orbital motion), rotational (a similar rotating diamond burr but operated like a drill bit), laser (an optical fiber carries short high-energy pulses of UV or near-IR light to target and vaporize the plaque; aka. photoablation), and directional (the catheter has a sharp blade or cutting cylinder at its tip applied directly to the plaque, with excised debris captured in a chamber). The objective of the first three techniques is to pulverize the plaque into very fine particles that are tiny enough to pass safely through the bloodstream and be filtered out by the body.

While angioplasty and atherectomy are effective in treating atherosclerotic plaque in large arteries, these techniques are not commonly used for the penile arteries due to the technical challenges, high risk of complications, and the diffuse nature of atherosclerosis in this region. The penile arteries are much smaller in diameter and have thinner (more delicate) walls than the 3-10 mm coronary, femoral, and other peripheral arteries in which these techniques are usually employed. Angioplasty and atherectomy catheters are typically 1300-2300 μm and 1600-2700 μm in diameter, respectively, although 400-670 μm microcatheters have sometimes been used in more distal arteries in the brain and elsewhere. The risk of restenosis⁴⁸⁹ (a rapid recurrence of the obstruction) is higher in the smaller penile arteries. Finally, atherosclerosis in the penile arteries is often diffuse rather than focal, meaning that it affects a longer segment of the artery. Angioplasty and atherectomy are more effective in treating focal, localized plaques rather than diffuse disease, making these conventional techniques less suitable for penile arteries. In the last few decades there have been a few studies of the use of percutaneous transluminal balloon angioplasty on the internal iliac, internal pudendal, dorsal penile and cavernosal arteries with limited success,⁴⁹⁰ but as of 2024 this procedure was still regarded as highly experimental.

Let's do a preliminary scaling analysis for a nanocatheter that performs plaque debridement in the penile arteries as suggested in [Section 5.2.1.1](#). The large arterial system of the penis has a total vascular length of $L_{\text{penart}} \sim 71 \text{ cm}$ and an intimal vascular surface area of $A_{\text{penart}} \sim 33.2 \text{ cm}^2$ ([Section 5.2.1.1](#)). In a case of severe ED where all arteries are $f_{\text{occlude}} \sim 30\%$ volumetrically occluded by plaque, about $V_{\text{plaque}} \sim 0.4 \text{ cm}^3$ of plaque would need to be removed ([Section 5.2.1.1](#)). To complete the job in $t_{\text{NC}} \sim 1 \text{ hour}$ (3600 sec), during debridement the nanocatheter must be moved through the arteries at an average speed of $v_{\text{NC}} = L_{\text{penart}} / t_{\text{NC}} \sim 0.2 \text{ mm/sec}$, comfortably slower than the $v_{\text{cath}} \sim 1 \text{ mm/sec}$ speed estimated earlier ([Section 5.2.1](#)) for nanocatheter transit through solid soft tissue. The nanocatheter must excise and remove plaque material at the rate of $\beta_{\text{NC}} = V_{\text{plaque}} / t_{\text{NC}} \sim 111 \times 10^6 \mu\text{m}^3/\text{sec}$. To achieve this rate using a 100 μm

⁴⁸⁸ https://en.wikipedia.org/wiki/Atherectomy#/media/File:Blausen_Atherectomy_eng.svg.

⁴⁸⁹ <https://en.wikipedia.org/wiki/Restenosis>.

⁴⁹⁰ Wang TD, Lee CK, Chia YC, Tsoi K, Buranakitjaroen P, Chen CH, Cheng HM, Tay JC, Teo BW, Turana Y, Sogunuru GP, Wang JG, Kario K; HOPE Asia Network. Hypertension and erectile dysfunction: The role of endovascular therapy in Asia. *J Clin Hypertens* (Greenwich). 2021 Mar;23(3):481-488; <https://www.ncbi.nlm.nih.gov/pmc/articles/PMC8029574/pdf>.

diameter nanocatheter, debrided plaque material must pass through an internal debris disposal channel of areal cross-section $A_{\text{debris}} \sim 1000 \mu\text{m}^2$ (e.g., $33 \mu\text{m} \times 33 \mu\text{m}$) at a flow velocity of $v_{\text{debris}} \sim \beta_{\text{NC}} / A_{\text{debris}} \sim 0.111 \text{ m/sec}$, conveying the debris the length of the nanocatheter and out of the body.

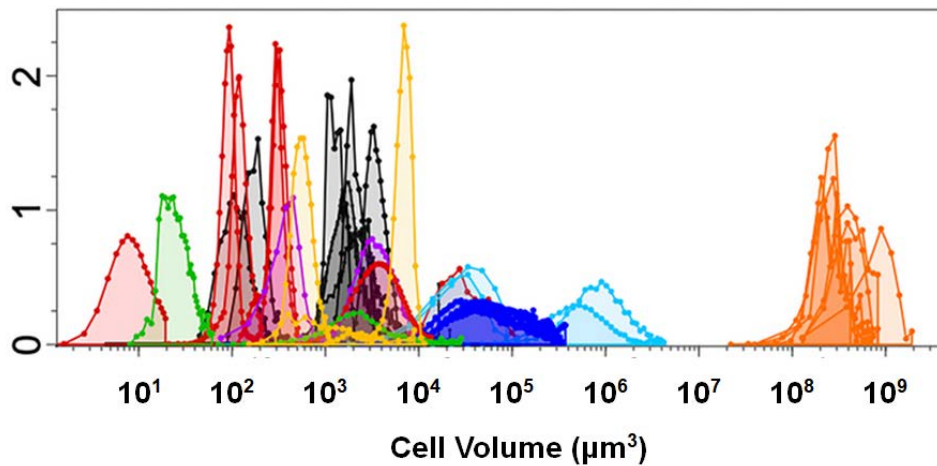
A cutting tool will be mounted on the apex of the nanocatheter to separate the plaque material from the viable surface of the intimal arterial wall. Lacking a detailed design of the cutting tool, for computational convenience in this scaling study we shall simply presume that the tool deploys a cone-shaped diamondoid cutting blade composed of overlapping linked lengthwise narrow slats, open-mouthed in the forward direction of travel, the radius of whose open mouth matches that of the original plaque-free arterial vessel whose representative radius for all penile arteries may be taken as $R_{\text{penart}} \sim A_{\text{penart}} / 2\pi L_{\text{penart}} \sim 744 \mu\text{m}$ with an average plaque thickness of $x_{\text{plaque}} \sim V_{\text{plaque}} / A_{\text{penart}} \sim 120 \mu\text{m}$. There are sensors along the rim of the cone to differentiate between plaque and viable vascular tissue as cutting progresses, allowing the device to adjust in real time the cutting depth by altering the local radius of the conical surface by tilting the wall-forming slats forward or backward, thus ensuring the capture of all plaque material but nothing more. As the tool is moved forward, plaque is separated from the arterial wall and forced into an annular drain at the base of the cone which connects directly to the debris disposal channel inside the nanocatheter.

Ignoring fine points of cutting tool design and operational alternatives,⁴⁹¹ the cutting power required to push the rim of the cutting tool through plaque may be approximated as $P_{\text{cutting}} \sim 2\pi R_{\text{penart}} x_{\text{rim}} E_{\text{plaque}} v_{\text{NC}} \sim 0.19\text{-}1.9 \times 10^{-7} \text{ W}$ (soft), $0.37\text{-}1.1 \times 10^{-6} \text{ W}$ (fibrous), and $0.0019\text{-}0.019 \text{ W}$ (calcified), taking cutting tool rim thickness $x_{\text{rim}} = 2 \mu\text{m}$ and the Young's modulus $E_{\text{plaque}} = 10\text{-}100 \text{ kPa}$ for soft plaque, $0.2\text{-}0.6 \text{ MPa}$ for fibrous plaque, and $1\text{-}10 \text{ GPa}$ for calcified plaque. Ignoring heat conduction or convection, local heating at the cutting site may produce temperature increases of $\Delta T \sim P_{\text{cutting}} / C_V V_{\text{cutting}} \sim 0.00001\text{-}0.0001 \text{ K/sec}$ (soft), $0.0002\text{-}0.0006 \text{ K/sec}$ (fibrous), and $0.8\text{-}8 \text{ K/sec}$ (calcified), taking the volumetric heat capacity for plaque as $C_V \sim 2 \times 10^6 \text{ J/m}^3\text{-K}$ (soft), $2.5 \times 10^6 \text{ J/m}^3\text{-K}$ (fibrous), and $3 \times 10^6 \text{ J/m}^3\text{-K}$ (calcified), and approximating the thermal cutting volume as $V_{\text{cutting}} \sim 2\pi R_{\text{penart}} x_{\text{plaque}} (R_{\text{penart}} - R_{\text{cath}}) / \sin(\theta_{\text{cone}}) \sim 0.779 \text{ mm}^3$ for a cone wall/axis angle of $\theta_{\text{cone}} = 30^\circ$. The higher thermal loads generated by excising calcified plaque can be offset by circulating cooling water through the (very thermally conductive) diamondoid cutting tool via an internal channel of cross-sectional area $A_{\text{coolant}} \sim 100 \mu\text{m}^2$ at a flow speed of $v_{\text{coolant}} \sim P_{\text{cutting,max}} / C_V \Delta T_{\text{coolant}} A_{\text{coolant}} \sim 1.3 \text{ m/sec}$, taking maximum calcified plaque cutting power $P_{\text{cutting,max}} = 0.019 \text{ W}$, volumetric heat capacity for water $C_V \sim 4 \times 10^6 \text{ J/m}^3\text{-K}$, and coolant temperature change $\Delta T_{\text{coolant}} \sim 37 \text{ K}$ (e.g., $T_{\text{in}} \sim 273 \text{ K}$, $T_{\text{out}} \sim 310 \text{ K}$).

⁴⁹¹ The actual tool might have beveled or serrated edges to improve cutting efficiency, the conical cutting tool might rotate or reciprocate axially, the inner cone walls could include manipulatory mechanisms to hasten the debris flow, the system could employ vacuum-based debris aspiration, and so forth. Also, if the hour-long procedure blocks the blood flow through various arteries, the nanocatheter should exude oxygen and other time-critical nutrients and should absorb metabolic wastes such as CO_2 , in order to maintain the viability of the tissues serviced by those arteries for the duration of the surgery.

5.2.4.3 Whole Cell Transport and Emplacement

A nanocatheter instrument could be threaded into the penile tissues to deliver whole biological cells to repair sites where replacement living cells are needed, and to transport nanorobots to those sites to perform tissue repairs and later retrieve and export them from the body when the job is done. Individual autologous living replacement cells can be manufactured to order in cell mills⁴⁹² using the patient's own genomic data. Vasculocyte-class nanorobots (Section 5.2.1.1) could help debride nonfunctional cells, herd new cells into position in the tissue as they are delivered by the nanocatheter, and perform various on-site repairs including essential nanomanipulation and cytosolic injection of the existing tissue and new cells alike.



There is considerable variation in size between cell types and even within each cytotype, as illustrated by the chart above,⁴⁹³ but a 100 μm diameter nanocatheter should be able to transport all but the largest human cells, probably up to $\sim 10^6 \mu\text{m}^3$ in volume. Tissue repair in connection with erectile dysfunction may require transporting multiple types of cells, but two types – arterial penile endothelial cells (Section 5.2.1.1(1)) and Leydig cells (Section 5.2.3) – are probably of greatest interest:

The typical penis has $N_{\text{penileEC}} \sim N_{\text{largeEC}} + N_{\text{helicineEC}} + N_{\text{sinusoidEC}} \sim 3300 \times 10^6$ **arterial penile endothelial cells**, comprising:

(1) the **large penile artery** system (including the pudendal, dorsal, bulbourethral, and cavernosal arteries), which has a total length of $L_{\text{penart}} \sim 71$ cm and a total intimal vascular surface

⁴⁹² Freitas RA Jr. Cell Mills: Nanofactory Manufacture of Biological Components. IMM Report No. 53, 15 June 2024; <http://www.imm.org/Reports/rep053.pdf>.

⁴⁹³ modified from: Hatton IA, Galbraith ED, Merleau NSC, Miettinen TP, Smith BM, Shander JA. The human cell count and size distribution. Proc Natl Acad Sci U S A. 2023 Sep 26;120(39):e2303077120; <https://www.ncbi.nlm.nih.gov/pmc/articles/PMC37722043/>.

area of $A_{\text{penart}} \sim 33.2 \text{ cm}^2$ (Section 5.2.1.1). Large-artery endothelial cells typically measure 10-20 μm (width) x 20-40 μm (length) x 1-2 μm (thickness), with a representative volume of $V_{\text{largeEC}} \sim 570 \mu\text{m}^3$ (range 200-1600 μm^3) and a representative intimal vascular surface area of $A_{\text{largeEC}} \sim 450 \mu\text{m}^2$ (range 200-1000 μm^2). Hence there are $N_{\text{largeEC}} = A_{\text{penart}} / A_{\text{largeEC}} \sim 7.4 \times 10^6$ endothelial cells lining the intimal surface of the large penile arteries.

(2) the **helicine arteries** (smaller arteries that lead to the sinusoids of the corpora cavernosa), which have a diameter of 100-300 μm and a length in the erect state of $\sim 3 \text{ mm}$. There are 30-100 helicine arteries in each corpus cavernosum, of which there are two in the penis, giving a total length of $L_{\text{helicine}} \sim 16 \text{ cm}$ (range 9-30 cm) and a total intimal vascular surface area of $A_{\text{helicine}} \sim 1.9 \text{ cm}^2$ (range 0.9-2.8 cm^2). Helicine endothelial cells typically measure 7.5-15 μm (width) x 15-30 μm (length) x 1-2 μm (thickness), with a representative volume of $V_{\text{helicineEC}} \sim 310 \mu\text{m}^3$ (range 110-900 μm^3) and a representative intimal vascular surface area of $A_{\text{helicineEC}} \sim 220 \mu\text{m}^2$ (range 110-450 μm^2). Hence there are $N_{\text{helicineEC}} = A_{\text{helicine}} / A_{\text{helicineEC}} \sim 8.6 \times 10^5$ endothelial cells lining the intimal surface of the helicine arteries.

(3) the **sinusoids** of the corpora cavernosa (spaces that fill with blood during erection), which during erection can be crudely modeled as spherical⁴⁹⁴ with inside diameters of $d_{\text{sinusoid}} = 2r_{\text{sinusoid}}$. The change in volume of the corpora cavernosa during erection is $\Delta V_{\text{CC}} = V_{\text{erect}} - V_{\text{flaccid}} = 77 \text{ cm}^3$, taking the erect penile volume as $V_{\text{erect}} \sim 141 \text{ cm}^3$ and the flaccid penile volume as $V_{\text{flaccid}} \sim 64 \text{ cm}^3$ (Section 2.5), which crudely approximates the unchanging volume of penile tissue surrounding the sinusoids. If each sinusoid is surrounded by a wall composed of endothelial cells, smooth muscle cells, and other connective tissue that is x_{CCwall} thick, giving an outside radius for each sinusoid of $R_{\text{sinusoid}} \sim r_{\text{sinusoid}} + x_{\text{CCwall}}$, and if there are an estimated $N_{\text{CC}} \sim 50,000$ sinusoids in both corpora cavernosa, then $r_{\text{sinusoid}} = (3 \Delta V_{\text{CC}} / 4\pi N_{\text{CC}})^{1/3} \sim 720 \mu\text{m}$, $R_{\text{sinusoid}} = [r_{\text{sinusoid}}^3 + (3V_{\text{flaccid}} / 4\pi N_{\text{CC}})]^{1/3} \sim 880 \mu\text{m}$, and the trabecular⁴⁹⁵ walls separating adjacent sinusoids are about $2 x_{\text{CCwall}} = 2 (R_{\text{sinusoid}} - r_{\text{sinusoid}}) \sim 320 \mu\text{m}$ thick. In this model, the representative intimal surface area for all sinusoids would be $A_{\text{sinusoid}} \sim 4\pi r_{\text{sinusoid}}^2 N_{\text{CC}} \sim 3300 \text{ cm}^2$. Sinusoid endothelial cells typically measure 5-10 μm (width) x 10-20 μm (length) x 1-2 μm (thickness), with a representative volume of $V_{\text{sinusoidEC}} \sim 100 \mu\text{m}^3$ (range 50-200 μm^3) and a representative intimal vascular surface area of $A_{\text{sinusoidEC}} \sim 100 \mu\text{m}^2$ (range 50-200 μm^2), hence there are $N_{\text{sinusoidEC}} = A_{\text{sinusoid}} / A_{\text{sinusoidEC}} \sim 3260 \times 10^6$ endothelial cells lining the intimal surface of the sinusoids.

Additionally, the two human male testicles include $N_{\text{Leydig}} \sim 300 \times 10^6$ **Leydig cells** (range 200-700 $\times 10^6$ cells), which are androgen-secreting cells (Section 5.2.3) roughly spherical or

⁴⁹⁴ The fully inflated sinusoids in the erectile tissue of the penis do not take on uniform shapes like spheres or cubes but rather assume shapes that are largely determined by the surrounding trabeculae and the overall structure of the corpora cavernosa. They may be polygonal or irregular in shape, or ovoid or ellipsoidal in areas where the trabeculae are less dense, or tubular or elongated in regions where the trabeculae are more aligned in parallel or perpendicular orientations.

⁴⁹⁵ The trabeculae are fibrous and muscular structures that form the supportive framework around the sinusoids. They consist of smooth muscle fibers and collagenous connective tissue that provide structural support to the erectile tissue. This is the tissue separating adjacent sinusoidal voids during full penile erection.

polygonal in shape, typically measuring 15-20 μm in diameter with a representative volume of $V_{\text{EC}} \sim 2800 \mu\text{m}^3$ (range 1800-4200 μm^3) per cell.

Consider a transport nanocatheter with a 100 μm outside diameter and 90 μm inside diameter (i.e., 5 μm thick walls), carrying separate outgoing and return streams of $d_{\text{container}} = 20 \mu\text{m}$ wide containers, each of volume $V_{\text{container}} = (\pi/6) d_{\text{container}}^3 = 4200 \mu\text{m}^3$ and containing one penile endothelial or Leydig cell, moving at a fairly conservative velocity of $v_{\text{transport}} \sim 2 \text{ mm/sec}$ through two $\sim 20 \mu\text{m}$ wide columns. Even such an inefficiently-designed nanocatheter could deliver $n_{\text{cells}} \sim v_{\text{transport}} / d_{\text{container}} \sim 100 \text{ cells/sec}$ to the terminus of the device, fast enough for $N_{\text{cath}} = 10$ nanocatheters to replace 1% of all arterial penile endothelial cells in $t_{1\%} \sim (0.01) N_{\text{penileEC}} / n_{\text{cells}}$ $N_{\text{cath}} \sim 33,000 \text{ sec}$ ($\sim 9 \text{ hrs}$) or 1% of all Leydig cells in $t_{1\%} \sim (0.01) N_{\text{Leydig}} / n_{\text{cells}}$ $N_{\text{cath}} \sim 3000 \text{ sec}$ ($\sim 0.8 \text{ hr}$).

Inside the nanocatheter, a ciliary array⁴⁹⁶ of 100 nm long telescoping manipulator arms,⁴⁹⁷ each with a 100 nm armswing arc positioned $x_{\text{manip}} = 100 \text{ nm}$ apart along the inner surface of a $\sim 20 \mu\text{m}$ wide delivery column $L_{\text{NC}} = 10 \text{ cm}$ in length, would provide $d_{\text{container}} / x_{\text{manip}} = 200$ manipulators in continuous contact with each container during transport, with $N_{\text{manipNC}} = L_{\text{NC}} / x_{\text{manip}} = 10^6$ manipulators along the entire inside length of the nanocatheter. Each manipulator dissipates $P_{\text{manip}} \sim 0.1 \text{ pW}$ while in continuous motion at a 1 cm/sec transport velocity *in vacuo*, so the power draw is a modest $N_{\text{manipNC}} P_{\text{manip}} \sim 0.1 \mu\text{W}$ for each nanocatheter.

At the nanocatheter terminus, a working nanomechanical toolhead equipped with thousands of independent manipulators and sensors branching outward from the central trunk on retractile stalks can receive and install the new cells. Mobile surgical nanorobots imported into the body through the nanocatheter could also physically manipulate cells⁴⁹⁸ arriving through the nanocatheter, and reposition those cells as desired within tissue voids or other spaces previously cleared or debrided.⁴⁹⁹ Discarded cells and other debris can be transported out of the body in the return stream of otherwise empty containers inside the nanocatheter.

⁴⁹⁶ Freitas RA Jr. Nanomedicine, Volume I: Basic Capabilities, Landes Bioscience, Georgetown TX, 1999; Section 9.3.4, "Manipulator Arrays"; <http://www.nanomedicine.com/NMI/9.3.4.htm>.

⁴⁹⁷ Freitas RA Jr. Nanomedicine, Volume I: Basic Capabilities, Landes Bioscience, Georgetown TX, 1999; Section 9.3.1.4, "Telescoping Manipulators"; <http://www.nanomedicine.com/NMI/9.3.1.4.htm>.

⁴⁹⁸ Leong TG, Randall CL, Benson BR, Bassik N, Stern GM, Gracias DH. Tetherless thermobiochemically actuated microgrippers. Proc Natl Acad Sci U S A. 2009 Jan 20;106(3):703-8; <http://www.ncbi.nlm.nih.gov/pmc/articles/PMC2630075/>. Gach PC, Wang Y, Phillips C, Sims CE, Allbritton NL. Isolation and manipulation of living adherent cells by micromolded magnetic rafts. Biomicrofluidics. 2011 Sep;5(3):32002-3200212; <http://www.ncbi.nlm.nih.gov/pmc/articles/PMC3194786/>.

⁴⁹⁹ Freitas RA Jr. The Alzheimer Protocols: A Nanorobotic Cure for Alzheimer's Disease and Related Neurodegenerative Conditions. IMM Report No. 48, June 2016; Section 5.3.2.2, "Intracranial Debridement"; <http://www.imm.org/Reports/rep048.pdf>.

5.2.4.4 Cytosolic Intervention in Individual Cells

A nanocatheter instrument could be threaded into the penile tissues to deliver cytosolic modification agents and nanomachine instrumentalities into individual smooth muscle cells – for example, reversing the switch from a contractile to a synthetic phenotype in response to atherosclerotic changes ([Section 5.2.1.1\(3\)](#)) or reversing the over-expression of the phosphodiesterase type 5 (PDE5) enzyme by smooth muscle cells in the corpora cavernosa ([Section 5.2.3](#)), by the insertion of appropriate biochemical agents into the cytosol of the misbehaving cells as described earlier. These injections may be performed (1) by nanorobots that have navigated via the bloodstream to the affected smooth muscles cells within the penile tissues, (2) by nanorobots that are locally released at the appropriate sites from the terminus of a nanocatheter, or (3) by a nanomechanical toolhead at the tip of a nanocatheter which is equipped with the appropriate manipulation,⁵⁰⁰ surface-sensing,⁵⁰¹ and cytosolic-sampling⁵⁰² mechanisms.

If the total smooth muscle cell (SMC) volume in the corpora cavernosa is $V_{\text{smcCC}} \sim 15 \text{ cm}^3$ and if the typical SMC is roughly cylindrical with diameter $d_{\text{smc}} \sim 6 \text{ }\mu\text{m}$ (range 3-10 μm), length $L_{\text{smc}} \sim 150 \text{ }\mu\text{m}$ (range 100-200 μm), and volume $V_{\text{smc}} \sim 4000 \text{ }\mu\text{m}^3$ (range 700-16,000 μm^3), then there are $N_{\text{smcCC}} \sim V_{\text{smcCC}} / V_{\text{smc}} \sim 4 \times 10^9$ SMCs in the corpora cavernosa. A set of $N_{\text{cath}} = 10$ nanocatheters – each mounted with a nanomechanical guided-tractor toolhead equipped with $n_{\text{tent}} = 1000$ separately targetable tentacle manipulators that can reposition, sense, sample, and inject SMCs at $v_{\text{tent}} \sim 0.1 \text{ cell/sec}$ (i.e., 10 sec spent on each cell) – could service $\sim 1\%$ of all penile SMCs in $t_{\text{smc}} \sim (0.01) N_{\text{cath}} N_{\text{smcCC}} / n_{\text{tent}} v_{\text{tent}} \sim 40,000 \text{ sec}$ ($\sim 11 \text{ hrs}$). This requires a mean velocity of the nanocatheter through the tissues of $(V_{\text{smcCC}} / N_{\text{cath}})^{1/3} / t_{\text{smc}} \sim 0.3 \text{ }\mu\text{m/sec}$,

⁵⁰⁰ Freitas RA Jr. Nanomedicine, Volume I: Basic Capabilities. Landes Bioscience, Georgetown, TX, 1999; Section 9.3.2, “Nanoscale End-Effectors and Tool Tips”; <http://www.nanomedicine.com/NMI/9.3.2.htm>.

⁵⁰¹ Freitas RA Jr. Nanomedicine, Volume I: Basic Capabilities. Landes Bioscience, Georgetown, TX, 1999; Section 4.2.8, “Chemotactic Sensor Pads”; <http://www.nanomedicine.com/NMI/4.2.8.htm>; and Section 4.2.9, “Receptor Sensors”; <http://www.nanomedicine.com/NMI/4.2.9.htm>.

⁵⁰² Freitas RA Jr. Nanomedicine, Volume I: Basic Capabilities. Landes Bioscience, Georgetown, TX, 1999; Section 8.5.3.12, “Cytonavigational Issues”; <http://www.nanomedicine.com/NMI/8.5.3.12.htm>; and Section 9.2.4, “Capillarity and Nanoscale Fluid Flow”; <http://www.nanomedicine.com/NMI/9.2.4.htm>. Freitas RA Jr. The ideal gene delivery vector: Chromalloyocytes, cell repair nanorobots for chromosome replacement therapy. J Evol Technol 2007;16:1-97; Section 6.1, “Proliferating Cells”; <http://jetpress.org/v16/freitas.pdf>. Freitas RA Jr. Chapter 23. Comprehensive Nanorobotic Control of Human Morbidity and Aging. In: Fahy GM, West MD, Coles LS, Harris SB, eds, The Future of Aging: Pathways to Human Life Extension, Springer, New York, 2010; Section 23.6.4.4, “Modifying Cellular Controls and Cycles”; Section 23.6.4.6, “Organelle Testing, Replacement, or Repair”; and Section 23.6.4.8, “Intracellular Environmental Maintenance”; <http://www.nanomedicine.com/Papers/Aging.pdf>. Freitas RA Jr. The Alzheimer Protocols: A Nanorobotic Cure for Alzheimer’s Disease and Related Neurodegenerative Conditions. IMM Report No. 48, June 2016; Section 5.2.2, “Remove Intracellular Aggregates”; <http://www.imm.org/Reports/rep048.pdf>. Freitas RA Jr. Cryostasis Revival: The Recovery of Cryonics Patients through Nanomedicine. Alcor Life Extension Foundation, Scottsdale AZ, 2022; Section 4.10, “Molecular Extraction”; and Section 4.12.2.1, “Preliminary Cell Inspection and Small Debris Cleanup”; <https://www.alcor.org/cryostasis-revival/>.

comparable to the observed 0.05-0.7 $\mu\text{m}/\text{sec}$ speed of natural leukocyte and fibroblast amoeboid motion through extracellular tissue.⁵⁰³

5.2.4.5 Tissue and Nerve Repair

A nanocatheter instrument could be threaded into the penile tissues to correct degenerative changes in the tunica albuginea that can weaken the ability of the tunica to compress the veins, leading to venogenic ED (Section 3.1). The tunica albuginea is a tough, fibrous layer that surrounds the corpora cavernosa, composed mostly of collagen fibers (mainly type I and type III collagen) that provide structural integrity and ~5% elastin fibers, interwoven with a collagen network, that help provide flexibility during the expansion of the corpora cavernosa and allows the tunica to stretch and then return to its original shape after the erection subsides.⁵⁰⁴

Degenerative changes can include (1) a decrease in collagen content or a shift in the balance between collagen types, or (2) a loss of elasticity when elastin fibers become damaged or lose their normal function, or from localized fibrosis (e.g., due to Peyronie's Disease), or from repeated microtrauma due to mechanical stresses creating microscopic tears that heal improperly forming less flexible scar tissue.

Repairing such damage will require deployment either of cell repair nanorobots analogous to the biological fibroblast (Section 5.2.1.2) or a nanocatheter equipped with a nanomechanical guided tractor toolhead having terminal manipulators similarly capable of repairing or replacing the collagenous sheath. The tunica albuginea is roughly a cylindrical annulus of diameter $D_{\text{erect}} \sim 3.7$ cm, length $L_{\text{erect}} \sim 13.1$ cm, and thickness $x_{\text{tunica}} \sim 1.5$ mm, giving a total solid volume of $V_{\text{tunica}} = \pi D_{\text{erect}} L_{\text{erect}} x_{\text{tunica}} \sim 23 \text{ cm}^3$. A 100 μm diameter transport nanocatheter carrying separate outgoing and return streams of $d_{\text{container}} = 20 \mu\text{m}$ wide containers, each of volume $V_{\text{container}} = (\pi/6) d_{\text{container}}^3 = 4200 \mu\text{m}^3$ filled with replacement tunica wall material and moving at $v_{\text{transport}} \sim 2$ mm/sec through one of two ~20 μm wide columns, could deliver $V_{\text{material}} \sim v_{\text{transport}} V_{\text{container}} / d_{\text{container}} \sim 420,000 \mu\text{m}^3/\text{sec}$ to the terminus of the device, fast enough for $N_{\text{cath}} = 10$ nanocatheters to replace 1% of all tunica albuginea wall material in $t_{1\%} \sim (0.01) V_{\text{tunica}} / V_{\text{material}} N_{\text{cath}} \sim 55,000$ sec (~15 hrs).

⁵⁰³ Peacock EE Jr. Wound Repair. W.B. Saunders Company, Philadelphia, 1984; https://books.google.com/books/about/Wound_Repair.html?id=ZVdsAAAAMAAJ. Stefano GB, Shipp MA, Scharer B. A possible immunoregulatory function for [Met]-enkephalin-Arg6-Phe7 involving human and invertebrate granulocytes. J Neuroimmunol. 1991 Feb;31(2):97-103; <https://pubmed.ncbi.nlm.nih.gov/1991823/>. Keller HU, Zimmermann A, Cottier H. Cell shape, movement and chemokinesis. Adv. Biosci. 1987;66:21-27.

⁵⁰⁴ Other components of the tunica albuginea include proteoglycan and glycosaminoglycan molecules that are part of the extracellular matrix. They play a role in maintaining tissue hydration and structural integrity, and help modulate the interaction between collagen and elastin fibers and contribute to the viscoelastic properties of the tunica. A few fibroblast cells are also present in the tunica and are responsible for the synthesis, maintenance, and repair of the extracellular matrix, including collagen, elastin, and proteoglycans.

A single repair tool of width $w_{\text{tool}} = 10 \mu\text{m}$ mounted on a telescoping manipulator,⁵⁰⁵ with the nanocatheter tip translating at $v_{\text{scan}} = 10 \mu\text{m/sec}$ across the tunica surface performing debridement or fibrous replacement to a tissue depth of $d_{\text{manip}} = 10 \mu\text{m}$ during each pass, would allow tissue repairs at $V_{\text{tool}} = w_{\text{tool}} d_{\text{manip}} v_{\text{scan}} \sim 1000 \mu\text{m}^3/\text{sec}$.⁵⁰⁶ One such repair tool mounted on the tips of each of $N_{\text{toolmanip}} = 100$ manipulators coordinated on the toolhead of each of $N_{\text{cath}} = 100$ nanocatheters can repair $V_{\text{repair}} = N_{\text{cath}} N_{\text{toolmanip}} V_{\text{tool}} \sim 10^7 \mu\text{m}^3/\text{sec}$ of tunica tissue, enabling $\sim 1\%$ of the tunica albuginea to be repaired in $t_{1\%} = (0.01) V_{\text{tunica}} / V_{\text{repair}} \sim 23,000 \text{ sec}$ ($\sim 6 \text{ hrs}$). Repairing moderate fibrosis of the corpora cavernosa ([Section 5.2.1.2](#)) at a similar treatment speed should require roughly similar resources.

A nanocatheter instrument could also be employed to repair nerve axons damaged by demyelination, degeneration by compression or entrapment, or by direct trauma or surgical injury, located in the pelvis, the spinal column, or the brain. The previously outlined repair of demyelinated pelvic splanchnic nerves using nanorobots ([Section 5.2.2](#)) could equally well be performed by a nanocatheter with a multimanipulator toolhead as described above for the tunica albuginea. Extra care must be taken during neuron repair or replacement operations in the brain because neurons are packed more tightly in the brain than are cells in other tissues, leaving less space for nanodevices to operate.⁵⁰⁷

5.3 Nanorobotic Symptomatic Treatments for ED

Medical nanorobots can provide symptomatic relief from ED without correcting the underlying organic problem that is causing the condition. Correction of complex medical conditions such as hypertension, atherosclerosis, and diabetes may require relatively complex nanorobotic

⁵⁰⁵ Freitas RA Jr. Nanomedicine, Volume I: Basic Capabilities. Landes Bioscience, Georgetown, TX, 1999; Section 9.3.1.4, “Telescoping Manipulators”; <http://www.nanomedicine.com/NMI/9.3.1.4.htm>.

⁵⁰⁶ Assume for computational convenience that the $D_{\text{cath}} = 100 \mu\text{m}$ diameter nanocatheter has a square cross-section with an apical area $A_{\text{apicalNC}} = D_{\text{cath}}^2 \sim 10,000 \mu\text{m}^2$, with $A_{\text{manip}} \sim A_{\text{apicalNC}} / N_{\text{toolmanip}} = 100 \mu\text{m}^2$ allocated to each of 100 tissue manipulators with a repair tool at the tip of each manipulator. Each manipulator is roughly cylindrical, $d_{\text{manip}} = 10 \mu\text{m}$ in length and $w_{\text{manip}} = 3 \mu\text{m}$ in width, leaving $A_{\text{manip}} - w_{\text{manip}}^2 \sim 91 \mu\text{m}^2$ at the apex of each manipulator to accommodate supply feeds for replacement tools, incoming consumables, outgoing waste streams, and even space to allow the deployment and retrieval of nanorobots a few microns in size if needed. Each manipulator has an accessible arc of $\pm 5 \mu\text{m}$ from the vertical centerline and is located $10 \mu\text{m}$ from its neighboring manipulators on the nanocatheter. The manipulators can swing through a full $10 \mu\text{m}$ arc in 0.001 sec (i.e., $\sim 1000 \text{ Hz}$ operation) and move at $v_{\text{manip}} \sim 1 \text{ cm/sec} = 10,000 \mu\text{m/sec}$. The tool at the manipulator apex can trace out the perimeters of 100 squares each $1 \mu\text{m}^2$ in area in $400 \mu\text{m}$ of travel, and repeating 10 times to cover $10 \mu\text{m}$ depth at $1 \mu\text{m}$ 3D resolution requires $v_x \sim 4000 \mu\text{m/sec}$ of travel, leaving $(v_{\text{manip}} - v_x) / v_{\text{manip}} \sim 60\%$ of the scan time for specific tissue manipulation and repair functions. The two nanocatheter supply columns could transport $V_{\text{material}} \sim 420,000 \mu\text{m}^3/\text{sec}$ of materials to and from the terminus of the nanocatheter, or $V_{\text{material}} / N_{\text{toolmanip}} = 4200 \mu\text{m}^3/\text{manipulator-sec} > V_{\text{tool}} \sim 1000 \mu\text{m}^3/\text{manipulator-sec}$, the material requirement for the repair tool.

⁵⁰⁷ Freitas RA Jr. The Alzheimer Protocols: A Nanorobotic Cure for Alzheimer’s Disease and Related Neurodegenerative Conditions. IMM Report No. 48, June 2016; Section 5.3.2, “Reconstruction of Neural Tissues”; <http://www.imm.org/Reports/rep048.pdf>.

interventions, hence might not be available until more sophisticated nanorobots become available. Simple symptomatic relief might be available sooner in time, or without having to undergo a significant medical procedure, because fixing a symptom can often be easier and quicker than permanently curing multiple underlying diseases. An impatient user might choose this option.

There are several convenient methods to achieve effective vasodilation sufficient to establish and maintain a normal erection, using erectogenic nanorobots operating in the penile tissues ([Section 5.3.1](#)). Nanorobots deployed in the brain can also be employed to artificially stimulate sexual arousal in cases where male hypoactive sexual desire disorder⁵⁰⁸ is the primary symptom of the dysfunction ([Section 5.3.2](#)). It is also possible that some men, after receiving a curative treatment ([Section 5.2](#)) enabling them to have normal and fully natural erections, might still make use of a symptomatic treatment to enhance and extend their natural responses. Nanorobotic systems can also enhance or extend the male orgasmic response ([Section 5.3.3](#)).

5.3.1 Erection via Vasodilator or Inflatable Nanorobots (Lifters)

The simplest possible symptomatic nanorobotic treatment for erectile dysfunction, using the simplest possible nanorobots which may be called “lifters”,⁵⁰⁹ would be to deploy site-specific devices analogous to pharmacytes⁵¹⁰ that could deliver the vasodilator nitric oxide (NO)⁵¹¹ or other vasodilative biochemical agents to the appropriate penile tissues, triggering the normal cycle of muscle cell relaxation, the filling of the corpora cavernosa with blood, and the consequent squeezing shut of the venous drainage network, resulting in a near-normal erection.

There are two independent sources for NO in the penile vasculature:

(1) **Endothelial NO.** Nitric oxide is synthesized by endothelial cells (via endothelial nitric oxide synthase, or eNOS) and then diffuses across the very short distances into the adjacent smooth muscle cells of the blood vessels, helping to relax these cells and thereby dilate the vessels, which enhances blood flow. This diffusion is a localized event, with the NO only influencing cells very close to where it is produced and not typically entering the bloodstream in significant quantities.

⁵⁰⁸ Belu CF, Corsini-Munt S, Dubé JP, Wang GA, Rosen NO. Partner responses to low desire among couples coping with male hypoactive sexual desire disorder and associations with sexual well-being. *J Sex Med.* 2023 Jun 28;20(7):955-964; <https://www.ncbi.nlm.nih.gov/pmc/articles/PMC10311074/pdf>.

⁵⁰⁹ Proposed alternative names for the lifters includes “androbots”, “erectors”, peniforms”, “vascuformers”, and “vasculifters”.

⁵¹⁰ Freitas RA Jr. Pharmacytes: an ideal vehicle for targeted drug delivery. *J Nanosci Nanotechnol.* 2006 Sep-Oct;6(9-10):2769-75; <http://www.nanomedicine.com/Papers/JNNPharm06.pdf>.

⁵¹¹ https://en.wikipedia.org/wiki/Biological_functions_of_nitric_oxide#Vasodilation_and_smooth_muscles.

(2) **Neuronal NO.** Nitric oxide produced by neuronal nitric oxide synthase (nNOS) in nerve endings diffuses directly into adjacent smooth muscle cells by passing through the small synaptic or junctional gaps between cells. This diffusion is also highly localized.

Given the objective to get nitric oxide into the penile smooth muscle cells to cause them to relax, there are at least two simple approaches. Nanorobots could release nitric oxide into the blood volume immediately adjacent to the endothelial cells lining the penile vasculature, allowing diffusion to carry the NO into the endothelial cells, and thence into the SMCs by further diffusion ([Section 5.3.1.1](#)). More efficiently, nanorobots could inject NO directly into the endothelial cells ([Section 5.3.1.2](#)) which would then diffuse into the smooth muscle cells, triggering their relaxation and the desired erection.

In another scenario, nanorobots lining the inner walls of the penile sinusoids could physically inflate, mechanically forcing the corpora cavernosa to expand, yielding an erection ([Section 5.3.1.3](#)). In cases of venous leakage or venogenic ED, nanorobots lining the inner walls of the penile venous vasculature could arrange themselves into a configuration that significantly blocks the outflow of blood, slowly forcing the corpora cavernosa to expand, yielding an erection. ([Section 5.3.1.4](#)).

We conclude this Section with a discussion of methods for infusing these nanorobots into the body ([Section 5.3.1.5](#)), extracting them from the body after temporary symptomatic relief has been achieved ([Section 5.3.1.6](#)), and controlling the nanorobots while they are on-station inside the body ([Section 5.3.1.7](#)).

5.3.1.1 Bloodstream Diffusion of Nitric Oxide

In the simplest case, lifter nanorobots transiently anchored⁵¹² on the intimal surface of the penile arterial vasculature could release nitric oxide (NO) into the blood volume immediately adjacent to the endothelial cells (ECs) lining the penile vasculature, allowing diffusion to carry the NO into the endothelial cells, and thence through the intercellular spaces into the smooth muscle cells (SMCs) by further diffusion, triggering the normal cycle of SMC relaxation leading to erection.

An endothelial cell cytoplasmic NO concentration of ~3 nM is minimally sufficient to activate the soluble guanylate cyclase (sGC) enzyme in SMCs and elicit an erectile response in the corpora cavernosa, whereas a steady-state NO concentration of 10 nM produces 30-50% maximal vasodilation⁵¹³. Concentrations much higher than 10 nM probably wouldn't proportionally increase the activation of sGC as the enzyme may already be saturated with NO, and much higher concentrations risk NO participating in less beneficial reactions such as forming peroxynitrite

⁵¹² Freitas RA Jr. Nanomedicine, Volume I: Basic Capabilities. Landes Bioscience, Georgetown, TX, 1999; Section 9.4.3.3, "Anchoring and Dislodgement Forces"; <http://www.nanomedicine.com/NMI/9.4.3.3.htm>.

⁵¹³ Liu X, Yan Q, Baskerville KL, Zweier JL. Estimation of nitric oxide concentration in blood for different rates of generation. Evidence that intravascular nitric oxide levels are too low to exert physiological effects. J Biol Chem. 2007 Mar 23;282(12):8831-6; <https://www.sciencedirect.com/science/article/pii/S0021925819834683/pdf>.

through interactions with superoxide anions, a potent oxidant that could lead to cellular damage if the balance of NO production and antioxidant defenses is disrupted. The fraction of NO in the endothelial cells that migrates back into the bloodstream is likely under 5%.

For NO to diffuse into endothelial cells from the bloodstream and achieve a cytosolic concentration of $c_{\text{NO-EC}} \sim 3\text{-}10\text{ nM}$, the external concentration (in the vascular space) does not need to be much higher than this range, due to the high diffusivity and permeability of NO (a small lipophilic molecule) across biological membranes as well as the thinness of the endothelial barrier. Maintaining an NO concentration in the range of approximately 5-15 nM in the vascular spaces would likely drive the endothelial cytosolic NO concentration to the desired level of 3-10 nM, accounting for some degradation and binding in the vascular space.

If one nanorobot is anchored over every $A_{\text{NO}} \sim 1000\text{ }\mu\text{m}^2$ of intimal vascular surface, spanning 2-5 individual endothelial cells,⁵¹⁴ then to maintain a $c_{\text{NO}} = 5\text{-}15\text{ nM}$ NO concentration in the fluid nearest the EC plasma membranes, given a normal capillary bloodflow past the anchored nanorobot at $v_{\text{NO}} \sim 1\text{ mm/sec}$, the robot would have to emit NO at the rate of $c_{\text{NO}} A_{\text{NO}} v_{\text{NO}} \sim 5\text{-}15 \times 10^{-18}\text{ moles/sec}$. However, the half-life of free NO in the bloodstream is $\tau_{\text{NO}} \sim 1\text{-}5\text{ sec}$,⁵¹⁵ giving a degradation rate $k_{\text{NO}} \sim \ln(2) / \tau_{\text{NO}} \sim 0.14\text{-}0.69\text{ sec}^{-1}$, so to maintain the desired steady-state concentration each nanorobot must emit $n_{\text{NO}} \sim c_{\text{NO}} A_{\text{NO}} v_{\text{NO}} / k_{\text{NO}} \sim 0.07\text{-}1.1 \times 10^{-16}\text{ moles/sec}$, or $n_{\text{NOmol}} \sim n_{\text{NO}} N_A = \mathbf{0.4\text{-}7 \times 10^7\text{ molecules/sec}}$ of nitric oxide, taking Avogadro's number $N_A = 6.023 \times 10^{23}\text{ molecules/mole}$.

There are at least three possible sources for the required nitric oxide: (1) pressure tank storage and (2) onboard synthesis, both of which are feasible and could be employed in tandem, and (3) local absorption, which is not:

(1) Pressure tank storage. Nitric oxide is relatively stable as a free radical and should not spontaneously decompose if stored at high pressure in chemically inert diamondoid containers in the complete absence of oxygen. A 1000-atm onboard NO storage tank of volume $V_{\text{tank}} = 0.1 V_{\text{nanorobot}} \sim 1\text{ }\mu\text{m}^3$ in each $V_{\text{nanorobot}} \sim 10\text{ }\mu\text{m}^3$ nanorobot, holding $c_{\text{tankNO}} \sim 142 \times 10^{26}\text{ NO molecules/m}^3$,⁵¹⁶ could store enough nitric oxide to support $t_{\text{NO}} \sim V_{\text{tank}} c_{\text{tankNO}} / n_{\text{NOmol}} \sim 900\text{ sec}$ (range 200-3600 sec) or $\sim 0.25\text{ hr}$ of NO-emission operations using a fleet of $A_{\text{penile}} / A_{\text{NO}} \sim 335 \times 10^6$ nanorobots, assuming the typical penis has $A_{\text{penile}} \sim A_{\text{penart}} + A_{\text{helicine}} + A_{\text{sinusoid}} \sim 3350\text{ cm}^2$ of intimal vascular surface (Section 5.2.4.3). A $t_{\text{hr}} = 3600\text{ sec}$ (1 hr) erectile mission would require

⁵¹⁴ The representative intimal surface area of endothelial cells in the large penile arteries, the helicine arteries, and the sinusoids of the corpora cavernosa are $\sim 450\text{ }\mu\text{m}^2$, $\sim 220\text{ }\mu\text{m}^2$, and $\sim 100\text{ }\mu\text{m}^2$, respectively.

⁵¹⁵ NO quickly reacts with oxygen, superoxide, and other molecules in the blood. Hemoglobin, found in red blood cells, rapidly binds to NO, converting it into nitrate and nitrosyl-hemoglobin. This swift interaction limits the range and duration of NO's biological effects, ensuring that its actions remain highly localized and transient.

⁵¹⁶ Freitas RA Jr. Nanomedicine, Volume I: Basic Capabilities. Landes Bioscience, Georgetown, TX, 1999; Table 10.1, "Van der Waals Equation Gas Constants"; <https://www.nanomedicine.com/NMI/Tables/10.1.jpg>.

$N_{\text{erection}} \sim t_{\text{hr}} A_{\text{penile}} / t_{\text{NO}} A_{\text{NO}} \sim 1.33 \times 10^9$ nanorobots covering $N_{\text{erection}} V_{\text{nanorobot}}^{2/3} / A_{\text{penile}} \sim 1.8\%$ of the available intimal vascular surface.

If nanorobots initially emit NO at a standard calibration rate, then subsequently adjust their anchorage location by moving up or down the resulting 2D concentration gradient to establish a preset target calibration rate, then the nanorobots can space themselves fairly evenly across the vascular surface without being able to directly “see” each other to ensure proper spacing, with one robot in every $\sim 1000 \mu\text{m}^2$ patch of vascular surface. Alternatively, the nanorobots can reposition themselves using an ultrasonic acoustic mesh network,⁵¹⁷ since in their final positions the robots would be $\sim A_{\text{NO}}^{1/2} \sim 32 \mu\text{m}$ apart and acoustic positional navigation⁵¹⁸ and communication⁵¹⁹ between nanorobots should work well out to at least $\sim 100 \mu\text{m}$ separation.

(2) Onboard synthesis. Establishing and maintaining an erection requires the emission of up to $n_{\text{NOall}} \sim n_{\text{NOmol}} A_{\text{penile}} / A_{\text{NO}} \sim 2.4 \times 10^{16}$ molecules/sec of nitric oxide throughout the penile vascular system. Nitric oxide could be continuously chemically synthesized⁵²⁰ onboard the nanorobot using ambient N_2 and O_2 dissolved in the bloodstream at an energy cost of 90.3 kJ/mole or $E_{\text{NO}} \sim 150$ zJ/molecule of NO,⁵²¹ requiring a fleet power of at least $n_{\text{NOall}} E_{\text{NO}} \sim 3.5$ mW at 100% energy efficiency. There are about $c_{\text{N}_2} = 1.8 \times 10^5$ molecules/ μm^3 of molecular nitrogen and $c_{\text{O}_2\text{-A}} = 7.3 \times 10^4$ molecules/ μm^3 of molecular oxygen in human arterial blood plasma, but we’ll avoid impacting normal cellular metabolism by conservatively assuming only the $c_{\text{O}_2\text{-V}} = 3 \times 10^4$ molecules/ μm^3 of venous plasma molecular oxygen are available for NO synthesis. Each robot in a fleet of $N_{\text{synth}} \sim 10^9$ nanorobots would have to extract the “excess” venous oxygen (the limiting resource) from $n_{\text{NOall}} / c_{\text{O}_2\text{-V}} N_{\text{synth}} \sim 800 \mu\text{m}^3/\text{sec}$ of blood plasma, which seems reasonable given the volumetric plasma flow past the robot is $V_{\text{nanorobot}}^{2/3} V_{\text{NO}} \sim 4600 \mu\text{m}^3/\text{sec}$. A 7 nm x 14 nm x 14 nm sorting rotor of volume $V_{\text{rotor}} \sim 1372 \text{ nm}^3/\text{rotor}$ should collect $n_{\text{rotor}} \sim 3000 \text{ O}_2$ molecules/rotor-sec from serum with $c_{\text{O}_2\text{-V}} = 0.3 \times 10^4 \text{ O}_2$ molecules/ nm^3 ,⁵²² so each nanorobot needs $N_{\text{rotors}} \sim n_{\text{NOall}} / 2 n_{\text{rotor}} N_{\text{synth}} \sim 4000$ rotors/nanorobot with a fairly modest total rotor volume of $V_{\text{AllRotors}} = V_{\text{rotor}} N_{\text{rotors}} \sim 0.005 \mu\text{m}^3$ per $\sim 10 \mu\text{m}^3$ robot.

⁵¹⁷ https://en.wikipedia.org/wiki/Mesh_networking.

⁵¹⁸ Freitas RA Jr. Nanomedicine, Volume I: Basic Capabilities. Landes Bioscience, Georgetown, TX, 1999; Section 8.3.3, “Microtransponder Networks”; <http://www.nanomedicine.com/NMI/8.3.3.htm>.

⁵¹⁹ Freitas RA Jr. Nanomedicine, Volume I: Basic Capabilities. Landes Bioscience, Georgetown, TX, 1999; Section 7.2.2, “Acoustic Broadcast Communication”; <http://www.nanomedicine.com/NMI/7.2.2.htm>; and Section 7.3.2, “Mobile Networks”; <http://www.nanomedicine.com/NMI/7.3.2.htm>.

⁵²⁰ The Birkeland-Eyde process (https://en.wikipedia.org/wiki/Birkeland-Eyde_process.) uses an electric arc on an N_2/O_2 mixture to achieve the reaction $\text{N}_2 + \text{O}_2 \rightarrow 2\text{NO}$ with a 30-50% yield of NO relative to other oxides of nitrogen; the use of intense UV combined with higher temperature, low O_2 concentration, and rapid cooling might increase the NO yield as high as 90-95%. Mechanochemical synthesis processes are expected to be more energy efficient, with $\sim 100\%$ yields of NO.

⁵²¹ https://en.wikipedia.org/wiki/Standard_enthalpy_of_formation.

⁵²² Freitas RA Jr. Nanomedicine, Volume I: Basic Capabilities. Landes Bioscience, Georgetown, TX, 1999; Section 4.2.3, “Counting Rotors”; <http://www.nanomedicine.com/NMI/4.2.3.htm>.

Once erection occurs and the volumetric blood flow rate falls by 90%, the nanorobots must draw their required oxygen (and nitrogen) from a tenfold larger volume of blood than before, in the corpora cavernosa. The total volume of blood in the erect corpora cavernosa is $V_{CC} \sim V_{erect} - V_{flaccid} = 77 \text{ cm}^3$, containing $n_{O_2-CC} = V_{CC} c_{O_2-V} \sim 2.3 \times 10^{18}$ molecules of available O_2 , enough to synthesize $2n_{O_2-CC} \sim 4.6 \times 10^{18}$ molecules of NO which would be sufficient to maintain an erection for $2n_{O_2-CC} / n_{NOall} \sim 200 \text{ sec}$. Conveniently, the entire blood volume of the corpora cavernosa is exchanged with fresh oxygenated arterial blood every $t_{exch-erect} \sim 200 \text{ sec}$ during an erection (see below), so the inflow of O_2 and N_2 from new blood should just allow the synthesis of enough NO to maintain the erection indefinitely. (There is enough N_2 available to sustain more than twice this rate.)

A previous study⁵²³ estimated that mechanosynthetic chemical fabrication modules of volume $V_{fab} \sim 0.001 \text{ } \mu\text{m}^3$ and power consumption $P_{fab} \sim 0.094 \text{ pW/module}$ could synthesize $n_{fab} \sim 10^5$ simple molecules/module-sec from elemental precursors, so a nanorobot equipped with $n_{modules} = n_{NOall} / n_{fab} N_{synth} \sim 240$ fab modules of volume $V_{modules} = n_{modules} V_{fab} \sim 0.24 \text{ } \mu\text{m}^3$ drawing $P_{modules} = n_{modules} P_{fab} \sim 23 \text{ pW}$ ($\sim 12\%$ of the usual $\sim 200 \text{ pW}$ nanorobot power budget) could synthesize the required $n_{NOall} / N_{synth} \sim 2.4 \times 10^7$ molecules/robot-sec of nitric oxide. For comparison, the proposed mechanosynthetic chemical fabrication modules achieve a productivity of 5×10^{22} molecules/sec-kg, comparable to the biological productivity of 3×10^{23} molecules/sec-kg for eNOS enzyme in HUVEC cells⁵²⁴ which uses L-citrulline, not N_2/O_2 , precursors.⁵²⁵

(3) Local absorption. The ambient concentration of NO in human plasma has been estimated as 0.001-0.030 nM,⁵²⁶ or $c_{NO} \sim 0.06\text{-}1.8 \times 10^{-11}$ molecules/nm³, a very low concentration from which sorting rotors can only extract $n_x \sim 10^{-4}$ molecules/rotor-sec.⁵²⁷

⁵²³ Freitas RA Jr. The Whiskey Machine: Nanofactory-Based Replication of Fine Spirits and Other Alcohol-Based Beverages. IMM Report No. 47, May 2016; Section 5.3.2, "Quantitative Production of Ethanol and Congeners"; <http://www.imm.org/Reports/rep047.pdf>.

⁵²⁴ Hedengran KK, Andersen MR, Szecsi PB, Lindh C, Uldbjerg N, Stender S. Environmental tobacco smoke exposure during pregnancy has limited effect on infant birth weight and umbilical vein endothelial nitric oxide synthase. *Acta Obstet Gynecol Scand*. 2018 Nov;97(11):1309-1316; <https://obgyn.onlinelibrary.wiley.com/doi/10.1111/aogs.13419>.

⁵²⁵ From the Hedengran *et al.* paper, the reported eNOS concentration in HUVECs (Human Umbilical Vein Endothelial Cells) was $1.65 \pm .92 \text{ ng}/10^6 \text{ ECs}$ (mean \pm SD) in nonsmokers and eNOS activity was $52.0 \pm 20.6 \text{ pmol L-citrulline}/\text{min}/10^6 \text{ ECs}$ in nonsmokers. This means the eNOS activity was $(52.0 \pm 20.6 \text{ pmol L-citrulline}/\text{min})/(1.65 \pm .92 \text{ ng})$ ($1 \text{ pmol NO} / 1 \text{ pmol L-citrulline}$) = $31.5 \text{ pmol}/\text{min-ng}$ = $31.5 \times 10^6 \text{ pmol}/\text{min-mg}$ = $3.16 \times 10^{23} \text{ molecules}/\text{sec-kg}$.

⁵²⁶ Liu X, Yan Q, Baskerville KL, Zweier JL. Estimation of nitric oxide concentration in blood for different rates of generation. Evidence that intravascular nitric oxide levels are too low to exert physiological effects. *J Biol Chem*. 2007 Mar 23;282(12):8831-6; <https://www.sciencedirect.com/science/article/pii/S0021925819834683/pdf>.

⁵²⁷ Freitas RA Jr. Nanomedicine, Volume I: Basic Capabilities. Landes Bioscience, Georgetown, TX, 1999; Section 4.2.3, "Counting Rotors"; <http://www.nanomedicine.com/NMI/4.2.3.htm>.

Producing $n_{\text{NOall}} \sim 2.4 \times 10^{16}$ molecules/sec would require a rotor volume of $n_{\text{NOall}} V_{\text{rotor}} / n_x$
 $N_{\text{absorb}} \sim 300,000 \mu\text{m}^3/\text{nanorobot}$ (assuming an $N_{\text{absorb}} \sim 10^9$ nanorobot fleet), which is clearly infeasible.

What if we simply increased the NO concentration globally throughout the entire bloodstream, or just locally closer to the penis? The time it takes for blood to flow through the penile large artery system (including the pudendal, dorsal, bulbourethral, and cavernosal arteries) to reach the first venous drainage vessels in the corpora cavernosa may be $t_{\text{exch-rest}} \sim 10\text{-}30$ sec in the resting state, $t_{\text{exch-init}} \sim 10\text{-}15$ sec during the initial stages of sexual arousal and tumescence, slowing to $t_{\text{exch-erect}} \sim 200$ sec during an erection due to venous occlusion and increased resistance to arterial inflow. Therapeutic levels of inhaled nitric oxide (used in medicine) produce blood concentrations of $0.001\text{-}1 \mu\text{M}$,⁵²⁸ with toxic effects⁵²⁹ appearing in the $10\text{-}100 \mu\text{M}$ range. If the half-life of NO in the blood is $\tau_{\text{NO}} \sim 3$ sec (range $1\text{-}5$ sec), then the NO blood concentration entering the arteries would have to be raised to borderline toxic levels of $c_{\text{NO-art}} \sim (1/2)\exp[-(t_{\text{exch-rest}}/\tau_{\text{NO}})] c_{\text{NO-CC}} \sim 0.1\text{-}10 \mu\text{M}$ (resting) in order to guarantee the NO concentration remains at or above the minimum erection stimulative level of $c_{\text{NO-CC}} \sim 10$ nM (range $5\text{-}15$ nM) throughout the entire corpora cavernosal flow path during the pre-erection period. Once erection has occurred and blood flow has slowed ~ 10 -fold from the resting rate, it will not be possible to create a nontoxic initial arterial NO concentration throughout the corpora cavernosa high enough to maintain the erection,⁵³⁰ whereupon the erection will fail.

⁵²⁸ Micromolar blood concentrations of NO are the result from inhaling 20-160 ppm of NO mixed with air in typical therapeutic treatments (e.g., ~ 40 ppm NO inhalant produces a $\sim 1 \mu\text{M}$ blood concentration) for antiviral,^{*} COPD,[†] cardiac surgery,[‡] and other treatments.^{**}

^{*} Garren MR, Ashcraft M, Qian Y, Douglass M, Brisbois EJ, Handa H. Nitric oxide and viral infection: Recent developments in antiviral therapies and platforms. *Appl Mater Today*. 2021 Mar;22:100887; <https://www.ncbi.nlm.nih.gov/pmc/articles/PMC7718584/pdf>.

[†] Giuriato G, Paneroni M, Venturelli M, Layec G. Strategies targeting the NO pathway to counteract extra-pulmonary manifestations of COPD: A systematic review and meta-analysis. *Nitric Oxide*. 2022 Nov 1;128:59-71, <https://pubmed.ncbi.nlm.nih.gov/35977691/>.

[‡] Estanove S, Girard C, Bastien O, Piriou V, Lehot JJ. Le monoxyde d'azote inhalé: applications thérapeutiques en chirurgie cardiaque [Inhaled nitric oxide: therapeutic applications in cardiac surgery]. *Bull Acad Natl Med*. 2000;184(8):1715-26; <https://pubmed.ncbi.nlm.nih.gov/11471390/>.

^{**} Biban P. Somministrazione di ossido nitrico per via inalatoria nei neonati [Administration of inhaled nitric oxide in newborns]. *Minerva Anestesiol*. 2004 Apr;70(4):245-50; <https://pubmed.ncbi.nlm.nih.gov/15173704/>.

⁵²⁹ e.g., measurable increases in methemoglobin formation, oxidative damage, and other signs of NO-related toxicity including systemic vasodilation and reduced blood pressure, hyperperfusion of the brain and kidneys, and inhibition of platelet function.

⁵³⁰ It might be possible to extend the reach of the excess NO if the NO-absorptive mechanisms in the blood were overwhelmed with excess NO, allowing the NO half life to be considerably extended. However, doing so could have toxic results. For example, one primary absorptive mechanism is the conversion of hemoglobin (Hb) to methemoglobin (MetHb).^{*} The blood normally contains 2% MetHb, but levels of **20%-30%** produce anxiety, headache, and dyspnea on exertion, and **30%-50%** produces fatigue, confusion, dizziness, tachypnea, and palpitations.[†] If all the Hb in the $\sim 0.4 \text{ cm}^3/\text{sec}$ of blood passing through the corpora cavernosa became NO-saturated as MetHb, then after a 1-hr erection the blood concentration of MetHb would rise to $(0.4 \text{ cm}^3/\text{sec})(3600 \text{ sec/hr})/(5400 \text{ cm}^3 \text{ whole-body blood volume}) \sim 27\%$, a mid-range toxic level.

5.3.1.2 Endothelial Cell Injection of Nitric Oxide

In a closely related scenario, lifter nanorobots transiently anchored⁵³¹ to individual endothelial cells (ECs) lining the penile vasculature could inject nitric oxide (NO) directly into the cytosol of the ECs using a $\sim 1 \mu\text{m}$ long microneedle,⁵³² allowing diffusion to carry the NO through the ECs and the intercellular spaces into the smooth muscle cells (SMCs) by diffusion, thereby triggering the normal cycle of SMC relaxation leading to erection.

A steady-estate endothelial cell cytoplasmic NO concentration of $c_{\text{NO-EC}} \sim 3\text{-}10 \text{ nM}$ should be sufficient to activate the soluble guanylate cyclase (sGC) enzyme in SMCs and elicit an erectile response in the corpora cavernosa (Section 5.3.1.1). The typical penis has $N_{\text{penileEC}} \sim 3.3 \times 10^9$ arterial penile endothelial cells of average representative volume $V_{\text{penileEC}} \sim (N_{\text{largeEC}} V_{\text{largeEC}} + N_{\text{helicineEC}} V_{\text{helicineEC}} + N_{\text{sinusoidEC}} V_{\text{sinusoidEC}}) / N_{\text{penileEC}} \sim 102 \mu\text{m}^3$ (Section 5.2.4.3). If we assume rapid diffusion of NO through the ECs (en route to the SMCs) giving an effective NO half-life of $\tau_{1/2} \sim 0.1 \text{ sec}$ in the ECs, then the required NO injection rate is $n_{\text{NO-EC}} \sim c_{\text{NO-EC}} V_{\text{penileEC}} N_A (\ln(2) / \tau_{1/2}) \sim 4300 \text{ NO molecules/sec}$ for each EC. The simplest approach involves anchoring one vasculomobile nanorobot atop each endothelial cell, requiring a fleet of $N_{\text{penileEC}} \sim 3.3 \times 10^9$ nanorobots each injecting 4300 NO molecules/sec directly into the cytosol of its designated EC. A nanorobot equipped with the pressure tank described in Section 5.3.1.1(1) would hold $V_{\text{tank}} c_{\text{tankNO}} \sim 142 \times 10^{10}$ molecules of NO, providing $3.3 \times 10^6 \text{ sec}$ (~ 38 days) of erectile capacity, while a nanorobot equipped with onboard NO synthesis could provide erectile capacity virtually indefinitely. Positioning one nanorobot of contact area $A_{\text{contact}} \sim V_{\text{nanorobot}}^{2/3} \sim 4.6 \mu\text{m}^2$ over each EC having a representative intimal vascular surface of $A_{\text{sinusoidEC}} \sim 100 \mu\text{m}^2$ (range 50-200 μm^2) would only cover $A_{\text{contact}} / A_{\text{sinusoidEC}} \sim 4.6\%$ of the intimal vascular surface in the corpora cavernosa.

Endothelial cells have a typical turnover time of a few months (i.e., $\sim 3 \times 10^7 \text{ ECs/day}$), so nanorobots anchored to ECs for that amount of time are likely to be removed from the intimal vascular surface along with the damaged or senescent ECs. The normal EC turnover process in the corpora cavernosa is apoptosis, in which the cell self-digests and dismantles itself into apoptotic bodies that are either absorbed by neighboring cells or digested by roving phagocytes without being released into the bloodstream. Attached nanorobots could free themselves from

* <https://en.wikipedia.org/wiki/Methemoglobin>.

† https://en.wikipedia.org/wiki/Methemoglobin#Methemoglobin_saturation.

⁵³¹ Freitas RA Jr. Nanomedicine, Volume I: Basic Capabilities. Landes Bioscience, Georgetown, TX, 1999; Section 9.4.3.3, “Anchoring and Dislodgement Forces”; <http://www.nanomedicine.com/NMI/9.4.3.3.htm>.

⁵³² Freitas RA Jr. The ideal gene delivery vector: Chromalloyocytes, cell repair nanorobots for chromosome replacement therapy. J Evol Technol 2007;16:1-97; Section 3.2, “Proboscis Manipulator”; <http://jetpress.org/v16/freitas.pdf> (injection manipulator). Freitas RA Jr. Cryostasis Revival: The Recovery of Cryonics Patients through Nanomedicine. Alcor Life Extension Foundation, Scottsdale AZ, 2022; Section 4.10.2, “Alternative to Targeted Extraction: Tissue Washout”; <https://www.alcor.org/cryostasis-revival/> (injection micropipette).

neighboring cells or phagocytes by several means,⁵³³ or they could simply relocate their temporary anchorage to another cell upon detecting apoptotic activity in their designated EC, but the default residence period should probably be set fairly conservatively, perhaps ~1 day.

5.3.1.3 Mechanical Sinusoid Inflation

In another scenario, lifter nanorobots transiently anchored⁵³⁴ to individual endothelial cells (ECs) lining the sinusoids of the corpora cavernosa could physically inflate, e.g., using compressed gas, mechanically forcing the corpora cavernosa to expand, yielding an erection. This method could be used to guarantee erection when the entire biochemical erectile infrastructure is malfunctioning but the physical microstructure of the corpora cavernosa remains intact.

Previously we estimated that the corpora cavernosa can be crudely modeled as including $N_{CC} \sim 50,000$ roughly spherical sinusoids⁵³⁵ that expand to a radius of $R_{\text{sinusoid}} \sim 880 \mu\text{m}$ when the sinusoids fill with blood during an erection, with $N_{\text{sinusoidEC}} \sim 3260 \times 10^6$ endothelial cells lining the $A_{\text{sinusoid}} \sim 3300 \text{ cm}^2$ intimal surface area of the sinusoids (Section 5.2.4.3). In the present scenario, sinusoid inflation⁵³⁶ is mechanically induced by the inflation of circumferential bumpers⁵³⁷ enclosing the perimeter of $N_{\text{inflation}} = A_{\text{sinusoid}} h_{\text{nanorobot}} / V_{\text{nanorobotINFL}} \sim 1.5 \times 10^9$ nanorobots from a pre-inflation robot volume $V_{\text{nanorobot}} = 10 \mu\text{m}^3$ to a post-inflation robot volume $V_{\text{nanorobotINFL}} = 300 \mu\text{m}^3$, assuming the nanorobots are $h_{\text{nanorobot}} = 1.33 \mu\text{m}$ thick. The bumpers of each robot must provide $\Delta V = V_{\text{nanorobotINFL}} - V_{\text{nanorobot}} \sim 290 \mu\text{m}^3$ of gas at $p_{\text{erect}} \sim 120 \text{ mmHg}$ (0.16 atm) pressure to establish and maintain an erection (Section 2.5), requiring $n_{\text{inflateN}_2} = p_{\text{erect}} \Delta V / R_{\text{gas}} T_{\text{body}} \sim 1.1 \times 10^9$ nitrogen molecules at body temperature $T_{\text{body}} = 310 \text{ K}$ and universal gas constant $R_{\text{gas}} = 1.36 \times 10^{-28} \text{ m}^3\text{-atm/molecule-K}$, and are inflated using compressed nitrogen gas from an onboard buffer storage tank holding $c_{\text{tankN}_2} \sim 106 \times 10^{26} \text{ N}_2 \text{ molecules/m}^3$ at $p_{\text{storage}} \sim$

⁵³³ Freitas RA Jr. Nanomedicine, Volume IIA: Biocompatibility. Landes Bioscience, Georgetown, TX, 2003; Section 15.4.3.6, "Phagocyte Avoidance and Escape"; <http://www.nanomedicine.com/NMIIA/15.4.3.6.htm>.

⁵³⁴ Freitas RA Jr. Nanomedicine, Volume I: Basic Capabilities. Landes Bioscience, Georgetown, TX, 1999; Section 9.4.3.3, "Anchoring and Dislodgement Forces"; <http://www.nanomedicine.com/NMI/9.4.3.3.htm>.

⁵³⁵ The corpora cavernosa sinusoids are larger in the center of the corpora and smaller in the periphery and have a grape-like appearance, enabling blood within the penis to transfer easily from the top to the bottom of the corpora, and allowing the penis to have a common intracavernosal pressure and a common penile rigidity. Peripheral sinusoids have a greater individual surface area than central sinusoids, which aids in the passive process of corporal veno-occlusion by sub-tunical venule compression against the tunica albuginea (<https://www.bumc.bu.edu/sexualmedicine/physicianinformation/male-genital-anatomy/>).

⁵³⁶ Although this analysis emphasizes sinusoid inflation, the same method could be employed to force open the large penile arteries, which are $A_{\text{penart}} / A_{\text{sinusoid}} \sim 1\%$ of the total penile vascular intimal surface area, and the helicine arteries, which are $A_{\text{helicine}} / A_{\text{sinusoid}} \sim 0.5\%$ of the total.

⁵³⁷ Freitas RA Jr. Nanomedicine, Volume I: Basic Capabilities. Landes Bioscience, Georgetown, TX, 1999; Section 5.4, "Metamorphic Bumpers"; <http://www.nanomedicine.com/NMI/5.4.htm>.

1000 atm pressure,⁵³⁸ requiring an onboard storage tank of volume $V_{\text{tankN}_2} = n_{\text{inflateN}_2} / c_{\text{tankN}_2} \sim 0.1 \mu\text{m}^3/\text{robot of compressed N}_2$.

Risk of mechanical damage. If there is no nitric oxide emission and the smooth muscle cells remain in their contracted state, unrelaxed and not compliant to the expansion pressure, then a rapid forced expansion of the sinusoids by the robotic devices could stress, tear, or mechanically damage the smooth muscle cells, the endothelial cells, and other components of penile tissue including connective tissue and nerve fibers. However, endothelial cells respond to shear stress by emitting nitric oxide, allowing the smooth muscle cells to relax. Shear stress on endothelial cells typically results from the flow of blood over the surface of these cells, but the lateral movement of the expanding nanorobot bumpers might create a similar stress – only 1-2 Pa ($\sim 10^{-5}$ atm) of shear stress is necessary to elicit the nitric oxide emission response from endothelial cells in the corpora cavernosa, activating mechanotransduction pathways leading to NO release which facilitates the relaxation of smooth muscle cells. Endothelial cells begin generating NO within 1-5 sec after being activated by shear forces, though peak NO production will require 30 sec to several minutes. The nanorobot fleet should re-apply the shear stress (e.g., by briefly “shrugging”) on roughly the same timescale to maintain NO production. Precise control over the inflation speed and volume of the nanorobots can ensure the generation of appropriate shear stress, with feedback mechanisms that monitor endothelial response and adjust inflation parameters accordingly would enhance the safety and efficacy of this approach. The nanorobots might need to release supplemental NO if ECs cannot generate a sufficient amount, or might employ a more gradual expansion rate if SMCs have become unresponsive to NO.

Risk of anoxia. Coating the sinusoid surface with nanorobots creates a risk of anoxia (lack of oxygen) and subsequent tissue damage or death. Tissue cells can begin to experience hypoxia (reduced oxygen) within minutes if blood flow is completely obstructed, with significant tissue damage (critical anoxia) occurring within 20-30 minutes of severe oxygen deprivation with permanent damage or cell death if the anoxic conditions persist for more than an hour.⁵³⁹ But the use of an inflatable nanorobotic shell leaves the interiors of the sinusoids open and available to fill with blood, allowing bloodborne oxygen and other nutrients to continue supplying the underlying endothelial cells via internal transport streams such as molecular conveyors⁵⁴⁰ or nanopipettes⁵⁴¹ transporting molecules (most critically, glucose, O₂ and CO₂) between the blood-

⁵³⁸ Freitas RA Jr. Nanomedicine, Volume I: Basic Capabilities. Landes Bioscience, Georgetown, TX, 1999; Table 10.2, “Gas Molecules Packed into a Pressure Vessel”; <https://www.nanomedicine.com/NMI/Tables/10.2.jpg>.

⁵³⁹ For a short period such as 1 hour, the primary concern for cellular health is maintaining adequate oxygen and glucose supply. The absence of other nutrients like amino acids, electrolytes, vitamins, fatty acids, and trace elements for this short duration is unlikely to cause permanent damage or cell death, as cells have internal reserves and buffering capacities to handle short-term deficiencies and can temporarily adjust their metabolism in response to short-term nutrient deprivation.

⁵⁴⁰ Freitas RA Jr. Nanomedicine, Volume I: Basic Capabilities. Landes Bioscience, Georgetown, TX, 1999; Section 3.4.3, “Internal Transport Streams”; <http://www.nanomedicine.com/NMI/3.4.3.htm>.

⁵⁴¹ Freitas RA Jr. Nanomedicine, Volume I: Basic Capabilities. Landes Bioscience, Georgetown, TX, 1999; Section 9.2.4, “Capillarity and Nanoscale Fluid Flow”; <http://www.nanomedicine.com/NMI/9.2.4.htm>.

contacting and endothelium-contacting faces of the nanorobots using an appropriate array of molecular sorting rotors on either face.⁵⁴² Alternatively, selected nanorobots could be briefly deflated and re-inflated in a pattern and on a schedule that would periodically allow all endothelial cells at least brief direct access to blood without compromising the mechanical integrity of the robotic support shell.

Other risks: (1) Biocompatible nanorobot surfaces must be employed to minimize immune system reactions; (2) repeated mechanical expansion might lead to tissue remodeling or fibrosis over time, so tissue health should be monitored regularly and the frequency and duration of device use should be limited appropriately; (3) mechanical expansion too fast might cause discomfort or pain, so the system must ensure sufficiently gradual inflation to minimize discomfort; and (4) nanorobot design should be optimized to minimize impact on sensory nerves, as the presence of inflation devices might affect sensation during erection.

5.3.1.4 Venous Occlusion

In a final scenario, lifter nanorobots transiently anchored⁵⁴³ to individual endothelial cells (ECs) lining the venous vessels that drain blood from the sinusoids of the corpora cavernosa could arrange themselves into a configuration that significantly blocks the outflow of blood, slowly forcing the corpora cavernosa to expand, yielding an erection. This method would most likely only be used in cases of venous leakage or venogenic ED ([Section 3.1](#)), or in combination with NO injection ([Section 5.3.1.1](#) or [Section 5.3.1.2](#)) or mechanical inflation ([Section 5.3.1.3](#)) in cases where the entire biochemical erectile infrastructure is malfunctioning but the physical microstructure of the corpora cavernosa remains intact.

Normally, erections occur because arterial inflow into the corpora cavernosa increases significantly while venous outflow is restricted by the compression of the subtunical venules. What happens if the subtunical venules are partially blocked but there has been no sexual arousal, neural initiation, or increased arterial inflow?

50% Blockage. With a baseline blood flow of 2-5 cm³/min (typical for the flaccid state) and a 50% reduction in venous outflow due to partial blockage of the venules, blood would

⁵⁴² An inflated $V_{\text{nanorobotINFL}} = 300 \mu\text{m}^3$ nanorobot that is $h_{\text{nanorobot}} = 1.33 \mu\text{m}$ thick covers $n_{\text{EC-infl}} \sim V_{\text{nanorobotINFL}} / h_{\text{nanorobot}} \sim 2.25$ endothelial cells of intimal vascular surface area of $A_{\text{sinusoidEC}} \sim 100 \mu\text{m}^2$ ([Section 5.2.4.3](#)). If each $100 \mu\text{m}^3$ sinusoid EC cell consumes $\sim 810,000$ molecules/sec of O_2 , $\sim 90,000$ molecules/sec of glucose, and generates $\sim 810,000$ molecules/sec of CO_2 , then 2.25 ECs will require importing $n_{\text{O}_2} \sim 1,800,000$ molecules/sec of O_2 and $200,000$ molecules/sec of glucose, and exporting $1,800,000$ molecules/sec of CO_2 . A $7 \text{ nm} \times 14 \text{ nm} \times 14 \text{ nm}$ sorting rotor of volume $V_{\text{rotor}} \sim 1372 \text{ nm}^3/\text{rotor}$ should collect $n_{\text{rotor}} \sim 3000$ O_2 molecules/rotor-sec from serum with $c_{\text{O}_2\text{-v}} = 0.3 \times 10^{-4}$ O_2 molecules/ nm^3 ([Section 5.3.1.1](#)), so each nanorobot needs $N_{\text{rotors}} \sim n_{\text{O}_2} / n_{\text{rotor}} \sim 600$ rotors of volume $V_{\text{AllRotors}} = V_{\text{rotor}} N_{\text{rotors}} \sim 0.0008 \mu\text{m}^3$ per robot to import all oxygen required to support the underlying endothelial cells, with a similar rotor count to handle the glucose and CO_2 transfers.

⁵⁴³ Freitas RA Jr. Nanomedicine, Volume I: Basic Capabilities. Landes Bioscience, Georgetown, TX, 1999; Section 9.4.3.3, "Anchoring and Dislodgement Forces"; <http://www.nanomedicine.com/NMI/9.4.3.3.htm>.

accumulate within the corpora cavernosa, but the rate at which the corpora cavernosa would fill with blood would be very slow if the inflow rate is so low (far lower than during sexual arousal). The slow rate of blood accumulation at such low inflow levels might not be sufficient to achieve a full erection because erections also require a certain level of pressure within the corpora cavernosa to become rigid. If the subtunical venules are partially blocked, leading to some degree of blood retention, the penis might show some increase in size, but this would occur very slowly, potentially over an hour, and the result might be a state of partial tumescence rather than a full, functional erection that would not be equivalent to a normal erection in terms of function or stability. That is, while some increase in penile size might occur due to the slow accumulation of blood, achieving a normal, functional erection solely through 50% blockage of venous outflow without increased arterial inflow seems unlikely.

70% Blockage. With the arterial inflow remaining at the baseline rate of $2\text{--}5\text{ cm}^3/\text{min}$, the increased restriction of venous outflow would cause a greater and faster accumulation of blood compared to a 50% blockage. This could result in a faster onset of tumescence, although it would still occur much slower than during an arousal-induced erection. The penis might reach a state closer to full tumescence, but without the typical full rigidity of an erection because the high pressures and full engorgement of arousal-induced erections wouldn't be achieved.

90% Blockage. With a 90% reduction in venous outflow, the blood trapped in the corpora cavernosa would lead to a more significant and rapid accumulation than with lesser degrees of blockage, resulting in a much quicker approach to full tumescence. Although the penis might achieve full tumescence due to the high volume of trapped blood, the rigidity typically associated with a normal erection might still be lacking because the high intracavernosal pressure necessary for full rigidity and functional sexual intercourse might not be reached without the enhanced arterial inflow that occurs during sexual arousal.

So venous occlusion alone in an otherwise normal or unexcited penis is unlikely by itself to produce a completely normal erection. In cases where the arterial inflow increases by natural or artificial means but venous leakage exists, venous occlusion probably would restore the user's ability to establish and maintain a normal erection.

The subtunical venules are the vessels most directly involved in the veno-occlusive mechanism because they are located just beneath the tunica albuginea and are the first to be compressed when the erectile tissues expand. In a simplified model, we may assume that the venules form a network (i.e., the subtunical venular plexus) of $N_{\text{venule}} \sim 2000$ (range 300-3000) vessels of diameter $d_{\text{venule}} \sim 300\text{ }\mu\text{m}$ (range 100-400 μm) and length $L_{\text{venule}} \sim 3\text{--}10\text{ mm}$ that drains blood from the corpora cavernosa at $1\text{--}3\text{ cm}^3/\text{sec}$ during flaccidity or early detumescence and up to $3\text{--}8\text{ cm}^3/\text{sec}$ at the peak rate during detumescence, with an average flow velocity of $v_{\text{venule}} \sim 4\text{ n}_{\text{plexus}} / \pi d_{\text{venule}}^2 N_{\text{venule}} \sim 3.5\text{ cm}/\text{sec}$, taking $n_{\text{plexus}} \sim 5\text{ cm}^3/\text{sec}$. The venules could be blocked to $f_{\text{block}} \sim 90\%$ using vasculomobile nanorobots capable of forming temporary vascular gates⁵⁴⁴ or

⁵⁴⁴ Freitas RA Jr. Chapter 23. Comprehensive Nanorobotic Control of Human Morbidity and Aging. In: Fahy GM, West MD, Coles LS, Harris SB, eds, *The Future of Aging: Pathways to Human Life Extension*, Springer, New York, 2010; Section 23.6.3.5.1, "Vascular Gates"; <http://www.nanomedicine.com/Papers/Aging.pdf>.

multilayer ringsets⁵⁴⁵ blocking the venule lumina by stacking $N_{\text{occlude}} \sim \pi d_{\text{venule}}^2 f_{\text{block}} N_{\text{venule}} / 4$. $V_{\text{nanorobot}}^{2/3} \sim 27 \times 10^6$ nanorobots, each of volume $V_{\text{nanorobot}} \sim 10 \mu\text{m}^3$. The rest of the outlying venous penile vasculature with a total luminal cross-sectional area⁵⁴⁶ of $A_{\text{venous}} \sim 100 \text{ mm}^2$ could also be $\sim 90\%$ blocked using an additional similarly-deployed $N_{\text{occludeAll}} \sim f_{\text{block}} A_{\text{venous}} / V_{\text{nanorobot}}^{2/3} \sim 19 \times 10^6$ nanorobots, if necessary.

5.3.1.5 Nanorobot Infusion

The curative treatments for erectile dysfunction (Section 5.2) will most likely take place in a hospital or clinical setting under the direct and constant supervision of medical personnel. Such procedures will employ the various appropriate methods for nanorobot infusion and extraction as have been previously described in professional contexts ranging from emergency care⁵⁴⁷ to cell repair,⁵⁴⁸ where it is expected that the robots will be removed from the body immediately after the curative treatment is concluded.

In the case of purely symptomatic treatments for erectile dysfunction, the infusion and extraction of nanorobots will occur well outside of clinics and hospitals, probably in someone's bedroom. Such nanorobots must be able to reliably enter the body and find their way into the penile tissues largely on their own, and they must also be able to exit the body quickly and completely without any assistance from complex external medical apparatuses.

Each of the symptomatic nanorobotic treatments for erectile dysfunction described in this Section requires the transport of simple nanorobots, aka. "lifters", into the human body from the outside, targeting the appropriate penile tissues such as the large penile arteries, the helicine arteries, and the sinusoids of the corpora cavernosa in the penis. For concreteness, we can specify the typical task as importing $N_{\text{robots}} \sim 10^9$ nanorobots each of volume $V_{\text{nanorobot}} \sim 10 \mu\text{m}^3$, for a total dosage of $V_{\text{dosage}} \sim 10 \text{ mm}^3$ of robots, into the penile arteries and sinusoids, transacting data and control instructions with the robots while they are on station, and then exporting them out again after the user is finished enjoying his erection, using the quickest and simplest possible route.

⁵⁴⁵ Hogg T, Freitas RA Jr. Chemical power for microscopic robots in capillaries. *Nanomedicine*. 2010 Apr;6(2):298-317; <http://www.nanomedicine.com/Papers/NanoPowerModel2010.pdf>.

⁵⁴⁶ The total luminal cross-section area of the venous penile vasculature above the subtunical venular plexus can be crudely estimated as $A_{\text{venous}} \sim 100 \text{ mm}^2$ (range 12-329 mm^2), comprising the superficial dorsal vein of the penis (3.1-12.6 mm^2), the 2-6 circumflex veins (1.6-42.6 mm^2), the 2-4 crural veins (2.4-21.3 mm^2), the 3-4 bulbourethral veins (2.4-12.4 mm^2), and the ~ 300 smaller veins (2.4-240 mm^2).

⁵⁴⁷ Freitas RA Jr. Exploratory design in medical nanotechnology: a mechanical artificial red cell. *Artif Cells Blood Substit Immobil Biotechnol*. 1998 Jul;26(4):411-30; Section 4, "Therapeutics and Performance"; <https://www.tandfonline.com/doi/pdf/10.3109/10731199809117682>.

⁵⁴⁸ Freitas RA Jr. The ideal gene delivery vector: Chromalloyocytes, cell repair nanorobots for chromosome replacement therapy. *J Evol Technol* 2007;16:1-97; Section 5.2, "Detailed Sequence of Chromalloyocyte Activities"; <http://jetpress.org/v16/freitas.pdf>.

For maximum comfort, convenience, and effectiveness, the leading administration route appears to be a **metered dose inhaler for lung entry** by the nanorobots. A single dose from a metered dose inhaler for asthma medications typically involves intaking $50\text{--}100\text{ cm}^3$ of air containing $10\text{--}20\text{ mm}^3$ of aerosolized liquid medication, consistent with a 50% suspension of a 10 mm^3 dose of vasculomobile nanorobots in 10 mm^3 of a neutral carrier fluid for a total aerosolized inhalation volume of 20 mm^3 . Once inhaled deeply into the lungs, the fluid-suspended robots initially settle onto the air-contacting side of the pulmonary alveoli⁵⁴⁹ or perambulate to the alveoli if they're deposited higher in the respiratory tree.⁵⁵⁰ A pair of lungs contain ~480 million alveoli (each $100\text{--}300\text{ }\mu\text{m}$ in diameter) that provide a $70\text{--}80\text{ m}^2$ surface for gas exchange, so on average there may only be a few nanorobots in each alveolus during the dosing process.

The robots histonate⁵⁵¹ through the alveolar epithelial cell layer (consisting of Type I pneumocytes)⁵⁵² and the basement membrane of the alveolar epithelium, then pass through the interstitial space or interstitium (which includes connective tissue such as elastic fibers and extracellular matrix), then penetrate the basement membrane of the capillary endothelium and the capillary endothelial cell layer, finally arriving in the lumenal volume of the pulmonary capillaries to enter the bloodstream after a journey of $0.2\text{--}0.6\text{ }\mu\text{m}$, taking $t_{\text{gap}} \sim 3\text{ sec}$ to execute the transit. The robots then flow with the blood from the pulmonary capillaries through the pulmonary venules and the pulmonary veins ($\sim 0.5\text{ cm}$), the left atrium of the heart ($2\text{--}4\text{ cm}$), the mitral (bicuspid) valve and the left ventricle ($\sim 2\text{ cm}$), and finally the aortic valve ($\sim 1\text{ cm}$), entering the headwaters of the aorta after a journey of $\sim 6.5\text{ cm}$ (range $5.5\text{--}7.5\text{ cm}$) at an average flow velocity of $20\text{--}30\text{ cm/sec}$, requiring less than $\sim 1\text{ sec}$ of travel time. Vessel navigation is relatively unimportant for this part of the journey because essentially all paths lead to the aorta.

After passing the aortic valve, the vasculomobile nanorobots are programmed to immediately move to the nearest vascular wall as quickly as possible and transiently adhere to that surface, then begin perambulating downstream at $v_{\text{vasculo}} \sim 1\text{ cm/sec}$ along the vascular wall.⁵⁵³ If the entire nanorobot fleet of total vascular contact area $A_{\text{fleet}} \sim N_{\text{robots}} V_{\text{nanorobot}}^{2/3} \sim 46\text{ cm}^2$ managed to quickly precipitate onto the $\sim 52\text{ cm}^2$ first section of the ascending aorta before the first arterial

⁵⁴⁹ https://en.wikipedia.org/wiki/Pulmonary_alveolus.

⁵⁵⁰ If deposited in the respiratory bronchioles or even higher in the bronchial tree, nanorobots may be caught in the protective mucociliary clearance mechanism that's intended to keep micron-size particles out of the lungs. Nanorobots that can swim through mucus moving at $\sim 1.4\text{ cm/min}$ and can also avoid ingestion by mobile phagocytes present in the airways and alveoli may continue their journey along with the rest of the fleet. Those that cannot will be swept into the esophagus and gastrointestinal tract, then eliminated from the body in the normal manner. Freitas RA Jr. Nanomedicine, Volume I: Basic Capabilities. Landes Bioscience, Georgetown, TX, 1999, Section 8.2.2, "Navigational Bronchography"; <http://www.nanomedicine.com/NMI/8.2.2.htm>.

⁵⁵¹ Freitas RA Jr. Nanomedicine, Volume I: Basic Capabilities. Landes Bioscience, Georgetown, TX, 1999, Section 9.4.4, "Histonation"; <http://www.nanomedicine.com/NMI/9.4.4.htm>.

⁵⁵² https://en.wikipedia.org/wiki/Pulmonary_alveolus#Type_I_cells.

⁵⁵³ Freitas RA Jr. Nanomedicine, Volume I: Basic Capabilities, Landes Bioscience, Georgetown TX, 1999; Section 9.4.3.5, "Legged Ambulation"; <http://www.nanomedicine.com/NMI/9.4.3.5.htm>.

branch points in the aortic arch,⁵⁵⁴ then the robots would have a **~0.88** sub-monolayer coverage on the vascular surface, which is pretty crowded. However, about 30-40% of the blood that enters the aortic arch is distributed away from the aorta into the brachiocephalic trunk, the left common carotid and the left subclavian arteries which supply blood to the head, neck, and upper limbs, respectively. Robots diverted into these side arteries can finish settling out there, then crawl back upstream to the aortic arch to rejoin the main robot fleet that is crawling south into the descending aorta. If the robots distributed themselves evenly over the vascular surfaces of these three major arteries and the aortic arch, then the total available vascular surface increases to 187 cm²,⁵⁵⁵ yielding a much less crowded **~0.25** sub-monolayer coverage. Adding the ~57 cm² surface area of the descending aorta down to the next major branchings (the bronchial and posterior intercostal arteries) increases the settling surface to ~243 cm²,⁵⁵⁶ further dropping the robots to **~0.19** sub-monolayer coverage; and so forth.

The vasculomobile nanorobots must travel ~70 cm from the aortic valve to the internal pudendal artery in the penis,⁵⁵⁷ plus as much as ~20 cm more for robots temporarily diverted into side arteries, which requires **~90 sec** (1.5 min) to traverse at a crawling velocity of $v_{\text{vasculo}} \sim 1$ cm/sec. Navigation is key during this part of the journey because the traveling robots must choose the correct turn at every vascular branch along the way to the internal pudendal artery. A comprehensive analysis is beyond the scope of this paper and requires very specific and yet-to-be experimentally collected molecular information, but it should be possible to distinguish the desired vascular branch at each junction by a combination of observables available to the nanorobots including molecular surface markers, flow velocities, and other means.⁵⁵⁸ Robots that discover they have taken the incorrect branch can reverse course, return upstream to the junction where the wrong choice was made, then resume travel along the correct branch.

For example, while the **bronchial** and **posterior intercostal** arteries that branch off from the **thoracic aorta** (the desired path for the nanorobots) share many common vascular markers, the bronchial arteries may express higher levels of markers related to angiogenesis, inflammation, and oxygen sensing, reflecting their role in lung physiology. The posterior intercostal arteries

⁵⁵⁴ Pre-aortic arch aorta: diameter ~ 3 cm (range 2.5-3.5 cm), length ~ 5.5 cm (range 5-6 cm), area = **51.8 cm²** (range 39.3-66.0 cm²).

⁵⁵⁵ Pre-aortic arch aorta (51.8 cm²) + aortic arch (diameter ~ 3 cm, length ~ 4.5 cm, area ~ 42.4 cm²) + brachiocephalic trunk (diameter ~ 1.25 cm, length ~ 4.5 cm, area ~ 17.7 cm²) + left common carotid artery (diameter ~ 0.7 cm, length ~ 17.5 cm, area ~ 38.5 cm²) + left subclavian artery (diameter ~ 1.05 cm, length ~ 11 cm, area ~ 36.3 cm²) = **186.7 cm²**.

⁵⁵⁶ Pre-aortic arch aorta, aortic arch, and branches (186.7 cm²) + pre-branch post-aortic branch (diameter ~ 3 cm, length ~ 6 cm, area ~ 56.5 cm²) = **243.2 cm²**.

⁵⁵⁷ Aortic valve to ascending aorta (5-6 cm) + ascending aorta to aortic arch (4-5 cm) + aortic arch to descending thoracic aorta (~20 cm) + descending thoracic aorta to abdominal aorta (15-20 cm) + abdominal aorta to common iliac artery (10-12 cm) + common iliac artery to internal iliac artery (4-5 cm) + internal iliac artery to internal pudendal artery (6-8 cm) = **70 cm** (range 64-76 cm).

⁵⁵⁸ Freitas RA Jr. Nanomedicine, Volume I: Basic Capabilities, Landes Bioscience, Georgetown TX, 1999; Chapter 8, "Navigation"; <http://www.nanomedicine.com/NMI/8.1.htm>.

may show more tissue-specific metabolic and extracellular matrix markers related to their role in supplying the chest wall. Differences in shear stress-related molecules and adhesion proteins may also provide clues for distinguishing these arteries.

As another example, the internal iliac artery branches into the internal pudendal artery and several others including the superior gluteal, inferior gluteal, and obturator arteries. The **internal pudendal artery** (the desired path for the nanorobots) may be distinguished from other branches of the internal iliac artery by its higher expression of sex hormone receptors (androgen and estrogen receptors), molecules involved in the nitric oxide and prostacyclin signaling pathways (eNOS, GC, IP receptors), and angiogenesis-related markers (VEGF receptors). Additionally, the presence of neuropeptide Y receptors and specific adhesion molecules in the internal pudendal artery may reflect its role in controlling blood flow to the genitalia and perineum. These molecular markers, when sampled by a small mobile device, could help identify when the device is within the internal pudendal artery versus other arteries in the pelvic region.

After reaching the internal pudendal artery, the robots need only swim⁵⁵⁹ another 5-10 cm, following a path through the deep artery of the penis, to reach the sinusoids of the corpora cavernosa, taking $t_{\text{pudendal}} \sim \mathbf{5-10 \text{ sec}}$ at a speed of $v_{\text{nano}} = 1 \text{ cm/sec}$,⁵⁶⁰ for a total lung-to-penis transit time of $\sim \mathbf{100 \text{ sec}}$.

Several alternative nanorobot entry routes might include:

(1) **Topical administration for dermal entry.** Nanorobots could be suspended in a carrier liquid that the user applies directly onto the skin of the penis. The nanorobots must then histonate⁵⁶¹ through $x_{\text{tissue}} \sim 2-7 \text{ mm}$ of tissue⁵⁶² to reach and enter the sinusoids of the corpora cavernosa of the penis in $t_{\text{dermal}} \sim x_{\text{tissue}} / v_{\text{ECM}} \sim 20-70 \text{ sec}$ by traversing tissue at $v_{\text{ECM}} = 100 \mu\text{m/sec}$.⁵⁶³ A flaccid penis that is $L_{\text{flaccid}} \sim 9 \text{ cm}$ in length and $D_{\text{flaccid}} \sim 3 \text{ cm}$ in diameter has a cylindrical external surface area of $A_{\text{flaccid}} \sim \pi D_{\text{flaccid}} L_{\text{flaccid}} \sim 85 \text{ cm}^2$, of which $\sim 70\%$ or $A_{\text{DermalRoute}} \sim (70\%) A_{\text{flaccid}} = 60 \text{ cm}^2$ overlays the corpora cavernosa. Sending $N_{\text{robots}} \sim 10^9$

⁵⁵⁹ Freitas RA Jr. Nanomedicine, Volume I: Basic Capabilities. Landes Bioscience, Georgetown, TX, 1999; Section 9.4.2, "Sanguination"; <http://www.nanomedicine.com/NMI/9.4.2.htm>.

⁵⁶⁰ Freitas RA Jr. Nanomedicine, Volume I: Basic Capabilities. Landes Bioscience, Georgetown, TX, 1999; Section 9.4.2.4, "Force and Power Requirements"; <http://www.nanomedicine.com/NMI/9.4.2.4.htm>.

⁵⁶¹ Freitas RA Jr. Nanomedicine, Volume I: Basic Capabilities. Landes Bioscience, Georgetown, TX, 1999; Section 9.4.4, "Histonatation"; <http://www.nanomedicine.com/NMI/9.4.4.htm>.

⁵⁶² The estimated path length includes the thickness of the skin epidermis (50-150 μm) + dermis of skin (500-2000 μm) + subcutaneous tissue and dartos fascia (200-500 μm) + Buck's fascia, the deep fascia of the penis (500-1000 μm) + the space between Buck's fascia and the tunica albuginea (500-1000 μm) + tunica albuginea of the corpora cavernosa (500-1500 μm) + trabeculae or supporting tissue inside the corpora cavernosa (100-500 μm) + sinusoid intima or the endothelial cell lining of the sinusoids (1-2 μm) = **2351-6652 μm** (2-7 mm).

⁵⁶³ Freitas RA Jr. Nanomedicine, Volume I: Basic Capabilities. Landes Bioscience, Georgetown, TX, 1999; Section 9.4.4.2, "ECM Brachiation"; <http://www.nanomedicine.com/NMI/9.4.4.2.htm>.

nanorobots through a $A_{\text{DermalRoute}} \sim 60 \text{ cm}^2$ tissue surface in $t_{\text{dermal}} \sim 100 \text{ sec}$ (allowing $t_{\text{gap}} \sim 3 \text{ sec}$ for “biochemically-mediated endothelial gap width management” while crossing each of the eight tissue layers leading into the sinusoids)⁵⁶⁴ requires an areal transit rate of $a_{\text{dermal}} = N_{\text{robots}} / t_{\text{dermal}}$. $A_{\text{DermalRoute}} \sim 1670 \text{ robots/sec-mm}^2$, or $\sim 1 \text{ robot/sec}$ moving past each $A_{\text{epicell}} \sim 600 \mu\text{m}^2$ epithelial cell on the epidermis of the penis. Mechanical damage during nanorobot histopenetration is proportional to the volume of disturbed tissue. The tissue volume required to be displaced by a given population of passing nanorobots is minimized if transit tunnel volumes are reused by successive nanorobots – that is, if nanorobots histopenetrate in linear convoys⁵⁶⁵ to minimize unnecessary perforation of the epidermis and underlying tissues. In this case the tissue holing fraction would be $f_{\text{hole}} \sim V_{\text{nanorobot}}^{2/3} / A_{\text{epicell}} \sim 0.8\%$, well below the holing fractions generally regarded as an acceptable and fully biocompatible maximum degree of tissue intrusion.⁵⁶⁶ Small-scale movements on the order of microns are unlikely to activate nociceptors (pain sensation) in most of the layers traversed, but the robots would need to distinguish penile and finger epidermis for users applying the robot-laden lotion with their hands, a minor additional complexity.

(2) **Oral administration for gastrointestinal entry.** Nanorobots could be administered in a pill that is swallowed, by mouth, by the user. Most efficiently, a motorized $1 \text{ cm} \times 3.6 \text{ mm}$ cylindrical “pillbot” of volume $\sim 100 \text{ mm}^3$ carrying a $V_{\text{dosage}} \sim 10 \text{ mm}^3$ nanorobot cargo swims or crawls the $\sim 25 \text{ cm}$ distance from the stomach through the duodenum plus the $\sim 250 \text{ cm}$ length of the jejunum in $\sim 275 \text{ sec}$ ($\sim 4.6 \text{ min}$), traveling at $\sim 1 \text{ cm/sec}$. Upon entering the jejunum, the pillbot continually disgorges its cargo of $N_{\text{robots}} \sim 10^9$ nanorobots at a steady rate, emptying its cargo by the end of the jejunum and then exiting the body with the stool in due course. The jejunum is the primary site of nutrient absorption in the intestines, so it has the highest capillary density to maximize nutrient transport into the bloodstream, which also facilitates nanorobot entry. Specifically, the jejunum is $\sim 2.75 \text{ cm}$ (range $2.5\text{--}3 \text{ cm}$) in diameter and $\sim 250 \text{ cm}$ in length, giving a luminal surface area of $\sim 2160 \text{ cm}^2$ (range $1960\text{--}2360 \text{ cm}^2$) with a capillary density of $\sim 20,000 \text{ capillaries/cm}^2$ (range $15,000\text{--}25,000$) for a total of $N_{\text{capillaries}} \sim 43.2 \times 10^6$ capillaries. This implies a transit requirement of $N_{\text{robots}} / t_{\text{oral}} N_{\text{capillaries}} \sim 0.09 \text{ robots/capillary-sec}$ for an assumed $t_{\text{jejunum}} \sim 250 \text{ sec}$ jejunal delivery time, which gives each robot $\sim 11 \text{ sec}$ to transit the intestinal wall and enter a capillary, with a total of $N_{\text{robots}} / N_{\text{capillaries}} \sim 23$ nanorobots entering each capillary during the delivery time. Transiting the jejunal wall requires passing through $x_{\text{mucosa}} \sim 175 \mu\text{m}$ of mucosa including the epithelial layer ($20\text{--}30 \mu\text{m}$ thick, comprising a single layer of columnar epithelial cells) and lamina propria ($100\text{--}200 \mu\text{m}$ thick, comprising a loose connective tissue layer containing small blood vessels, lymphatic vessels or lacteals, and immune cells) where the capillaries are located, a travel time of $t_{\text{mucosal}} \sim 2 t_{\text{gap}} + x_{\text{mucosa}} / v_{\text{ECM}} \sim 8 \text{ sec}$.

⁵⁶⁴ Freitas RA Jr. Nanomedicine, Volume I: Basic Capabilities. Landes Bioscience, Georgetown, TX, 1999; Section 9.4.4.1, “Nanorobot Diapedesis”; <http://www.nanomedicine.com/NMI/9.4.4.1.htm>.

⁵⁶⁵ Freitas RA Jr. Nanomedicine, Volume IIA: Biocompatibility. Landes Bioscience, Georgetown, TX, 2003; Section 15.5.2.3, “Nanorobot Convoy Formation”; <http://www.nanomedicine.com/NMIIA/15.5.2.3.htm>.

⁵⁶⁶ Freitas RA Jr. Nanomedicine, Volume IIA: Biocompatibility. Landes Bioscience, Georgetown, TX, 2003; Section 15.6.3, “Cellular Intrusiveness”; <http://www.nanomedicine.com/NMIIA/15.6.3.htm>.

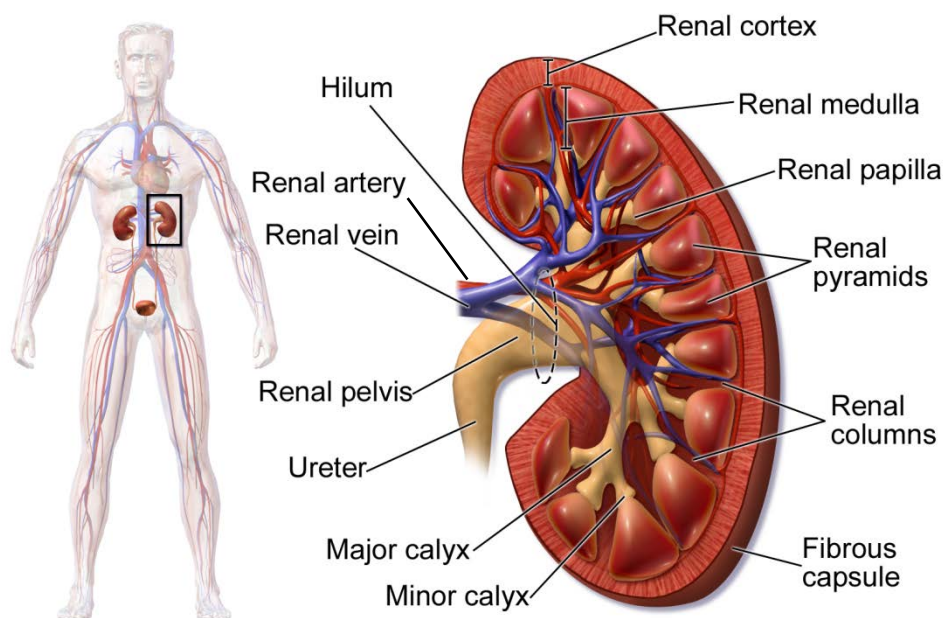
The vasculomobile nanorobots then traverse the $x_{\text{jejunum}} \sim 44 \text{ cm}$ path⁵⁶⁷ from the jejunum to the internal pudendal artery in $x_{\text{jejunum}} / v_{\text{vasculo}} \sim \mathbf{44 \text{ sec}}$, plus another $t_{\text{pudendal}} \sim \mathbf{5-10 \text{ sec}}$ to reach the sinusoids of the corpora cavernosa after reaching the internal pudendal artery, for a total entry time of $\sim \mathbf{335 \text{ sec (5.6 min)}}$ into the sinusoids.

(3) **Nanocatheter injection for direct entry.** A nanocatheter ([Section 5.2.4](#)) painlessly inserted through the skin of the penis can use its intelligent nanomechanical guided tractor toolhead to drag the tip into contact with the internal pudendal artery, from which would be dispensed the $N_{\text{robots}} \sim 10^9$ nanorobots as fast as possible directly into the artery. There are two internal pudendal arteries, one on each side of diameter $D_{\text{ipa}} \sim 2.5 \text{ mm}$ (range 2-3 mm) and length $L_{\text{ipa}} \sim 5 \text{ cm}$ (range 4-6 cm), giving a total intimal surface area of $A_{\text{ipa}} = 2\pi D_{\text{ipa}} L_{\text{ipa}} \sim 7.5 \text{ cm}^2$ (range 5.0-11.3 cm^2) and total lumenal volume of $V_{\text{ipa}} = (\pi/2) D_{\text{ipa}}^2 L_{\text{ipa}} \sim 0.46 \text{ cm}^3$ (range 0.25-0.85 cm^3) for both arteries, and an extremely safe $2V_{\text{dosage}} / \pi D_{\text{ipa}}^2 v_{\text{IPA}} t_{\text{inject}} \sim 0.01\%$ nanocrit, assuming a $t_{\text{inject}} \sim \mathbf{10 \text{ sec}}$ nanocatheter injection time and an arterial blood flow velocity of $v_{\text{IPA}} \sim 200 \text{ mm/sec}$, for a total entry time of $t_{\text{inject}} + t_{\text{pudendal}} \sim \mathbf{15-20 \text{ sec}}$ into the sinusoids.

⁵⁶⁷ Jejunum to superior mesenteric artery (15-20 cm) + superior mesenteric artery to abdominal aorta (2-3 cm) + abdominal aorta to internal iliac artery (15-20 cm) + internal iliac to internal pudendal artery (5-8 cm) = **44 cm** (range 37-51 cm).

5.3.1.6 Nanorobot Extraction

Except for the most advanced medical nanosystems with optimized biocompatibility,⁵⁶⁸ nanorobots left inside the human body indefinitely will eventually fail or get permanently sequestered in the lymph nodes⁵⁶⁹ or granulomas,⁵⁷⁰ perhaps after circulation or on-station times of days, weeks, or months. For maximum comfort, convenience, and effectiveness, the leading extraction route appears to be **retrograde vascular transit to the bladder** via the renal (kidney) arterial tree (image, below),⁵⁷¹ followed by excretion in the urine.



Kidney Anatomy

Vasculomobile nanorobots following this self-excretory pathway would depart from the sinusoids of the corpora cavernosa and crawl along the walls of a series of 11 vascular spaces leading to the

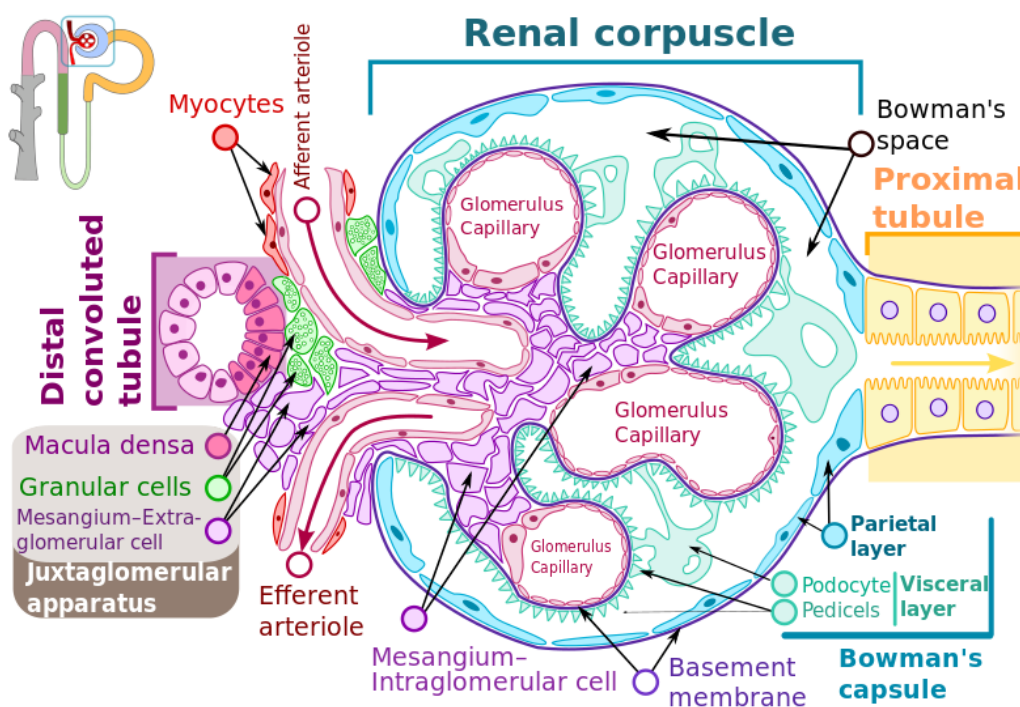
⁵⁶⁸ Freitas RA Jr. Nanomedicine, Volume IIA: Biocompatibility, Landes Bioscience, Georgetown, TX, 2003; <http://www.nanomedicine.com/NMIIA.htm>.

⁵⁶⁹ Freitas RA Jr. Nanomedicine, Volume IIA: Biocompatibility, Landes Bioscience, Georgetown, TX, 2003; Section 15.4.3.4, "Particle Clearance from the Lymphatics"; <http://www.nanomedicine.com/NMIIA/15.4.3.4.htm>.

⁵⁷⁰ Freitas RA Jr. Nanomedicine, Volume IIA: Biocompatibility, Landes Bioscience, Georgetown, TX, 2003; Section 15.4.3.5, "Foreign Body Granulomatous Reaction"; <http://www.nanomedicine.com/NMIIA/15.4.3.5.htm>.

⁵⁷¹ Blausen.com staff. [Medical gallery of Blausen Medical 2014](https://en.wikipedia.org/wiki/Kidney#/media/File:Blausen_0592_KidneyAnatomy_01.png). WikiJournal of Medicine 2014; 1 (2); https://en.wikipedia.org/wiki/Kidney#/media/File:Blausen_0592_KidneyAnatomy_01.png.

entrance of one of the $\sim 2 \times 10^6$ “renal corpuscles” (image, below)⁵⁷² in both kidneys, in the sequence listed in the table below, for a total travel length of 51-70 cm, implying a travel time of $t_{\text{renaltravel}} \sim 51\text{-}70$ sec at $v_{\text{vasculo}} \sim 1$ cm/sec, and a total vascular wall surface area of $A_{\text{renalpath}} \sim 1331$ cm².



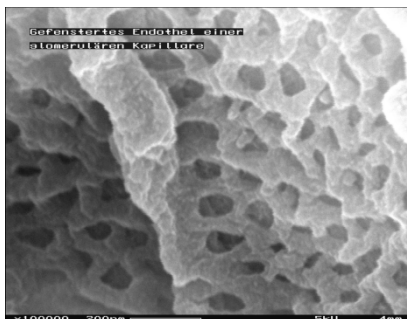
Sequence of vessels traversed during retrograde vascular transit to the bladder and the fractional monolayer coverage of the endothelium by the nanorobot fleet

Seq. #	Names of vessels (in the order traversed)	# of Vessels	Diam. (mm)	Length (cm)	Area (cm ²)	ML*	Blood (cm/sec)
1	Helicine arteries	~ 100	0.02	0.1-0.3	1.3	0.0143	
2	Cavernosal arteries	2	1.5	10-15	11.8	0.0980	
3	Internal pudendal arteries	2	2.5	4-6	7.9	0.0587	
4	Internal iliac arteries	2	6.5	6-8	28.6	0.0227	
5	Common iliac arteries	2	9	4-5	25.4	0.0164	
6	Abdominal aorta	1	25	20-25	176.7	0.0118	
7	Renal arteries	2	5	4-5	14.1	0.0296	10-20
8	Interlobar arteries	10-20	1.5	1-2	10.6	0.0131	4-6
9	Arcuate arteries	10-20	1	1-1.5	5.8	0.0200	2-3
10	Cortical radiate arteries	400-600	0.45	1-2	106.0	0.0013	1-1.5
11	Afferent arterioles	$\sim 2 \times 10^6$	0.02	0.05-0.1	942.5	7×10^{-6}	0.5-1

* Fractional monolayer coverage of robots: $ML_{\text{robots}} = N_{\text{robots}} V_{\text{nanorobot}}^{2/3} L_{\text{vessel}} / A_{\text{vessel}} v_{\text{vasculo}} t_{\text{extraction}}$

⁵⁷² https://commons.wikimedia.org/wiki/File:Renal_corpuscle-en.svg.

The fleet of robots next enters the $\sim 2 \times 10^6$ glomerulus capillaries in both kidneys, with each corpuscle harboring 10-20 mm of capillaries, each comprising ~ 100 shorter capillary loops of 100-300 μm length, providing $A_{\text{glom}} \sim 4 \text{ m}^2$ of endothelial filtration surface in both kidneys. Having reached the capillaries, the nanorobots must now histonate⁵⁷³ through the fenestrated endothelium⁵⁷⁴ (0.05-0.1 μm thick), the glomerular basement membrane (0.2-0.3 μm thick), and the podocytes⁵⁷⁵ (5-10 μm thick) which are specialized epithelial cells wrapping around the capillaries, finally reaching the Bowman's space containing the accumulating free liquid filtrate that will become urine, allowing the nanorobots to be excreted through the urethra at the next urination.



The traveling nanorobots can determine the end of their vascular journey because the fenestrated endothelium consists of endothelial cells about 5-10 μm wide, 10-20 μm long, and 0.2-1 μm thick, whose surface is thoroughly perforated by 10^3 - 10^4 holes/cell through which fluid can flow, with each hole about 70-100 nm in diameter and 50-100 nm in depth (image, left).⁵⁷⁶ The nanorobots can easily detect this unique surface using tactile sensors analogous to reading Braille,⁵⁷⁷ since the afferent arteriole has a continuous endothelial lining with no fenestrations, making it readily distinguishable from the glomerulus capillaries.⁵⁷⁸ Extracting $N_{\text{robots}} \sim 10^9$ nanorobots through $\sim 2 \times 10^6$ glomerulus capillaries (fed by $\sim 2 \times 10^6$ afferent arterioles) in an extraction time of $t_{\text{extraction}} \sim 500 \text{ sec}$ ($\sim 8.3 \text{ min}$) requires a clearance rate of $N_{\text{robots}} / t_{\text{extraction}} \sim 2 \times 10^6$ robots/sec through both kidneys, or ~ 1 robot/sec through each capillary or afferent arteriole throughout the $t_{\text{extraction}} \sim 500 \text{ sec}$ extraction time.

Just to be clear: Nanorobots will *not* be moving into the urine in the same manner used by fluid leaving the blood, i.e., via the 70-100 nm wide holes or “fenestra” (image above, left). Rather, the robots will travel from the capillary lumen into Bowman's spaces by gently tunneling through temporary gaps opened between neighboring endothelial cells lining the capillary surface, using

⁵⁷³ Freitas RA Jr. Nanomedicine, Volume I: Basic Capabilities. Landes Bioscience, Georgetown, TX, 1999; Section 9.4.4, “Histonatation”; <http://www.nanomedicine.com/NMI/9.4.4.htm>.

⁵⁷⁴ [https://en.wikipedia.org/wiki/Glomerulus_\(kidney\)#Lining](https://en.wikipedia.org/wiki/Glomerulus_(kidney)#Lining).

⁵⁷⁵ <https://en.wikipedia.org/wiki/Podocyte>.

⁵⁷⁶ Scanning electron microscope view of the inner surface of an opened (broken) capillary with fenestrae visible (100,000x magnification); https://en.wikipedia.org/wiki/File:Inner_view_of_fenestrae_in_capillary_of_glomerulus_in_Scanning_Electron_Microscope_magnification_100,000x.GIF.

⁵⁷⁷ <https://en.wikipedia.org/wiki/Braille>.

⁵⁷⁸ If necessary, other methods for uniquely identifying the endothelium might include (1) cell surface markers (e.g., podocalyxin, VEGF receptors, or eNOS), (2) a decrease in measured blood flow or a pressure gradient indicative of glomerular filtration, or (3) detection of higher oxygen tension in the glomerulus than in other parts of the nephron.

techniques similar to diapedesis⁵⁷⁹ and locomotion through intercellular spaces⁵⁸⁰ as commonly employed by phagocytes⁵⁸¹ and bacteria⁵⁸² in the human body. (Phagocytic cells have been indirectly observed to traverse the glomerular filtration barrier under specific pathological conditions,⁵⁸³ and in rare cases motile organisms like *Leptospira*⁵⁸⁴ or *Borrelia*⁵⁸⁵ may actively migrate through fenestrations or damaged glomerular filtration membrane using flagellar motility and enzymes like hyaluronidases.) Each endothelial cell in a renal corpuscle has a luminal area of $A_{\text{renalEC}} \sim 50\text{-}200 \mu\text{m}^2$, (vs. only $V_{\text{nanorobot}}^{2/3} \sim 4.64 \mu\text{m}^2$ for a nanorobot), so there are $N_{\text{glomEC}} \sim A_{\text{glom}} / A_{\text{renalEC}} \sim 20\text{-}80 \times 10^9$ endothelial cells in both kidneys, through which only $N_{\text{robots}} \sim 10^9$ nanorobots must pass.

A few navigational complexities must be noted. All of the paths leading from the penile helicine arteries to the cavernosal, internal pudendal, internal iliac, and common iliac arteries into the abdominal aorta involve movement from smaller to larger diameter vessels with progressively increasing blood velocities, so nanorobots monitoring these parameters in the vessels through which they pass should not get lost at intervening junctions if they continue moving continuously upstream. However, once in the abdominal aorta, the robots know that the entry to the two renal arteries lies 20-25 cm further upstream, but there are three other possibly-distracting renal-adjacent arteries that branch off from the aorta – the superior mesenteric artery (1-2 cm

⁵⁷⁹ Freitas RA Jr. Nanomedicine, Volume I: Basic Capabilities. Landes Bioscience, Georgetown, TX, 1999, Section 9.4.4.1, “Nanorobot Diapedesis”; <http://www.nanomedicine.com/NMI/9.4.4.1.htm>.

⁵⁸⁰ Freitas RA Jr. Nanomedicine, Volume I: Basic Capabilities. Landes Bioscience, Georgetown, TX, 1999; Section 9.4.4.2, “ECM Brachiation”; <http://www.nanomedicine.com/NMI/9.4.4.2.htm>.

⁵⁸¹ https://en.wikipedia.org/wiki/Leukocyte_extravasation.

⁵⁸² <https://en.wikipedia.org/wiki/Shigella#Pathogenesis>.

⁵⁸³ Kimura M, Nagase M, Hishida A, Honda N. Intramesangial passage of mononuclear phagocytes in murine lupus glomerulonephritis. Am J Pathol. 1987 Apr;127(1):149-56; <https://pmc.ncbi.nlm.nih.gov/articles/PMC1899589/pdf>.

⁵⁸⁴ Amatredjo A, Campbell RS, Trueman KF. A study of nephritis of beef cattle in North Queensland. Aust Vet J. 1976 Sep;52(9):398-402; <https://pubmed.ncbi.nlm.nih.gov/1016164/>. Dierauf LA, Vandenbroek DJ, Roletto J, Koski M, Amaya L, Gage LJ. An epizootic of leptospirosis in California sea lions. J Am Vet Med Assoc. 1985 Dec 1;187(11):1145-8; <https://pubmed.ncbi.nlm.nih.gov/4077625/>. Scialfa E, Brihuega B, Venzano A, Morris WE, Bolpe J, Schettino M. First isolation of *Leptospira interrogans* from *Lycalopex griseus* (South American gray fox) in Argentina shows new MLVA genotype. J Wildl Dis. 2013 Jan;49(1):168-72; <https://pubmed.ncbi.nlm.nih.gov/23307384/>. Silva F, Brandão M, Esteves A. A Rare Presentation of Leptospirosis. Eur J Case Rep Intern Med. 2016 Aug 26;3(6):000447; <https://pmc.ncbi.nlm.nih.gov/articles/PMC6346843/pdf>. Hailat NQ, Mafrag ZA, Gharaibeh MH, Alzuheir IM. Pathological and molecular study of kidneys in apparently healthy cattle and sheep with special reference to *Leptospira* species in central and northern Jordan. Vet World. 2023 Dec;16(12):2488-2496; <https://pmc.ncbi.nlm.nih.gov/articles/PMC10844780/pdf>.

⁵⁸⁵ Kwiatkowska E, Golembiewska E, Ciechanowski K, Kędzierska K. Minimal-Change Disease Secondary to *Borrelia burgdorferi* Infection. Case Rep Nephrol. 2012;2012:294532; <https://pmc.ncbi.nlm.nih.gov/articles/PMC3914252/pdf>. Rolla D, Conti N, Ansaldo F, Panaro L, Lusenti T. Post-infectious glomerulonephritis presenting as acute renal failure in a patient with Lyme disease. J Renal Inj Prev. 2013 Nov 8;3(1):17-20; <https://pmc.ncbi.nlm.nih.gov/articles/PMC4206044/pdf>.

upstream), the gonadal arteries (0-2 cm upstream), and the inferior mesenteric artery (3-5 cm downstream) – that the nanorobots should avoid, in favor of the renal arteries, by monitoring:

(1) **Diameter differences.** The renal arteries typically have diameters of 4-6 mm while the gonadal arteries are much smaller (2-3 mm) and the superior and inferior mesenteric arteries are slightly larger (5-9 mm), so the robots could be programmed to recognize and follow arteries only in the 4-6 mm range, ignoring vessels outside this range.

(2) **Flow rate and blood velocity.** The blood flow rate and velocity in the renal arteries are relatively consistent due to the kidneys' constant need for filtration, whereas the superior and inferior mesenteric arteries may have more variable flow based on digestive processes, and the gonadal arteries also have much lower flow rates. Robots could measure flow dynamics to distinguish the renal artery from nearby vessels.

(3) **Endothelial cell markers.** The endothelial cells of the renal arteries may express unique markers related to kidney function, such as VEGF receptors, angiopoietin, and specific integrins that guide blood to the kidneys, whereas the mesenteric and gonadal arteries may express markers related to their target tissues (digestive organs or reproductive organs), allowing the device to detect surface molecules or proteins specific to those vascular regions and avoid them.

Once the nanorobots have correctly entered the renal artery, 90-95% of the blood flow eventually passes through the glomerular capillaries for filtration, but 5-10% of the blood entirely bypasses filtration. These non-glomerular pathways include a few small arterial branches from the main renal artery that carry non-glomerular blood, a few smaller arteries branching off from each of the several interlobar arteries that carry non-glomerular blood to the renal capsule and cortical tissues, and a few still smaller arteries that branch off from the arcuate and cortical radiate arteries that carry non-glomerular blood to the renal capsule, renal cortex, and renal medulla. These side branches may be detected (and avoided) by nanorobots perambulating along the primary arterial walls by:

(1) **Measuring vessel diameter.** Detect when the diameter narrows below a threshold to avoid entering smaller non-glomerular branches.

(2) **Analyzing blood flow patterns.** Use sensors to measure local blood flow rates. The nanorobot could identify non-glomerular vessels by detecting abnormally low or irregular flow.

(3) **Sampling blood chemistry.** Identify differences in solute concentrations, oxygen levels, or metabolic waste products, signaling non-glomerular pathways.

(4) **Detecting endothelial molecular markers.** Use molecular detection to identify endothelial cells lining the glomerular arterioles and capillaries based on specific filtration-related markers, helping distinguish them from non-glomerular pathways.

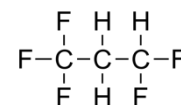
Uniformly distributing a fleet of $N_{\text{robots}} = 10^9$ nanorobots with total vascular contact area $A_{\text{fleet}} \sim N_{\text{robots}} V_{\text{nanorobot}}^{2/3} \sim 46 \text{ cm}^2$ over the total vascular wall surface area of $A_{\text{renalpath}} \sim 1331 \text{ cm}^2$, assuming a path travel time $t_{\text{renaltravel}} \sim 51\text{-}70 \text{ sec}$ during a $t_{\text{extraction}} \sim 500 \text{ sec}$ overall extraction period might seem to imply an average of only $ML_{\text{robots}} \sim (A_{\text{fleet}} / A_{\text{renalpath}}) (t_{\text{renaltravel}} / t_{\text{extraction}}) \sim 0.004\text{-}0.005$ monolayer coverage of robots over the entire vascular path and extraction time. However, the table above shows that most vessels comprising the vascular extraction path are

bottlenecked at monolayer coverages of $ML_{\text{robots}} \sim 0.01\text{-}0.1$, given the velocity and extraction parameters chosen.

5.3.1.7 Nanorobot Control

Once the nanorobots are properly emplaced in penile tissue, how do we control them? There are several classes of control tasks of interest. First, a user must be able to turn the robots on or off, quickly generating or extinguishing an erection, possibly repeatedly. Second, users may want to be able to order the robots to perform more complex coordinated activities, or alter their operating parameters while they are deployed inside the body. Third, a user must be able to command the robots to exit the body.

Turning the robots on or off, or commanding them to terminate all activities and exit the body, should require transmitting only a relatively few bits of information to the devices, even if the commands employ modest “password” type coding to prevent accidental or unintended messaging. A simple onboard timer could handle both these tasks but would lack flexibility once the robots are deployed. A more flexible approach might involve the inhalation of a biocompatible volatile artificial messenger molecule consisting of a digitally encoded hydrofluorocarbon⁵⁸⁶ (e.g., 1,1,1,3,3-pentafluoropropane, with H and F atoms representing “0” and “1”, respectively; image, right)⁵⁸⁷ whose unnatural presence in the bloodstream could be rapidly detected by chemical sensors on the nanorobots deployed in the penis, allowing the message to be quickly decoded and acted upon. Alternatively, the deeply-inhaled scent of a specific perfume or sexual partner might serve a similar function.



Robots deployed in the penis could also detect certain mechanical sounds generated by the user, such as a coded series of hand slaps applied to the buttocks or thighs.⁵⁸⁸ A hand of palm area $A_{\text{hand}} \sim 100 \text{ cm}^2$ and mass $m_{\text{hand}} \sim 0.4 \text{ kg}$ ⁵⁸⁹ that strikes skin at $v_{\text{slap}} \sim 1 \text{ m/sec}$ with a $t_{\text{slap}} \sim 0.1 \text{ sec}$ impact duration applies a pressure impulse of $p_{\text{slap}} \sim m_{\text{hand}} v_{\text{slap}} / t_{\text{slap}}$ $A_{\text{hand}} \sim 0.0040 \text{ atm}$ at a distance up to $x_{\text{slap}} \sim 30 \text{ cm}$ from penile-embedded nanorobots, which can detect a pressure wave (assumed planar) of amplitude $A_x \sim p_{\text{slap}} e^{-(\alpha v x_{\text{slap}})} \sim 0.0039 \text{ atm}$, taking the slap acoustic frequency $\nu \sim 1000 \text{ Hz}$ (range 100-3000 Hz) and amplitude absorption coefficient $\alpha \sim 8.3 \times 10^{-6}$

⁵⁸⁶ Freitas RA Jr. Nanomedicine, Volume I: Basic Capabilities. Landes Bioscience, Georgetown, TX, 1999; Section 7.2.1.1, “Ideal Messenger Molecule”; <http://www.nanomedicine.com/NMI/7.2.1.1.htm>.

⁵⁸⁷ <https://en.wikipedia.org/wiki/Pentafluoropropane>.

⁵⁸⁸ Freitas RA Jr. Nanomedicine, Volume I: Basic Capabilities. Landes Bioscience, Georgetown, TX, 1999; Section 7.4.2.1, “Mechanical Inmessaging”; <http://www.nanomedicine.com/NMI/7.4.2.1.htm>.

⁵⁸⁹ Ferrè ER, Joel J, Cadete D, Longo MR. Systematic underestimation of human hand weight. Curr Biol. 2023 Jul 24;33(14):R758-R759; <https://www.cell.com/action/showPdf?pii=S0960-9822%2823%2900673-5>.

sec/m for human soft tissue.⁵⁹⁰ This wave can be detected by *in vivo* nanorobots with an onboard acoustic sensor of volume $V_{\text{sensor}} \sim k_B T_{\text{body}} e^{\text{SNR}} / A_x \sim 0.02 \mu\text{m}^3$,⁵⁹¹ assuming a signal/noise ratio (SNR) ~ 10 , human body temperature $T_{\text{body}} = 310 \text{ K}$, and Boltzmann's constant $k_B = 1.38 \times 10^{-23} \text{ J/K}$. With the aid of an onboard clock, the nanorobots could count the number of slaps and detect pauses between each series of slaps, allowing the user to send numerically coded commands such as "123" to tumesce the penis, "321" to de-tumesce, and so forth. The clapping of hands⁵⁹² or a hand-held vibrator appliance⁵⁹³ with programmable waveforms and digital encoding that is briefly applied to the groin or abdomen could serve a similar function.

Ordering the robots to perform more complex or coordinated activities, or altering their operating parameters after deployment inside the body, requires the ability to transmit information-rich signals into the body that the nanorobots can hear and decode. The simplest method would probably involve using a modified cell phone with an innocuous ultrasound speaker attachment, permitting transmission of high-frequency ultrasound commands,⁵⁹⁴ probably in the 0.1-1 MHz range that lies well beyond human hearing. Complex commands or parameter adjustments could be generated via a user-friendly interface and transmitted into the body by pressing the phone against the skin.⁵⁹⁵

A billion mechanically active remote-controlled nanorobots loaded into a penis could perform several additional interesting physical tasks. Robots that can exchange messages acoustically because they lie within $\sim 100 \mu\text{m}$ of each other in the penile tissue,⁵⁹⁶ or because they are in physical contact with their neighbors through "communicating junctions" on their perimeters,⁵⁹⁷ can display various coordinated activities. For example, they could alter the penile inflationary pattern to express specific patterns of bumps or ridges on the surface of the penis, analogous to those found on the exteriors of ribbed condoms⁵⁹⁸ that are said to provide extra pleasure for one's

⁵⁹⁰ Freitas RA Jr. Nanomedicine, Volume I: Basic Capabilities. Landes Bioscience, Georgetown, TX, 1999; Table 4.2 in Section 4.9.1.3, "Respiratory Audition"; <http://www.nanomedicine.com/NMI/4.9.1.3.htm>.

⁵⁹¹ Freitas RA Jr. Nanomedicine, Volume I: Basic Capabilities. Landes Bioscience, Georgetown, TX, 1999; Section 4.5.1, "Minimum Detectable Pressure"; <http://www.nanomedicine.com/NMI/4.5.1.htm>.

⁵⁹² https://en.wikipedia.org/wiki/The_Clapper.

⁵⁹³ [https://en.wikipedia.org/wiki/Vibrator_\(sex_toy\)](https://en.wikipedia.org/wiki/Vibrator_(sex_toy)).

⁵⁹⁴ Freitas RA Jr. Nanomedicine, Volume I: Basic Capabilities. Landes Bioscience, Georgetown, TX, 1999; Section 7.2.2, "Acoustic Broadcast Communication"; <http://www.nanomedicine.com/NMI/7.2.2.htm>.

⁵⁹⁵ Freitas RA Jr. Nanomedicine, Volume I: Basic Capabilities. Landes Bioscience, Georgetown, TX, 1999; Section 6.4.1, "Acoustic Power Transmission"; <http://www.nanomedicine.com/NMI/6.4.1.htm>.

⁵⁹⁶ Freitas RA Jr. Nanomedicine, Volume I: Basic Capabilities. Landes Bioscience, Georgetown, TX, 1999; Section 7.2.2.2, "Free-Tissue Acoustic Channel Capacity"; <http://www.nanomedicine.com/NMI/7.2.2.2.htm>.

⁵⁹⁷ Freitas RA Jr. Nanomedicine, Volume I: Basic Capabilities. Landes Bioscience, Georgetown, TX, 1999; Section 5.4.2, "Transbumper Communication"; <http://www.nanomedicine.com/NMI/5.4.2.htm>.

⁵⁹⁸ https://en.wikipedia.org/wiki/Condom#Ribbed_and_studded.

partner. Bumpered robots in the sinusoids (Section 5.3.1.3) could adjust the inflation levels of neighboring sinusoids of diameter $2R_{\text{sinusoid}} \sim 1.76 \text{ mm}$, thus creating features at or below the 5-10 mm limit of tactile spatial resolution for the penile skin or the vaginal wall, with the specific pattern, depth and spacing of features all under user control. More complexly, these surface patterns could be made to vary over time to create traveling waves, e.g., including vibrations at the specific acoustic frequencies most likely to induce orgasms in women,⁵⁹⁹ or at higher frequencies that provide a buzzing sensation⁶⁰⁰ analogous to vibrator sex toys.⁶⁰¹ The nanorobots could also collectively exhibit dynamic behaviors in which the patterns and movements are altered in response to stimuli such as temperature, stress, or the bending and compressive forces that are transmitted through the penile tissues during copulation. Nanorobots in the penis could also detect the users pulse rate⁶⁰² or the melody of ejaculation and other copulatory sounds,⁶⁰³ and modify their behavior accordingly.

⁵⁹⁹ According to sexual lore, * in 1992 a car dealer in Daytona Beach, FL, organized an experiment to find the most “stimulating” frequency using a tone generator and an in-car sub woofer, and determined that the ideal clitoral resonant frequency most likely to trigger female orgasms averaged at 33 Hz. Subsequent animal studies confirmed that pelvic nerve stimulation at 32 Hz caused significantly increased clitoral blood flow in female New Zealand White rabbits.[†] The physiological basis for the response, finally discovered in 2024,[‡] appears to be tiny sensory cells called Krause corpuscles that are present in the human and animal clitoris and act as genital vibration detectors. These cells are present at $\sim 1500 \text{ cells/mm}^3$ in the clitoris, have a mechanical stimulation threshold of only 1-10 mN, and have optimal sensitivity to 40-80 Hz mechanical vibrations, most especially in the low-frequency end of the range.

* e.g., see <https://www.youtube.com/watch?v=oLKIQ55P-es>, and many mentions in Playboy magazine.

[†] Min K, Munarriz R, Berman J, Kim NN, Goldstein I, Traish AM, Stankovic MR. Hemodynamic evaluation of the female sexual arousal response in an animal model. *J Sex Marital Ther.* 2001 Oct-Dec;27(5):557-65; <https://pubmed.ncbi.nlm.nih.gov/11554219/>.

[‡] Qi L, Iskols M, Greenberg RS, Xiao JY, Handler A, Liberles SD, Ginty DD. Krause corpuscles are genital vibrotactile sensors for sexual behaviours. *Nature.* 2024 Jun;630(8018):926-934; <https://www.nature.com/articles/s41586-024-07528-4.pdf>.

⁶⁰⁰ A selection of vibrators commonly employed for sexual stimulation were measured to produce average displacements of $37\text{--}783 \mu\text{m}$ and mechanical accelerations of $18\text{--}311 \text{ m/sec}^2$ at vibratory frequencies ranging from 43-148 Hz. Prause N, Roberts V, Legarretta M, Cox LMR. Clinical and research concerns with vibratory stimulation: a review and pilot study of common stimulation devices. *Sexual and Relationship Therapy*, 2012 Feb12;27(1):17-34; <https://citeseerx.ist.psu.edu/document?repid=rep1&type=pdf&doi=c8994948355c2c08a1fb818b7bf195f08f11d5f2>.

⁶⁰¹ [https://en.wikipedia.org/wiki/Vibrator_\(sex_toy\)](https://en.wikipedia.org/wiki/Vibrator_(sex_toy)).

⁶⁰² Freitas RA Jr. *Nanomedicine, Volume I: Basic Capabilities*. Landes Bioscience, Georgetown, TX, 1999; Section 4.9.1.2, “Blood Pressure and Pulse Detection”; <http://www.nanomedicine.com/NMI/4.9.1.2.htm>.

⁶⁰³ Freitas RA Jr. *Nanomedicine, Volume I: Basic Capabilities*. Landes Bioscience, Georgetown, TX, 1999; Section 4.9.1.4, “Mechanical Body Noises”; <http://www.nanomedicine.com/NMI/4.9.1.4.htm>.

5.3.2 Nanorobotic Stimulation of Sexual Arousal in Men (Lustbots)

Traditionally, an aphrodisiac is a substance alleged to increase libido, sexual desire, sexual attraction, sexual pleasure, or sexual behavior, including both psychological and physiological effects.⁶⁰⁴ Nanorobots will be able to influence neural pathways by directly detecting,⁶⁰⁵ then stimulating or suppressing action potentials in specific nerves or groups of nerves,⁶⁰⁶ and can inject or extract specific hormones or other biologically active biochemicals into specific neural cells or groups of cells.⁶⁰⁷ A coordinated fleet of such nanaphrodisiac nanorobots, aka. “lustbots”, should be able to artificially create powerful subjective sensations and physiological expressions of sexual arousal in a human male, even in the absence of traditional external tactile, olfactory, auditory, or visual stimuli that would typically induce sexual arousal in a human male – e.g., a eurythmic female body shape with superior callipygean, bathyclopian, and calliskelous endowments. We outline the physiological requirements ([Section 5.3.2.1](#)), technical details ([Section 5.3.2.2](#)), and some aspects of nanorobotic lust control for men ([Section 5.3.2.3](#)) and women ([Section 5.3.2.4](#)), then briefly describe the alternative of virtual orgasms ([Section 5.3.2.5](#)).

5.3.2.1 Physiological Requirements

A region of the hypothalamus called the **Medial Preoptic Area (mPOA)**⁶⁰⁸ is where male “appetitive” sexual arousal originates.⁶⁰⁹ There are two mPOAs in the brain, one on each side of the bilaterally symmetrical hypothalamus. The mPOA integrates a wide variety of sensory and physiological inputs that are crucial for sexual behavior and arousal, including:

(1) **hormonal** inputs, such as testosterone and aromatized testosterone (converted into estradiol) that bind to intracellular receptors in the mPOA, and oxytocin and vasopressin (involved in social bonding and sexual behavior)⁶¹⁰ that can modulate mPOA activity;

(2) **sensory** inputs, such as (A) odor-related information from the olfactory bulb, (B) somatosensory signals from the genital region through the spinal cord via the **Periaqueductal Gray (PAG)**⁶¹¹ and the brainstem that carry tactile sensory information during sexual activity, and (C) visual and auditory signals containing cues that are perceived as sexually relevant; and

⁶⁰⁴ <https://en.wikipedia.org/wiki/Aphrodisiac>.

⁶⁰⁵ Freitas RA Jr. Nanomedicine, Volume I: Basic Capabilities. Landes Bioscience, Georgetown, TX, 1999; Section 4.8.6, “Noninvasive Neuroelectric Monitoring”; <http://www.nanomedicine.com/NMI/4.8.6.htm>.

⁶⁰⁶ Freitas RA Jr. Nanomedicine, Volume I: Basic Capabilities. Landes Bioscience, Georgetown, TX, 1999; Section 7.4.5.6, “Outmessaging to Neurons”; <http://www.nanomedicine.com/NMI/7.4.5.6.htm>.

⁶⁰⁷ Freitas RA Jr. Nanomedicine, Volume I: Basic Capabilities. Landes Bioscience, Georgetown, TX, 1999; Section 7.4.5.3, “Outmessaging to Cells”; <http://www.nanomedicine.com/NMI/7.4.5.3.htm>.

⁶⁰⁸ https://en.wikipedia.org/wiki/Preoptic_area#Medial_preoptic_nucleus.

⁶⁰⁹ https://en.wikipedia.org/wiki/Sexually_dimorphic_nucleus.

⁶¹⁰ https://en.wikipedia.org/wiki/Effects_of_hormones_on_sexual_motivation#Oxytocin_and_vasopressin.

⁶¹¹ https://en.wikipedia.org/wiki/Periaqueductal_gray.

(3) **neural** inputs from the amygdala⁶¹² (which processes emotional and social cues, including sexual motivation and fear or anxiety), the **Bed Nucleus of the Stria Terminalis (BNST)**⁶¹³ that conveys stress and anxiety signals, and components of the limbic system like the hippocampus⁶¹⁴ and other parts of the hypothalamus,⁶¹⁵ both of which modulate the mPOA's role in sexual behavior.

Once activated, the mPOA sends signals to various parts of the brain and body to initiate and regulate sexual behavior, collectively constituting the experience of sexual arousal, including:

(1) **Ventral Tegmental Area (VTA)**. The mPOA projects to the VTA, influencing dopamine release and modulating the rewarding aspects of sexual behavior. (By “projection”, we mean neurons in the sending region that have long extensions (axons) that reach and form synapses (connections) with neurons in the receiving region.) The VTA sends dopaminergic⁶¹⁶ projections to the **Nucleus Accumbens (NAc)**,⁶¹⁷ facilitating the sensation of pleasure and reward that reinforces sexual behavior and arousal. Dopamine release in the **Prefrontal Cortex (PFC)**⁶¹⁸ helps modulate cognitive control, decision-making, and the regulation of impulsive behaviors during sexual arousal, and the dopamine release affects emotional processing, especially concerning sexual stimuli, in the amygdala. The VTA also affects the hippocampus, influencing memory and learning processes that reinforce the rewarding aspects of sexual experiences.

(2) **Spinal Cord**. The mPOA communicates with neurons in the spinal cord (especially at the sacral spinal cord, S2-S4) to regulate the parasympathetic nerves that control genital blood flow and erection. The mPOA also sends signals to the thoracolumbar spinal cord (T10-L2) to control ejaculation through sympathetic nerves.

(3) **Periaqueductal Gray (PAG)**. The mPOA projects to the PAG to control autonomic responses associated with sexual arousal (heart rate, blood pressure, and breathing) as well as defensive behaviors. This is crucial for balancing arousal with anxiety.

(4) **Lateral Hypothalamus**. The mPOA communicates with the lateral hypothalamus⁶¹⁹ to regulate feeding and arousal states, which are closely linked.

(5) **Amygdala and BNST**. The mPOA sends feedback to these regions, further modulating emotional responses related to sexual behavior.

Stimulating the mPOA alone should initiate and sustain the majority of the physiological and sensory aspects of sexual arousal, particularly the neural pathways and autonomic responses.

⁶¹² <https://en.wikipedia.org/wiki/Amygdala#Function>.

⁶¹³ https://en.wikipedia.org/wiki/Stria_terminalis#Bed_nucleus_of_the_stria_terminalis.

⁶¹⁴ <https://en.wikipedia.org/wiki/Hippocampus>.

⁶¹⁵ <https://en.wikipedia.org/wiki/Hypothalamus>.

⁶¹⁶ <https://en.wikipedia.org/wiki/Dopaminergic>.

⁶¹⁷ https://en.wikipedia.org/wiki/Nucleus_accumbens#Reward_and_reinforcement.

⁶¹⁸ https://en.wikipedia.org/wiki/Prefrontal_cortex#Executive_function.

⁶¹⁹ https://en.wikipedia.org/wiki/Lateral_hypothalamus#Function.

However, to fully replicate the complex experience of every aspect of sexual arousal, including all of the pleasurable sensations, emotional components, and motivational drives, modulating other areas like the VTA, NAc, and emotional centers (e.g., the amygdala) might further enhance the effect.

Finally, to maximize and sustain the artificial arousal it might also be useful to suppress several inhibitory factors such as:

(1) **Serotonin**. Serotonin⁶²⁰ can either inhibit or facilitate sexual behavior depending on its levels and the receptors it interacts with. Reducing serotonin activity in certain brain regions like the lateral hypothalamus (where it inhibits sexual function) could remove barriers to arousal.

(2) **Prolactin**. Elevated prolactin levels are associated with reduced sexual desire post-orgasm,⁶²¹ so suppressing prolactin during the period of arousal would prevent the post-orgasmic refractory period and help maintain sexual motivation.

(3) **Adrenaline and Cortisol**. The adrenal glands produce adrenaline⁶²² and other stress-related hormones.⁶²³ Lowering adrenaline and cortisol⁶²⁴ levels could reduce stress and anxiety, promoting a more relaxed state conducive to arousal.

(4) **Amygdala**. Certain regions tied to anxiety⁶²⁵ or inhibition could be suppressed.

5.3.2.2 Technical Details

Each mPOA (Medial Preoptic Area) in humans is a small structure with a volume of about 1-2 mm³ and a mass of around 1-2 mg, with the two mPOAs containing a total of 200,000 to 500,000 neurons with an average neuronal size of 10-20 µm in diameter and volume $V_{\text{neuron}} \sim 10,000 \mu\text{m}^3$. To elicit an artificial arousal state, let's consider an input simulant approach in which resident nanorobots stimulate all relevant input channels leading into the mPOA, triggering the mPOA to produce its normal arousal response. Nanorobots would need to artificially generate all normal hormonal, sensory, and neural inputs to the mPOA that occur during sexual arousal, as follows:

* For the **artificial hormonal inputs**, testosterone binds to free-floating intracellular receptors that translocate to the cell nucleus and alter gene expression in the cell (a relatively slow response), whereas oxytocin and vasopressin bind to neuron membrane-bound receptors, modulating the ion channels and increasing the neuron's action potential firing rate (a relatively rapid response). To obtain a "natural" response, testosterone in estimated concentrations of $c_{\text{testo}} \sim 3\text{-}10 \mu\text{g/L}$ should be applied to the 20-40% of mPOA neurons ($N_{\text{testo}} \sim 40,000\text{-}200,000$ cells), probably mostly concentrated in the **Sexually Dimorphic Nucleus (SDN)**⁶²⁶ within the mPOA

⁶²⁰ https://en.wikipedia.org/wiki/Serotonin#Biological_role.

⁶²¹ https://en.wikipedia.org/wiki/Prolactin#In_humans.

⁶²² https://en.wikipedia.org/wiki/Adrenaline#Emotional_responses.

⁶²³ https://en.wikipedia.org/wiki/Stress_hormone.

⁶²⁴ <https://en.wikipedia.org/wiki/Cortisol#Stress>.

⁶²⁵ <https://en.wikipedia.org/wiki/Amygdala#Anxiety>.

⁶²⁶ https://en.wikipedia.org/wiki/Sexually_dimorphic_nucleus.

that is particularly sensitive to testosterone, that cytosolically express androgen or estrogen receptors or which exhibit axonal projections to regions like the VTA, NAc, and PAG. A single dose should produce effects in gene expression that can persist for days, amounting to $m_{\text{testo}} \sim c_{\text{testo}} V_{\text{neuron}} \sim 3 \times 10^{-17} \text{ gm/nanorobot}$ or $m_{\text{testo}}/\rho_{\text{testo}} \sim 0.3\text{--}1 \times 10^{-4} \mu\text{m}^3/\text{nanorobot}$, assuming one nanorobot per neuron and testosterone density $\rho_{\text{testo}} \sim 1 \text{ gm/cm}^3$. Oxytocin and vasopressin probably must be applied at concentrations at least 10 times higher than the 1-10 ng/L baseline circulating levels, or $c_{\text{oxyvaso}} \sim 0.2 \mu\text{g/L}$ for both hormones, on the 5-20% of mPOA neurons ($N_{\text{oxyvaso}} \sim 5,000\text{--}20,000$ cells) that express OXTR and AVPR receptors on their plasma membranes or which exhibit axonal projections to regions like the VTA and NAc. The duration of effectiveness is several minutes to hours, so we'll assume a capacity for administering up to $n_{\text{oxyvaso}} \sim 100$ doses to maintain sexual arousal over multiple hours, hence the dosage per nanorobot for both hormones is $m_{\text{oxyvaso}} \sim n_{\text{oxyvaso}} c_{\text{oxyvaso}} V_{\text{neuron}} \sim 2 \times 10^{-16} \text{ gm/nanorobot}$ or $m_{\text{oxyvaso}}/\rho_{\text{oxyvaso}} \sim 2 \times 10^{-4} \mu\text{m}^3/\text{nanorobot}$, assuming one nanorobot per neuron and hormone density $\rho_{\text{oxyvaso}} \sim 1 \text{ gm/cm}^3$. The volume of all three hormones that must be carried onboard a lustbot represents a minuscule $\sim 0.01\%$ of the volume of a $V_{\text{nanorobot}} \sim 10 \mu\text{m}^3$ nanorobot. A total of $N_{\text{hormone}} \sim N_{\text{testo}} + N_{\text{oxyvaso}} \sim 200,000$ nanorobots are required to execute the mission.

* For the **artificial sensory inputs**, sensory inputs to the mPOA related to sexual arousal are transmitted via nerve connections (axons), and the signals are received at synapses on neurons within the mPOA that allow sensory information (olfactory,⁶²⁷ somatosensory,⁶²⁸ visual⁶²⁹ and auditory⁶³⁰ cues) to be integrated into the neuronal circuits in the mPOA. There are likely up to a billion sensory-related synaptic connections throughout the SDN and other regions of the mPOA, but the number of pre-synaptic axons entering the mPOA for sensory processing is likely in the range of tens to hundreds of thousands, so a reasonable estimate is that we will require up to $N_{\text{sensory}} \sim 200,000$ nanorobots positioned on or within axons, if one nanorobot per axon is sufficient to provide the $\sim 50 \text{ pW}$ required to artificially trigger and maintain the requisite action potentials in each axon ([Section 5.3.3.1](#)), well within the capacity of an individual nanorobot.⁶³¹

⁶²⁷ **Odor-related** information passes through axons from the olfactory bulb to regions of the mPOA that integrate information from the amygdala and other limbic structures. The synaptic inputs from the amygdala and hypothalamic areas form direct synapses with neurons in the mPOA.

⁶²⁸ Sensory neurons from the genital region carry **tactile** information through the dorsal root ganglia of the spinal cord to the sacral spinal cord (S2-S4), which is then relayed through ascending pathways to the brainstem and the PAG, both of which pass the information through axons to the mPOA, where action potentials are converted into chemical signals at synapses in the mPOA.

⁶²⁹ **Visual** inputs are processed through the retina, which sends signals to the visual cortex, from which sexually relevant visual stimuli are relayed to the amygdala, hippocampus, and prefrontal cortex, which process emotional and motivational aspects of the stimuli and then pass the information through axons to the mPOA.

⁶³⁰ **Auditory** inputs, like vocalizations or sounds related to sexual activity, are processed through the auditory cortex and similarly relayed to the amygdala and hippocampus, which process their emotional significance and relay the information via axonal pathways to the mPOA.

⁶³¹ For example, the maximum power output of a $\sim 12 \mu\text{m}^3$ microbivore (which was not optimized for action potential generation) has been estimated as $\sim 200 \text{ pW}$. Freitas RA Jr. Microbivores: Artificial mechanical

Note that an artificially triggered action potential in the middle of a pre-synaptic axon can propagate in both directions, including backward toward the neuron's cell body. However, this retrograde propagation usually doesn't cause major complications because the cell body and dendrites are not involved in action potential generation, and because the neuron's structural and physiological properties often minimize any negative effects of backward action potentials. In most cases, the desired forward (anterograde) propagating synaptic outputs would occur without disruption, but careful placement of stimulation and understanding of refractory periods can help prevent any unintended backflow.

The sensation of continuous sexual arousal under intermittent stimulation of sensory neurons depends on how the brain integrates the incoming sensory signals over time. Neuronal circuits involved in arousal, including those in the mPOA and SDN, are capable of temporal integration of sensory inputs, meaning that they can sustain a physiological and psychological state of arousal even if the sensory inputs are not continuous. The brain can integrate episodic sensory signals and maintain a sustained state of arousal for some time even after the sensory input stops, because arousal involves neural plasticity and ongoing hormonal signaling (e.g., testosterone, oxytocin) that continue to influence the brain even in the absence of direct sensory input. Neurons in the mPOA and SDN exhibit aftereffects following activation, meaning that once sensory pathways are stimulated, the neurons can remain active for a period even after the stimulus ends. The brain's reward circuitry, particularly involving the VTA and NAc, can also sustain sexual motivation and arousal once activated. Refractory periods occur naturally: Natural sensory inputs during sexual arousal do not occur in a perfectly continuous stream, with normal fluctuations in sensory input intensity (e.g., tactile stimulation during sexual activity). The brain is accustomed to processing this intermittent input. As a result, a sensory stimulation with a 10% duty cycle in which action potentials are triggered at 10-50 Hz for only 1 second every 10 seconds should produce a continuous sensation of arousal since the 1 second of activation is enough to sustain the arousal circuits for many seconds afterward.

* For the **artificial neural inputs**, the amygdala probably sends several tens of thousands of axons to the mPOA, originating primarily from the medial and central nuclei of the amygdala, following the amygdalofugal pathway.⁶³² The mPOA also receives thousands to tens of thousands of axons from the ventral BNST and dorsal BNST and thousands of axons from the ventral regions of the hippocampus and from the ventromedial hypothalamus and other hypothalamic nuclei. This implies a requirement for up to $N_{\text{neural}} \sim 100,000$ nanorobots positioned on or within these neural input axons, again assuming that one nanorobot per axon is sufficient to artificially trigger the requisite action potentials in each axon.

The above analysis suggests that a total of $N_{\text{stim}} = N_{\text{hormone}} + N_{\text{sensory}} + N_{\text{neural}} \sim 500,000$ nanorobots, if properly positioned along the correct axons at pre-synaptic positions, should suffice to artificially generate all the hormonal, sensory, and neural inputs to the mPOA that

phagocytes using digest and discharge protocol. J Evol Technol 2005;14:1-52;
<http://www.jetpress.org/volume14/freitas.html>.

⁶³² https://en.wikipedia.org/wiki/Amygdalofugal_pathway.

would normally occur during natural sexual arousal,⁶³³ even in the complete absence of organically produced normal inputs.

It should be noted that there may be an estimated ~300,000 axons that promote sexual arousal, ~20,000 axons that inhibit sexual arousal,⁶³⁴ and ~10,000 axons involved purely in non-arousal functions,⁶³⁵ projecting into the mPOA. In the simplest scenario where all mPOA-entering axons are stimulated without regard to function, the outcome would likely be a sensation of sexual arousal, because the excitatory inputs related to arousal (~300,000 axons) vastly outnumber the inhibitory inputs. The inhibitory signals (~20,000 axons) would likely dampen the intensity of the arousal but not extinguish it, while the non-arousal inputs (~10,000 axons) would have minimal direct effect on arousal but might engage other unrelated physiological processes. Side effects might include mixed physiological responses in which the individual feels aroused but also experiences conflicting sensations like stress or anxiety, or just a less coherent experience of arousal due to the simultaneous activation of arousal and inhibitory inputs.

If the nanorobots can identify and avoid artificially stimulating any inhibitory mPOA-terminating axons that originate in the BNST, amygdala, or PAG, the result would be a stronger and more natural sensation of sexual arousal.⁶³⁶ Axons from each of these inhibitory sources possess membrane and cytosolic molecular markers that may allow a nanorobot equipped with the appropriate surface-sensing⁶³⁷ and cytosolic-sampling⁶³⁸ mechanisms to distinguish them from

⁶³³ An alternative strategy in which resident nanorobots are positioned in all of the output structures of the mPOA and artificially generate false output signals of the requisite strength and pattern to duplicate a normal arousal response, but without directly triggering activity from the mPOA, would likely require a similarly sized nanorobot fleet.

⁶³⁴ These would include specific axons originating in the bed nucleus of the stria terminalis or BNST (inhibits the mPOA in response to stress, anxiety, or fear, requiring survival-related behaviors), amygdala (inhibits the mPOA in response to stress or threatening stimuli), periaqueductal gray or PAG (inhibits arousal in response to aversive stimuli such as pain or when defensive behaviors are triggered), and lateral hypothalamus or LH (inhibits the mPOA when feeding behavior is prioritized over reproductive behavior).

⁶³⁵ These would include specific axons originating in the VTA, NAc and other parts of the hypothalamus that regulate maternal and parental behaviors, and in the reticular formation and other parts of the hypothalamus that control thermoregulation.

⁶³⁶ In the extreme case where nanorobots actively **suppress*** action potentials in mPOA-terminating axons that originate in the BNST, amygdala, or PAG, excluding all inhibitory inputs might make the sexual arousal feel unnaturally strong, leading to an intense but less regulated arousal response which could feel overwhelming or uncontrolled. The exclusion of inhibitory signals could also lead to an extended period of arousal, as there would be less feedback to reduce or stop the arousal.

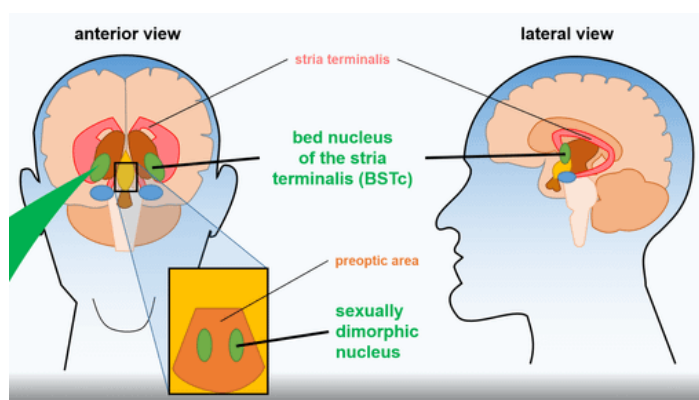
* Freitas RA Jr. Nanomedicine, Volume I: Basic Capabilities. Landes Bioscience, Georgetown, TX, 1999; Section 7.4.5.4, "Cell Message Modification"; <http://www.nanomedicine.com/NMI/7.4.5.4.htm>; and Section 7.4.5.6, "Outmessaging to Neurons"; <http://www.nanomedicine.com/NMI/7.4.5.6.htm>.

⁶³⁷ Freitas RA Jr. Nanomedicine, Volume I: Basic Capabilities. Landes Bioscience, Georgetown, TX, 1999; Section 4.2.8, "Chemotactic Sensor Pads"; <http://www.nanomedicine.com/NMI/4.2.8.htm>; and Section 4.2.9, "Receptor Sensors"; <http://www.nanomedicine.com/NMI/4.2.9.htm>.

axons originating from other sources. Specifically, BNST-originating axonal membranes express corticotropin-releasing hormone (CRHR1) receptors and vasopressin (V1aR) receptors, and axonal cytosol may express corticotropin-releasing factor (CRF) and neurotensin. Amygdala-originating axonal membranes express oxytocin (OXTR) receptors and vasopressin (V1aR) receptors, and axonal cytosol may express gamma-aminobutyric acid (GABA), GABAergic markers such as glutamate decarboxylase (GAD65/67), and corticotropin-releasing factor (CRF). PAG-originating axonal membranes express mu-opioid (MOR) receptors and cannabinoid (CB1) receptors, and axonal cytosol may express enkephalin peptides and tryptophan hydrolase (TPH). (Neurotransmitter receptors are commonly found on the plasma membranes of dendrites, cell bodies, and synaptic sites, but not generally on axons, making these markers harder for the nanorobots to find.)

Focusing the artificial stimulation on just the sexually dimorphic nucleus (SDN)⁶³⁹ within the mPOA would produce an even stronger and more natural sexual arousal response with fewer side effects, since the SDN is specialized for sexual behavior, and might allow using a smaller nanorobot fleet.

There are an estimated 50,000-100,000 axons in each of the left and right human SDNs (image, right). An SDN-focused nanophrodisiac medication might be introduced into the body via a simple nose spray. An infusion of $N_{\text{stim}} \sim 500,000$ nanorobots, each of volume $V_{\text{nanorobot}} \sim 10 \mu\text{m}^3$, represents a dosage volume of $V_{\text{dosage}} = N_{\text{stim}} V_{\text{nanorobot}} \sim 0.005 \text{ mm}^3$ which is only $\sim 0.01\%$ of the typical single-dose 25-100 microliter output volume of a commonplace metered-dose asthma inhaler. The nasal cavity is highly vascularized, allowing efficient transfer of drugs directly to



⁶³⁸ Freitas RA Jr. Nanomedicine, Volume I: Basic Capabilities. Landes Bioscience, Georgetown, TX, 1999; Section 8.5.3.12, "Cytonavigational Issues"; <http://www.nanomedicine.com/NMI/8.5.3.12.htm>. Freitas RA Jr. The ideal gene delivery vector: Chromalloyocytes, cell repair nanorobots for chromosome replacement therapy. J Evol Technol 2007;16:1-97; Section 6.1, "Proliferating Cells"; <http://jetpress.org/v16/freitas.pdf>. Freitas RA Jr. Chapter 23. Comprehensive Nanorobotic Control of Human Morbidity and Aging. In: Fahy GM, West MD, Coles LS, Harris SB, eds, The Future of Aging: Pathways to Human Life Extension, Springer, New York, 2010; Section 23.6.4.4, "Modifying Cellular Controls and Cycles"; Section 23.6.4.6, "Organelle Testing, Replacement, or Repair"; and Section 23.6.4.8, "Intracellular Environmental Maintenance"; <http://www.nanomedicine.com/Papers/Aging.pdf>. Freitas RA Jr. The Alzheimer Protocols: A Nanorobotic Cure for Alzheimer's Disease and Related Neurodegenerative Conditions. IMM Report No. 48, June 2016; Section 5.2.2, "Remove Intracellular Aggregates"; <http://www.imm.org/Reports/rep048.pdf>. Freitas RA Jr. Cryostasis Revival: The Recovery of Cryonics Patients through Nanomedicine. Alcor Life Extension Foundation, Scottsdale AZ, 2022; Section 4.10, "Molecular Extraction"; and Section 4.12.2.1, "Preliminary Cell Inspection and Small Debris Cleanup"; <https://www.alcor.org/cryostasis-revival/>.

⁶³⁹ https://en.wikipedia.org/wiki/Sexually_dimorphic_nucleus.

the nervous system.⁶⁴⁰ More importantly, the intranasal delivery method has already been used to transport large mesenchymal stem cells, 8-20 μm in size, into the brain with transit times ranging from a few hours to a few days,⁶⁴¹ entirely bypassing the blood-brain barrier (BBB),⁶⁴² so this method appears sufficient to accommodate the passage of a medical nanorobot measuring several microns in size that is attempting to enter the brain.

Other methods for safe nanorobot ingress to (and egress from) the brain have been detailed elsewhere.⁶⁴³ For example, vasculomobile nanorobots such as the vasculocyte could walk the vascular walls from an entry point in the nasal tissues all the way to the SDN. On such a journey, the robots would pass through, in sequence, (1) the capillaries of the inner nasal walls (either left or right nostril), (2) one of the two anterior ethmoidal arteries (either left or right), (3) one of the two ophthalmic arteries (either left or right), (4) one of the two internal carotid arteries (either left or right), (5) one of the two anterior cerebral arteries (either left or right), (6) the anterior communicating artery (part of the Circle of Willis), (7) one of the hypothalamic perforating arteries,⁶⁴⁴ (8) a series of several progressively smaller hypothalamic arterioles, finally reaching (9) the capillary bed in the SDN in the hypothalamus, employing a variety of navigational

⁶⁴⁰ https://en.wikipedia.org/wiki/Intranasal_drug_delivery.

⁶⁴¹ Danielyan L, Schäfer R, von Ameln-Mayerhofer A, Buadze M, Geisler J, Klopfer T, Burkhardt U, Proksch B, Verleysdonk S, Ayturan M, Buniatian GH, Gleiter CH, Frey WH 2nd. Intranasal delivery of cells to the brain. *Eur J Cell Biol*. 2009 Jun;88(6):315-24; <http://www.ncbi.nlm.nih.gov/pubmed/19324456/>. Danielyan L, Schäfer R, von Ameln-Mayerhofer A, Bernhard F, Verleysdonk S, Buadze M, Lourhmati A, Klopfer T, Schaumann F, Schmid B, Koehle C, Proksch B, Weissert R, Reichardt HM, van den Brandt J, Buniatian GH, Schwab M, Gleiter CH, Frey WH 2nd. Therapeutic efficacy of intranasally delivered mesenchymal stem cells in a rat model of Parkinson disease. *Rejuvenation Res*. 2011 Feb;14(1):3-16; <http://www.ncbi.nlm.nih.gov/pubmed/21291297/>. Reitz M, Demestre M, Sedlacik J, Meissner H, Fiehler J, Kim SU, Westphal M, Schmidt NO. Intranasal delivery of neural stem/progenitor cells: a noninvasive passage to target intracerebral glioma. *Stem Cells Transl Med*. 2012 Dec;1(12):866-73; <http://www.ncbi.nlm.nih.gov/pmc/articles/PMC3659670/pdf>. Balyasnikova IV, Prasol MS, Ferguson SD, Han Y, Ahmed AU, Gutova M, Tobias AL, Mustafi D, Rincón E, Zhang L, Aboody KS, Lesniak MS. Intranasal delivery of mesenchymal stem cells significantly extends survival of irradiated mice with experimental brain tumors. *Mol Ther*. 2014 Jan;22(1):140-8; <http://www.ncbi.nlm.nih.gov/pmc/articles/PMC3978787/pdf>.

⁶⁴² https://en.wikipedia.org/wiki/Blood%E2%80%93brain_barrier.

⁶⁴³ Freitas RA Jr. The Alzheimer Protocols: A Nanorobotic Cure for Alzheimer's Disease and Related Neurodegenerative Conditions. IMM Report No. 48, June 2016; Section 4.3, "Medical Nanorobots: Ingress to, and Egress from, the Brain"; <http://www.imm.org/Reports/rep048.pdf>.

⁶⁴⁴ A perforating artery is a small artery that typically arises from larger arteries and penetrates deeper into tissues or organs, often passing through a membrane or surface layer to reach their target area. They supply blood to the internal structures of tissues or organs. In the brain, perforating arteries arise from major arteries like the anterior cerebral artery and "perforate" the surface of the brain to supply deep structures such as the hypothalamus or basal ganglia. These arteries tend to take direct, often vertical, paths through the tissue layers they perforate, serving deep or internal regions.

techniques⁶⁴⁵ (and see discussion below). The estimated travel distance of $x_{\text{nasal-SDN}} \sim 14$ cm (range 11-17 cm) might be traversed as fast as $x_{\text{nasal-SDN}} / v_{\text{nano}} \sim \mathbf{14 \text{ sec}}$ (~ 0.23 min) by vasculomobile nanorobots ambulating across vascular surfaces at a top speed of $v_{\text{nano}} \sim 1$ cm/sec.⁶⁴⁶ The robots might need an additional ~ 10 sec to transit the BBB⁶⁴⁷ to enter the SDN tissues,⁶⁴⁸ then a similar period of time to traverse the SDN extracellular spaces.⁶⁴⁹ Typically about 1-3 neurons and perhaps 30-100 axons may reside between adjacent SDN capillaries that are spaced 20-50 μm apart, so the tissue penetrating nanorobots should not have too far to travel to reach their action stations. The user could begin to feel lustful sensations in $t_{\text{lust}} \sim \mathbf{30-60 \text{ sec}}$.

For sequential navigation during a journey through the arteries in the order listed above, nanorobots can periodically sample the endothelial cells lining the arterial walls for markers to determine their location within the arterial system, using molecular sampling to detect specific membrane-bound receptors or intracellular proteins that are more prevalent or uniquely expressed in certain arteries. Possible useful markers for each arterial segment may include:

(1) The **anterior ethmoidal artery** supplies the nasal cavity and the ethmoid sinuses and is closely associated with the respiratory system and the immune response in mucosal tissues. Useful markers may include **VCAM-1** (vascular cell adhesion molecule-1)⁶⁵⁰ and **ICAM-1** (intercellular adhesion molecule-1),⁶⁵¹ which are often upregulated in the endothelial cells of arteries involved in mucosal immune responses, such as those supplying the nasal cavity; and **eNOS** (endothelial nitric oxide synthase),⁶⁵² whose elevated expression may be associated with arteries in the nasal region due to the need for vasodilation in response to environmental conditions.

(2) The **ophthalmic artery** supplies the eyes and orbit, and its endothelial cells are likely influenced by the oxygen demands of ocular tissues and light exposure. Useful markers may

⁶⁴⁵ Freitas RA Jr. Nanomedicine, Volume I: Basic Capabilities. Landes Bioscience, Georgetown, TX, 1999; Chapter 8, "Navigation"; <http://www.nanomedicine.com/NMI/8.1.htm>.

⁶⁴⁶ Freitas RA Jr. Nanomedicine, Volume I: Basic Capabilities. Landes Bioscience, Georgetown, TX, 1999; Section 9.4.3.5, "Legged Ambulation"; <http://www.nanomedicine.com/NMI/9.4.3.5.htm>.

⁶⁴⁷ Freitas RA Jr. The Alzheimer Protocols: A Nanorobotic Cure for Alzheimer's Disease and Related Neurodegenerative Conditions. IMM Report No. 48, June 2016; Section 4.3.1, "Blood-Brain Barrier (BBB) Penetration"; <http://www.imm.org/Reports/rep048.pdf>.

⁶⁴⁸ Freitas RA Jr. Nanomedicine, Volume I: Basic Capabilities. Landes Bioscience, Georgetown, TX, 1999; Section 9.4.4.1, "Nanorobot Diapedesis"; <http://www.nanomedicine.com/NMI/9.4.4.1.htm>.

⁶⁴⁹ Freitas RA Jr. Nanomedicine, Volume I: Basic Capabilities. Landes Bioscience, Georgetown, TX, 1999; Section 9.4.4.2, "ECM Brachiation"; <http://www.nanomedicine.com/NMI/9.4.4.2.htm>. Freitas RA Jr. The Alzheimer Protocols: A Nanorobotic Cure for Alzheimer's Disease and Related Neurodegenerative Conditions. IMM Report No. 48, June 2016; Section 4.3.4, "Nanorobotic Transit Through Extracellular Spaces"; <http://www.imm.org/Reports/rep048.pdf>

⁶⁵⁰ <https://en.wikipedia.org/wiki/VCAM-1>.

⁶⁵¹ <https://en.wikipedia.org/wiki/ICAM-1>.

⁶⁵² https://en.wikipedia.org/wiki/Endothelial_NOS.

include **ET-1** (endothelin-1),⁶⁵³ a vasoconstrictive peptide often upregulated in arteries associated with the eyes, possibly due to the need to regulate blood flow tightly to the retina; and **VEGF** (vascular endothelial growth factor),⁶⁵⁴ because arteries associated with ocular blood flow might express higher levels of VEGF due to the high metabolic demands of retinal cells, though VEGF is not exclusive to this artery.

(3) The **internal carotid artery**, a major blood vessel supplying the brain that must maintain high flow rates and be protected against mechanical stress. Useful markers may include **PECAM-1** (platelet endothelial cell adhesion molecule-1, aka. CD31),⁶⁵⁵ which is important for maintaining the integrity of large arteries and responding to shear stress, and may be particularly prominent in the internal carotid artery due to the vessel's size and the high blood flow it experiences; and **laminin**⁶⁵⁶ and **integrins**,⁶⁵⁷ because laminin receptors may be more highly expressed in large arteries like the internal carotid, where vascular integrity under high pressure is key.

(4) The **anterior cerebral artery** (ACA), which supplies the medial portions of the frontal lobe and superior medial parietal lobe, with specific demands related to cognitive function and control of motor functions. Useful markers may include **aquaporin-4**,⁶⁵⁸ which may be involved in regulating water transport in arterial segments like the ACA that supply the brain, though it is more commonly found in the blood-brain barrier; and **claudins**⁶⁵⁹ and **occludins**,⁶⁶⁰ tight junction proteins critical to the blood-brain barrier that could be more expressed in cerebral arteries to ensure the selective permeability of brain vasculature.

(5) The **anterior communicating artery**, which connects the anterior cerebral arteries and plays a crucial role in the Circle of Willis (critical for maintaining blood supply redundancy in the brain). Useful markers may include **N-cadherin**⁶⁶¹ and **β -catenin**,⁶⁶² cell adhesion molecules that could be uniquely upregulated in this region to help maintain vessel integrity under the Circle of Willis' network of connections; and again **eNOS** (endothelial nitric oxide synthase), which may be highly expressed to facilitate vasodilation when necessary, given the Circle of Willis' role in regulating cerebral blood flow.

(6) The **hypothalamic arteries**, which supply the hypothalamus, a region that regulates a wide range of homeostatic processes and has some unique features related to the blood-brain barrier. Useful markers may include **GLUT1** (glucose transporter-1)⁶⁶³ because the hypothalamic arteries might have specialized regulation of glucose transport reflecting the metabolic needs of the hypothalamus, even though GLUT1 is found throughout the brain's blood vessels; and **leptin**

⁶⁵³ https://en.wikipedia.org/wiki/Endothelin_1.

⁶⁵⁴ https://en.wikipedia.org/wiki/Vascular_endothelial_growth_factor.

⁶⁵⁵ <https://en.wikipedia.org/wiki/CD31>.

⁶⁵⁶ <https://en.wikipedia.org/wiki/Laminin>.

⁶⁵⁷ <https://en.wikipedia.org/wiki/Integrin>.

⁶⁵⁸ <https://en.wikipedia.org/wiki/Aquaporin-4>.

⁶⁵⁹ <https://en.wikipedia.org/wiki/Claudin>.

⁶⁶⁰ <https://en.wikipedia.org/wiki/Occludin>.

⁶⁶¹ <https://en.wikipedia.org/wiki/Cadherin-2>.

⁶⁶² https://en.wikipedia.org/wiki/Catenin_beta-1.

⁶⁶³ <https://en.wikipedia.org/wiki/GLUT1>.

receptors⁶⁶⁴ and **insulin receptors**,⁶⁶⁵ which may be more highly expressed on endothelial cells reflecting the integration of bloodborne metabolic signals, since the hypothalamus regulates appetite and energy homeostasis.

Finally, axons in the SDN can be navigationally distinguished from other axons in the mPOA by their preferentially high concentration of **androgen receptors** (AR),⁶⁶⁶ **estrogen receptors** (ER α and ER β),⁶⁶⁷ and **aromatase** (CYP19A1)⁶⁶⁸ and **neuronal nitric oxide synthetase** (nNOS)⁶⁶⁹ enzymes which are free in the axonal cytosol of SDN axons.

What is the power requirement for the fleet? Artificially stimulating the sensation of sexual arousal apparently requires the infusion of $N_{stim} \sim 500,000$ nanorobots, each of volume $V_{nanorobot} \sim 10 \mu m^3$. The maximum power draw of each robot is assumed to be $P_{robot} \sim 200$ pW/nanorobot similar to the oxygen/glucose-powered microbivore,⁶⁷⁰ but even during their stimulatory activities these nanorobots don't need to operate continuously at full power. For instance, the hormonal inputs require a capacity for administering up to $n_{oxyvaso} \sim 100$ doses over multiple hours to maintain sexual arousal, or $n_{dose} \sim 100$ sec/dose. If each dosing requires $t_{dose} \sim 10$ sec/dose, that's an $f_{duty} \sim t_{dose} / n_{dose} \sim 10\%$ duty cycle for those 200,000 robots. An $f_{duty} \sim 10\%$ duty cycle is also acceptable for the $\sim 300,000$ sensory and neural stimulation robots, as previously described, so the continuous power demand for the fleet is $P_{fleet} = f_{duty} N_{stim} P_{robot} \sim 10 \mu W$, which can be provided by metabolizing $n_{glu} = P_{fleet} / E_{glu} \sim 4.2 \times 10^{12}$ glucose molecules/sec and $n_{O2} = P_{fleet} / E_{O2} \sim 2.5 \times 10^{13}$ oxygen molecules/sec assuming the nanorobots consume glucose ($E_{glu} \sim 2400$ zJ/molecule) and oxygen ($E_{O2} \sim 400$ zJ/molecule) to produce onboard power in an oxyglucose engine⁶⁷¹ at $\sim 50\%$ efficiency. There are about $c_{glu} = 2.3 \times 10^6$ molecules/ μm^3 of glucose and $c_{O2} = 7.3 \times 10^4$ molecules/ μm^3 of oxygen in human arterial blood plasma, and the SDN is supplied with $n_{SDN} \sim 5.3$ mm³/sec of arterial blood⁶⁷² which provides a total of $n_{SDNglu} = n_{SDN} c_{glu} \sim 1.2 \times 10^{16}$ glucose molecules/sec and $n_{SDNO2} = n_{SDN} c_{O2} \sim 3.9 \times 10^{14}$ oxygen molecules/sec, so the power demands of the nanorobot fleet can be satisfied by drawing $n_{glu} / n_{SDNglu} \sim 0.04\%$ of the **glucose** and $n_{O2} / n_{SDNO2} \sim 6.4\%$ of the **oxygen** from the passing blood supply.⁶⁷³ A 1000-atm

⁶⁶⁴ https://en.wikipedia.org/wiki/Leptin_receptor.

⁶⁶⁵ https://en.wikipedia.org/wiki/Insulin_receptor.

⁶⁶⁶ https://en.wikipedia.org/wiki/Androgen_receptor.

⁶⁶⁷ https://en.wikipedia.org/wiki/Estrogen_receptor.

⁶⁶⁸ <https://en.wikipedia.org/wiki/Aromatase>.

⁶⁶⁹ <https://en.wikipedia.org/wiki/NOS1>.

⁶⁷⁰ Freitas RA Jr. Microbivores: Artificial mechanical phagocytes using digest and discharge protocol. J Evol Technol 2005;14:1-52; Section 3.2.1, "Power Supply and Fuel Buffer Tankage"; <http://www.jetpress.org/volume14/freitas.html>.

⁶⁷¹ Freitas RA Jr. Nanomedicine, Volume I: Basic Capabilities. Landes Bioscience, Georgetown, TX, 1999; Section 6.3.4.4, "Glucose Engine"; <http://www.nanomedicine.com/NMI/6.3.4.4.htm>.

⁶⁷² If the SDN has a tissue volume of 1-2 mm³, a capillary density of 400-500 capillaries/mm³, and a flow rate of $\sim 8.3 \times 10^{-3}$ mm³/sec, then the total flow rate to the SDN is ~ 5.3 mm³/sec (range 3.3-8.3 mm³/sec).

⁶⁷³ The solubility of oxygen in biological tissues is quite good, and oxygen readily diffuses into cells. The oxygen content inside the 1-2 μm thick endothelial cells constituting the BBB in brain capillaries should be

onboard buffer storage tank of volume $V_{\text{tank}} = 0.1 V_{\text{nanorobot}} \sim 1 \mu\text{m}^3$ on each nanorobot, holding $c_{\text{tankO}_2} \sim 111 \times 10^{26} \text{ O}_2 \text{ molecules/m}^3$,⁶⁷⁴ could store enough oxygen to support $t_{\text{O}_2} \sim V_{\text{tank}} N_{\text{stim}} / c_{\text{tankO}_2} / n_{\text{SDNO}_2} \sim 14 \text{ sec}$ of fleet operations.

When the mission is completed, the nanorobot fleet can exit the body by the shortest possible vascular path, which is a travel distance of 5-9 cm to the conjunctiva⁶⁷⁵ of the eye. The devices would navigate through the hypothalamic capillaries (1-2 mm), flow into the anterior cerebral artery (1-2 cm), then into the internal carotid artery (2-3 cm), branch into the ophthalmic artery (1-1.5 cm), and finally transition through the small conjunctival capillaries (0.5-1 cm), exiting the body via the surface of the conjunctiva, i.e., through tear ducts. The typical volume of fluid secreted from the surface of the conjunctiva through the tear ducts (from the combined secretions of the lacrimal glands, accessory lacrimal glands, and conjunctival goblet cells) is 1-2 mm³/min during baseline (non-stimulated) tear secretion. This fluid is secreted onto the surface of the conjunctiva and drains through the puncta (tiny openings in the eyelids) into the tear ducts and ultimately into the nasal passages via the nasolacrimal duct. The excretion of the entire nanorobot fleet of volume $V_{\text{dosage}} \sim 0.005 \text{ mm}^3$ represents only 15-30% of the volume of normal fluid secretion every second. This should be entirely unnoticeable to the human user, especially since the nanorobot size of $V_{\text{nanorobot}}^{1/3} \sim 2.2 \mu\text{m}$ is well below the 3-10 μm particle size detection threshold for the conjunctiva.

5.3.2.3 Nanorobot Control

After sniffing a single dose from the nanaphrodisiac inhaler and waiting a minute or so for the lustbots to get into position in the mPOA and SDN, the user is ready to become artificially sexually aroused. In the simplest mode of operation, the nanorobots may be programmed to begin stimulation as soon as they arrive, simulating the gradual upramp that is experienced during the natural arousal sensation. In the default setting, an onboard timer should limit the period of artificial arousal to some reasonable duration, perhaps an hour, to avoid uncomfortably long or unending states of arousal, mentally roughly equivalent to the physical pathology of priapism⁶⁷⁶ in the case of erections. As an additional default setting, the robots should be programmed to detach from the mPOA/SDN and extract themselves from the body after some set maximum time period has elapsed.

Users must be careful not to indulge in “too much of a good thing”. An artificially-stimulated state of endless arousal might be subjectively similar to aspects of the pathological medical conditions such as Persistent Genital Arousal Disorder (PGAD),⁶⁷⁷ which includes physiological

85-90% of the blood concentration, and the oxygen content inside a neural cell or other tissue lying below the endothelial cells should be 50-70% of bloodstream levels, depending on the tissue's metabolic activity.

⁶⁷⁴ Freitas RA Jr. Nanomedicine, Volume I: Basic Capabilities. Landes Bioscience, Georgetown, TX, 1999; Table 10.2, “Gas Molecules Packed into a Pressure Vessel”; <https://www.nanomedicine.com/NMI/Tables/10.2.jpg>.

⁶⁷⁵ <https://en.wikipedia.org/wiki/Conjunctiva>.

⁶⁷⁶ <https://en.wikipedia.org/wiki/Priapism>.

⁶⁷⁷ https://en.wikipedia.org/wiki/Persistent_genital_arousal_disorder.

symptoms in the penis,⁶⁷⁸ or compulsive sexual behavior disorder⁶⁷⁹ or hypersexuality,⁶⁸⁰ which does not.⁶⁸¹ The subjective experience of persistent overstimulation of the SDN might include an **intensely focused sexual desire** manifesting as a strong, almost biological compulsion toward sexual activity⁶⁸² without the complexity of compulsive behaviors seen in hypersexuality, and a primarily **urge-driven behavior** in which the desire feels more instinctual or primal, as the SDN is heavily influenced by hormonal signals (like testosterone) which are more directly tied to sexual arousal. SDN overstimulation might result in feelings of arousal or the urge for sexual activity but not necessarily lead to compulsive or excessive sexual behaviors in other contexts. The experience would likely be dominated by an increase in sexual drive with a sharp focus on sexual behaviors and a lessened ability to suppress these urges, but still confined to the sexual aspect of cognition.

The operating modes and parameters of the nanorobots may be altered before or after deployment using high-frequency ultrasonic communications,⁶⁸³ probably in the 0.1-1 MHz range that lies well beyond human hearing. Most conveniently, a miniature ultrasound speaker could be attached to or installed in the user's cell phone, allowing coded messages to be transmitted to *in vivo* nanorobots when the cell phone is pressed to the head or relayed through an earbud, using a software application with a user-friendly interface. Operational items that might be available for user control might include:

(1) **Arousal onset.** The user could program the nanorobots to wait until they've all arrived on station before beginning arousal, rather than employing the default gradual upramp.

(2) **Calendared arousal.** The user could program the nanorobots to "turn him on" at a particular time of day.

⁶⁷⁸ PGAD is characterized by unrelenting and unwanted genital arousal, which can persist for hours, days, or longer, even after sexual activity or climax has occurred. People with PGAD may experience feelings of genital swelling, throbbing, or tingling, along with the sensation of being on the verge of orgasm without relief. The condition can cause significant discomfort, embarrassment, and emotional distress.

⁶⁷⁹ https://en.wikipedia.org/wiki/Compulsive_sexual_behaviour_disorder.

⁶⁸⁰ <https://en.wikipedia.org/wiki/Hypersexuality>.

⁶⁸¹ In compulsive sexual behavior disorder the affected individual experiences excessive or uncontrollable sexual thoughts, urges, or desires, often leading to a preoccupation with sex. These thoughts and desires persist despite not being accompanied by physiological arousal or genital symptoms like penile tingling, erections, or throbbing. Hypersexuality is more about the mental and emotional aspects of sexual desire and often manifests in a compulsive need for sexual activities, fantasy, or behavior, even when it's not physically pleasurable or wanted.

⁶⁸² [https://en.wikipedia.org/wiki/Vulcan_\(Star_Trek\)#Mating_drive](https://en.wikipedia.org/wiki/Vulcan_(Star_Trek)#Mating_drive).

⁶⁸³ Freitas RA Jr. Nanomedicine, Volume I: Basic Capabilities. Landes Bioscience, Georgetown, TX, 1999; Section 7.2.2, "Acoustic Broadcast Communication"; <http://www.nanomedicine.com/NMI/7.2.2.htm>.

(3) **Arousal intensity.** The user could turn the intensity of the arousal sensation up or down, experimenting with different degrees of arousal, instantaneously and upon user command.

(4) **Arousal duration.** The experience of arousal could be set last for hours or longer, subject to a maximum period consistent with medical health.

(5) **Patterned arousal.** The user could specify a particular programmed arousal sequence in which arousal intensity follows a sinusoidal, square wave, or staircase pattern, or has a variety of timeouts or spikes, or any other periodic or randomized pattern. As one fanciful example that only a nerd could love, intensity levels from 0-9 could be sequentially activated to match the digits of pi (i.e., 3.1415926...), allowing the user to be “aroused by pi”.⁶⁸⁴

(6) **Conditional arousal.** Execution of particular patterns of arousal could be driven by the detection of specific sensory inputs. For example, the detection of the onset of natural arousal could trigger the artificial stimulation, powerfully amplifying the natural sensation. Because the fleet is positioned to receive natural olfactory, somatosensory, visual and auditory sensory inputs, different arousal programs could be triggered by the users conscious perception of specific smells (a particular perfume), sounds (a person’s voice), sights (a particular color), or mechanosensory information related to touch, pain, or temperature. Arousal could be patterned after external inputs such as the undulations of complex music playing on the radio that’s processed via the cell phone app.

(7) **Conditional de-arousal.** Artificial stimulation of arousal could be terminated upon detection of the absence of specific sensory inputs, including all of the ones mentioned in (6), the absence of natural arousal signals, or the detection of orgasm or ejaculation.

(8) **Calendared removal.** Rather than flushing the robots out of the body shortly after use, the nanorobots could be programmed to remain in the body for a longer period of time, subject to medical biocompatibility limits, thus remaining available for multiple sessions of sexual activity if so desired.

5.3.2.4 Female Arousal

The nanorobotic arousal methods described in the present work pertain only to the elicitation of **sexual arousal in males**. Once these methods become widely available, men should remain alert to the possibility of abuse of this technology by others. For example, unscrupulous women (or, in some cases, other men) might employ lustbots as a date rape⁶⁸⁵ instrumentality to artificially and irresistibly sexually arouse male victims with the objective of inducing them to engage in sexual activities in which they would normally be unwilling to participate.

⁶⁸⁴ Arithmophilia is sexual attraction or arousal by numbers or mathematical concepts; https://map-wiki.com/index.php/List_of_paraphilias#Objects.

⁶⁸⁵ https://en.wikipedia.org/wiki/Date_rape.

In one scenario, the offending robots could be delivered using a fragrant perfume that the male is likely to inhale deeply. The robotic particles would remain suspended in air and not settle out for very long periods of time because the thermal velocity⁶⁸⁶ $v_{\text{thermal}} \sim (3 k_B T_{\text{body}} / m_{\text{nanorobot}})^{1/2} = 925 \text{ } \mu\text{m/sec}$ of a $V_{\text{nanorobot}} \sim 10 \text{ } \mu\text{m}^3$ nanorobot exceeds its terminal velocity⁶⁸⁷ of $v_{\text{terminal}} = 2 \text{ g}$ $R_{\text{nanorobot}}^2 (\rho_{\text{nanorobot}} - \rho_{\text{air}}) / 9 \eta_{\text{air}} \sim 200 \text{ } \mu\text{m/sec}$ in sea-level room-temperature air of density $\rho_{\text{air}} = 1.29 \text{ kg/m}^3$ and viscosity $\eta_{\text{air}} = 1.89 \times 10^{-5} \text{ Pa-sec}$, assuming nanorobots of density $\rho_{\text{nanorobot}} \sim 1500 \text{ kg/m}^3$, mass $m_{\text{nanorobot}} \sim \rho_{\text{nanorobot}} V_{\text{nanorobot}} \sim 1.5 \times 10^{-14} \text{ kg}$, and radius $R_{\text{nanorobot}} \sim 0.5 V_{\text{nanorobot}}^{1/3} \sim 1.08 \text{ } \mu\text{m}$. The nefarious deed requires delivering $V_{\text{dosage}} \sim 0.005 \text{ mm}^3$ of particles or $N_{\text{stim}} \sim 500,000$ airborne robots to the victim. If the mass density of nanorobots suspended as aerosolized perfume molecules is $\sim 0.2 \text{ gm/m}^3$ in a small spray cloud⁶⁸⁸ with perhaps $c_{\text{perfumebots}} \sim 0.1 \text{ gm/m}^3$ in the air immediately above the skin, then the male victim need only inhale $m_{\text{nanorobot}} N_{\text{stim}} / c_{\text{perfumebots}} \sim 75 \text{ cm}^3$ of nanorobot-infused air to receive the nasal dosage needed to ensure effective arousal, less than the volume $V_{\text{sniff}} \sim 200 \text{ cm}^3$ of a single typical casual sniff targeted for scent detection.⁶⁸⁹

One obvious technological defense that could be established by government regulation would be to legally require the manufacture of all lustbots to include a chemical sensor that can detect the bloodstream presence of an engineered long-lived⁶⁹⁰ but harmless messenger molecule which, if detected in the bloodstream, immediately compels the nanorobots to abort their arousal-stimulating mission and exit the body immediately. This messenger molecule might be a digitally encoded hydrofluorocarbon⁶⁹¹ that is nasally administered by a concerned male as a precautionary measure prior to his social encounter. To more aggressively protect unwitting males against the threat of being unknowingly dosed with bootleg or illegal lustbots having disabled or missing messenger molecule detectors, potential victims could nasally self-administer a counter-dose of SDN-targeting protective nanorobots that would stand guard in the mPOA and actively prevent rogue robots from illegally co-opting the arousal function of the SDN.

⁶⁸⁶ Freitas RA Jr. Nanomedicine, Volume I: Basic Capabilities. Landes Bioscience, Georgetown, TX, 1999; Section 3.2.1, "Brownian Motion", Eqn. 3.3; <http://www.nanomedicine.com/NMI/3.2.1.htm>.

⁶⁸⁷ Freitas RA Jr. Nanomedicine, Volume I: Basic Capabilities. Landes Bioscience, Georgetown, TX, 1999; Section 3.2.5, "Nanocentrifugal Sortation", Eqn. 3.10; <http://www.nanomedicine.com/NMI/3.2.5.htm>.

⁶⁸⁸ If a typical perfume spray dispenses $V_{\text{spray}} \sim 0.15 \text{ cm}^3/\text{spray}$ of liquid that is 10% nanorobots by volume (with $\rho_{\text{nanorobot}} \sim 1500 \text{ kg/m}^3$) in a cloud of volume $V_{\text{cloud}} \sim 0.1 \text{ m}^3$ (i.e., cloud diameter $\sim 46 \text{ cm}$), then the mass density of nanorobots in the cloud would be $(10\%) V_{\text{spray}} \rho_{\text{nanorobot}} / V_{\text{cloud}} \sim 0.2 \text{ gm/m}^3$.

⁶⁸⁹ $V_{\text{sniff}} = (2 \text{ nostrils}) (\sim 1 \text{ cm}^2/\text{nostril}) (\sim 1 \text{ m/sec air velocity}) (\sim 1 \text{ sec/sniff}) \sim 200 \text{ cm}^3$.

⁶⁹⁰ Very short-chain hydrofluorocarbons such as the common refrigerant HFC-134a ($\text{C}_2\text{H}_2\text{F}_4$; <https://en.wikipedia.org/wiki/1,1,1,2-tetrafluoroethane>) are extremely volatile and can be eliminated from the blood in minutes to hours via exhalation, but somewhat larger and less-volatile HFCs, such as HFC-245fa, aka. 1,1,1,3,3-pentafluoropropane ($\text{C}_3\text{H}_3\text{F}_5$; <https://en.wikipedia.org/wiki/pentafluoropropane>) or others with higher tissue accumulation due to lipophilicity, would not be eliminated for hours to a few days. Most HFCs are not extensively metabolized in the body.

⁶⁹¹ Freitas RA Jr. Nanomedicine, Volume I: Basic Capabilities. Landes Bioscience, Georgetown, TX, 1999; Section 7.2.1.1, "Ideal Messenger Molecule"; <http://www.nanomedicine.com/NMI/7.2.1.1.htm>.

Might lustbots also be employed to sexually arouse women? The biological regulation of sexual arousal in human females⁶⁹² apparently involves a more complex interplay of hormonal, neural, and sensory mechanisms than in males, with notable differences between the genders in how these mechanisms operate and their complexity of action:

(1) **Hormonal inputs.** **Estrogen** enhances female sexual desire, often referred to as “proceptivity” or the drive to seek out sexual interaction, in contrast with males where testosterone primarily drives sexual desire and arousal. Estrogen’s effects on sexual behavior are primarily mediated through the **Ventromedial Hypothalamus (VMH)**,⁶⁹³ a region that is highly sensitive to estrogen and integrates hormonal signals, influencing arousal by modulating sexual motivation and receptivity. Estrogen also influences sexual behavior by modulating other VMH neurotransmitter systems such as dopamine, oxytocin, and serotonin, which contribute to sexual arousal and reward. Estrogen does act on the mPOA, but its role in females is more about integrating motivational cues and coordinating sexual behaviors, rather than directly triggering arousal. Women normally have much lower **testosterone** levels than men, but women with relatively high testosterone levels often report higher sexual desire, partly mediated through the mPOA. Testosterone enhances the amygdala’s sensitivity to sexually salient stimuli, enhancing sexual motivation, and may also enhance sexual motivation via its effects on the brain’s reward centers, particularly the nucleus accumbens, which mediates the reward aspects of sexual behavior in both sexes. On the suppression side, **progesterone** (which rises during the post-ovulation luteal phase of the female menses) has the opposite effect, dampening sexual motivation and promoting more nurturing or affiliative behaviors, mediated through the VMH.

(2) **Sensory inputs.** Both males and females rely on sensory inputs from the genitals for arousal, but female arousal is often more diffuse and can involve increased sensitivity in areas beyond the genitals, such as the breasts and inner thighs. Sexual arousal in females also tends to be more context-dependent, with a heavier reliance on external factors like emotional intimacy and security, relationship quality, mood, and psychological states like stress or anxiety, whereas sexual arousal in males is more directly linked to visual or tactile stimuli, though emotional and relational factors can also play a role.

(3) **Neural inputs.** The VMH plays a larger role in female sexual receptivity, motivation and behavior than in men. The amygdala is critical in emotional processing and the appraisal of stimuli, which is reflected in differences in amygdala activation during sexual stimuli. The **anterior cingulate cortex (ACC)**,⁶⁹⁴ which helps regulate emotional and social behaviors, is more activated in females during sexual arousal, indicating that the social context and relationship quality play a more pronounced role in female sexual arousal compared to males. The mPOA and SDN (key for male sexual arousal) also play a role in females, but other brain regions take on more prominent roles. Finally, there is a difference in hemispheric activation between males and females during sexual arousal. Males tend to show more localized brain activation (e.g., in the

⁶⁹² Wise NJ, Frangos E, Komisaruk BR. Brain Activity Unique to Orgasm in Women: An fMRI Analysis. *J Sex Med.* 2017 Nov;14(11):1380-1391; <https://pmc.ncbi.nlm.nih.gov/articles/PMC5675825/pdf>.

⁶⁹³ https://en.wikipedia.org/wiki/Ventromedial_nucleus_of_the_hypothalamus.

⁶⁹⁴ https://en.wikipedia.org/wiki/Anterior_cingulate_cortex.

hypothalamus) while females exhibit more diffuse brain activation across multiple areas involved in emotional processing, relationship appraisal, and sensory input.

The **VMH (ventromedial hypothalamus)** in women is similar in size to the mPOA in men, with each of the left and right VMHs having a volume of about 2-4 mm³ and a mass of around 2-5 mg, and with the two VMHs containing a total of 400,000 to 1,000,000 neurons and a similar number of axons. Estrogen receptors (ER α and ER β)⁶⁹⁵ and progesterone receptors (PRs)⁶⁹⁶ are both expressed on the same neurons in the ventrolateral part of the VMH (VMHvI), the most important subregion for sexual behavior in females as it contains a high density of both estrogen and progesterone receptors. The strategy for nanorobots seeking to elicit female sexual arousal would be to release estrogen into the VMHvI or to release artificial molecules designed to permanently bind to the ERs, leaving them continuously activated until a separate artificial molecule is released that removes the first. The PRs should be blocked in the same manner, inhibited from activation until a separate artificial molecule is released that removes the first. To maximize the VMH contribution to the arousal sensation, the nanorobots could:

- (1) stimulate D1 dopamine receptors⁶⁹⁷ in VMHvI neurons or induce increased local dopamine production to amplify sexual arousal and the brain's reward system;
- (2) selectively increase glutamate receptor⁶⁹⁸ activation (e.g., NMDA or AMPA receptors) to heighten the excitatory signals involved in sexual arousal;
- (3) inhibit GABAergic signaling⁶⁹⁹ in the VMHvI by reducing GABA receptor activity (e.g., GABA_A⁷⁰⁰ or GABA_B⁷⁰¹ receptors) to reduce inhibitory tone;
- (4) release oxytocin⁷⁰² or stimulate oxytocin release in circuits connected to the VMH by directly stimulating oxytocin-producing neurons or increasing receptor sensitivity; and
- (5) inhibit specific serotonin receptors (e.g., 5-HT_{2A} receptors)⁷⁰³ in the VMHvI or connected regions to reduce inhibitory effects on sexual behavior.

Sexual arousal in women would also be enhanced by stimulation of specific target areas in the **ACC (anterior cingulate cortex)**, which is deeply involved in integrating emotional and cognitive information, processing the social context of sexual arousal, and contributing to the subjective experience of arousal. Each of the two ACCs in women are 2-3 cm³ and 1-1.5 gm in size, with both ACCs containing a total of 600-1,000 million neurons and a similar number of axons, perhaps ~400 times larger than the SDN. To maximize the ACC contribution to the female arousal sensation, the nanorobots could:

⁶⁹⁵ https://en.wikipedia.org/wiki/Estrogen_receptor.

⁶⁹⁶ https://en.wikipedia.org/wiki/Progesterone_receptor.

⁶⁹⁷ https://en.wikipedia.org/wiki/Dopamine_receptor#D1-like_family.

⁶⁹⁸ https://en.wikipedia.org/wiki/Glutamate_receptor.

⁶⁹⁹ <https://en.wikipedia.org/wiki/GABAergic>.

⁷⁰⁰ https://en.wikipedia.org/wiki/GABAA_receptor.

⁷⁰¹ https://en.wikipedia.org/wiki/GABAB_receptor.

⁷⁰² <https://en.wikipedia.org/wiki/Oxytocin>.

⁷⁰³ https://en.wikipedia.org/wiki/5-HT2A_receptor.

(1) stimulate the pregenual ACC (pgACC; 0.4-0.8 cm³, 0.2-0.4 gm, 80-120 million neurons each) to heighten the emotional/social aspects of arousal and make the experience more intense and pleasurable;

(2) stimulate the subgenual ACC (sgACC; 0.3-0.6 cm³, 0.15-0.3 gm, 60-100 million neurons each) to enhance the integration of emotional context and reward processing during sexual arousal and further intensify the emotional experience;

(3) stimulate the dorsal ACC (dACC; 0.8-1.5 cm³, 0.4-0.6 gm, 150-200 million neurons each) to improve attentional focus on sexual cues, amplifying arousal by making the individual more aware and engaged with the stimuli;

(4) increase dopamine,⁷⁰⁴ oxytocin, and endorphin⁷⁰⁵ levels in the ACC to enhance pleasure, emotional bonding, and reward;

(5) increase glutamate⁷⁰⁶ and norepinephrine⁷⁰⁷ signaling in the ACC to amplify emotional intensity and attentional focus on sexual stimuli; and

(6) modulate serotonin by promoting 5-HT_{1A}⁷⁰⁸ receptor activation and inhibiting 5-HT_{2A}⁷⁰⁹ receptor activity in the ACC to enhance arousal.⁷¹⁰

While nanorobotic stimulation of sexual arousal in women is apparently more complex than for men,⁷¹¹ it can probably be accomplished using similar mechanisms as previously outlined for males ([Section 5.3.2.2](#)) though likely requiring 100-200 million nanorobots – still only a 1-2 mm³

⁷⁰⁴ <https://en.wikipedia.org/wiki/Dopamine>.

⁷⁰⁵ <https://en.wikipedia.org/wiki/Endorphins>.

⁷⁰⁶ [https://en.wikipedia.org/wiki/Glutamate_\(neurotransmitter\)](https://en.wikipedia.org/wiki/Glutamate_(neurotransmitter)).

⁷⁰⁷ <https://en.wikipedia.org/wiki/Norepinephrine>.

⁷⁰⁸ https://en.wikipedia.org/wiki/5-HT1A_receptor.

⁷⁰⁹ https://en.wikipedia.org/wiki/5-HT2A_receptor.

⁷¹⁰ https://en.wikipedia.org/wiki/Flibanserin#Activity_profile.

⁷¹¹ On the other hand, according to a report from the early days of deep brain stimulation in 1986,* a 48-year-old woman with a stimulating nVPL electrode implanted in her right ventral thalamus started to compulsively self-stimulate when she discovered that it could produce erotic sensations. This pleasurable response was heightened by continuous stimulation at 75% maximal amplitude, frequently augmented by short bursts at maximal amplitude. Though sexual arousal was prominent, no orgasm occurred with these brief increases in stimulation intensity. Despite several episodes of paroxysmal atrial tachycardia and development of adverse behavioral and neurological symptoms during maximal stimulation, compulsive use of the stimulator developed. At its most frequent, the patient self-stimulated throughout the day, neglecting personal hygiene and family commitments. A chronic ulceration developed at the tip of the finger used to adjust the amplitude dial and she frequently tampered with the device in an effort to increase the stimulation amplitude.

* Portenoy RK, Jarden JO, Sidtis JJ, Lipton RB, Foley KM, Rottenberg DA. Compulsive thalamic self-stimulation: a case with metabolic, electrophysiologic and behavioral correlates. *Pain*. 1986 Dec;27(3):277-290; <https://www.wireheading.com/intracran/compulsive-selfstimulation.pdf>. See also: <https://mindhacks.com/2008/09/16/erotic-self-stimulation-and-brain-implants/>.

nanomachine dose, roughly 200-400 times larger than the male dosage, based on relative neural tissue volumes. Further technical details of lustbots for women are outside of the scope of the present discussion of male erectile dysfunction and are deferred to a future work. However, similar protections against abusive use of lustbots should be offered for potential female victims as were previously described for potential male victims.

5.3.3 Male Orgasms on Demand (Ecstasytes)

Besides the social and health⁷¹² benefits, the **pleasurable experience of an orgasm** is one of the principal objectives of a penile erection. Nanorobots called “ecstasytes” stationed in the penile tissues ([Section 5.3.3.1](#)) or in the brain ([Section 5.3.3.2](#)) can help generate or manage the scheduling and intensity of such experiences, and create the possibility of continuous orgasms ([Section 5.3.3.3](#)).

5.3.3.1 Penile Orgasm Management

As concisely summarized elsewhere,⁷¹³ a man feels an intense and highly pleasurable pulsating sensation of neuromuscular euphoria as he nears orgasm during stimulation of the penis. These pulsating sensations originate from the contractions of pelvic floor muscles that begin in the anal sphincter⁷¹⁴ and travel to the tip of the penis, commonly described as a “throbbing” or “tingling” sensation. They eventually increase in speed and intensity as the orgasm approaches, until a final “plateau” (the orgasmic) pleasure is sustained for several seconds. In the throes of orgasm, a human male experiences 3-15 rapid, rhythmic contractions of the anal sphincter, the prostate,⁷¹⁵ and the bulbospongiosus muscles of the penis at a contraction frequency of ~1.4 Hz. The sperm are transmitted up the vasa deferentia⁷¹⁶ from the testicles, into the prostate gland as well as through the seminal vesicles, where they are combined with a secretion produced by the prostate to produce semen. Except in cases of “dry orgasm”, contraction of the anal sphincter and prostate force stored semen to be expelled through the urethral channel⁷¹⁷ of the penis. The process produces a pleasurable feeling over **3-10 sec**, although ejaculation⁷¹⁸ may continue for a few more

⁷¹² A widely-reported 1997 study* of 918 men in South Wales, UK, found that participants who had two or more orgasms per week had a **50% lower mortality risk from all causes** than those who had orgasms less often than monthly; a 2001 follow-up study† found that having orgasms twice or more a week **reduced the risk of fatal heart attack by 35%**. A 2004 study‡ of 29,342 U.S. men aged 46-81 years found that each increment of 3 orgasms per week across a lifetime was associated with a **15% decrease in risk of total prostate cancer**.

* Davey Smith G, Frankel S, Yarnell J. Sex and death: are they related? Findings from the Caerphilly Cohort Study. *BMJ*. 1997 Dec 20-27;315(7123):1641-4;

<https://www.ncbi.nlm.nih.gov/pmc/articles/PMC2128033/pdf>.

† Ebrahim S, May M, Ben Shlomo Y, McCarron P, Frankel S, Yarnell J, Davey Smith G. Sexual intercourse and risk of ischaemic stroke and coronary heart disease: the Caerphilly study. *J Epidemiol Community Health*. 2002 Feb;56(2):99-102; <https://www.ncbi.nlm.nih.gov/pmc/articles/PMC1732071/pdf>.

‡ Leitzmann MF, Platz EA, Stampfer MJ, Willett WC, Giovannucci E. Ejaculation frequency and subsequent risk of prostate cancer. *JAMA*. 2004 Apr 7;291(13):1578-86; <https://jamanetwork.com/journals/jama/articlepdf/198487/joc32368.pdf>.

⁷¹³ <https://en.wikipedia.org/wiki/Orgasm#Males>.

⁷¹⁴ https://en.wikipedia.org/wiki/External_anal_sphincter.

⁷¹⁵ <https://en.wikipedia.org/wiki/Prostate>.

⁷¹⁶ https://en.wikipedia.org/wiki/Vas_deferens.

⁷¹⁷ <https://en.wikipedia.org/wiki/Urethra>.

⁷¹⁸ <https://en.wikipedia.org/wiki/Ejaculation>.

seconds after the euphoric sensation gradually tapers off. After ejaculation, a man typically⁷¹⁹ cannot achieve another orgasm until after a refractory period that can last anywhere from less than a minute to several hours or days depending on age and other individual factors.

How could ecstasy nanorobots modulate or control the male orgasm? The process of orgasm in men, particularly the neuromuscular euphoria and muscle contractions, involves a network of nerves that control both sensation and motor responses in the pelvic floor, prostate, and penile muscles. Most notably, the **pudendal nerve**⁷²⁰ is the primary nerve involved in male orgasm, responsible for both sensory and motor innervation to the external genitalia, perineum, and anal sphincter, with a diameter of 2-4 mm in the pelvic region. It is heavily involved in controlling the contractions of the bulbospongiosus muscle (crucial for the ejaculation process and the pleasurable pulsating sensation felt during orgasm) via its perineal nerve branch, and external anal sphincter contractions (via its inferior rectal nerve branch) which are rhythmic during orgasm, and also plays a significant role in transmitting the pleasurable sensations during stimulation of the penis (via its penile dorsal nerve branch). The pelvic splanchnic nerves innervate the bladder, rectum, and the prostate (regulating prostate contraction), but most importantly connect downstream with the **cavernous nerves**⁷²¹ which are primarily responsible for controlling the erectile response by regulating blood flow into the corpora cavernosa and maintaining erection. The direct stimulation by nanorobots of the two pudendal nerves (left and right) and the two cavernous nerves (left and right) should be sufficient to artificially generate an orgasm-like response, even in the absence of sexual arousal, because these nerves play key roles in both the sensory and motor aspects of orgasm, as well as in erection and genital muscle contractions.⁷²² Electrical stimulation of the pudendal nerve can trigger ejaculation and orgasmic-like responses in men with spinal cord injuries or other conditions that impair normal sexual function,⁷²³ bypassing the brain's role in sexual arousal.⁷²⁴ (Direct electrical stimulation of orgasm in women is much more widely employed and reported.)⁷²⁵

⁷¹⁹ Interviews with multiorgasmic men suggested that (1) detumescence does not always follow an orgasm, (2) a nonejaculatory orgasm can occur prior to as well as after an ejaculatory orgasm, and (3) it is possible for men to have a series of orgasms. Dunn ME, Trost JE. Male multiple orgasms: a descriptive study. Arch Sex Behav. 1989 Oct;18(5):377-87; <https://pubmed.ncbi.nlm.nih.gov/2818169/>.

⁷²⁰ https://en.wikipedia.org/wiki/Pudendal_nerve.

⁷²¹ https://en.wikipedia.org/wiki/Cavernous_nerves.

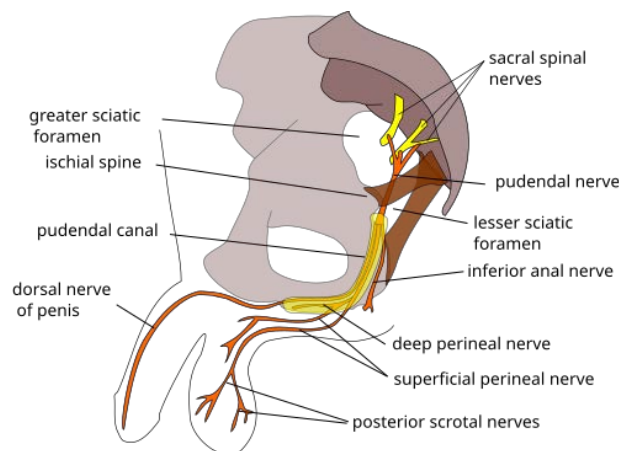
⁷²² Stimulation of the pudendal nerve can trigger the rhythmic muscle contractions in the pelvic floor and perineum, which are essential for ejaculation and are experienced as pleasurable pulsations during orgasm, and can induce sensory feedback from the genitals, which also contributes to the pleasurable sensations associated with orgasm. Stimulation of the cavernous nerves can induce vasodilation in the penile arteries and relaxation of the smooth muscle in the erectile tissue (corpora cavernosa), creating the physical conditions of orgasm by establishing and maintaining the erectile state.

⁷²³ Meng Z, Wang Z. [Treatment and mechanism study of electromagnetic stimulation and vibrational massage for patients with ejaculatory incompetence]. Sheng Wu Yi Xue Gong Cheng Xue Za Zhi. 2004 Feb;21(1):74-5, 80 (Chinese); <https://pubmed.ncbi.nlm.nih.gov/15022469/>. Alexander M, Rosen RC. Spinal cord injuries and orgasm: a review. J Sex Marital Ther. 2008;34(4):308-24; <https://pubmed.ncbi.nlm.nih.gov/18576233/>. Alexander M, Marson L. Orgasm and SCI: what do we know? Spinal Cord. 2018 Jun;56(6):538-547; <https://pubmed.ncbi.nlm.nih.gov/29259346/>.

During sexual arousal, the frequency of action potentials in these nerves progressively increases as stimulation becomes more intense or prolonged. The firing rate of a pudendal nerve is perhaps 0.1-5 Hz at rest, increasing during sexual excitement and eventually reaching 20-100 Hz during the rapid muscle contractions and sensory feedback associated with the orgasmic response. The orgasmic response is triggered when the cumulative sensory input and motor drive to these nerves reach a certain threshold level of neural activation.

Nanorobot deployment to pudendal

nerves. After the pudendal nerve originates from the S2, S3, and S4 nerve roots in the sacral region of the spinal cord, it runs as a single nerve for 4-5 cm before branching first into the inferior anal nerve,⁷²⁶ then further branching into the perineal and dorsal nerves ~2 cm further on (image, right).⁷²⁷ While a single unbranched trunk, the pudendal nerve runs parallel to, and lies within 1-3 mm of, the pudendal artery, separated by only a small amount of loose connective tissue rich in extracellular matrix (ECM) components, including collagen



fibers, proteoglycans, and elastic fibers. Nanorobots administered as described earlier ([Section 5.3.1.5](#)) could exit the artery anywhere along this segment and histonate directly across this narrow space to the pudendal nerve, but it may be challenging to determine the ideal arterial exit

⁷²⁴ “In the 1970s, experimenters noticed that bare speaker wires could deliver a jolt and began using recorded and live sound for electrostimulation....Although early e-stim units used only a simple, pulsed, sinusoidal wave, newer units use more complex wave forms and also allow for the use of ambient sound or prerecorded wave forms like music or specially designed computer files for specific types of stimulation. There are now sites dedicated to the creation of MP3 files specifically for erotic journeys or symphonies, which can include such routines as rewards, punishments, very strong, and pleasantly soft portions.” https://en.wikipedia.org/wiki/Erotic_electrostimulation#History.

⁷²⁵ Sipski ML. Sexual response in women with spinal cord injury: neurologic pathways and recommendations for the use of electrical stimulation. *J Spinal Cord Med.* 2001 Fall;24(3):155-8; <https://pubmed.ncbi.nlm.nih.gov/11585234/>. Meloy TS, Southern JP. Neurally augmented sexual function in human females: a preliminary investigation. *Neuromodulation.* 2006 Jan;9(1):34-40; <https://pubmed.ncbi.nlm.nih.gov/22151591/>. Surbeck W, Bouthillier A, Nguyen DK. Bilateral cortical representation of orgasmic ecstasy localized by depth electrodes. *Epilepsy Behav Case Rep.* 2013 Apr 13;1:62-5; <https://www.ncbi.nlm.nih.gov/pmc/articles/PMC4150648/pdf>. Chaton L, Chochoi M, Reyns N, Lopes R, Derambure P, Szurhaj W. Localization of an epileptic orgasmic feeling to the right amygdala, using intracranial electrodes. *Cortex.* 2018 Dec;109:347-351; <https://pubmed.ncbi.nlm.nih.gov/30126613/>. Zimmerman LL, Gupta P, OGara F, Langhals NB, Berger MB, Bruns TM. Transcutaneous Electrical Nerve Stimulation to Improve Female Sexual Dysfunction Symptoms: A Pilot Study. *Neuromodulation.* 2018 Oct;21(7):707-713; <https://www.ncbi.nlm.nih.gov/pmc/articles/PMC6218940/pdf>.

⁷²⁶ https://en.wikipedia.org/wiki/Inferior_anal_nerves.

⁷²⁷ https://en.wikipedia.org/wiki/File:Pudendal_nerve.svg.

angle without the guidance of an external navigation system.⁷²⁸ A more reliable course for vasculomobile nanorobots would be to exit the pudendal artery into the inferior rectal artery, at the first downstream junction of the pudendal artery as it passes through the lesser sciatic foramen just before entering the pudendal canal. The ecstacytes would then follow the inferior rectal artery and exit into any of numerous arterioles that branch off from the artery and run alongside or into the connective tissue surrounding the pudendal nerve (which contribute to the nerve's blood supply), finally leading into the vasa nervorum⁷²⁹ (the capillary bed that supplies oxygen to the pudendal nerve), a total path length of ~1 cm. The nanorobots can avoid entering arterioles that lead to other tissues such as the perianal skin or lower rectum that do not lead to the pudendal nerve, by monitoring vessel size and diameter,⁷³⁰ blood flow velocity and pressure,⁷³¹ endothelial biochemical markers,⁷³² or metabolic environment and oxygen levels.⁷³³

What is the power requirement for nanorobots surrounding the pudendal nerve to artificially stimulate an orgasm? Assuming electrical stimulation,⁷³⁴ the typical resting membrane potential

⁷²⁸ Freitas RA Jr. Nanomedicine, Volume I: Basic Capabilities. Landes Bioscience, Georgetown, TX, 1999; Section 8.3.3, "Microtransponder Networks"; <http://www.nanomedicine.com/NMI/8.3.3.htm>.

⁷²⁹ https://en.wikipedia.org/wiki/Vasa_nervorum.

⁷³⁰ Vasa nervorum are typically very small (5-10 μm) capillary-like vessels, much smaller than the arterioles supplying larger tissues like the anal canal or skin. As you move downstream along the inferior rectal artery, the arterioles leading to the vasa nervorum would likely be smaller in diameter than those supplying muscle or connective tissue.

⁷³¹ The blood flow velocity in arterioles leading to the vasa nervorum would likely be lower than in arterioles serving larger, high-demand tissues like the rectal or perianal muscles. Vasa nervorum typically have a low flow rate and are designed for sustained, small-volume supply to nerve fibers. We might expect lower velocity and lower pressure in the arterioles supplying the pudendal nerve compared to arterioles that supply surrounding tissues like muscles or skin, which need higher flow to meet metabolic demands.

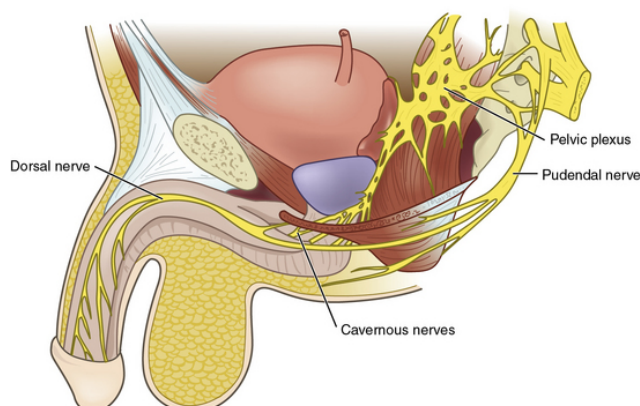
⁷³² Endothelial cells of vasa nervorum may express unique surface molecules or receptors related to nerve-specific growth factors or neuronal maintenance, possibly including (1) Nerve Growth Factor (NGF) receptors (essential for the maintenance and survival of neurons), since blood vessels supporting nerve tissues (vasa nervorum) may express markers related to NGF signaling or other neurotrophic factors like brain-derived neurotrophic factor or BDNF; (2) Vascular Endothelial Growth Factor (VEGF) receptors (vasa nervorum may express receptors specific for VEGF-A or related molecules that promote the vascularization of nerves); or (3) Neural Cell Adhesion Molecules (NCAMs), as endothelial cells in vasa nervorum may also express NCAMs or similar molecules which promote close associations with neural tissue. Arterioles supplying muscle or skin might express more general endothelial markers that are less specialized for nerve tissue, such as smooth muscle actin (SMA) or keratinocyte-specific markers in the skin's blood supply.

⁷³³ Nerve tissue has a lower metabolic demand than muscle, skin, or glandular tissue, so the oxygen consumption in the arterioles leading to the vasa nervorum may be lower. Nerves are more sensitive to hypoxia (low oxygen), so arterioles feeding vasa nervorum might have specific adaptations for consistent oxygen delivery, such as specialized hemoglobin binding proteins or other oxygen-sensing molecules.

⁷³⁴ It is theoretically possible to stimulate the pudendal nerve by purely mechanical means if the nanorobots can apply localized forces (such as compression, stretching, or shearing) on the nerve fibers. The force required would likely be in the range of 1-10 μN , sufficient to deform the nerve membrane and open

of a nerve cell is about -70 mV and an action potential is triggered when the membrane potential reaches around -55 mV (the threshold potential). To stimulate an action potential, the nanorobots must depolarize the membrane by around 15-20 mV, depending on the exact characteristics of the neuron. For peripheral nerves like the pudendal nerve, the duration of a stimulus required to elicit an action potential is 0.1-1 msec for myelinated fibers and 1-10 msec for unmyelinated fibers.⁷³⁵ A threshold energy of $E_{\text{trigger}} \sim I_{\text{stim}} \Delta V_{\text{nerve}} \tau_{\text{stim}} \sim 50 \text{ pJ}$ is required to trigger an $E_{\text{APot}} \sim 246,800 \text{ pJ}$ action potential in a single myelinated axon with a stimulus current of $I_{\text{stim}} \sim 2.5 \mu\text{A}$,⁷³⁶ assuming the stimulus for each action potential is applied over $\tau_{\text{stim}} \sim 1 \text{ msec}$ with a voltage differential of $\Delta V_{\text{nerve}} \sim 20 \text{ mV}$. To trigger an orgasmic event, the nanorobots would need to stimulate multiple axonal fibers in the pudendal nerve, both sensory and motor. Assuming a pudendal nerve includes $N_{\text{axons}} \sim 10,000$ axons and taking the maximum orgasmic stimulation frequency as $\nu_{\text{orgasm}} \sim 100 \text{ Hz}$, the stimulation power required from the nanorobot fleet to provoke and maintain an orgasm totals $P_{\text{orgasm}} \sim E_{\text{trigger}} \nu_{\text{orgasm}} N_{\text{axons}} \sim 50 \mu\text{W}$, or **$\sim 50 \text{ pW/nanorobot}$ for a fleet of $\sim 1,000,000$ nanorobots** emplaced around each of the two pudendal nerves. The average spacing between adjacent capillaries of the vasa nervorum is generally in the range of 50-100 μm , well within the most convenient $\sim 100 \mu\text{m}$ acoustic communication range of nanorobots,⁷³⁷ enabling the ecstacyte robot fleet at each nerve to coordinate its stimulation activities in real time.

Nanorobot deployment to cavernous nerves. The cavernous nerves (image, right),⁷³⁸ 1-2 mm in diameter, originate from the pelvic plexus (also called the inferior hypogastric plexus), a network of autonomic nerves that includes fibers from the pelvic splanchnic nerves⁷³⁹ (parasympathetic) and hypogastric nerves⁷⁴⁰ (sympathetic). These autonomic fibers (primarily parasympathetic) that contribute to the cavernous nerves first converge into two primary nerve bundles



– the left cavernous nerve and the right cavernous nerve. The cavernous nerves run alongside the prostate, where they are known as part of the prostatic plexus⁷⁴¹ in men. Branching begins at this

mechanosensitive ion channels, thereby triggering an action potential. The key to success would be precise application of force to avoid damaging the nerve while delivering consistent stimulation to the axons.

⁷³⁵ The pudendal nerve contains a mix of both myelinated and unmyelinated axons, as it carries sensory, motor, and autonomic fibers that innervate the pelvic floor, perineum, and genitalia.

⁷³⁶ Wang Y, Wang R, Xu X. Neural Energy Supply-Consumption Properties Based on Hodgkin-Huxley Model. *Neural Plast.* 2017;2017:6207141; <https://www.ncbi.nlm.nih.gov/pmc/articles/PMC5337805/pdf>.

⁷³⁷ Freitas RA Jr. *Nanomedicine, Volume I: Basic Capabilities.* Landes Bioscience, Georgetown, TX, 1999; Section 7.2.2, “Acoustic Broadcast Communication”; <http://www.nanomedicine.com/NMI/7.2.2.htm>.

⁷³⁸ <https://thoracickey.com/vasculogenic-erectile-dysfunction-3/>.

⁷³⁹ https://en.wikipedia.org/wiki/Pelvic_splanchnic_nerves.

⁷⁴⁰ https://en.wikipedia.org/wiki/Hypogastric_nerve.

⁷⁴¹ [https://en.wikipedia.org/wiki/Prostatic_plexus_\(nervous\)](https://en.wikipedia.org/wiki/Prostatic_plexus_(nervous)).

stage, with the first smaller branches from the cavernous nerves innervating the prostate and seminal vesicles, followed by extensive additional branching after the cavernous nerves pass by the prostate and move into the perineal region, innervating the corpora cavernosa and other structures. Ecstacytes should be sent into the 2-3 cm of intact (unbranched) cavernous nerves immediately upstream of the prostate. The internal pudendal artery passes within 3-10 mm of the intact cavernous nerve and directly supplies the vasa nervorum of this nerve with arterial blood, probably through small collateral arterioles. Nanorobots can distinguish the small arterioles branching off the internal pudendal artery that lead to the vasa nervorum of the unbranched section of the cavernous nerves, and avoid other arterioles that lead elsewhere, by monitoring physical characteristics, biochemical markers, and environmental cues as discussed above for the pudendal nerve. Finally, each cavernous nerve may include ~1000 axons, so the power requirement for orgasm control might be **~50 pW/nanorobot for a fleet of ~100,000 nanorobots** emplaced around each of the two cavernous nerves.

Orgasm-controlling ecstasy nanorobots will allow men to become regularly **multiorgasmic**. Normal male multiple orgasms can occur in two forms: sporadic multiorgasms, with interorgasmic intervals of several minutes, and condensed multiorgasms, with rapid bursts within a few seconds to 2 minutes. In one study of naturally multiorgasmic men,⁷⁴² male participants reported experiencing between 2 and 30 orgasms within a certain period, though the more common range is between 2 and 4 consecutive orgasms, typically within minutes. Unfortunately, multiple orgasms are relatively rare in men, with less than 10% of men in their 20s and less than 7% of men after age 30 yrs reporting the ability to experience them.⁷⁴³ Nanorobots can correct this unfortunate natural limitation.

To estimate the nanorobotically-assisted multiorgasmic potential of men, we consider the bulbospongiosus muscles⁷⁴⁴ which are involved in male orgasmic contractions. These contain skeletal muscle fibers (voluntary striated muscle fibers) that are predominantly type II muscle fibers (aka. fast-twitch fibers) best suited for short bursts of powerful, rapid pulsations. Isolated type II fibers have an absolute refractory period (when the muscle fiber cannot respond to any further stimuli) of 1-2 msec, a relative refractory period (when the muscle can be stimulated again but requires a stronger stimulus) of 10-30 msec. The muscle fiber requires at least ~3 seconds under optimal conditions to recover fully for another maximal contraction. However, with heavy loads or sustained contractions, recovery time can range from $\tau_{\text{recovery}} \sim 30\text{-}120$ sec depending on the intensity of contraction and the duration of effort.⁷⁴⁵ This suggests that nanorobots should be

⁷⁴² Griffin-Mathieu G, Berry M, Shtarkshall RA, Amsel R, Binik YM, Gérard M. Exploring Male Multiple Orgasm in a Large Online Sample: Refining Our Understanding. *J Sex Med*. 2021 Sep;18(9):1652-1661; <https://pubmed.ncbi.nlm.nih.gov/34404626/>.

⁷⁴³ Wibowo E, Wassersug RJ. Multiple Orgasms in Men-What We Know So Far. *Sex Med Rev*. 2016 Apr;4(2):136-148; <https://pubmed.ncbi.nlm.nih.gov/27872023/>.

⁷⁴⁴ https://en.wikipedia.org/wiki/Bulbospongiosus_muscle.

⁷⁴⁵ Crow MT, Kushmerick MJ. Chemical energetics of slow- and fast-twitch muscles of the mouse. *J Gen Physiol*. 1982 Jan;79(1):147-66; <https://pmc.ncbi.nlm.nih.gov/articles/PMC2215489/pdf>. Maglischo EW. Part II: Training Fast Twitch Muscle Fibers: Why and How. *J Swimming Res*. 2012;19:1; <https://www.rowperfect.co.uk/wp-content/uploads/2012/01/Training-fast-twitch-fibers.pdf>. See also:

able to provide a sustained cadence of $\tau_{\text{recovery}}^{-1} \sim \mathbf{0.5-2 \text{ orgasms/min}}$ throughout lovemaking sessions of indefinitely long duration, entirely competitive with the average $\sim \mathbf{0.3-1 \text{ orgasms/min}}$ reported by multiorgasmic college women in a 2021 study, in which 34% of the apparently insatiable women reported “partner tired” as their reason for ending the series of orgasms.⁷⁴⁶ Note that in a classic 1954 experiment,⁷⁴⁷ rats with electrodes wired directly to their pleasure centers voluntarily self-stimulated themselves up to $\sim \mathbf{12 \text{ times/min}}$ – essentially enjoying nearly continuous ecstasy ([Section 5.3.3.3](#)) – and ignoring food and all other distractions until the current was turned off.⁷⁴⁸

Orgasm-controlling nanorobots should also allow the male **climax to be indefinitely delayed** (under user control) while avoiding the discomfort of epididymal hypertension⁷⁴⁹ and greatly expanding, even redefining, the possibilities for edging.⁷⁵⁰ Note that if ecstasy artificially suppressed or blocked signals traveling through the pudendal nerve, the sensation of penile stimulation would be diminished or absent, and the motor signals needed to contract the pelvic floor muscles for ejaculation and orgasm would be interrupted, effectively preventing orgasm even in the presence of significant arousal. Suppression of the pelvic splanchnic or cavernous nerves would prevent adequate blood flow into the penis, leading to erectile dysfunction, in which case an orgasm might be less likely to occur even with high arousal. Suppressing the hypogastric nerve⁷⁵¹ would prevent the emission of semen from the prostate, vas deferens, and seminal

<https://strengthrx.com/muscle-fiber-types-energy-systems-and-time-to-failure-a-comprehensive-breakdown/>.

⁷⁴⁶ Gérard M, Berry M, Shtarkshall RA, Amsel R, Binik YM. Female Multiple Orgasm: An Exploratory Internet-Based Survey. *J Sex Res.* 2021 Feb;58(2):206-221; https://www.researchgate.net/profile/Ronny-Shtarkshall/publication/340728686_Female_Multiple_Orgasm_An_Exploratory_Internet-Based_Survey/links/5ec18dca92851c11a87027c1/Female-Multiple-Orgasm-An-Exploratory-Internet-Based-Survey.pdf.

⁷⁴⁷ Olds J, Milner P. Positive reinforcement produced by electrical stimulation of septal area and other regions of rat brain. *J Comp Physiol Psychol.* 1954 Dec;47(6):419-27; <https://seminarioneurounam.wordpress.com/wp-content/uploads/2014/04/olds-milner.pdf>.

⁷⁴⁸ Research in the decades following Olds and Milner’s 1954 study suggested that the environment can affect self-stimulation behavior in rats. Studies in the 1970s and later explored how environmental enrichment (larger spaces, social interaction, natural stimuli) impacts rats’ self-stimulation behavior and generally found that rats in enriched environments might not self-stimulate to the exclusion of all other activities as they do in confined settings. In novel* or enriched environments, rats often show more balanced behavior, interspersing self-stimulation with other activities such as social interactions, exploration, and feeding.

* e.g., De Witte P. Enhanced self-stimulation in the home cage but not in a novel cage environment after naloxone injection. *Arch Int Pharmacodyn Ther.* 1982 Dec;260(2):255-64; <https://pubmed.ncbi.nlm.nih.gov/7165428/>.

⁷⁴⁹ This is a painful condition that occurs when orgasm is delayed too long after the beginning of sexual arousal or activities, colloquially described as “blue balls” in men and “blue vulva” in women; https://en.wikipedia.org/wiki/Epididymal_hypertension.

⁷⁵⁰ [https://en.wikipedia.org/wiki/Edging_\(sexual_practice\)](https://en.wikipedia.org/wiki/Edging_(sexual_practice)).

⁷⁵¹ https://en.wikipedia.org/wiki/Hypogastric_nerve.

vesicles into the urethra, artificially creating a “dry orgasm”,⁷⁵² an advanced form of birth control⁷⁵³ for men conceptually similar to today’s far more primitive experimental vas-occlusive methods.⁷⁵⁴

For completeness, it should be noted that for some men an important objective of penile erection is the insemination of a female to produce offspring. For men who are stalwartly fixated on this objective, nanorobots could enable **orgasmless ejaculation** from an erect penis that is capable of penetrative intercourse by selective stimulation of the pelvic splanchnic nerves (which facilitate the expulsion of semen through smooth muscle contractions of the prostate and seminal vesicles), the hypogastric nerve (that assists the emission phase of ejaculation where sperm and seminal fluid are transported from the vas deferens and prostate into the urethra), and the perineal nerve (that controls the muscular contractions of the bulbospongiosus which are crucial for the ejaculation process). Further details of this intervention are outside the scope of this paper.

5.3.3.2 Virtual Orgasms

Virtual reality devices⁷⁵⁵ allow a user to vicariously enjoy a sensory experience that is not actually occurring in the physical world. Similarly, ecstacytes that are carefully deployed throughout the human brain could create a virtual orgasm, or “vorgasm”, by directly stimulating those parts of the brain that would normally be activated during sexual activity leading to male climax. The nanorobot deployment could be structured so as to produce either a **simulated vorgasm**⁷⁵⁶ in which an exact replica of the normal biological sensations of ecstatic orgasm is experienced in the user’s conscious mind even in the complete absence of penile tissue stimulation or related sensory inputs, or an **augmented vorgasm**⁷⁵⁷ in which simulated sensations generated by nanorobots in the brain are interactively combined with actual sensations produced during copulation in the natural manner by physical penile tissue stimulation and other natural inputs and responses. (Of course, orgasms in human uploads⁷⁵⁸ would be easier and more direct.)

Deploying a fleet of ecstacytes to generate episodic or continuous virtual orgasms will likely require more precisely positioned and coordinated neural targeting than other applications previously described in this paper. Specifically, artificial stimulation of action potentials in the Medial Preoptic Area (mPOA)⁷⁵⁹ [~89,300 neurons] and Paraventricular Nucleus (PVN)⁷⁶⁰

⁷⁵² Shindel AW. Anejaculation: Relevance to Sexual Enjoyment in Men and Women. J Sex Med. 2019 Sep;16(9):1324-1327; <https://pubmed.ncbi.nlm.nih.gov/31488287/>.

⁷⁵³ https://en.wikipedia.org/wiki/Male_contraceptive.

⁷⁵⁴ https://en.wikipedia.org/wiki/Vas-occlusive_contraception.

⁷⁵⁵ https://en.wikipedia.org/wiki/Virtual_reality.

⁷⁵⁶ https://en.wikipedia.org/wiki/Simulated_reality.

⁷⁵⁷ https://en.wikipedia.org/wiki/Augmented_reality.

⁷⁵⁸ https://en.wikipedia.org/wiki/Mind_uploading.

⁷⁵⁹ Within the ~100,000 neurons of the **mPOA**, the nanorobots should stimulate action potentials in: (1) ~50,000 **GABAergic neurons** (to disinhibit other parts of the hypothalamus and brainstem, effectively boosting sexual arousal and helping simulate orgasmic peak sensations), (2) ~30,000 **glutamatergic neurons** (to stimulate downstream dopaminergic pathways, particularly the reward centers, enhancing

[~20,000 neurons] in the hypothalamus, and also in the Nucleus Accumbens (NAc) [~1.95 million neurons],⁷⁶¹ Ventral Tegmental Area (VTA) [~45,000 neurons],⁷⁶² Periaqueductal Gray (PAG) [~373,000 neurons],⁷⁶³ and insular cortex [~2.45 million neurons],⁷⁶⁴ would address the

feelings of pleasure and euphoria during simulated orgasm), **(3) ~3000 dopaminergic neurons** (to directly enhance the release of dopamine in critical regions that mediate the pleasure and euphoric aspects of orgasm thus ensuring the user perceives peak sexual satisfaction), **(4) ~3000 kisspeptin neurons** (to amplify the brain's sexual arousal signals and help replicate the neuroendocrine responses that peak during orgasm), and **(5) ~3000 nitric oxide producing neurons** (to enhance the physiological correlates of orgasm, such as the perception of bodily arousal or muscle contractions). The robots should also suppress action potentials in ~300 **serotonergic neurons** in the mPOA (to reduce dampening effects on arousal, leading to increased arousal and a quicker onset of orgasm since the serotonin-induced delay mechanism is weakened).

⁷⁶⁰ Within the ~30,000 neurons of the **PVN**, the nanorobots should stimulate action potentials in: **(1) ~4000 oxytocinergic neurons** (to release oxytocin into the nucleus accumbens (NAc), amygdala, prefrontal cortex (PFC), hippocampus, brainstem and spinal cord, to help simulate the neurochemical state associated with orgasm which emphasizes the emotional and bonding aspects of the orgasmic experience), **(2) ~3000 vasopressinergic neurons** (to release vasopressin into the NAc, amygdala, PFC, bed nucleus of the stria terminalis (BNST), brainstem and spinal cord, to enhance emotional intensity and reward circuits in combination with oxytocin, contributing to a more profound orgasmic experience), **(3) ~3000 dopaminergic axonal projections** into the PVN (enhance dopamine release in pleasure-related areas such as the nucleus accumbens, heightening the feeling of euphoria during orgasm), and **(4) ~10,000 parvocellular neurons** that project to the brainstem and spinal cord (to activate autonomic responses, enhancing the physiological sensations associated with orgasm such as increased heart rate, blood pressure, muscle contractions, and warmth).

⁷⁶¹ Within the ~2 million neurons of the **NAc**, the nanorobots should stimulate action potentials in neurons that integrate incoming signals from the mPOA and PVN to mediate the reward and euphoria associated with orgasm, particularly the ~880,000 **D1-receptor-expressing Medium Spiny Neurons** (to amplify the reward signals from the dopaminergic inputs already stimulated). The robots should also suppress action potentials in ~1,070,000 **D2-receptor-expressing Medium Spiny Neurons** (which typically inhibit reward-related behaviors when activated).

⁷⁶² Within the ~50,000 neurons of the **VTA**, the nanorobots should stimulate action potentials in ~35,000 **dopaminergic neurons** (triggering release of dopamine in the NAc via the mesolimbic pathway, the prefrontal cortex via the mesocortical pathway, and the amygdala, amplifying the sensation of pleasure and reward). The robots should also suppress action potentials in ~10,000 **GABAergic neurons** in the VTA (reducing their inhibitory effect on the dopaminergic neurons and allowing the dopaminergic neurons to fire more freely, leading to more dopamine release in the NAc and other target areas which would enhance the feelings of euphoria, pleasure, and reward). The requirement that nanorobots *stimulate* GABAergic neurons in the mPOA but *suppress* GABAergic neurons in the **VTA** is not contradictory because stimulating the mPOA neurons allows the body to remove the “brakes” on sexual arousal and facilitate the physiological and motivational drive for orgasm, whereas suppressing the VTA neurons allows for a boost in dopamine which enhances the pleasure and reward sensations that are central to the orgasmic experience.

⁷⁶³ Within the ~500,000 neurons of the **PAG**, the nanorobots should stimulate action potentials in: **(1) ~100,000 glutamatergic neurons** (to enhance the autonomic responses associated with orgasm such as increased heart rate, muscle contractions, and the overall feeling of bodily arousal), **(2) ~80,000 GABAergic neurons in the ventrolateral PAG or vIPAG** (to disinhibit the excitatory circuits that project to areas like the rostral ventromedial medulla (RVM) which can enhance autonomic responses (e.g., heart rate, breathing) and emotional arousal associated with orgasm, generally increasing arousal, euphoria, and

core components of the orgasmic experience, including pleasure, euphoria, autonomic sensations, and emotional satisfaction. (Additionally stimulating the 0.4-0.6 billion neuron anterior cingulate cortex (ACC) would produce a richer emotional experience with more pronounced emotional satisfaction, bonding, and depth than a purely physical and pleasure-driven experience.) Finally, electrical stimulation of parts of the sensory cortex [~ 6 -13 million neurons]⁷⁶⁵ could recreate the perception of peak tactile sensations in the absence of actual motor control or sensory feedback from the penile tissues or elsewhere in the body. Artificial generation of a orgasm thus appears to require the precise placement and operation of ~ 11 -18 million nanorobots on each side of the

emotional intensity), (3) $\sim 40,000$ **GABAergic neurons in the dorsolateral PAG or dIPAG** (to allow for greater sensory input and emotional amplification, contributing to the intense sensory experiences of orgasm by opening the circuits that promote the integration of strong sensory inputs during the peak of orgasmic pleasure), and (4) $\sim 150,000$ **opioid receptor-expressing neurons** (to mimic the release of natural opioids, increasing the sense of euphoria and well-being associated with orgasm and amplifying the pleasure and emotional relief that occur at the peak of orgasm). The robots should also suppress action potentials in the network of ~ 3000 **serotonergic axonal projections into the PAG from the Raphe nuclei** (offering a faster onset of orgasm, followed by prolonged and smoother sensations, without reducing emotional intensity too much).

⁷⁶⁴ Within the 60-80 million neurons of the **insular cortex**, the nanorobots should stimulate action potentials in: (1) $\sim 1,000,000$ **Layer 5/6 viscerosensory neurons** (to simulate sensations like increased heart rate, warmth, and bodily tension, which are typical during the climax of orgasm, crucial for replicating the physical sensation of bodily changes during orgasm), (2) $\sim 200,000$ **Layer 6 autonomic modulatory neurons** (to amplify the perception of bodily arousal, such as increased heart rate, rapid breathing, and muscle tension, mimicking the physical sensations associated with orgasm), and (3) $\sim 1,000,000$ **glutamatergic pyramidal neurons** (to enhance the sensation of body awareness and emotional arousal, intensifying the overall experience of orgasm, in neurons located throughout different layers of the insular cortex that project to regions involved in emotional processing such as the amygdala and prefrontal cortex). The robots should also moderately and selectively stimulate action potentials in the $\sim 150,000$ **Layer 2/3 GABAergic interneurons** (that control emotional intensity and sensory integration) and the $\sim 100,000$ **Layer 5/6 GABAergic interneurons** (that modulate autonomic functions and integrate body-state signals), preventing overstimulation while maintaining the pleasure, sensory richness, and emotional satisfaction that define a fulfilling orgasm.

⁷⁶⁵ Within the 10-15 million neurons of the **sensory cortex**, the nanorobots should stimulate action potentials in: (1) ~ 1 -2 million **Layer 4 neurons in the primary somatosensory cortex (S1)** (to simulate the tactile sensations typically associated with orgasm, even if no input is coming from the lower body, resulting in the perception of pressure, warmth, and movement across the skin, which are sensations linked to the peak of orgasm), (2) ~ 0.5 -1.5 million **Layer 5 pyramidal neurons in the primary somatosensory cortex (S1)** (to create a more integrated body-state sensation during orgasm, contributing to the full-body experience of heightened tactile arousal and movement coordination), (3) ~ 1 -2 million **neurons in the secondary somatosensory cortex (S2)** (to enhance the emotional intensity of the tactile sensations, helping (A) simulate the pleasure and satisfaction associated with orgasm, (B) bind tactile sensations into a coherent whole to make the experience feel smooth and natural, and (C) make the tactile sensations feel emotionally pleasurable or rewarding), (4) ~ 3 -6 million **Layer 2/3 pyramidal neurons (interconnected cortical layers)** (to simulate a diffuse whole-body tactile experience and ensure that the tactile sensations felt during orgasm are widespread and coordinated across different body parts, as is common in a peak orgasmic experience), and (5) ~ 0.5 -1.5 million **Layer 6 neurons (thalamocortical loop)** (to help maintain the continuity, persistence and rhythm of the tactile sensations, creating a more fluid and prolonged sensory experience throughout orgasm).

brain (there is one of each of the aforementioned brain regions in each hemisphere), giving a total whole-brain $0.22\text{--}0.36\text{ mm}^3$ robot dose assuming one robot per neuron.

Further details of this intervention are outside the scope of the present paper because the generation of orgasms might obviate the need for penile erection if the user's primary or sole objective is to seek pleasurable sensations,⁷⁶⁶ making this matter off-topic in a discussion primarily concerned with treatments for erectile dysfunction.

5.3.3.3 Continuous Orgasms

Extending the male physical orgasmic experience beyond the usual 3-10 sec to a duration of many minutes (or longer) of continuous orgasm⁷⁶⁷ would require significant alterations to typical biological feedback mechanisms, such as extending dopaminergic and oxytocinergic activation, preventing the refractory period, and managing physical sensitivity and fatigue.⁷⁶⁸ Suppressing or

⁷⁶⁶ e.g., like the indefatigable electrically self-stimulating rats, in: Olds J, Milner P. Positive reinforcement produced by electrical stimulation of septal area and other regions of rat brain. *J Comp Physiol Psychol*. 1954 Dec;47(6):419-27; <https://seminarioneuounam.wordpress.com/wp-content/uploads/2014/04/olds-milner.pdf>.

⁷⁶⁷ "il Dormiglione" (The Orgasmatron), from Woody Allen's *The Sleeper* (1972); https://www.youtube.com/watch?v=jBmCe_Vt76M. See also: <https://www.youtube.com/watch?v=uZvpIE5g5Fo>.

⁷⁶⁸ To enable a continuous physical orgasm, nanorobots would have to prevent muscle fatigue in the bulbospongiosus, ischiocavernosus, prostate, and anal sphincter muscles that are responsible for ejaculation contractions and the pleasurable pulsating sensations felt during orgasm. Nanorobots equipped with onboard tankage (or capable of simple-molecule synthesis; [Section 5.3.1.1](#)) and sorting rotors (both intracellular and extracellular) positioned at each muscle cell could actively manage several critical metabolic pathways by injecting or extracting biochemicals from the cytosol allowing muscles to contract indefinitely without fatigue, by: (1) **extracting lactic acid** (whose accumulation during anaerobic metabolism contributes to muscle fatigue by lowering intracellular pH), (2) **extracting hydrogen ions** (the pH drop caused by excess H^+ from glycolysis can inhibit enzyme activity and contractile proteins), (3) **injecting bicarbonate ions** into the cytosol (HCO_3^- buffers the H^+ ions, maintaining pH balance and delaying fatigue), (4) **transporting potassium ions** into the cytosol (continuous contractions require K^+ replenishment to avoid muscle cell depolarization), (5) **transporting sodium ions** out of the cytosol (Na^+ accumulation inside muscle cells during prolonged contraction can disrupt ionic gradients, so removing excess ions helps maintain normal cell excitability), (6) **extracting reactive oxygen species** (continuous muscle contraction generates ROS that can damage cellular components and contribute to fatigue), (7) **transporting metabolic byproducts** out of the cytosol, including inorganic phosphate (which accumulates during ATP breakdown and interferes with muscle contraction by reducing calcium sensitivity of contractile proteins) and ammonia (a byproduct of amino acid metabolism during prolonged exercise, whose accumulation can cause fatigue), (8) **managing calcium ion flows** within the cytosol by extracting excess calcium (to avoid overload and allow proper muscle relaxation) or injecting calcium (if calcium release from the sarcoplasmic reticulum becomes insufficient to sustain contraction) as needed to sustain contractions without fatigue, and (9) **importing enough extracellular oxygen and glucose** into the cytosol to offset anaerobic conditions created by continuous muscle contraction. Additionally, to help protect the muscle cell against thermal stress and protein denaturation during the intense activity of continuous contraction, nanorobots should **raise the cytosolic concentration of heat shock proteins** from normal

delaying the full inhibition of certain brain circuits via GABAergic neurons (which create a release of tension that is part of the orgasmic experience) could prevent the rapid peak-and-drop pattern of a standard orgasm. Extending orgasm without causing discomfort would also require methods to desensitize the pain pathways while keeping pleasure circuits active, such as modulating the activity of nociceptors or increasing endorphin release.

Just as muscles become fatigued after prolonged exertion and sensory systems like olfaction become desensitized to a constant stimulus, neural circuits involved in orgasm are subject to similar adaptive mechanisms that reduce responsiveness after prolonged stimulation. Producing a continuous orgasm of lengthy duration would require eliminating several mechanisms of neural habituation including diminishing dopamine response, neurotransmitter depletion, receptor desensitization, GABAergic inhibition and homeostasis, and fatigue in cortical and subcortical networks. While various methods by which ecstacy nanorobots can achieve these objectives are readily imagined,⁷⁶⁹ further detailed analysis of the technical and implementation issues is beyond the scope of this paper.

levels near 1-10 μM to 50-100 μM to provide a strong buffer against ongoing thermal stress, ensuring that the cell maintains proper protein folding capacity and avoids degradation pathways that contribute to fatigue or cell death. This would require multiple nanorobots to inject into, and later extract from, the cytosol of each bulbospongiosus muscle cell ($\sim 50 \mu\text{m}$ diameter, $\sim 1000 \mu\text{m}$ long) approximately $\Delta V_{\text{Hsp70}} \sim \Delta c_{\text{Hsp}} V_{\text{Mcell}} m_{\text{Hsp70}} / \rho_{\text{Hsp70}} \sim 7300 \mu\text{m}^3/\text{cell}$ of heat shock proteins, taking cell volume $V_{\text{Mcell}} = 2 \times 10^6 \mu\text{m}^3$, required Hsp concentration change $\Delta c_{\text{Hsp}} \sim 70 \mu\text{M}$, and molecular weight and density of Hsp70 (a typical Hsp; <https://en.wikipedia.org/wiki/Hsp70>) of $m_{\text{Hsp70}} = 70,000 \text{ gm/mole}$ and $\rho_{\text{Hsp70}} \sim 1.35 \text{ gm/cm}^3$, respectively, assuming the nanorobots cannot more efficiently upregulate rapid natural Hsp production.

⁷⁶⁹ **Neurotransmitter depletion** could be prevented using devices that can enter neurons or surrounding cells and continuously inject supplemental dopamine, serotonin, or other necessary neurotransmitters as they become depleted, which would maintain the activation of reward and pleasure pathways in the brain without allowing depletion to occur. **Receptor desensitization** could be counteracted by nanorobots that enter cells and manipulate the receptors themselves, either by preventing desensitization or by artificially re-sensitizing receptors once they have become unresponsive, possibly by injecting molecules that block receptor internalization or recycling processes. **Homeostatic inhibitory mechanisms** could be overridden either by targeting GABAergic interneurons or other inhibitory neurons in areas like the mPOA, nucleus accumbens, or VTA to reduce their activity (either by injecting chemicals that block GABA receptors or by electrically inhibiting the neurons themselves, preventing them from dampening the pleasure signals), or by electrically stimulating only the excitatory neurons involved in pleasure and orgasm while avoiding or suppressing inhibitory neurons, bypassing the circuits responsible for shutting down the orgasmic experience and allowing the pleasurable sensations to be extended indefinitely. **Neural excitability** might be maintained either by injecting ion channel modulators that enhance the excitability of neurons, allowing them to continue firing without the typical fatigue (e.g., injecting calcium channel modulators to keep neurons firing at higher rates, preventing the usual decline in excitability) or by directing nanorobots to periodically adjust the internal ion balance of neurons, actively restoring the neurons' excitability by modulating the ionic environment (e.g., injecting potassium or calcium buffers), thus preventing neurons from becoming overworked and reducing the likelihood of circuit failure due to fatigue. The male **refractory period** might be suppressed by injecting molecules that block the production or release of prolactin during orgasm (e.g., dopamine agonists such as bromocriptine), preventing its inhibitory effects on arousal and pleasure, and modulating oxytocin release (by either inhibiting its release or blocking its receptors temporarily). **Neural fatigue** in pleasure circuits due to prolonged stimulation of the ventral tegmental area and nucleus accumbens during orgasmic experiences, leading to neural fatigue in the dopamine pathways, could be prevented by nanorobots targeting and stimulating supporting neural networks in the prefrontal cortex or hypothalamus that modulate the activity of the pleasure circuits,

After outlining the above theoretical approach to achieving continuous orgasms of unbounded duration using nanorobots, the author asked the online AI assistant ChatGPT4o to survey the human literary universe and conceptualize how to describe the sensation of a lengthy continuous orgasm, based on how people have described shorter orgasmic experiences, but now magnified and stretched over time. The enlightening responses fell into eight categories, including “unrelenting waves of pleasure”,⁷⁷⁰ “heightened sensory experience”,⁷⁷¹ “loss of time and space”,⁷⁷² “euphoria and emotional intensity”,⁷⁷³ “sensory overload and intensity”,⁷⁷⁴ “body-wide

creating an alternating pattern of stimulation that prevents any one network from becoming fatigued, or by using controlled bursts of stimulation to keep neurons firing without inducing fatigue, as alternating between stimulation of different groups of neurons could maintain a high level of pleasure perception while giving individual neurons time to recover. **Pain sensitivity and discomfort** could be mitigated by selectively targeting nociceptors (pain receptors) in the genital region to inhibit their activity by injecting local anesthetic molecules or neurotransmitters that suppress pain signaling (e.g., endorphins or enkephalins) or by selectively enhancing sensory circuits that provide pleasure while suppressing pain circuits, requiring real-time feedback from the sensory neurons to determine which neurons should be inhibited or excited to maintain pleasure without discomfort.

⁷⁷⁰ The hallmark of a continuous orgasm might be described as **unceasing waves of pleasure** that ebb and flow through the body without a break. Instead of the rapid climax and sharp decline typical of an orgasm, the sensations would persist at or near the peak of intensity for an extended period. The individual might feel as if they are suspended in a state of euphoria, with each wave of pleasure building on the previous one without fading. Possible descriptions: *“It feels like being caught in an endless surge of bliss, where every nerve in my body is alive and vibrating with pleasure.”* *“The sensation is one of rolling, pulsating waves – each crest more intense than the last, but instead of breaking, they just keep coming, flowing through me.”*

⁷⁷¹ A prolonged orgasm would likely be accompanied by an **amplified perception of bodily sensations**. The brain’s sensory circuits would remain hyper-engaged, meaning the person might feel ultra-sensitive to every small movement, touch, or internal shift. There might be an overwhelming awareness of pleasure in every part of the body, not just the genitals. Possible descriptions: *“It’s as if every inch of my skin is tingling, hypersensitive to the faintest breath or touch. I’m consumed by the sensation, and it radiates outward from my core.”* *“The pleasure isn’t localized – it spreads, seeping into my limbs, my chest, my head. It’s as though I’m dissolving into the feeling.”*

⁷⁷² An extended orgasm might also lead to a profound sense of **disconnection from time and space**. As the brain’s reward and pleasure circuits remain activated, cognitive processes related to time might become blurred, leading to a sense of timelessness or immersion in the experience. Possible descriptions: *“Time feels meaningless – I can’t tell if it’s been seconds, minutes, or hours. The sensation is so all-encompassing that I’ve lost my sense of everything else.”* *“I’m floating in the pleasure – my body feels distant, and I’m existing entirely within the sensations, detached from everything around me.”*

⁷⁷³ An extended orgasm could intensify the **emotional and euphoric components** of the experience. The prolonged release of dopamine, oxytocin, and endorphins would likely create an overwhelming sense of joy, ecstasy, and even emotional vulnerability. Feelings of connection, love, and profound satisfaction might be drawn out over the course of the experience. Possible descriptions: *“It feels like I’m overflowing with joy, love, and euphoria – like every beautiful emotion I’ve ever felt has been magnified and is washing over me in waves.”* *“It’s an emotional high that is almost too much to handle. I feel incredibly vulnerable, but also deeply connected to myself and the experience, like a blissful surrender.”*

muscle contractions”,⁷⁷⁵ “emotional and physical exhaustion”,⁷⁷⁶ and “psychological impact”.⁷⁷⁷ In sum, the sensation of a continuous orgasm lasting many minutes or longer would likely be described as an overpowering, euphoric, and all-consuming experience, marked by heightened pleasure, emotional intensity, and a profound loss of time and self. While pleasurable at first, the intensity might become overwhelming or exhausting over time, leading to a sense of sensory and emotional overload. It could feel like floating in a state of bliss that is both exhilarating and demanding, with pleasure waves moving through the body, skirting the edge of overstimulation.

It is unclear if “status orgasmus” (e.g., a 43-second orgasmic state recorded in one female subject by Masters and Johnson in 1966)⁷⁷⁸ or Expanded Sexual Response (ESR) in women (reportedly

⁷⁷⁴ While the prolonged pleasure might be exhilarating at first, there could also be elements of overwhelm or even **sensory overload** if the intensity is sustained for too long. As the brain and body are not typically used to experiencing such prolonged pleasure, the person might describe the feeling as being overstimulated or even helpless in the face of such intensity. Possible descriptions: *“The pleasure is so intense, it’s almost unbearable – like I’m teetering on the edge of bliss and overwhelm, but I can’t pull back, and I don’t want to.” “It feels as though I’m caught in an unstoppable flood of sensation, and I have no control over how much pleasure I’m experiencing. It’s exhilarating, but it’s also almost too much.”*

⁷⁷⁵ The physical aspect of orgasm involves rhythmic **muscle contractions**, particularly in the pelvic floor. During a continuous orgasm, these contractions might be extended or sustained, leading to a sensation of muscular tension and release spread across the entire body. The person might feel locked in a state of pleasurable tension, punctuated by ongoing, involuntary spasms of blissful release. Possible descriptions: *“My entire body is caught in this rhythm of tightening and releasing – like every muscle is being stimulated to the point of exhaustion, but instead of tiring, the sensation only grows.” “The contractions come in waves, but they never let go completely – it feels like being pulled taut, then released into a state of relaxation, only to tighten again.”*

⁷⁷⁶ While pleasurable, the unrelenting nature of a prolonged orgasm might eventually lead to **emotional and physical exhaustion**. The continuous stimulation might feel overwhelming as the body struggles to cope with the intensity over a long period. This could lead to a sensation of helpless surrender to the pleasure, as if the person is at the mercy of their body’s responses. Possible descriptions: *“I’m overwhelmed by the pleasure, it’s almost exhausting – but in a way that makes me want more. It feels like I’m being carried by the sensation, and I can’t resist it.” “It’s a beautiful kind of exhaustion, where every moment is filled with pleasure, but I can feel my body getting worn down, even though the sensation hasn’t stopped.”*

⁷⁷⁷ Experiencing an extended orgasm might have a significant **psychological impact** as well. The sheer intensity and duration could blur the lines between pleasure and pain at times, particularly if the experience becomes overwhelming. However, if the stimulation remained pleasurable, the individual might describe a profound sense of fulfillment or transcendence. Possible descriptions: *“It’s almost too intense to handle, but it feels like I’ve reached a state of pure bliss, something beyond anything I’ve ever known.” “There’s a point where the pleasure almost becomes painful because it’s so intense, but it’s like I’ve reached a new level of sensation, something that’s hard to describe.”*

⁷⁷⁸ Masters WH, Johnson VE. Human Sexual Response. Little, Brown and Company, 1966; <https://www.amazon.com/Human-Sexual-Response-William-Masters/dp/0316549878>.

lasting 1-15 min or more)⁷⁷⁹ is a true continuous orgasm or merely a series of multiorgasmic events. It appears that ESR has not yet been formally reported or confirmed in males.

5.4 Nanorobotic Prostheses for ED

A prosthesis⁷⁸⁰ or prosthetic implant is an artificial device that either replaces a missing body part (which has been lost through surgery, physical trauma, disease, or congenital disorder) or restores the normal functions of a nonfunctional body part, such as a male penis afflicted with erectile dysfunction. In this Section we describe four conceptual designs for nanorobotic prostheses to eliminate ED of progressively greater versatility and sophistication, including:

(1) a “Maypole implant” comprising a cylindrical-shaped macroscale nanomechanical robot that is implanted in the penis like a traditional penile implant, but with greatly improved sexual performance characteristics ([Section 5.4.1](#));

(2) a nanorobotic condom or “nanoglove” that provides a motorized flexible sheath that can expand into the shape and size of a fully erect penis, with full sensory feedback from the condom exterior to the enveloped biological organ ([Section 5.4.2](#));

(3) a “lifter mesh” implanted throughout the penile tissue that provides geometric control and the benefits of direct skin-on-skin contact during coitus ([Section 5.4.3](#)); and

(4) a “utility penis” that represents the ultimate multifunctional and maximally versatile penile prosthesis ([Section 5.4.4](#)).

5.4.1 Maypole Implant

A penile prosthesis, aka. penile implant ([Section 4.6](#)), is a medical device surgically implanted within the penis to allow men with erectile dysfunction to achieve an erection. The most common type of penile implant (image, right),⁷⁸¹ intended to closely mimic the natural erection process, consists of a pair of sterile-saline fluid-filled cylinders implanted into the cavernous body of the



⁷⁷⁹ Sayin HU. Doors of Female Orgasmic Consciousness: New Theories on the Peak Experience and Mechanisms of Female Orgasm and Expanded Sexual Response. *NeuroQuantology* 2012 Nov; 10(4):692-714; https://www.academia.edu/download/32946238/SAYIN-NeuroQuantology-13-Doors_of_Female_Orgasmic_Consciousness.pdf. Sayin HU. Five Cases with Expanded Sexual Response (ESR). *Ann Clin Case Stud*. 2019;1:10-19; https://www.academia.edu/download/59525416/Sayin-U-Annals_of-Clinical-Case-Studies-Five-cases-with-expanded-sexual-response-esr-2019-1-1-100520190604-78645-z3i3wq.pdf.

⁷⁸⁰ <https://en.wikipedia.org/wiki/Prosthesis>.

⁷⁸¹ https://en.wikipedia.org/wiki/Penile_implant#/media/File:Penile_Implant.png.

penis, a pump placed in the scrotum, and a fluid reservoir placed in the abdomen. A simple similarly-sized ($\sim 25 \text{ cm}^3$) nanorobotic penile implant would comprise a cylindrical-shaped nanomechanical robot with gas-tight expansible internal chambers with metamorphic walls,⁷⁸² a $V_{\text{tank}} \sim 30 \text{ mm}^3$ diamondoid pressure tank⁷⁸³ containing compressed nitrogen gas stored at $p_{\text{storage}} \sim 1000 \text{ atm}$,⁷⁸⁴ pressure valves and gas pumps to empty and refill the tank,⁷⁸⁵ expansion sensors to measure device inflation, nanomotors to laterally and longitudinally flex the robot in various controlled motions, acoustic/vibration sensors to receive external control commands and import power from external sources from acoustic-powered energy generators,⁷⁸⁶ efficient energy storage systems,⁷⁸⁷ and a nanocomputer control system to monitor and coordinate all device activities.

Besides the quick-erection function bestowed by the conventional penile implant, a nanorobotic Maypole⁷⁸⁸ implant would additionally provide:

⁷⁸² Freitas RA Jr. Nanomedicine, Volume I: Basic Capabilities. Landes Bioscience, Georgetown, TX, 1999; Section 5.3, “Metamorphic Surfaces”; <http://www.nanomedicine.com/NMI/5.3.htm>.

⁷⁸³ The expansion chambers in each robot would need to receive $\Delta V \sim V_{\text{erect}} - V_{\text{flaccid}} = 77 \text{ cm}^3$ of N_2 gas at $p_{\text{erect}} \sim 0.16 \text{ atm}$ (120 mmHg) pressure to establish and maintain a penile erection equivalent in size to a natural erection (Section 2.5), requiring $n_{\text{inflateN}_2} = p_{\text{erect}} \Delta V / R_{\text{gas}} T_{\text{body}} \sim 2.92 \times 10^{20}$ nitrogen molecules at body temperature $T_{\text{body}} = 310 \text{ K}$ and universal gas constant $R_{\text{gas}} = 1.36 \times 10^{-28} \text{ m}^3\text{-atm/molecule-K}$. The robot would receive this gas from compressed nitrogen gas stored in an onboard diamondoid tank of volume $V_{\text{tankN}_2} = n_{\text{inflateN}_2} / n_{\text{tankN}_2} \sim \mathbf{27.6 \text{ mm}^3/\text{robot}}$ that holds $n_{\text{tankN}_2} \sim 106 \times 10^{26} \text{ N}_2 \text{ molecules/m}^3$ at $p_{\text{storage}} \sim 1000 \text{ atm}$ pressure. (Note that Zephyrs “special kit for large penis” (<https://en.zsimplants.ch/products/zsi-475/documents/surgeons>) uses $\Delta V \sim 70 \text{ cm}^3$ of fluid to inflate both cylinders.)

⁷⁸⁴ Freitas RA Jr. Nanomedicine, Volume I: Basic Capabilities. Landes Bioscience, Georgetown, TX, 1999; Table 10.2, “Gas Molecules Packed into a Pressure Vessel”; <https://www.nanomedicine.com/NMI/Tables/10.2.jpg>.

⁷⁸⁵ An onboard flywheel energy storage unit of volume $V_{\text{flywheel}} = p_{\text{storage}} V_{\text{tank}} / E_{\text{D,flywheel}} = \mathbf{0.06 \text{ mm}^3}$ stores enough energy to compress chamber N_2 back into the tank once, assuming flywheel energy density $E_{\text{D,flywheel}} \sim 50 \text{ MJ/L}$ ($5 \times 10^{10} \text{ J/m}^3$).^{*} For redundancy, each robot could harbor multiple such units which could be remotely recharged at leisure, but, as with regenerative braking,[†] much of the energy released during penile erection by the expansion of the compressed gas could probably be recaptured and stored for later use by the pumps for gas re-compression into the tank.

^{*} Freitas RA Jr. Nanomedicine, Volume I: Basic Capabilities. Landes Bioscience, Georgetown, TX, 1999; Section 6.2.2.2, “Flywheels”; <http://www.nanomedicine.com/NMI/6.2.2.2.htm>. Freitas RA Jr. Energy Density. IMM Report No. 50, 25 June 2019; Section 5.3.2, “Rotational Motion”; <http://www.imm.org/Reports/rep050.pdf>.

[†] https://en.wikipedia.org/wiki/Regenerative_braking.

⁷⁸⁶ Freitas RA Jr. Nanomedicine, Volume I: Basic Capabilities. Landes Bioscience, Georgetown, TX, 1999; Section 6.3, “Power Conversion”; <http://www.nanomedicine.com/NMI/6.3.htm>.

⁷⁸⁷ Freitas RA Jr. Nanomedicine, Volume I: Basic Capabilities. Landes Bioscience, Georgetown, TX, 1999; Section 6.2, “Energy Storage”; <http://www.nanomedicine.com/NMI/6.2.htm>.

⁷⁸⁸ <https://en.wikipedia.org/wiki/Maypole>.

(1) the ability to generate acoustic pressure or sound waves, similar to vibrators,⁷⁸⁹ that would excite participants of both genders during coitus, including vibrations at acoustic frequencies most likely to induce orgasms in women ([Section 5.3.1.7](#));

(2) the ability to rapidly alter penile size by varying its expansion parameters, allowing it to periodically mechanically oscillate in length (i.e., “thrust”), girth (i.e., “throb”), and volume;

(3) the ability to waggle the entire penis from side to side or up and down, or to move the tip of the penis to trace out circular, oval, Lissajous,⁷⁹⁰ or other kinematic motions; and

(4) real-time user control of all accessible penile dimensions, motions, and functions via tactile (e.g., slapping buttocks or thighs)⁷⁹¹ or acoustic (e.g., coded ultrasonic signals from an attachment to the users cell phone; [Section 5.3.2.3](#)) inmessaging at the user’s pelvis.

5.4.2 Nanorobotic Condom (Nanoglove)

A condom⁷⁹² is a sheath-shaped barrier device traditionally used during sexual intercourse to reduce the probability of pregnancy or a sexually transmitted infection. The external condom is rolled onto an erect penis before intercourse and works by forming a physical barrier which limits skin-to-skin contact, exposure to fluids, and blocks semen from entering the body of a sexual partner. Many condoms incorporate spermicides to enhance their contraceptive effectiveness, and some are designed to enhance the pleasure of the sexual act, e.g., by incorporating lubricants, patterned ribbing and studs⁷⁹³ (image, right),⁷⁹⁴ and other features that can create additional sensations during copulation. As will be described, the nanorobotic condom, or “nanoglove”, will be a robotic prosthesis⁷⁹⁵ that can do all of this and much more.



First, and most importantly in the context of the present paper, the nanorobotic condom eliminates the problem of erectile dysfunction by providing a motorized flexible sheath that can expand into the shape and size of a fully erect penis. Placed over the glans (tip) of a flaccid penis, the mechanized nanoglove unrolls itself along the shaft until it reaches the base of the penis,

⁷⁸⁹ Rullo JE, Lorenz T, Ziegelmann MJ, Meihofer L, Herbenick D, Faubion SS. Genital vibration for sexual function and enhancement: a review of evidence. *Sex Relation Ther.* 2018;33(3):263-274; <https://www.ncbi.nlm.nih.gov/pmc/articles/PMC7678782/pdf>.

⁷⁹⁰ https://en.wikipedia.org/wiki/Lissajous_curve.

⁷⁹¹ Freitas RA Jr. *Nanomedicine, Volume I: Basic Capabilities*. Landes Bioscience, Georgetown, TX, 1999; Section 7.4.2.1, “Mechanical Inmessaging”; <http://www.nanomedicine.com/NMI/7.4.2.1.htm>.

⁷⁹² <https://en.wikipedia.org/wiki/Condom>.

⁷⁹³ https://en.wikipedia.org/wiki/Condom#Ribbed_and_studded.

⁷⁹⁴ <https://www.amazon.com/Ultra-Standard-Condoms-Experience-Partner/dp/B0CQFLLWYN/>.

⁷⁹⁵ https://en.wikipedia.org/wiki/Prosthesis#Robotic_protheses.

where it creates a gentle adhesive seal just below the mons pubis near the abdominal wall and along the top of the scrotal sac on the underside while carefully avoiding pinching any pubic hairs. (Spray-on application⁷⁹⁶ is also possible.) Upon receiving the command to mantle the penis with a full erection, the $x_{\text{nanoglove}} \sim 1$ mm thick walls of the motorized condom contract until they come into direct contact with the foreskin (of uncircumcised males) or the epithelium (of circumcised males) of the penis, establishing thousands of weakly adhesive contact points. The nanoglove then slowly extends itself from the flaccid $L_{\text{flaccid}} \sim 9.2$ cm length to the full $L_{\text{erect}} \sim 13.1$ cm erection length, gently dragging the contact points forward and stretching the elastic penile tissues while maintaining a snug fit to the fully enclosed organ. At the same time, $N_{\text{chambers}} \sim A_{\text{erect}} / A_{\text{chamberA}} \sim 15,000$ balloon chambers each of area $A_{\text{chamberA}} \sim 1 \text{ mm}^2$ at the exterior surface of the nanorobotic condom, which are also in adhesive contact with $A_{\text{chamberB}} \sim 0.67 \text{ mm}^2$ of the external skin surface of the stretched penis,⁷⁹⁷ are filled with pressurized nitrogen gas, causing the balloons to expand to a length of $L_{\text{balloon}} \sim (0.5) (D_{\text{erect}} - D_{\text{contracted}}) \sim 6$ mm, taking $D_{\text{erect}} \sim 3.7$ cm, $D_{\text{contracted}} \sim 2.5$ cm,⁷⁹⁸ and $A_{\text{erect}} \sim \pi D_{\text{erect}} L_{\text{erect}} \sim 150 \text{ cm}^2$ as the outer surface area of an erect penis (or fully inflated nanoglove). The pressurized nitrogen gas can be provided either from an onboard tank (Section 5.4.1) or by direct air extraction.

In terms of its look and feel, the texture of the outer skin of the nanorobotic condom can be very soft and flexible, with surface corrugations at the 1-10 μm scale enabling it to feel velvety to the touch. Nanomotors embedded in the walls of the nanoglove would permit control over device length, width, stiffness, the size and number of time-variable surface ribbings and studs, and gross motions in all directions (within the physical operating envelope constraints of the device), allowing it to mechanically oscillate in length, girth, and sensible volume at a variety of frequencies. Much like the Maypole implant (Section 5.4.1), but applied over the entire external surface of the nanoglove, nanomachinery in the skin of the nanorobotic condom could generate acoustic vibrations and physical pulsations similar to vibrator sex toys. Nanoscale devices mounted in the condom walls could also provide perfect coloration,⁷⁹⁹ allowing the nanoglove exterior to project an image of a biologically normal penis; or, if the user is more adventurous, made to look like almost anything, from a yellow banana to the sleek silvery fuselage of a jet fighter with colorful racing stripes. Other nanoscale devices in the condom walls could create artificial heating in virtually any spatial or temporal pattern desired. As before, the user can exert real-time control over all accessible penile dimensions, motions, and functions via tactile (e.g., slapping buttocks or thighs)⁸⁰⁰ or acoustic (e.g., coded ultrasonic signals from an attachment to

⁷⁹⁶ https://en.wikipedia.org/wiki/Spray-on_condom.

⁷⁹⁷ The contact area on the surface of the stretched flaccid penis is $A_{\text{SFpenis}} \sim \pi D_{\text{contracted}} L_{\text{erect}} \sim 100 \text{ cm}^2$, so the base of each balloon chamber in contact with the penis is only $A_{\text{chamberB}} \sim (A_{\text{chamber}}) (A_{\text{SFpenis}} / A_{\text{erect}}) \sim 0.67 \text{ mm}^2$, taking $A_{\text{erect}} \sim 150 \text{ cm}^2$.

⁷⁹⁸ The flaccid penis of volume $V_{\text{flaccid}} = (\pi/4) D_{\text{flaccid}}^2 L_{\text{flaccid}} = (\pi/4) D_{\text{contracted}}^2 L_{\text{erect}} \sim 64 \text{ cm}^3$ is stretched to a length of $L_{\text{erect}} \sim 13.1$ cm which causes the diameter of the still-flaccid penis to contract from $D_{\text{flaccid}} \sim 3$ cm to $D_{\text{contracted}} \sim (4 V_{\text{flaccid}} / \pi L_{\text{erect}})^{1/2} \sim 2.5$ cm assuming an unchanged penile volume of V_{flaccid} .

⁷⁹⁹ Freitas RA Jr. Nanomedicine, Volume I: Basic Capabilities. Landes Bioscience, Georgetown, TX, 1999; Section 5.3.7, "Chromatic Modification"; <http://www.nanomedicine.com/NMI/5.3.7.htm>.

⁸⁰⁰ Freitas RA Jr. Nanomedicine, Volume I: Basic Capabilities. Landes Bioscience, Georgetown, TX, 1999; Section 7.4.2.1, "Mechanical Inmessaging"; <http://www.nanomedicine.com/NMI/7.4.2.1.htm>.

the user's cell phone; [Section 5.3.2.3](#)) in messaging from a device briefly touched to the user's pelvis.

However, the nanorobotic condom's most important feature is the network of sensory transducers embedded in the device's outer surface and directly connected to the user's penile epidermal sensorium, perhaps including one set of transducer channels for every balloon chamber. The penile skin includes biological tactile receptors for pressure, stretch, shear, edge, and touch with number densities in the 10-100/cm² range.⁸⁰¹ Sensors on the nanoglove exterior could detect sensory information on temperature, shear force, normal force, and so forth, and transmit this information to actuators that can directly stimulate the biological sensors on the penile surface, effectively transducing these sensations to the surface of the penis as if the penile surface had directly felt the sensations, aka. full penile force-feedback. In principle, sensors in contact with the penile surface could measure temperature changes and tissue movements within the organ and transduce these to nanoglove surface effectors, causing those temperatures or movements to be instantly replicated on the condom surface. This entire scheme would seem to meet Bill Gates' stated goal when he once offered a \$100,000 grant (for public health reasons) for a condom design that "significantly preserves or enhances pleasure" in order to encourage more males to adopt the use of condoms for safer sex.⁸⁰²



One particularly uncomfortable-looking and primeval analogue of the nanoglove employing only contemporary basic plastics technology is a penile support device consisting of a "penile cast" intended to be worn externally during intercourse (image, left).⁸⁰³

Apparently created by Japanese researcher Takehisa Iwai⁸⁰⁴ in the early 2010s, the device is composed of a body and

attachments that provide rigidity to the penile shaft, was available in three sizes (medium, large, and extra-large), and has two coronal glans openings to provide direct sensation during intercourse. Notes one overoptimistic reviewer: "There have been no published trials to establish the efficacy of the device at this time, [but] it may serve as an option for patients with end-organ failure who may not be candidates for, or unable to afford, penile implants." Penis sleeves (image, right)⁸⁰⁵ are used primarily to increase the stimulation of the person being penetrated.



⁸⁰¹ Freitas RA Jr. Nanomedicine, Volume I: Basic Capabilities. Landes Bioscience, Georgetown, TX, 1999; Section 7.4.6.1, "Somesthetic Outmessaging", Table 7.3; <http://www.nanomedicine.com/NMI/7.4.6.1.htm>.

⁸⁰² Jessica Chasmar, "Bill Gates offers \$100,000 grant for improved condoms," Washington Times, 24 Mar 2013; <https://www.washingtontimes.com/news/2013/mar/24/bill-gates-offers-100000-grant-improved-condoms/>.

⁸⁰³ Stein MJ, Lin H, Wang R. New advances in erectile technology. Ther Adv Urol. 2014 Feb;6(1):15-24; <https://www.ncbi.nlm.nih.gov/pmc/articles/PMC3891291/pdf>.

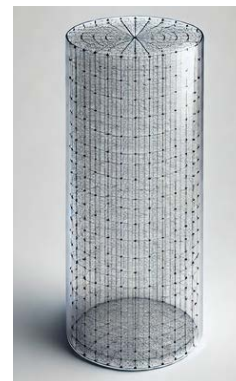
⁸⁰⁴ <https://www.omicsonline.org/author-profile/takehisa-iwai-246107/> and <https://www.researchgate.net/profile/Takehisa-Iwai>.

⁸⁰⁵ https://en.wikipedia.org/wiki/Sex_toy#Penile_toys.

Like conventional condoms, the future nanoglove may include a tip reservoir to catch and retain the ejaculate. However, unlike today's condoms, if the participants desire the condom could open an aperture at the tip allowing stored semen to be (1) forcefully ejected in a close approximation of a real ejaculation (but delayed in time or at increased velocity, and at the user's discretion), or (2) dribbled out slowly into a collection vessel for subsequent use in sperm-banking, IVF, genetic testing, or other reproduction-related applications.

5.4.3 Lifter Mesh Implant

The lifter mesh is a more intrusive implanted penile prosthesis that would provide geometric control and skin-on-skin contact during coitus. In this concept, a 3D web of linked biocompatible⁸⁰⁶ nanomechanical fibers (image, right) capable of motorized length extension or retraction by a fairly modest factor of $(V_{\text{erect}} / V_{\text{flaccid}})^{1/3} \sim 1.3$ (i.e., ~30%) is emplaced throughout the penile tissue. With proper design, telescoping extension of all the biocompatible-coated fibers by 30% in length would cause the fiber-embedded tissue to expand from the flaccid ($V_{\text{flaccid}} \sim 64 \text{ cm}^3$) to the erect ($V_{\text{erect}} \sim 141 \text{ cm}^3$) configuration.



How much longitudinal force must each fiber in the 3D lifter mesh provide, without buckling, to drive a flaccid penis into a mechanically erect state?

During a natural erection, vascular pressures rise from 10-20 mmHg (1300-2700 Pa) on the venous side to near or slightly above normal systolic systemic blood pressure of $p_{\text{erect}} \sim 120 \text{ mmHg}$ (16,000 Pa) temporarily during the peak of sexual arousal and rigidity (Section 2.5). For comparison, blood pressures exceeding ~140 mmHg (19,000 Pa) are considered hypertensive⁸⁰⁷ and the highest blood pressure ever recorded in a living human was 370 mmHg (49,000 Pa).⁸⁰⁸ Conservatively assuming a maximum fiber buckling force of $p_{\text{buckle}} \sim 30,000 \text{ Pa}$ and a Young's modulus for diamondoid fibers of $E_{\text{fiber}} \sim 5 \times 10^{10} \text{ N/m}^2$ for fibers of length of $L_{\text{fiber}} \sim 1 \text{ mm}$, the minimum fiber radius is $R_{\text{fiber}} \sim (4 L_{\text{fiber}}^2 p_{\text{buckle}} / \pi^2 E_{\text{fiber}})^{1/2} \sim 0.5 \text{ }\mu\text{m}$.⁸⁰⁹

The force required to mechanically expand the penis to its erect volume is $F_{\text{erect}} \sim \pi D_{\text{flaccid}} L_{\text{flaccid}} p_{\text{erect}} \sim 140 \text{ N}$. As the fibers in the penile-implanted lifter mesh extend, they must not exert so

⁸⁰⁶ Freitas RA Jr. Nanomedicine, Volume IIA: Biocompatibility. Landes Bioscience, Georgetown, TX, 2003; 15.5.3.6 "Non-Occluding Indwelling Vascular Obstructions"; <http://www.nanomedicine.com/NMIIA/15.5.3.6.htm>.

⁸⁰⁷ https://en.wikipedia.org/wiki/Blood_pressure.

⁸⁰⁸ Narloch JA, Brandstater ME. Influence of breathing technique on arterial blood pressure during heavy weight lifting. Arch Phys Med Rehabil. 1995 May;76(5):457-62; <https://pubmed.ncbi.nlm.nih.gov/7741618/>.

⁸⁰⁹ Freitas RA Jr. Nanomedicine, Volume I: Basic Capabilities. Landes Bioscience, Georgetown, TX, 1999; Section 9.3.1.2, "Nanocilium Manipulators"; <http://www.nanomedicine.com/NMI/9.3.1.2.htm>.

much force that they cut through the tissue, aka. the “wire strainer” effect.⁸¹⁰ The yield strength is where tissue begins to permanently deform but not break, which is much lower than the tensile strength which is the maximum load-bearing capacity beyond which the tissue actually breaks. Conservatively estimating the maximum yield strength of penile soft tissue as $Y_{\text{penile}} \sim P_{\text{erect}} \sim 16,000 \text{ Pa}$, an expanding hoop of fibers pressing laterally on soft tissue can safely apply $F_{\text{max}} = 2 R_{\text{fiber}} L_{\text{fiber}} Y_{\text{penile}} = 16 \mu\text{N}/\text{fiber}$, so to safely erect the penis we need $N_{\text{fibers}} = F_{\text{erect}} / F_{\text{max}} \sim 9 \times 10^6$ fibers of total length $N_{\text{fibers}} L_{\text{fiber}} \sim 9000 \text{ m}$ and total volume $V_{\text{fibers}} = \pi R_{\text{fiber}}^2 L_{\text{fiber}} N_{\text{fibers}} \sim 7 \text{ mm}^3$. There is also one nanorobot per fiber for control purposes, totaling $V_{\text{robs}} \sim N_{\text{fibers}} V_{\text{nanorobot}} \sim 0.09 \text{ mm}^3$, for a total volume intrusiveness of $(V_{\text{fibers}} + V_{\text{robs}}) / V_{\text{flaccid}} \sim 0.01\%$, well below the conservative safe limit for somatic intrusiveness of biocompatible foreign objects of 1-10% in local tissue volumes.⁸¹¹

An energy of $E_{\text{erect}} \sim (V_{\text{erect}} - V_{\text{flaccid}}) P_{\text{erect}} \sim 1 \text{ J}$ is required to erect the penis, or $P_{\text{erect}} \sim 40 \text{ mW}$ of power to complete the transition in $\sim 30 \text{ sec}$, demanding a power density of $P_D \sim P_{\text{erect}} / V_{\text{flaccid}} \sim 600 \text{ W/m}^3 \ll 6000\text{--}19,000 \text{ W/m}^3$ for testicular cells⁸¹² and $\sim 26,000 \text{ W/m}^3$ for a mature desktop nanofactory.⁸¹³ Power for each erection could be drawn from the equivalent of a single rechargeable flywheel battery of volume $E_{\text{erect}} / E_{D,\text{flywheel}} \sim 0.02 \text{ mm}^3$, or from natural sources.⁸¹⁴ Nanorobot infusion, extraction and control (Section 5.3.1), and orgasm management as previously described (Section 5.3.3.1) are still applicable except that this installation would be more “permanent” in nature, up to the appropriate maximum allowable *in vivo* residence time consistent with long-term biocompatibility constraints.

5.4.4 Utility Penis

An advanced form of nanorobotics technology called “utility fog” could be employed to enhance the performance of penis-coating prosthetics such as the nanoglove (Section 5.4.2), penile tissue-embedded prosthetics such as the lifter meshes (Section 5.4.3), or even whole-penis replacements to avoid the constraints of biological materials as with penile transplants (Section 4.9.5), creating a multifunctional and maximally versatile prosthesis called a “utility penis”. The device would

⁸¹⁰ Freitas RA Jr. Nanomedicine, Volume IIA: Biocompatibility. Landes Bioscience, Georgetown, TX, 2003; Section 15.5.3.4.3, “Nanorobotic Concussive Vasculopathy”; <http://www.nanomedicine.com/NMIIA/15.5.3.4.3.htm>.

⁸¹¹ Freitas RA Jr. Nanomedicine, Volume IIA: Biocompatibility. Landes Bioscience, Georgetown, TX, 2003; Section 15.6.1, “Somatic Intrusiveness”; <http://www.nanomedicine.com/NMIIA/15.6.1.htm>.

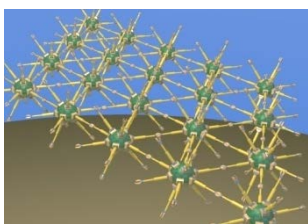
⁸¹² Freitas RA Jr. Nanomedicine, Volume I: Basic Capabilities. Landes Bioscience, Georgetown, TX, 1999; Section 6.5.2, “Thermogenic Limits *in vivo*”, Table 6.8; <http://www.nanomedicine.com/NMI/6.5.2.htm>.

⁸¹³ Freitas RA Jr. Energy Density. IMM Report No. 50, 25 June 2019, 516 pp; <http://www.imm.org/Reports/rep050.pdf>.

⁸¹⁴ The penis normally draws $P_{D,\text{human}} V_{\text{flaccid}} \sim 100 \text{ mW}$ even in the quiescent state, given the average human body basal power density of $P_{D,\text{human}} \sim 1000 \text{ W/m}^3$. Freitas RA Jr. Nanomedicine, Volume I: Basic Capabilities. Landes Bioscience, Georgetown, TX, 1999; Section 6.5.2, “Thermogenic Limits *in vivo*”, Table 6.8; <http://www.nanomedicine.com/NMI/6.5.2.htm>.

include neural interfaces to existing penile motor and sensory nerves, providing full sensory feedback for the user.

Also known as “programmable matter”⁸¹⁵ or “self-reconfiguring modular



robotics”,⁸¹⁶ and first conceptually applied to nanorobotics by Hall in 1993,⁸¹⁷ “utility fog” is a population of nanorobots (image, right) that can physically grasp each other in three dimensions (image, left), allowing them to collectively form



macroscale objects of virtually any size or shape. Nanorobots can quickly reconfigure the shape of the macroscale object they comprise by rapidly shifting their handgrips from one neighboring robot to another. According to the latest published technical description in the literature,⁸¹⁸ this active polymorphic material could be designed as a conglomeration of 10- μm nanorobotic cells (“foglets”) each of which has twelve arms, arranged on the 12 faces of a dodecahedron. “The arms telescope rather than having joints. The arms swivel on a universal joint at the base, and the gripper at the end can rotate about the arm’s axis. Each arm thus has four degrees of freedom, plus opening and closing the gripper. The only load-carrying motor on each axis is the extension/retraction motor. The swivel and rotate axes are weakly driven, able to position the arm in free air but not drive any kind of load; however, there are load-holding brakes on these axes.” The central body of the foglet is roughly spherical, 2 μm in diameter, and the arms are 0.5 μm in diameter and 5 μm long. Maximum dissipative power density of foglet nanorobots while in fastest motion⁸¹⁹ under maximum load can be estimated as $\sim 0.007 \text{ MW/L}$ ($p_s \sim 0.007 \text{ MW/kg}$),⁸²⁰ roughly comparable to medical

⁸¹⁵ Toffoli T, Margolus N. Programmable matter: Concepts and realization. Intl J High Speed Comput. 1993; 5(2):155-170; <https://books.google.com/books?hl=en&lr=&id=5HPrKf-nNuwC&oi=fnd&pg=PA263>. See also: https://en.wikipedia.org/wiki/Programmable_matter.

⁸¹⁶ https://en.wikipedia.org/wiki/Self-reconfiguring_modular_robot.

⁸¹⁷ Hall JS. Utility Fog: A Universal Physical Substance. Vision-21: Interdisciplinary Science and Engineering in the Era of Cyberspace, Westlake, OH; NASA Conference Publication CP-10129, 1993, pp. 115-126; <https://web.archive.org/web/20010525220851/http://www.aiveos.com/~bradbury/Authors/Computing/Hall-JS/UFAUPS.html>. See also: https://en.wikipedia.org/wiki/Utility_fog.

⁸¹⁸ Hall JS. Utility Fog: The stuff that dreams are made of. In: Crandall BC, ed. Nanotechnology: Molecular Speculations on Global Abundance. MIT Press, Cambridge MA, 1996, pp. 161-184; <https://www.amazon.com/Nanotechnology-Molecular-Speculations-Global-Abundance/dp/0262032376>. See also: <https://autogeny.org/Ufog.html>.

⁸¹⁹ Each layer of foglets can translate at a speed of up to $v_{\text{max}} \sim 5 \text{ m/sec}$ across a neighboring layer, during which about half the arms are linked between layers and the other half are not, with the tiny arms themselves moving back and forth as much as 100,000 times per second.

⁸²⁰ i.e., $\sim 700 \text{ kW/cm}^3$ with dissipative losses in the 10^{-5} range due to regenerative power capture. Hall JS. Utility Fog: The Stuff That Dreams Are Made Of. In: Crandall BC, ed. Nanotechnology: Molecular Speculations on Global Abundance. The MIT Press, Cambridge MA, 1996, Chapter 10, pp. 161-184; <https://www.amazon.com/Nanotechnology-Molecular-Speculations-Global-Abundance/dp/0262032376>. See also: <https://autogeny.org/Ufog.html>.

nanorobots such as microbivores ([Section 5.1.2](#)) and chromalloyocytes ([Section 5.1.3](#)) in their most active state.

Each foglet weighs $m_{\text{foglet}} \sim 0.20$ nanograms and contains $\sim 10^{13}$ atoms, with $c_{\text{foglets}} \sim 1$ billion foglets/cm³. Fully extended single-lattice 3D foglet material is estimated to have a bulk density of ~ 200 kg/m³, comparable to 150 kg/m³ for balsa wood and 250 kg/m³ for cork, with tensile, compressive, and fracture strengths of $\sim 1 \times 10^6$ N/m².⁸²¹ Fully contracted single-lattice 3D foglet material is ~ 1000 kg/m³, roughly the density of water. Double-lattice 3D foglet material that uses two interpenetrating foglet lattices should make a waterproof material when fully contracted, with density $\rho_{\text{foglets}} \sim 1800$ kg/m³, tensile strength $\sim 6 \times 10^7$ N/m² and flexural strength $\sim 8 \times 10^7$ N/m² comparable to ivory⁸²² or Corian structural plastic,⁸²³ and similar in density to glass sex toys.⁸²⁴

A penis constructed of foglet nanorobots could be inhumanly physically powerful if misused, so care must be taken to avoid injuring the recipient of the attentions of a **sexual “superman”**.⁸²⁵ An $x_{\text{nanoglove}} \sim 1$ mm thick layer of foglets coating the $A_{\text{erect}} \sim 150$ cm² outer surface area of an erect penis would consist of $N_{\text{fogglove}} \sim x_{\text{nanoglove}} A_{\text{erect}} c_{\text{foglets}} \sim 15 \times 10^9$ foglet nanorobots formed into an $m_{\text{fogglove}} = m_{\text{foglet}} N_{\text{fogglove}} \sim 3$ gm foglet-based nanoglove, or “fogglove”. Most fog motion is organized in layers, with each layer sliding by passing each other down hand-over-hand in bucket brigade fashion. If operated at a maximum speed of $v_{\text{max}} \sim 5$ m/sec under maximum load, a fogglove could extend from $L_{\text{flaccid}} \sim 9.2$ cm to $L_{\text{erect}} \sim 13.1$ cm in just $t_{\text{fogerection}} \sim (L_{\text{erect}} - L_{\text{flaccid}}) / v_{\text{max}} \sim 8$ msec, far faster than the 100-150 msec “blink of an eye”.⁸²⁶ Its brief power draw of $P_{\text{fogglove}} \sim m_{\text{fogglove}} p_s \sim 21$ W would heat the fogglove by no more than $\Delta T \sim \rho_{\text{diamond}} / p_s t_{\text{fogerection}} m_{\text{fogglove}} C_v \sim 0.01$ K, taking the volumetric heat capacity for diamond $C_v \sim 1.82 \times 10^6$ J/m³-K and diamond density $\rho_{\text{diamond}} = 3510$ kg/m³. Of course, the biological tissue of the human penis that would be enclosed by the fogglove cannot comfortably stretch nearly that fast. If operated at a more reasonable ~ 3.9 cm/sec giving a $t_{\text{fogerection}} \sim 1$ sec erection time, fogglove power demand (\approx velocity²) falls to $P_{\text{fogglove}} \sim 1$ mW, and the $E_{\text{fogerection}} \sim t_{\text{fogerection}} P_{\text{fogglove}} \sim 1$ mJ of energy required to produce one erection could be supplied for $n_{\text{erect}} \sim 1$ million erections by one rechargeable flywheel battery of volume $V_{\text{fly}} \sim n_{\text{erect}} E_{\text{fogerection}} / N_{\text{fogglove}} E_{\text{D,flywheel}} \sim 1.3$ μm^3 onboard each foglet nanorobot.

⁸²¹ https://www.matweb.com/search/datasheet_print.aspx?matguid=368427cdadb34b10a66b55c264d49c23,https://hal.science/hal-00561304v1/document.

⁸²² <https://whm.net/wp-content/uploads/2021/04/pa6-ivory.pdf>.

⁸²³ <https://www.hllmark.com/SiteAssets/Corian%20Design%20Specifications.pdf>.

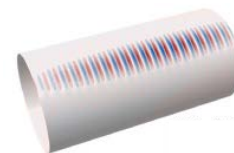
⁸²⁴ https://en.wikipedia.org/wiki/Sex_toy#Glass_sex_toys.

⁸²⁵ “Ejaculation of semen is entirely involuntary in the human male, and in all other forms of terrestrial life. It would be unreasonable to assume otherwise for a Kryptonian. But with Kryptonian muscles behind it, Kal-El’s semen would emerge with the muzzle velocity of a machine gun bullet.” Larry Niven. *Man of Steel*, *Woman of Kleenex*. *Knight: The Magazine for the Adult Male*, 1969 Dec; 7(8); <https://sff.calibre.jafner.net/download/14884/pdf/14884.pdf>. See also: https://en.wikipedia.org/wiki/Man_of_Steel,_Woman_of_Kleenex.

⁸²⁶ <https://www.ucl.ac.uk/news/2005/jul/blink-and-you-miss-it>.



An entire artificial penis composed of foglet nanorobots could rapidly (on 1-1000 msec timescales) reconfigure its external surface configuration, for example creating one or more



bulges (images, above left) that could form, expand, contract, or slide up and down the penile shaft at 1-100 Hz frequencies, or send rippling



surface waves in various patterns and frequencies across varying paths along the shaft (image, above right), or rapidly transform between ribbed and corkscrew patterns (images, left) or longitudinal traveling ridges (image, right). It could deploy a



small number of surplus foglet nanorobots to reform into various useful attachments to the shaft, as for example the separate clitoral stimulator pioneered by the notorious “Rabbit” vibrator (image, right).⁸²⁷ In the most extreme case where the human male flaccid penis volume of $V_{\text{flaccid}} \sim 64 \text{ cm}^3$ is entirely replaced with an implant of an equal volume of $N_{\text{foglets}} = c_{\text{foglets}} V_{\text{flaccid}} \sim 64 \times 10^9$ foglets, this is enough foglet material to form an annular $x_{\text{foglets}} \sim 1 \text{ mm}$ thick penile sheath about the width and length of the erect penis of a male horse,⁸²⁸ potentially enabling reenactment of a certain urban legend involving czarina Catharine the Great of Russia.⁸²⁹ There is also enough material to reform the utility penis into shapes resembling the five fingers of a human hand,⁸³⁰ or a flexible prehensile tongue,⁸³¹ or any other sexually useful configuration. Clearly there would be no difficulty adding modest amounts of penile length,



⁸²⁷ https://en.wikipedia.org/wiki/Rabbit_vibrator.

⁸²⁸ The distal end (inserted during copulation) of the erect penis of a stallion averages $D_{\text{stallion}} \sim 5.8 \text{ cm}$ in diameter and $L_{\text{stallion}} \sim 26 \text{ cm}$ in length (https://en.wikipedia.org/wiki/Stallion#Reproductive_anatomy), hence an $x_{\text{foglets}} \sim 1 \text{ mm}$ thick annulus having the aforementioned horse-erection dimensions has solid volume $V_{\text{horsefog}} \sim \pi D_{\text{stallion}} L_{\text{stallion}} x_{\text{foglets}} \sim 48 \text{ cm}^3$, leaving a $V_{\text{flaccid}} - V_{\text{horsefog}} \sim 16 \text{ cm}^3$ disk of foglets $\sim 1 \text{ cm}$ deep at the base through which biological vascular pathways can be rerouted and all essential human penile nerves may be interfaced to the foglet nanorobotic device.

⁸²⁹ Rounding V. Catherine the Great: Love, Sex, and Power. St. Martins Press, 2007; <https://www.amazon.com/Catherine-Great-Love-Sex-Power/dp/0312328877/>. See also: https://en.wikipedia.org/wiki/Legends_of_Catherine_the_Great#Death_while_having_sex_with_a_horse.

⁸³⁰ The mean hand and palm areas of a human male are $A_{\text{hand}} \sim 146.5 \text{ cm}^2$ and $A_{\text{palm}} \sim 77.9 \text{ cm}^2$,* leaving $A_{\text{fingers}} = A_{\text{hand}} - A_{\text{palm}} \sim 68.6 \text{ cm}^2$ for fingers (the primary digital tools during sexual activity) composed of an $x_{\text{foglets}} = V_{\text{flaccid}} / A_{\text{fingers}} \sim 0.9 \text{ mm}$ thick layer of foglets.

* Agarwal P, Sahu S. Determination of hand and palm area as a ratio of body surface area in Indian population. Indian J Plast Surg. 2010 Jan;43(1):49-53; <https://www.ncbi.nlm.nih.gov/pmc/articles/PMC2938623/pdf>.

⁸³¹ The dorsal and lateral surfaces of the human tongue have a mean area $A_{\text{tongue}} \sim 79.48 \text{ cm}^2$ (range 61.6-89.0 cm^2),* so a foglet aggregate of that shape would have walls $x_{\text{foglets}} = V_{\text{flaccid}} / A_{\text{tongue}} \sim 0.8 \text{ mm}$ thick.

* Naumova EA, Dierkes T, Sprang J, Arnold WH. The oral mucosal surface and blood vessels. Head Face Med. 2013 Mar 12;9:8; <https://www.ncbi.nlm.nih.gov/pmc/articles/PMC3639856/pdf>.

girth, features, functions, and speeds at the user's direction, subject only to device materials constraints.

5.5 Why Physical Sex?

Haptic⁸³² and teledildonic⁸³³ equipment can already communicate a partner's caresses and allow you to feel them. When fully immersive nanotechnology-based virtual reality becomes available,⁸³⁴ we'll be able to have as high-bandwidth of a sexual relationship electronically as in the flesh. Sociologist James Hughes has opined⁸³⁵ that sex in nano-neuro VR "will be far more intimate than in the flesh. We will be able to morph our genders, species, ages and numbers in VR, and open ourselves up to forms of tactile and emotional sharing that are impossible in the flesh-to-flesh. We can hold an orgy on the moons of Jupiter, on lambskin rugs, with cherubim as an attentive audience. When we are fully wired into one another's brains, body sex may seem no more intimate than a handshake, something one does for exercise with casual acquaintances. We will reserve fully immersive mind-melds for only those special half-dozen folks in our plural marriages."

Human beings who have been augmented via nanorobotic medicine into supermen⁸³⁶ with bodily parameters that are matters of design and choice "could enjoy the physical act of love as much as they pleased, which might be most of the time. But this isn't all they would be doing. The universe, both of nature and of man, is larger than any single emotional pattern. We shall grow sexually, to be sure, but we shall surely grow even more in other directions; our energies and satisfactions will take many channels, as they do now. In future generations, it seems most likely that sex will merge with the rest of life, that it will settle down and take its place within a whole new spectrum of experiences. But eventually it will indeed become a smaller aspect of life than it now seems – not because sex will shrink, but because life will expand." Perhaps sex will become just an entertaining hobby.⁸³⁷

⁸³² https://en.wikipedia.org/wiki/Haptic_technology.

⁸³³ <https://en.wikipedia.org/wiki/Teledildonics>.

⁸³⁴ Martins NRB, Angelica A, Chakravarthy K, Svidinenko Y, Boehm FJ, Opris I, Lebedev MA, Swan M, Garan SA, Rosenfeld JV, Hogg T, Freitas RA Jr. Human Brain/Cloud Interface. *Front Neurosci*. 2019 Mar 29;13:112; <https://www.ncbi.nlm.nih.gov/pmc/articles/PMC6450227/pdf>.

⁸³⁵ Hughes J. The Future of Sex. *IEET* 2003 Feb 9; <https://archive.ieet.org/articles/hughes20030209.html>. See also: Hughes J. From Virtual Sex to No Sex? *IEET* 2007 Feb 28; <https://archive.ieet.org/articles/hughes20070228.html>.

⁸³⁶ Ettinger RCW. *Man into Superman*, Avon, 1974; <https://www.amazon.com/Man-into-Superman-R-Ettinger/dp/0380000474/>. Online text of original 1972 edition at: <https://cryonics.org/wp-content/uploads/2020/05/ManIntoSuperman.pdf>.

⁸³⁷ Reitze BL. Sex Beyond Procreation – Sex as Hobby. *IEET* 2015 Jun 11; <https://archive.ieet.org/articles/reitze20150611.html>.

It is certainly possible that both penis and vagina might become sexually obsolescent in the future, if everything can be virtualized ([Section 5.3.3.2](#)) and all sexual contact could be perfectly simulated in the mind. If the virtual variety of sex is surpassingly ecstatic, people might come to prefer it over the natural variety which is less intimate and arguably produces mere pleasure but not ecstasy. Might sex become separated from physical contact when people can achieve orgasm simply by an act of will, anytime or anywhere? How might we wish to regulate the use of nanorobots that allow users to consciously overstimulate their pleasure centers (e.g., leading humans, like rats, to continuous self-activation while ignoring food and all other distractions until the current is turned off)⁸³⁸ which sounds like an irresistibly addictive euphorant drug vastly more powerful than heroin, fentanyl, methamphetamine, or crack cocaine? These and related important questions should be addressed in future work but are outside the scope of the present paper.

⁸³⁸ Olds J, Milner P. Positive reinforcement produced by electrical stimulation of septal area and other regions of rat brain. *J Comp Physiol Psychol.* 1954 Dec;47(6):419-27;
<https://seminarioneuromam.wordpress.com/wp-content/uploads/2014/04/olds-milner.pdf>.

6. Conclusions

This paper presents the first detailed technical analysis of the application of atomically precise nanorobots to the treatment of erectile dysfunction (ED) in human males. Also known as impotence, ED is characterized by the persistent inability to achieve or maintain an erection sufficient for satisfactory sexual performance – a multifactorial condition that can be influenced by psychological, neurological, hormonal, arterial, and penile anatomical components. The overall conclusion is that medical nanorobots should enable a man of any age or health status to physically consummate the sex act and fully satisfy both himself and his sexual partner, as frequently as desired.

After describing the normal physiological process by which male erections occur ([Section 2](#)) and how this normal process can fail, leading to erectile dysfunction ([Section 3](#)), we summarize the conventional clinical medical treatment strategies for the management of erectile dysfunction ([Section 4](#)). These methods are primarily pharmacological and mechanical, and offer only modest and temporary restoration of sexual function in some but not all patients, often accompanied by physical discomfort or undesirable side effects. The advent of nanofactories will make it possible to manufacture and deploy medical nanorobots ([Section 5.1](#)) to comprehensively treat and cure male erectile dysfunction ([Section 5](#)).

[Section 5.2](#) describes a range of nanorobotic treatments that would provide actual **permanent cures** for the underlying problems that are causing the ED. For example, vasculocytes are $\sim 8.3 \mu\text{m}^3$ “vasculomobile” nanorobots that could walk along the inside (intimal) surfaces of arteries or veins and navigate the branching vessels to reach specific locations in the vascular tree. About 400 million vasculocytes could clean out the **atherosclerotic plaque** (assuming $\sim 30\%$ occlusion) overlaying the endothelial cell lining of the eight primary penile arteries in ~ 6 hrs, permanently eliminating erectile dysfunction due to impaired blood flow ([Section 5.2.1.1](#)). Alternatively, a $100 \mu\text{m}$ diameter nanocatheter threaded into the penile arteries could perform plaque debridement in ~ 1 hr ([Section 5.2.4.2](#)). For **damaged endothelium**, ~ 10 nanocatheters could replace $\sim 1\%$ of all arterial penile endothelial cells in ~ 9 hr of treatment in which damaged cells are extracted and removed from the body while healthy new cells are transported to the repair site and installed ([Section 5.2.4.3](#)). To cure erectile dysfunction due to neurological defect, ~ 40 million cell repair nanorobots could **repair demyelinated pelvic splanchnic or pudendal nerves** in 1-2 hrs of onsite treatment activity ([Section 5.2.2](#)). A nanocatheter instrument could be threaded into the penile tissues to **correct degenerative tissue** changes in the tunica albuginea that can weaken the ability of the tunica to compress the penile veins, leading to venogenic ED. About 100 nanocatheters could repair $\sim 1\%$ of tunica albuginea penile sheath tissue in a ~ 6 hr treatment time ([Section 5.2.4.5](#)), and repairing moderate fibrosis of the corpora cavernosa should require roughly similar resources. **Cytosolic modification agents could be injected** into individual smooth muscle cells (SMCs) in the penile corpora cavernosa by (1) nanorobots that have navigated via the bloodstream to the affected smooth muscle cells within the penile tissues, (2) nanorobots that are locally released at the appropriate sites from the terminus of a nanocatheter, or (3) a nanomechanical toolhead at the tips of ~ 10 nanocatheters that could service $\sim 1\%$ of all penile SMCs in ~ 11 hrs ([Section 5.2.4.4](#)).

[Section 5.3](#) describes how medical nanorobots could provide **symptomatic relief** from ED without correcting the underlying organic problem that is causing the condition. Nanorobots called “**lifters**” to be deployed in penile tissues could achieve effective vasodilation or inflation sufficient to establish and maintain a normal erection ([Section 5.3.1](#)). Specifically, a fleet of ~ 1

billion nanorobots transiently anchored on the intimal surface of the penile arterial vasculature could release nitric oxide (NO) into the blood volume immediately adjacent to the endothelial cells lining the penile vasculature, allowing diffusion to carry the NO into the smooth muscle cells ([Section 5.3.1.1](#)), or the NO could be injected directly into the individual endothelial cells ([Section 5.3.1.2](#)). In either case, the robots trigger the normal cycle of SMC relaxation leading to an **erection that could be continuously maintained for ~1 hr** using compressed NO gas stored in onboard pressure tanks, **or maintained indefinitely** using onboard chemical synthesis of the required NO molecules. In another scenario, a fleet of ~1.5 billion lifter nanorobots anchored to endothelial cells lining the interior volume of the sinusoids in the corpora cavernosa could physically inflate (e.g., using compressed nitrogen gas), mechanically forcing the corpora cavernosa to expand, yielding an erection ([Section 5.3.1.3](#)). In cases of venogenic ED, ~27 million additional vasculomobile nanorobots could assemble into vascular gates creating a temporary ~90% blockage of the ~2000 subtunical venules through which venous blood exits the penis, thus providing sufficient venous occlusion to restore the ability to establish and maintain a normal erection ([Section 5.3.1.4](#)).

For maximum comfort, convenience, and effectiveness, the leading administration route for lifters appears to be a **metered dose inhaler for lung entry** by the nanorobots, allowing the devices to reach their assigned stations in the penile tissue in a **transit time of ~100 sec** ([Section 5.3.1.5](#)). The nanorobots later exit the body by passing through the kidney and into the bladder in a transit time of ~500 sec, thereafter to be excreted with the urine ([Section 5.3.1.6](#)). While on station, lifters may be activated or deactivated by user-generated mechanical sounds such as a coded series of hand slaps applied to the buttocks or thighs, or more complex instructions can be inmessaged to the robots using acoustic signals transmitted through a cell phone-attached ultrasound speaker pressed against the skin ([Section 5.3.1.7](#)). A billion mechanically active remote-controlled nanorobots loaded into a penis could alter the penile inflationary pattern to express specific patterns of bumps or ridges on the surface of the penis and cause these surface patterns to vary over time to create traveling waves including vibrations at the specific acoustic frequency most likely to induce orgasms in women, or exhibit other dynamic behaviors in response to sensed environmental information ([Section 5.3.1.7](#)).

A separate fleet of nanorobots called “**lustbots**” could be deployed in the brain of the human male to **artificially stimulate sexual arousal**, in cases where a lack of arousal plays a role in the ED pathology ([Section 5.3.2](#)). Approximately **500,000 nanorobots**, if properly positioned along the correct axons at pre-synaptic positions, should suffice to artificially generate all the hormonal, sensory, and neural inputs to the mPOA (Medial Preoptic Area) that would normally occur during natural sexual arousal ([Section 5.3.2.2](#)). There are ~300,000 axons projecting into the mPOA that promote sexual arousal. The ~20,000 axons that inhibit sexual arousal (originating in the BNST, amygdala, and PAG) possess detectable membrane and cytosolic molecular markers that should allow a nanorobot to distinguish them from axons originating from other sources, enabling nanorobots to avoid artificially stimulating them, creating a stronger and more natural sensation of sexual arousal. These vasculomobile nanorobots could be administered via a nasal spray or airborne perfume and might arrive on station at axons in the mPOA after a **~34 sec transit time**, later exiting the body via the conjunctiva of the eye. Men must remain alert (and perhaps proactively deploy defenses) against unscrupulous people who might surreptitiously employ lustbots as a date rape instrumentality to artificially and irresistibly arouse male victims with the objective of inducing them to engage in sexual activities in which they would normally be unwilling to participate ([Section 5.3.2.4](#)). The biological regulation of sexual arousal in human females is more complex than in males, probably requiring 100-200 million nanorobots (200-400 times larger than the male dosage) to effectuate reliable female arousal.

Lifters and lustbots can be supplemented by nanorobots called “**ecstasytes**” designed to **enhance or extend the male orgasmic response** (Section 5.3.3). A fleet of ~1 million nanorobots emplaced around each of the two pudendal nerves and ~100,000 nanorobots around each of the two cavernous nerves in the penis would enable modulation and control of the male orgasm, including triggering at least **2 orgasms/min**, or indefinitely delaying orgasm, entirely under user control (Section 5.3.3.1). Nanorobots carefully deployed throughout the human brain could create a “vorgasm” (virtual orgasm) by directly stimulating those parts of the brain that would normally be activated during sexual activity leading to male climax. Artificial generation of a vorgasm requires the precise placement and operation of **~11-18 million nanorobots on each side of the brain**, a total whole-brain 0.22-0.36 mm³ robot dose assuming one robot per neuron (Section 5.3.3.2). Extending the male orgasmic experience beyond the usual 3-10 sec to a **duration of many minutes (or longer) of continuous orgasm** appears feasible using nanorobots (Section 5.3.3.3).

Section 5.4 describes **nanorobotic penile prostheses** that can provide a reliable substitute for erectile functionality without directly curing or treating the underlying biological pathology of ED. Four possible approaches include: (1) a “**Maypole implant**” comprising a cylindrical-shaped macroscale nanomechanical robot that is implanted in the penis like a traditional penile implant, but with greatly improved sexual performance characteristics (Section 5.4.1); (2) a nanorobotic condom or “**nanoglove**” that offers a motorized flexible sheath that can expand into the shape and size of a fully erect penis, with **full sensory feedback** from the exterior of the condom to the enveloped biological organ (Section 5.4.2); (3) a motorized “**lifter mesh**” implanted throughout the penile tissue that provides geometric control and the benefits of direct skin-on-skin contact during coitus with a **30 sec erection time** (Section 5.4.3); and (4) a “**utility penis**” with a **1 sec erection time** that represents the ultimate multifunctional and maximally versatile penile prosthesis using a utility-fog based condom, implant, or whole-penis transplant (Section 5.4.4).

In the broader context of medical nanorobotics, a number of important regulatory, ethical, and safety concerns should be more comprehensively addressed in future publications, including (1) intellectual property issues and patents on sexual devices,⁸³⁹ (2) safety and biocompatibility⁸⁴⁰ (ensuring nanorobots are safe for long-term use, non-toxic, and biocompatible with human tissues), (3) regulatory approval (establishing frameworks for clinical trials, FDA (or equivalent) approval, and compliance with medical standards), (4) privacy and autonomy (addressing patient consent, data privacy, and autonomy regarding internal monitoring of therapeutic nanorobots), (5) potential misuse (including concerns over non-medical or military applications), and (6) long-term effects (assessing potential unknown effects from prolonged presence of nanorobots in the body).

⁸³⁹ Levins H. American Sex Machines: The Hidden History of Sex at the U.S. Patent Office, Adams Media Corp., 1996; <https://www.amazon.com/American-Sex-Machines-Hidden-History/dp/1558505342/>.

⁸⁴⁰ Freitas RA Jr. Nanomedicine, Volume IIA: Biocompatibility, Landes Bioscience, Georgetown, TX, 2003; <http://www.nanomedicine.com/NMIIA.htm>.